Online ISSN: 1920-3853

Vol. 8, No. 1, Feb 2014

Print ISSN : 1715-9997

# Canadian Journal of pure & applied sciences

an International Journal

SENRA

Academic Publishers

British Columbia

Print ISSN 1715-9997
Online ISSN 1920-3853

Volume 8, Number 1
Feb 2014

# CANADIAN JOURNAL OF PURE AND APPLIED SCIENCES

EDITOR
MZ Khan, SENRA Academic Publishers
Burnaby, British Columbia, Canada

ASSOCIATE EDITORS
Dongmei Zhou, Institute of Soil Science
Chines Academy of Sciences, China

Errol Hassan, University of Queensland
Gatton, Australia

Paul CH Li, Simon Fraser University
Burnaby, British Columbia, Canada

EDITORIAL STAFF
Jasen Nelson
Walter Leung
Sara Ali
Hao-Feng (howie) Lai
Ben Shieh
Alvin Louie

MANAGING DIRECTOR
Mak, SENRA Academic Publishers
Burnaby, British Columbia, Canada

The Canadian Journal of Pure and Applied Sciences (CJPAS-ISSN 1715-9997) is a peer reviewed multi-disciplinary specialist journal aimed at promoting research worldwide in Agricultural Sciences, Biological Sciences, Chemical Sciences, Computer and Mathematical Sciences, Engineering, Environmental Sciences, Medicine and Physics (all subjects).

Every effort is made by the editors, board of editorial advisors and publishers to see that no inaccurate or misleading data, opinions, or statements appear in this journal, they wish to make clear that data and opinions appearing in the articles are the sole responsibility of the contributor concerned. The CJPAS accept no responsibility for the misleading data, opinion or statements.

CJPAS is Abstracted/Indexed in:
Thomson Reuters, EBSCO, Ulrich's Periodicals Directory, Scirus, CiteSeerX, Index Copernicus, Directory of Open Access Journals, Google Scholar, CABI, Chemical Abstracts, Zoological Records, Global Impact Factor Australia, J-Gate, HINARI, WorldCat, British Library, European Library, Biblioteca Central, The Intute Consortium, Genamics JournalSeek, bibliotek.dk, OAJSE, Zurich Open Repository and Archive Journal Database. CJPAS has received:

Global Impact Factor for 2012 = 2.657
Index Copernicus Journals Evaluation for 2011 = 4.63

Frequency:
3 times a year (Feb, June and Oct.)

Editorial Office
E-mail: editor@cjpas.ca
: editor@cjpas.net

SENRA Academic Publishers
5919 129 B Street Surrey
British Columbia V3X 0C5 Canada
www.cjpas.net
E-mail: senra@cjpas.ca

## Board of Editorial Advisors

Richard Callaghan
University of Calgary, AB, Canada
David T Cramb
University of Calgary, AB, Canada
Matthew Cooper
Grand Valley State University, AWRI, Muskegon, MI, USA
Anatoly S Borisov
Kazan State University, Tatarstan, Russia
Ron Coley
Coley Water Resource & Environment Consultants, MB, Canada
Chia-Chu Chiang
University of Arkansas at Little Rock, Arkansas, USA
Michael J Dreslik
Illinois Natural History, Champaign, IL, USA
David Feder
University of Calgary, AB, Canada
David M Gardiner
University of California, Irvine, CA, USA
Geoffrey J Hay
University of Calgary, AB, Canada
Chen Haoan
Guangdong Institute for drug control, Guangzhou, China
Hiroyoshi Ariga
Hokkaido University, Japan
Gongzhu Hu
Central Michigan University, Mount Pleasant, MI, USA
Moshe Inbar
University of Haifa at Qranim, Tivon, Israel
SA Isiorho
Indiana University - Purdue University, (IPFW), IN, USA
Bor-Luh Lin
University of Iowa, IA, USA
Jinfei Li
Guangdong Coastal Institute for Drug Control, Guangzhou, China
Collen Kelly
Victoria University of Wellington, New Zealand
Hamid M.K.AL-Naimiy
University of Sharjah, UAE
Eric L Peters
Chicago State University, Chicago, IL, USA
Roustam Latypov
Kazan State University, Kazan, Russia
Frances CP Law
Simon Fraser University, Burnaby, BC, Canada
Guangchun Lei
Ramsar Convention Secretariat, Switzerland
Atif M Memon
University of Maryland, MD, USA
SR Nasyrov
Kazan State University,Kazan, Russia
Russell A Nicholson
Simon Fraser University, Burnaby, BC, Canada
Borislava Gutarts
California State University, CA, USA
Sally Power
Imperial College London, UK
Gordon McGregor Reid
North of England Zoological Society, UK
Pratim K Chattaraj
Indian Institute of Technology, Kharagpur, India
Andrew Alek Tuen
Institute of Biodiversity, Universiti Malaysia Sarawak, Malaysia
Dale Wrubleski
Institute for Wetland and Waterfowl Research, Stonewall, MB, Canada
Dietrich Schmidt-Vogt
Asian Institute of Technology, Thailand
Diganta Goswami
Indian Institute of Technology Guwahati, Assam, India
M Iqbal Choudhary
HEJ Research Institute of Chemistry, Karachi
Daniel Z Sui
Texas A&M University, TX, USA
SS Alam
Indian Institute of Technology Kharagpur, India
Biagio Ricceri
University of Catania, Italy
Zhang Heming
Chemistry & Environment College, Normal University, China
C Visvanathan
Asian Institute of Technology, Thailand
Indraneil Das
Universiti Malaysia, Sarawak, Malaysia
Gopal Das
Indian Institute of Technology , Guwahati, India
Melanie LJ Stiassny
American Museum of Natural History, New York, NY, USA
Kumlesh K Dev
Bio-Sciences Research Institute, University College Cork, Ireland.
Shakeel A Khan
University of Karachi, Karachi
Xiaobin Shen
University of Melbourne, Australia
Maria V Kalevitch
Robert Morris University, PA, USA
Xing Jin
Hong Kong University of Science & Tech.
Leszek Czuchajowski
University of Idaho, ID, USA
Basem S Attili
UAE University, UAE
David K Chiu
University of Guelph, Ontario, Canada
Gustavo Davico
University of Idaho, ID, USA
Andrew V Sills
Georgia Southern University Statesboro, GA, USA
Charles S. Wong
University of Alberta, Canada
Greg Gaston
University of North Alabama, USA


Member
**CANADIAN ASSOCIATION OF LEARNED JOURNALS**

Canadian Journal of pure & applied sciences

Volume 8, Number 1
February 2014

# CONTENTS

**PHYSICAL SCIENCES**

SENRA Academic Publishers, British Columbia
Vol. 8, No. 1, pp. 2663-2669, February 2014
Online ISSN: 1920-3853; Print ISSN: 1715-9997

Canadian Journal of pure&applied sciences

# CYTOSOLIC CALCIUM MEASUREMENT FOR SINGLE-CELL DRUG EFFICACY AND CARDIOTOXICITY EVALUATIONS USING MICROFLUIDIC BIOCHIPS

*XiuJun Li[1] and *Paul CH Li[2]
[1]Department of Chemistry, University of Texas at El Paso, El Paso, TX 79912, USA
[2]Department of Chemistry, Simon Fraser University, Burnaby, BC, V5A 1S6, Canada

## ABSTRACT

Intracellular calcium ($[Ca^{2+}]_i$) regulates a diverse range of cellular functions and signaling pathways. This review article aims to highlight applications of microfluidic single-cell analysis in drug discovery including drug efficacy test and drug side-effect test, based on intracellular calcium measurement.

**Keywords**: Cytosolic calcium, microfluidic chip, cytotoxicity, drug efficacy, drug cardiotoxicity, single-cell analysis, herbal ingredients, licorice.

## INTRODUCTION

Although medicinal herbs have been used in folk medicine with a long history, only recently has the screening of natural anticancer drugs from herbs gained much interest (Lee *et al*., 2007; Kanazawa *et al*., 2003; Srivastava and Gupta, 2007). Colorimetric cytotoxicity assays, such as the one using MTT (3-[4,5-dimethylthiazol-2-yl]-2,5-diphenyl tetrazolium bromide), are widely used for drug screening. However, these conventional assays usually require substantial amounts of herbal ingredients which are often expensive and limited in amount. In addition, these assays are time-consuming, usually taking ~ 4 days for experiments (Dell'Erba *et al*., 2005). Moreover, when screening for herbal compounds, the reliability and sensitivity of this assay are sometimes affected by the presence of antioxidants and colored substances that may lead to chemical and color interferences, respectively (Wang *et al*., 2006). Therefore, a new cell-based technique is needed to test the drug efficacy of herbal compounds.

It is well-known that intracellular calcium acts as a universal second messenger to regulate a diverse range of cellular functions (e.g., cell death and myocyte contraction) (Dorsam and Gutkind, 2007). In addition, the elevation of cytosolic $Ca^{2+}$ concentration or $[Ca^{2+}]_i$ is associated with the activation of cell membrane-bound G-protein-coupled receptors (GPCRs), which represent the drug targets of 50-60% of current therapeutic agents (Dorsam and Gutkind, 2007). Therefore, the cytosolic $Ca^{2+}$ measurement is now one of the most important cell-based assays in screening for new drug candidates (Monteith and Bird, 2005; Worley and Main, 2002). For example, it is found that various stimuli (e.g., anti-cancer drugs) can cause sustained $[Ca^{2+}]_i$ elevations, which disrupt the $Ca^{2+}$ homeostasis and result in cytotoxicity, and even cell death (Orrenius *et al*., 2003). Moreover, this disruption is believed to be an early event of cytotoxicity (Orrenius *et al*., 2003; Gurfinkel *et al*., 2006). Therefore, the effect of anticancer herbal compounds on cancer cells can be rapidly evaluated by $[Ca^{2+}]_i$ measurement.

During the process of drug discovery, drug biosafety (e.g. cardiac effect) must also be evaluated. It is known that any disturbance to cytosolic $Ca^{2+}$ may cause adverse effects on the contractility of myocytes, leading to cardiotoxicity (Missiaen *et al*., 2000). For instance, many chemicals or drugs (e.g., caffeine and cocaine) have undesirable side-effects on the heart as measured by their effects on the $[Ca^{2+}]_i$ mobilization (Sardao *et al*., 2002). A high plasma caffeine concentration (> 1-2 mM) is known to be lethal for adult humans, in which a large increase in cytosolic calcium occurs by emptying the internal store sarcoplasmic reticulum (SR) of heart muscle cells (Sardao *et al*., 2002). In addition, many anticancer drugs (e.g., daunorubicin, or DNR) have serious toxic effects on the heart (Olson and Mushlin, 1990). Therefore, the $[Ca^{2+}]_i$ measurements can provide useful information for cardiotoxicity of drug candidates before their animal tests and human trials.

Miniaturized microfluidic devices have been used for cellular analysis (see Fig. 1). They require much less reagent consumption when compared with the traditional microtiter plate-based assays. In addition, the small dimensions of microfluidic devices, which are compatible with the sizes of biological cells, allow for the study of a

*Corresponding author emails: xli4@utep.edu; paulli@sfu.ca

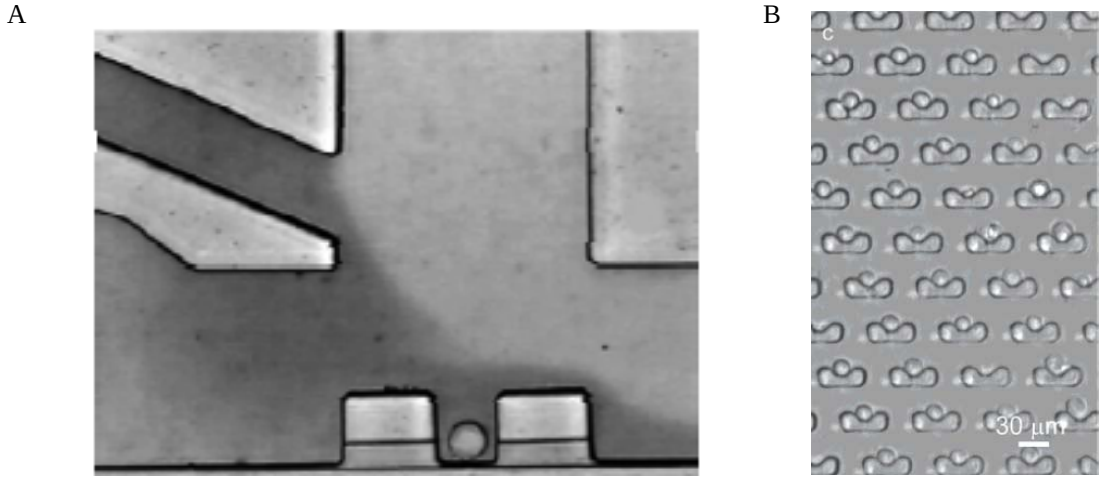


Fig. 1. Different microstructures for single-cell capture (A) from (Wheeler *et al*., 2003) and multiple single-cell capture (B) from (Di Carlo *et al*., 2006).

small number of cells, e.g., rare cells (Li *et al*., 2008). This has made the cell-based assay one of the most popular micro total analysis system (μTAS) applications (Dittrich *et al*., 2006; Li *et al*., 2012; Li *et al*., 2011; Kovarik *et al*., 2012). Among the microfluidics-based cellular applications, much emphasis has been placed on single-cell analysis (Sims and Allbritton, 2007; Di Carlo and Lee, 2006), which helps observe cellular heterogeneity and can provide information about cell-to-cell variations (Teruel and Meyer, 2002; Wheeler *et al*., 2003). For instance, Wheeler *et al*. (2003), Peng and Li (2004, 2005), Li *et al*. (2009), Yin *et al*. (2008), Yang *et al*. (2002), and Zhang *et al*. (2006) have measured calcium changes of spherical cells due to chemical stimuli using fluorescence detection. Furthermore, single cylindrically shaped cardiomyocytes (heart muscle cells) have been measured for calcium changes (Li and Li, 2005; Li *et al*., 2007; Li and Li, 2006; Kaji *et al*., 2003; Klauke *et al*., 2003; Cheng *et al*., 2006; Klauke *et al*., 2007; Klauke *et al*., 2006).

Among these microfluidic measurements on calcium, Li *et al*. quantified $[Ca^{2+}]_i$ of single cells (Li and Li, 2005), showing that only quantified $[Ca^{2+}]_i$, but not fluorescence intensity, can accurately represent the $[Ca^{2+}]_i$ changes of cells in response to drug stimulation. This quantitative method was applied to single cancer cells using a microfluidic biochip for drug efficacy test (see Fig. 2) (Li *et al*., 2009). This method quickly detected the sustained $[Ca^{2+}]_i$ increase, an early event of cytotoxicity, caused by different reagents on leukemia cancer cells. Meanwhile, by using a microfluidic chip with improved cell retention of cardiomyocytes (see Fig. 3), drug cardiotoxicity test on calcium mobilization of single cardiomyocytes from various chemicals (e.g. caffeine), the chemotherapeutic drugDNR, and anti-cancer drug candidate isoliquiritigenin (IQ) were studied (Li *et al*., 2007).

**Drug efficacy evaluations on cancer cells**

Daunorubicin, a highly effective chemotherapy drug of the anthracycline family, has been reported to cause apoptosis in leukemic cell lines, such as U937 and HL60 (Vial *et al*., 1997; Durrieu *et al*., 1998). Since $[Ca^{2+}]_i$ mobilization precedes the caspase activation in the apoptosis pathway (Durrieu *et al*., 1998), the $[Ca^{2+}]_i$ measurement method can reveal the early-stage information of cell death (Li *et al*., 2009).

The schematic diagram of the chip, the cell retention structure and single RAW cell retained within the structure are shown in figure 2A, 2B and 2C, respectively. Figure 2D shows the $[Ca^{2+}]_i$ mobilization of a single RAW cell (cell 1) by the DNR treatment. After DNR was added, $[Ca^{2+}]_i$ did not increase very much during the first 1200 s (see curve 1). Then a sustained $[Ca^{2+}]_i$ increase up to ~420 nM was observed after ~3800 s of the DNR treatment. A control experiment on another individual cell (cell 2) without Fluo-4 loading was performed, showing no obvious cellular fluorescence increase observed due to the DNR accumulation into the cell (see curve 2). This confirmed that DNR accumulation did not interfere with the fluorescent measurement of $[Ca^{2+}]_i$ because of the different emission wavelengths of DNR (585 nm) and Fluo 4-$Ca^{2+}$ (525 nm) (Li *et al*., 2008; Li and Li, 2005). At a higher concentration of DNR (35 μM), the $[Ca^{2+}]_i$ increase was even faster, and it was observed that some RAW cells died within ~4500 s.

Isoliquiritigenin (IQ), a flavonoid ingredient from licorice, was found to exhibit cytotoxic effects on human prostate

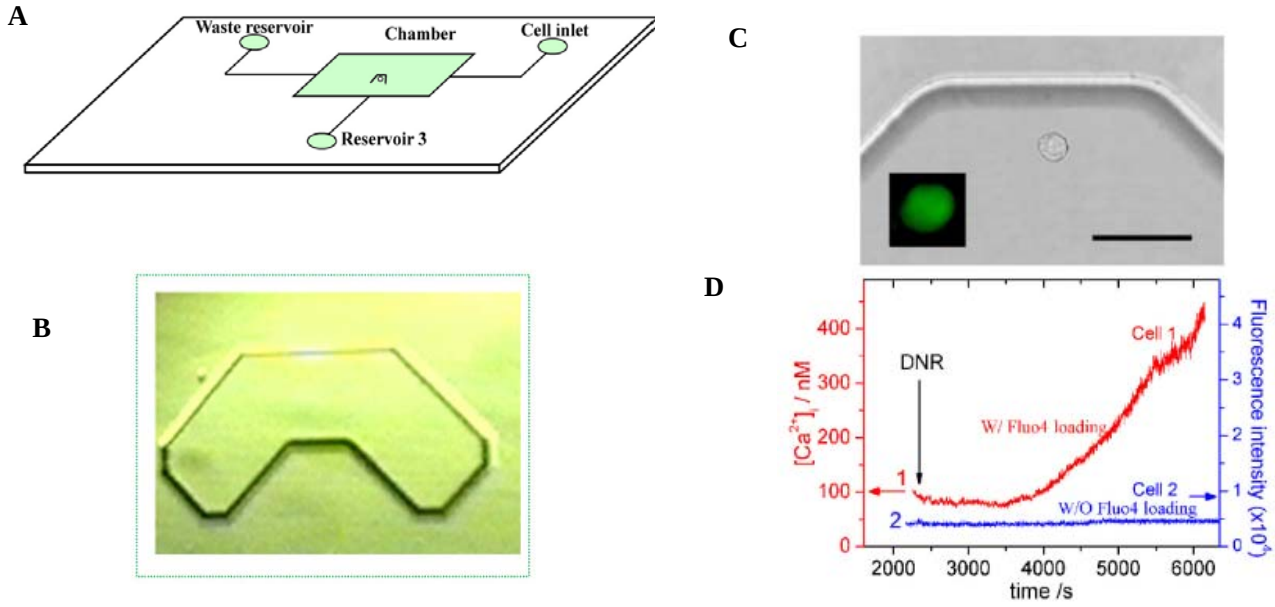


Fig. 2. Drug efficacy evaluations on cancer cells. (A) Microchip layout. (B) Single-cell capture structure. (C) A captured RAW 264.7 cell in the microstructure. (D) DNR-induced $[Ca^{2+}]_i$ mobilization on single leukemia RAW cells. The figure is adapted from Ref (Li *et al*., 2009).

(Kanazawa *et al*., 2003), gastric (Ma *et al*., 2001), heptoma (Hsu *et al*., 2005) and breast cancer cells (Maggiolini *et al*., 2002), and also on mouse renal (Yamazaki *et al*., 2002) and melanoma cells (Iwashita *et al*., 2000). As it was reported that the cytotoxic effect of IQ on gastric cancer cells may involve a calcium-dependent pathway (Ma *et al*., 2001), the anticancer effect of IQ on leukemia cells was investigated by monitoring $[Ca^{2+}]_i$ mobilization (Li *et al*., 2009).

It was shown that 50 μM IQ has caused a sustained $[Ca^{2+}]_i$ increase on a single cell reaching a level of 342±39 nM (n=3) after 1.5 h (Li *et al*., 2009). Glycyrrhizin (GL), which is a major ingredient of licorice (Pompei *et al*., 1979; Sung and Li, 2004), has various desirable pharmacological properties such as anti-viral (Cinatl *et al*., 2003), anti-inflammatory (Tanaka *et al*., 1987), has also been studied to see whether this ingredient has anticancer or cytotoxic effects on leukemia cells. But no sustained increase of $[Ca^{2+}]_i$ on single RAW cells from GL (up to 100 μM) was observed (Li *et al*., 2009).

**Drug cardiotoxicity evaluations on cardiomyocytes**

In drug development, after efficacy test of drug candidates, it is important to evaluate their cardiovascular safety. Figure 3C shows a single cardiomyocyte retained in the cell retention chamber of a chip with improved cell retention (Fig. 3A and B) for cylindrical cardiomyocytes as described elsewhere (Li *et al*., 2007).

The known cardiac effect of caffeine was first verified by the real-time monitoring of the $[Ca^{2+}]_i$ change on the contraction of a single cardiomyocyte (Li *et al*., 2007). After 40 mM caffeine was added, a rapid $[Ca^{2+}]_i$ increase of 580 ± 65 nM was observed, which was due to the transient release of $Ca^{2+}$ from SR (Bers, 1987). This $[Ca^{2+}]_i$ increase induced the cardiomyocyte to quickly contract by ~40% afterward. These $[Ca^{2+}]_i$ changes in cardiomyocytes indicate the early event of cardiotoxicity, as compared to the previous observations of cytotoxicity in RAW cells.

The effect of IQ on $[Ca^{2+}]_i$ of a single cardiomyocyte is shown in figure 3D (curve 1). Before drug treatment, the resting $[Ca^{2+}]_i$ was ~118 nM. After 100 μM IQ was introduced, $[Ca^{2+}]_i$ showed a slow increase after ~20 min (at ~4400 s), until it flattened off at ~279 nM after ~80 min (at ~8000 s). The results showed that IQ did increase the $[Ca^{2+}]_i$ of cardiomyocyte in a time-dependent manner, but the change was not dramatic, which indicated that IQ might have a low toxic effect on cardiomyocytes. For comparison, the cellular response of 3.5 μM of DNR was also measured, as shown in figure 3D as curve 2. It can be seen that the $[Ca^{2+}]_i$ increase due to DNR is much higher

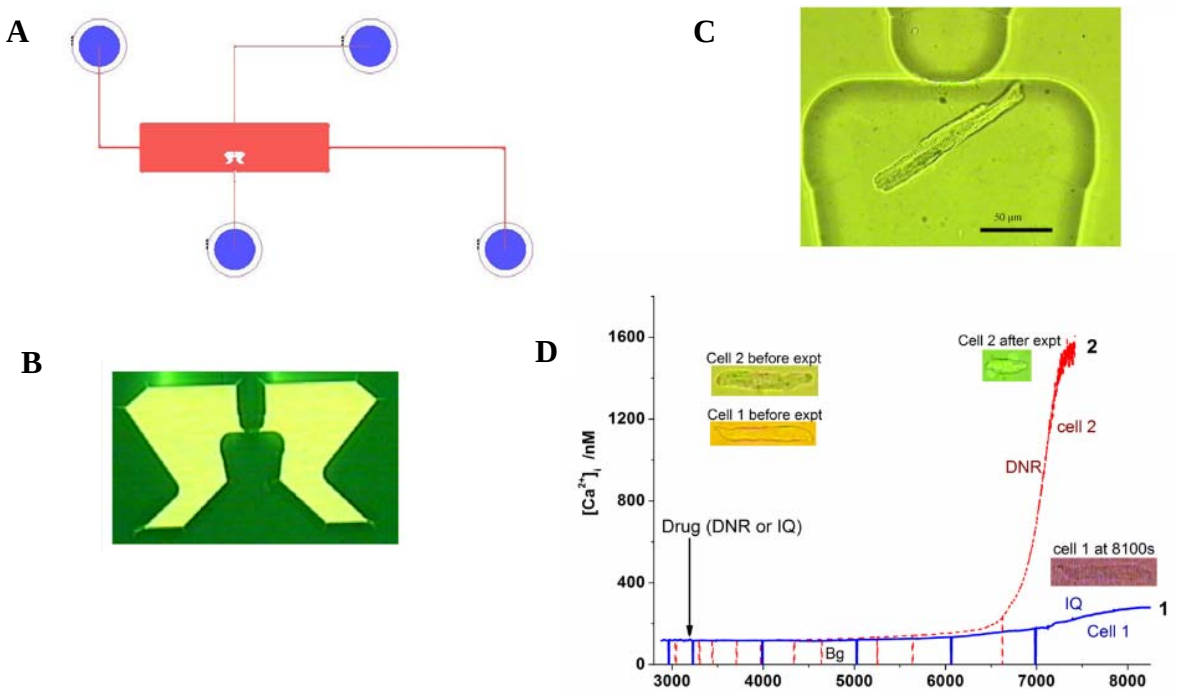


Fig. 3. Microfluidic single cell analysis for drug cardiotoxicity evaluation. (A) Chip layout. (B) Single-cell capture structure. (C) A single cardiomyocyte retained in the capture structure. (D) Cardiotoxicity evaluations on cardiomyocytes as depicted by the $[Ca^{2+}]_i$ responses after drug treatment of DNR and IQ. The figure is adapted from Li *et al.* (2007).

than that resulted from IQ. For instance, DNR caused $[Ca^{2+}]_i$ to increase up to 1563 nM, even when a much lower DNR concentration (3.5 μM) was used, while 100 μM IQ increased $[Ca^{2+}]_i$ only up to 279 nM. The very high $[Ca^{2+}]_i$ concentration of 1563 nM is detrimental to the cells (Olson and Mushlin, 1990), as it has been reported that $[Ca^{2+}]_i$ above ~$10^{-6}$ M or 1000 nM is lethal to cells (Hesketh *et al.*, 1983). More experiments show that the maximum $[Ca^{2+}]_i$ due to DNR and IQ within 90 min are 1507±80 nM and 255±35 nM (n=3), respectively. These data suggest that DNR has a much greater cytotoxic effect than IQ on cardiomyocytes. In addition to the $Ca^{2+}$ data, the microfluidic single-cell method provided the data of the cell morphology changes before and after the drug treatment (Fig. 3D). For instance, after DNR treatment, cell 2 showed cell shortening and membrane blebbing, which is indicative of an unhealthy or dying cell, while cell 1 still showed healthy status after the IQ treatment.

Although DNR is widely used in treatment of leukemia, the use of DNR is unfortunately limited by its potentially fatal cardiotoxicity (Olson and Mushlin, 1990; Olson *et al.*, 2000). As compared with DNR, IQ has less effect on $[Ca^{2+}]_i$ of heart muscle cells, and hence less cardiotoxicity. In conjunction with the finding from the previous section that 50 μM IQ has a cytotoxic effect on leukemia cells, IQ can be a potential drug candidate with less cardiotoxicity. But the findings of these cell-based in vitro tests are subject to the confirmation by in vivo assays.

## SUMMARY

Intracellular calcium measurement using microfluidic devices provides a versatile platform for drug discovery from drug efficacy test to side-effect test. Such an approach, together with the effort to develop high throughput capability and automation, will be useful to evaluate drug efficacy and cardiosafety, without the 4-day wait when using the conventional assays.

## ACKNOWLEDGEMENTS

Financial support from Natural Science and Engineering Research Council (NSERC) of Canada (Discovery Grant), UT STARS Award, UTEP IDR and URI programs is gratefully acknowledged.

**REFERENCES**


Bers, DM. 1987. Ryanodine and the calcium content of cardiac SR assessed by caffeine and rapid cooling contractures. Am. J. Physiol. 253:C408-15.

Cheng, W., Klauke, N., Sedgwick, H., Smith, GL. and Cooper, JM. 2006. Metabolic monitoring of the electrically stimulated single heart cell within a microfluidic platform. Lab Chip. 6:1424-31.

Cinatl, J., Morgenstern, B., Bauer, G., Chandra, P., Rabenau, H. and Doerr, HW. 2003. Treatment of SARS with human interferons. Lancet. 362:293-4.

Dell'Erba, C., Chiavarina, B., Fenoglio, C., Petrillo, G., Cordazzo, C., Boncompagni, E., Spinelli, D., Ognio, E., Aiello, C., Mariggio, MA. and Viale, M. 2005. Inhibition of cell proliferation, cytotoxicity and induction of apoptosis of 1,4-bis(1-naphthyl)-2,3-dinitro-1,3-butadiene in gastrointestinal tumour cell lines and preliminary evaluation of its toxicity in vivo. Pharmacol. Res. 52:271-82.

Di Carlo, D., Aghdam, N. and Lee, LP. 2006. Single-cell enzyme concentrations, kinetics, and inhibition analysis using high-density hydrodynamic cell isolation arrays. Anal. Chem. 78:4925-30.

Di Carlo, D. and Lee, LP. 2006. Dynamic single-cell analysis for quantitative biology. Anal. Chem. 78: 7918-25.

Dittrich, PS., Tachikawa, K. and Manz, A. 2006. Micro total analysis systems. Latest advancements and trends. Anal Chem. 78:3887-908.

Dorsam, RT. and Gutkind, JS. 2007. G-protein-coupled receptors and cancer. Nat. Rev. Cancer. 7:79-94

Durrieu, F., Belloc, F., Lacoste, L., Dumain, P., Chabrol, J., Dachary-Prigent, J., Morjani, H., Boisseau, MR., Reiffers, J., Bernard, P. and Lacombe, F. 1998. Caspase activation is an early event in anthracycline-induced apoptosis and allows detection of apoptotic cells before they are ingested by phagocytes. Exp. Cell Res. 240: 165-75.

Gurfinkel, DM., Chow, S., Hurren, R., Gronda, M., Henderson, C., Berube, C., Hedley, DW. and Schimmer, AD. 2006. Disruption of the endoplasmic reticulum and increases in cytoplasmic calcium are early events in cell death induced by the natural triterpenoid Asiatic acid. Apoptosis. 11:1463-71.

Hesketh, TR., Smith, GA., Moore, JP., Taylor, MV. and Metcalfe, JC. 1983. Free cytoplasmic calcium concentration and the mitogenic stimulation of lymphocytes. J. Biol. Chem. 258:4876-82.

Hsu, YL., Kuo, PL. and Lin, CC. 2005. Isoliquiritigenin induces apoptosis and cell cycle arrest through p53-dependent pathway in Hep G2 cells. Life Sci. 77:279-92.

Iwashita, K., Kobori, M., Yamaki, K. and Tsushida, T. 2000. Flavonoids inhibit cell growth and induce apoptosis in B16 melanoma 4A5 cells. Biosci. Biotechnol. Biochem. 64:1813-20.

Kaji, H., Nishizawa, M. and Matsue, T. 2003. Localized chemical stimulation to micropatterned cells using multiple laminar fluid flows. Lab Chip. 3:208-11.

Kanazawa, M., Satomi, Y., Mizutani, Y., Ukimura, O., Kawauchi, A., Sakai, T., Baba, M., Okuyama, T., Nishino, H. and Miki, T. 2003. Isoliquiritigenin inhibits the growth of prostate cancer. Eur. Urol. 43:580-6.

Klauke, N., Smith, G. and Cooper, JM. 2007. Microfluidic systems to examine intercellular coupling of pairs of cardiac myocytes. Lab Chip. 7:731-9.

Klauke, N., Smith, GL. and Cooper, J. 2003. Stimulation of single isolated adult ventricular myocytes within a low volume using a planar microelectrode array. Biophys. J. 85:1766-74.

Klauke, N., Smith, GL. and Cooper, J. 2006. Extracellular recordings of field potentials from single cardiomyocytes. Biophys. J. 91:2543-51.

Kovarik, M. L., Gach, PC., Ornoff, DM., Wang, Y., Balowski, J., Farrag, L. and Allbritton, NL. 2012. Micro total analysis systems for cell biology and biochemical assays. Anal Chem. 84:516-40.

Lee, C. K., Park, KK., Lim, SS., Park, JH. and Chung, WY. 2007. Effects of the licorice extract against tumor growth and cisplatin-induced toxicity in a mouse xenograft model of colon cancer. Biol. Pharm. Bull. 30:2191-5.

Li, XJ., Chen, YC. and Li, PCH. 2011. A simple and fast microfluidic approach of same-single-cell analysis (SASCA) for the study of multidrug resistance modulation in cancer cells. Lab on a Chip. 11:1378-1384.

Li, XJ., Huang, J., Tibbits, GF. and Li, PCH. 2007. Real-time monitoring of intracellular calcium dynamic mobilization of a single cardiomyocyte in a microfluidic chip pertaining to drug discovery. Electrophoresis 28:4723-4733.

Li, XJ. and Li, PCH. 2005. Microfluidic selection and retention of a single cardiac myocyte, on-chip dye loading, cell contraction by chemical stimulation, and quantitative fluorescent analysis of intracellular calcium. Anal. Chem. 77:4315-4322.

Li, XJ. and Li, PCH. 2006. Contraction study of a single cardiac muscle cell in a microfluidic chip. Methods Mol. Biol. 321:199-225.

Li, XJ., Ling, V. and Li, PCH. 2008. Same-single-cell analysis for the study of drug efflux modulation of multidrug resistant cells using a microfluidic chip. Anal. Chem. 80:4095-4102.

Li, XJ., Valadez, AV., Zuo, P. and Nie, Z. 2012. Microfluidic 3D cell culture: potential application for tissue-based bioassays. Bioanalysis 4:1509-1525.

Li, XJ., Xue, X. and Li, PCH. 2009. Real-time detection of the early event of cytotoxicity of herbal ingredients on single leukemia cells studied in a microfluidic biochip. Integr. Biol. 1:90-98.

Ma, J., Fu, NY., Pang, DB., Wu, WY. and Xu, AL. 2001. Apoptosis induced by isoliquiritigenin in human gastric cancer MGC-803 cells. Planta Med. 67:754-7.

Maggiolini, M., Statti, G., Vivacqua, A., Gabriele, S., Rago, V., Loizzo, M., Menichini, F. and Amdo, S. 2002. Estrogenic and antiproliferative activities of isoliquiritigenin in MCF7 breast cancer cells. J. Steroid Biochem. Mol. Biol. 82:315-22.

Missiaen, L., Robberecht, W., van den Bosch, L., Callewaert, G., Parys, JB., Wuytack, F., Raeymaekers, L., Nilius, B., Eggermont, J. and De Smedt, H. 2000. Abnormal intracellular ca(2+)homeostasis and disease. Cell Calcium 28:1-21.

Monteith, GR. and Bird, GS. 2005. Techniques: high-throughput measurement of intracellular Ca(2+) -- back to basics. Trends Pharmacol. Sci. 26:218-23.

Olson, RD., Li, X., Palade, P., Shadle, SE., Mushlin, PS., Gambliel, HA., Fill, M., Boucek, RJ. Jr. and Cusack, BJ. 2000. Sarcoplasmic reticulum calcium release is stimulated and inhibited by daunorubicin and daunorubicinol. Toxicol. Appl. Pharmacol. 169:168-76.

Olson, RD. and Mushlin, PS. 1990. Doxorubicin cardiotoxicity: analysis of prevailing hypotheses. Faseb J 4: 3076-86.

Olson, RD. and Mushlin, PS. 1990. Doxorubicin cardiotoxicity: analysis of prevailing hypotheses. Faseb J. 4: 3076-86.

Orrenius, S., Zhivotovsky, B. and Nicotera, P. 2003. Regulation of cell death: the calcium-apoptosis link. Nat. Rev. Mol. Cell Biol. 4:552-65.

Peng, XY. and Li, PCH. 2005. Extraction of pure cellular fluorescence by cell scanning in a single-cell microchip. Lab Chip 5:1298-302.

Peng, XY. and Li, PCH. 2004. A three-dimensional flow control concept for single-cell experiments on a microchip. 2. Fluorescein diacetate metabolism and calcium mobilization in a single yeast cell as stimulated by glucose and pH changes. Anal. Chem. 76:5282-92.

Pompei, R., Flore, O., Marccialis, MA., Pani, A. and Loddo, B. 1979. Glycyrrhizic acid inhibits virus growth and inactivates virus particles. Nature. 281:689-90.

Sardao, VA., Oliveira, PJ. and Moreno, AJ. 2002. Caffeine enhances the calcium-dependent cardiac mitochondrial permeability transition: relevance for caffeine toxicity. Toxicol Appl Pharmacol. 179:50-6.

Sims, CE. and. Allbritton, NL. 2007. Analysis of single mammalian cells on-chip. Lab Chip. 7(4):423-40.

Srivastava, JK. and Gupta, S. 2007. Antiproliferative and apoptotic effects of chamomile extract in various human cancer cells. J. Agric. Food Chem. 55:9470-8.

Sung, MW. and Li, PCH. 2004. Chemical analysis of raw, dry-roasted, and honey-roasted licorice by capillary electrophoresis. Electrophoresis. 25:3434-40

Tanaka, H., Hasegawa, T., Matsushita, M., Miichi, H. and Hayashi, S. 1987. Quantitative-evaluation of ocular antiinflammatory drugs based on measurements of corneal temperature in rabbits - dexamethasone and glycyrrhizin. Ophthalmic Res. 19: 213-220.

Teruel, MN. and Meyer, T. 2002. Parallel single-cell monitoring of receptor-triggered membrane translocation of a calcium-sensing protein module. Science. 295:1910-2.

Vial, JP., Belloc, F., Dumain, P., Besnard, S., Lacombe, F., Boisseau, MR., Reiffers, J. and Bernard, P. 1997. Study of the apoptosis induced in vitro by antitumoral drugs on leukaemic cells. Leuk. Res. 21:163-172.

Wang, X., Ge, J., Wang, K., Qian, J. and Zou, Y. 2006. Evaluation of MTT assay for measurement of emodin-induced cytotoxicity. Assay Drug Dev. Technol. 4:203-7.

Wheeler, AR., Throndset, WR., Whelan, RJ., Leach, AM., Zare, RN., Liao, YH., Farrell, K., Manger, ID. and Daridon, A. 2003. Microfluidic device for single-cell analysis. Anal. Chem. 75:3581-6.

Worley, JF. **3rd,** and Main, MJ. 2002. An industrial perspective on utilizing functional ion channel assays for high throughput screening. Receptors Channels. 8:269-82.

Yamazaki, S., Morita, T., Endo, H., Hamamoto, T., Baba, M., Joichi, Y., Kaneko, S., Okada, Y., Okuyama, T., Nishino, H. and Tokue, A. 2002. Isoliquiritigenin suppresses pulmonary metastasis of mouse renal cell carcinoma. Cancer Lett. 183:23-30.

Yang, M., Li, CW. and Yang, J. 2002. Cell docking and on-chip monitoring of cellular reactions with a controlled concentration gradient on a microfluidic device. Anal Chem. 74:3991-4001.

Yin, H., Pattrick, N., Zhang, X., Klauke, N., Cordingley, HC., Haswell, SJ. and Cooper, JM. 2008. Quantitative comparison between microfluidic and microtiter plate formats for cell-based assays. Anal. Chem. 80: 179-85.

Zhang, X., Yin, H., Cooper, JM. and Haswell, SJ. 2006. A microfluidic-based system for analysis of single cells based on Ca2+ flux. Electrophoresis. 27:5093-100

Received: Oct 17, 2013; Accepted: Dec 5, 2013

SENRA Academic Publishers, British Columbia
Vol. 8, No. 1, pp. 2671-2676, February 2014
Online ISSN: 1920-3853; Print ISSN: 1715-9997

Canadian Journal of pure&applied sciences

# DETECTION OF HUMAN PAPILLOMAVIRUS-21 GENOTYPES IN A SAMPLE OF IRAQI WOMEN WITH CERVICAL ABNORMALITIES AND CANCER

*Hula Y Fadhil[1], Dhuha S Saleh[1] and Faisal G Al-Hamdani[2]
[1]Department of Biology, College of Science, University of Baghdad, Baghdad-Al-Jadiria
[2]Department of Virology, National Central Public Health Laboratory
Ministry of Health, Baghdad-Al-Andlus Street, Iraq

## ABSTRACT

To determine the prevalence and genotypes of cervical HPV infection in Iraq by newly developed technique. In this study, 188 women with cervical dysplasia (CIN I, II/III), 7 women with squamous cervical cancer, 40 women with atypical squamous cell and cervicitis and 25 healthy women as control group were collected. For Detection of HPV types, DNA extracted from cervical exfoliated cells was evaluated by polymerase chain reaction and typing with genoarray test. HPV-DNA positive was found 28.94% (68/235) in the cases but was absent in the control group. In the cases, the detection rate of HPV DNA in cytological categories atypical squamous with chronic cervicitis, LSIL (CIN I), HSIL(CIN II-III), and cancer was 5% (2/40), 30.34% (44/145), 34.88%(15/43), and 100%(7/7), respectively. Seventeen different HPV genotypes were investigated among 68 infected women. Moreover, ten different HPV for the first time in Iraqi women were recorded. Our finding demonstrated a predominance of HPV-59 (14.4%) followed by HPV-16 (13.3%) of all infection, but HPV-16 the most common type in HSIL and cancer was observed. Our results provide evidence the genoarray using for detection was increasing the number of isolates. Since 28% of infected women had HPV-16 and -18, the HPV vaccine is importance to introduction. Moreover, HPV-16, - 45 and -18 were highly associated with increasing severity of the disease, thus the strongest risk factor for persistence of infection was the presence of these types.

**Keywords**: Human Papillomavirus (HPV), genotyping, genoarray test, Iraqi women.

## INTRODUCTION

Human papillomaviruses (HPVs) have been recognized as etiologic factors in cervical carcinoma, precancerous lesions of the cervix uteri, and several other anogenital cancers in females and males (Bosch *et al*., 2002; Mun˜oz *et al*., 2006). In addition; about 26% of head and neck cancers are linked to HPV infection (Gillison and Lowy, 2004). HPVs represent an extremely heterogeneous group of DNA viruses. Until now, more than 100 HPV types have been identified and fully sequenced (de Villiers *et al*., 2004). Approximately 40 HPV types infecting the anogenital epithelium are classified as either low risk (LR) or high risk (HR) on the basis of their oncogenic potentials. A recent meta-analysis has designated 15 anogenital HPV types as HR, with an additional 3 HPV types designated as probable HR types (Mun˜oz *et al*., 2003). A number of PCR-based HPV genotyping assays have been developed to amplify HPV DNA, followed by reverse hybridization against immobilized genotype-specific probes, allowing the simultaneous identification of a broad range of anogenital HPV genotypes. However, the different assays have potential variations in their abilities to detect different HPV types due to their different analytical sensitivities and specificities and their failure to detect specific variants (Brink *et al*., 2007; Molijn *et al*., 2005; Sabol *et al*., 2008). We used HPV GenoArray (Macroarray) test is a newly developed PCR-based HPV genotyping assay. It utilizes L1 consensus primers to simultaneously amplify 21 HPV genotypes, followed by flow through hybridization with immobilized genotype-specific probes (Grisaru *et al*., 2008). It is marked as Conformite´ Europe´enne (CE) for use in Europe and is currently being used in some hospitals in China. HPV GenoArray test kit (GA) and the Roche Linear Array (LA) assays were showed no significant difference in the rates of detection of both HPV genotyping assays and oncogenic genotypes (Liu *et al*., 2010). The results showed that there was a high level (93.8%) of the agreement between the results of that assay and those of the Amplicor HPV test (Grisaru *et al*., 2008). Currently, HPV infections are increased significantly among Iraqi women without vaccine and many studies detected some HPV genotypes with different samples, but as our knowledge there is no previous study investigated HPV-21 genotype. Thus, our study was designed to investigate the prevalence of HPVgenotypes that associated with different cervical histological changes in Iraqi women using the GenoArray assay for the first time in Iraq.

## MATERIALS AND METHODS

### Patients and specimens

Cervical exfoliated cells were prospectively collected from 188 women with cervical dysplasia (CIN I, II/III), 7

*Corresponding author email: hulayounis@scbaghdad.edu.iq

women with squamous cervical cancer, 40 women with atypical squamous cell and cervicitis and 25 healthy women as control group attending Women Health Center-Al-Alwia hospital and Al-kadhmia teaching hospital in Baghdad during 2011. Control group mainly depended on the absence of clinical symptoms and cervical cytological changes were referred for Pap smear examination. Pap smear swabs were inserted into the endocervix by a clinician and rotated in both directions to collect the exfoliated cervical samples. These samples were stored at -20°C until use for HPV detection and genotyping.

**Genomic DNA isolation from cervical swab samples**

Genomic DNA isolation was performed using the HPV DNA extraction kit according to the manufacturer's protocol (Hybribio Limited Corporation, Hong Kong). Briefly, 0.5ml of the cervix of the uterus cell preservation fluid was centrifuged at 14000rpm for 1min.The supernatant was discarded, and the HPV DNA was extracted with the HPV DNA extraction reagent.

**HPV genotyping test**

The genoarry test is an L1consensus primer-based PCR assay and is capable of amplifying 21 HPV genotypes, including 13 HR types (types 16, 18, 31, 33, 35, 39, 45, 51, 52, 56, 58, 59,and 68), 2 probable HR (PHR) types (types 53 and 66), and 6 low-risk (LR) and unknown-risk (UR) types (types 6, 11, 42, 43, 44, and CP8304 [HPV-81]). The assay was performed according to the manufacturer's protocol. Briefly, PCR was performed with a reaction volume of 25µl containing 5µl of DNA template, 19.25µl of the master mixture provided, and 0.75µl of DNA *Taq*po lymerase in thermocycler apparatus (Techine-UK). The amplification protocol was as follows: 9 min of denaturation at 95°C and 40 cycles of 20 s of denaturation at 95°C, 30 s of annealing at 55°C, and 30 s of elongation at 72°C, followed by a final extension for 5min at 72°C. The amplicon was subsequently denatured and subjected to hybridization. The assay utilized a flow through hybridization technique by actively directing the targeting molecules toward the immobilized probes within the membrane fibers, with the complementary molecules beingretained by the formation of duplexes. After a stringent wash, the hybridswere detected by the addition of the streptavidin-horseradish peroxidaseconjugate (provided with the kit), which binds to the biotinylated PCR products, and a substrate (nitrobluetetrazolium–5-bromo-4-chloro-3-indolylphosphate) to generate a purple precipitate at the probe dot.

## STATISTICAL ANALYSIS

The data and graphs were carried out using SPSS program version 20 IBM. The proportion and their frequencies were checked by applying the chi - square test. The P-values <0.05 considered statistically significant.

## RESULTS

**HPV Detection**

In the present study, HPV-DNA positive was found 28.94% of the cases but was absent in the control group. In the cases, the detection rate of HPV DNA in cytological categories atypical squamous with chronic cervicitis, LSIL(CIN I), HSIL (CIN II-III), and cancer was 5% (2/40), 30.34% (44/145), 34.88% (15/43), and 100% (7/7), respectively. Significant differences of positively HPV with cytological changes were observed ($P<0.05$) in women with cervical dysplasia and cancer from those with chronic cervicitis.

**HPV Genotypes of infected women**

Seventeen different HPV genotypes were investigated among 68 infected women. Fourteen of these HPV genotypes comprised 82.35% were HR-types and 17.56% were LR-type. The present study indicates presence of ten different HPV genotypes (HPV-39, -45, -51, -52, -53, -58, -59, -66, -68 and -44) were recorded for first time in Iraqi women with cervical lesions. Our finding demonstrated a predominance of HPV-59(14.4%) followed by HPV-16 (13.3%) (Table 1). On the other hand, genotypes-59, -16, -6, -39 and -11 were the five most common types detected in 62.2% of the types and 82.4%of the HPV positive cases. In the present study, type 16 was detected alone in 7/68 (10.3%) cases and in association with type -18 in one (1.5%) case. Type -18 was detected as monotype in three (4.4%) case. Thus, type -16 and -18 were detected alone and in association with each other types in 28% of the 68 cases. Type 59 was detected alone and in association with other types in 19.1% of cases.

In the current study, HPV-16, -45, and -56 were comprised of 57.14 % (4/7), 28.57% (2/7), and 14.29% (1/7) of SCC cases, respectively. Regarding the HPV-6 was detected as co-infector with HPV-45 in one case of SCC. It is remarkable the HPV-66 was detected as monotype in one case suffering from severs dysplasia, because these changes are the last stage for developing invasive cervical cancer. Although, the prevalence of most HPV types were non-significantly ($P>0.05$) among LSIL and HSIL, HPV-45 in HSIL and HPV-6, -11 in LSIL were significantly present ($P<0.0000001$) and ($P<0.05$), respectively.

Eleven cervical samples from women with genital wart as typical criteria of HPV infection were tested. Seven different HPV genotypes have been identified in these specimens, which included: HPV-6 (36.4%), HPV-11(18.2%), and HPV-16, -59,-39,-66 and 44 (9.09% of each).

**High and Low Risk Genotypes among infected women**

The frequency of different HPV genotypes accounted in 68 women was 90 subtypes where 74.4%were HR types

Table 1. HPV Genotypes Detected by Genoarray Technique.

| HPV genotype | No. of infected women [a] | % of total infected[b] |
|---|---|---|
| 16 | 12 | 13.3 |
| 18 | 7 | 7.8 |
| 33 | 1 | 1.1 |
| 35 | 2 | 2.2 |
| 39 | 9 | 10 |
| 45 | 3 | 3.3 |
| 56 | 1 | 1.1 |
| 58 | 5 | 5.5 |
| 51 | 1 | 1.1 |
| 59 | 13 | 14.4 |
| 52 | 1 | 1.1 |
| 66 | 8 | 8.9 |
| 53 | 2 | 2.2 |
| 68 | 2 | 2.2 |
| 44 | 1 | 1.1 |
| 6 | 13 | 14.4 |
| 11 | 9 | 10 |
| Women with Single genotype | 49 | 72.06 |
| Women with Mixed genotype | 19 | 27.94 |

Character (a) in the table indicates to number of infected women that harbor with either single or associated with other genotypes, (b) refers to genotype percentage of total genotypes frequency of all infected women.

and 25.6%LR types (Table 2). Forty five out of 68 infected women (66.18%) had HR types alone, whether single or multiple types, whereas14.7% (10/68) of infected women had HR types in association with LR types and 19.12% (13/68) had LR types alone. However, 80.9% of the positive women had HR-HPV types, thus those women are at risk of developing high-grade squamous intra epithelial lesions or invasive cervical cancer.

**Single and Multiple HPV Infection**

Figure 1 demonstrates that 72.06% (49/68) of infected women had single HPV types, they included that 60.29% (41/68) of the women with dysplasia (CIN I, II/III), compared with 8.83% (6/68) of patients with SCC, and 2.94% (2/68) had chronic cervicitis. As shown in fig. 1, infection with multiple HPV types was 27.94% (19/68) of the study patients; they are distributed to 26.47% (18/68) with dysplasia and 1.47% (1/68) with SCC cases. Appearance of mixed infection in CIN I more than CIN II/III and cancer was observed, whereasthe significant occurrence of single infection with HR-types in CIN II/III and SCC was reported ($P<0.01$).

On the other hand, out of single infections, 26.53% (13/49) were LR-types, HR-types other than HPV-16 constituted 59.18% (29/49), whereas HPV-16 comprised of 14.29% (7/49). Of the multiple infections, 26.32% (5/19) associated with HPV-16, 21.05% (4/19) were infected with HR-types other than HPV-16, and 52.63% (10/19) were infected with LR and HR-HPV types.

**DISCUSSION**

The close correlation between HPV infection and cervical cancer is well established, but there is a wide difference between the prevalence of infection and the occurrence of actual cancer (Yumin *et al*., 2012). The present study was demonstrated ten genotypes for the first time in our country which some of these were recorded in neighboring countries like Saudi Arabia, Iran and Turkey (Alsbeih *et al*., 2011; Zandi *et al*., 2010; Dursun *et al*., 2009). In this study, HPV-16 the most common type in SCC was explained the clearance more slowly than infections caused by other high-risk types (Kulmala *et al*., 2006). Moreover, other HR-HPV types were present in cervical cancer HPV-45 and HPV-56. Although, HPV-33 is one of the most types of cancer, our finding that low percentage (1.1%) of HPV types was present in CIN I. Contrast, Clifford *et al*. (2005a) reported that HPV-16,-18,-33 and -45 were the most four genotypes present in cervical cancer in North America. Also, Young *et al*. (2009) indicated that approximately 95% of cervical cancers in Korean women have been found to contain DNA of HR-HPV types, most commonly HPV-16, followed by HPV types -18, -31 and -45.Geographic differences in the relative prevalence of HPV genotypes may be related to the complex interplay among different

Table 2. Frequency of HPV genotypes according to infection type.

| HPV genotype | Frequency of genotypes as: | | *HPV genotype Co-infectors in mixed infection(NO. of infections) |
|---|---|---|---|
| | Single infection | Mixed infection | |
| 16 | 7 | 5 | 39(1),33(1),52(1),18+66(1),58+59(1) |
| 59 | 7 | 6 | 6(3), 39(1), 16+58(1), 11(1) |
| 66 | 5 | 3 | 11(1), 16+18(1), 18+51(1) |
| 6 | 7 | 6 | 59(3), 39(2), 45(1) |
| 11 | 5 | 4 | 66(1), 58(1), 18(1), 59(1) |
| 39 | 5 | 4 | 16(1), 59(1), 6(2) |
| 35 | 2 | 0 | - |
| 56 | 1 | 0 | - |
| 44 | 1 | 0 | - |
| 68 | 1 | 1 | 53(1) |
| 18 | 3 | 4 | 51+66(1), 16+66(1), 53(1), 11(1) |
| 45 | 2 | 1 | 6(1) |
| 58 | 3 | 2 | 11(1), 16+59(1) |
| 53 | 0 | 2 | 68(1), 18(1) |
| 33 | 0 | 1 | 16(1) |
| 51 | 0 | 1 | 66+18(1) |
| 52 | 0 | 1 | 16(1) |
| Total | 49 | 41 | |

Asterisk indicates that genotypes which appeared with detection genotype in the same infected women.

HPV genotypes and/or variants with host immunogenetic factors (e.g., HLA polymorphisms) (Hildesheim and Wang, 2002). Alternatively, a recent study showed that HPV 16 appeared less influenced by immune status than other HPV genotypes (Strickler *et al*., 2003). However, regional differences appear to become less pronounced with increasing severity of lesions, as HPV 16 becomes increasingly dominant (Clifford *et al*., 2005b). The strongest risk factor for persistence of infection is the presence of HPV-16 (Molano *et al*., 2003). This may explain HPV-16 in women with chronic cervicitis was observed. On the other hand, only one case (14.28%) of SCC genotypes has high-risk type infection in co-infection with HPV-6 was found. Based on the accepted model of cervical carcinogenesis, HPV-6 rarely integrates in the human genome (Coutlee *et al*., 2009). The investigators Garcia *et al*. (2011) suggested that the LR-HPVs persist in cancer lesions possibly as commensals and presence of other HPV types in the same lesions may represent concomitant infections. In contrary, HPV18 is unlikely to cause HSIL or worse cytologies despite its importance in causing 37% to 41% of cases of cervical adenocarcinoma. Moreover, Schiffman *et al*. (2005) showed that no one has been able to explain exactly why HPV18 tends to be ‘‘occult’’ at the stage of high-grade intraepithelial lesions (precancer), the target of cervical cancer screening. This may compare with the low prevalence of HPV-18 in HSIL of present study. The co-infection of HPV, that is, including two or more than two types of HPV in the same patient, is one of the main unsolved problems associated with the current HPV diagnosis and HPV vaccination. Our finding demonstrated that high rate 73.7% (14/19) of women with multiple infections was constituted CIN I in comparison with 26.3% (5/19) in CIN II/III and SCC. It remains to be determined if viral load of multiple HPV infections is indicative of an immunological response due to a combined effect among HPV types present in the infected area and whether or not it would predict a higher risk of infection persistence (Ahn *et al*., 2003). Furthermore, another study showed that mixed infections with HR-HPV genotypes are less likely to progress to cervical cancer than infections with single HR-HPV genotypes (Zuna *et al*., 2004). Thus, the high rate of single infections with HR-HPV types (approximately 53%) in this study population may also predict the higher risk of progression to invasive cancer. Nevertheless, Schellekens *et al*. (2004) reported significantly higher amount of multiple HPV infections in adenosquamous carcinoma in comparison with squamous cell carcinoma. These hypothesizes are confirmed by other study which showed that the infections with multiple HPV types may increase the risk

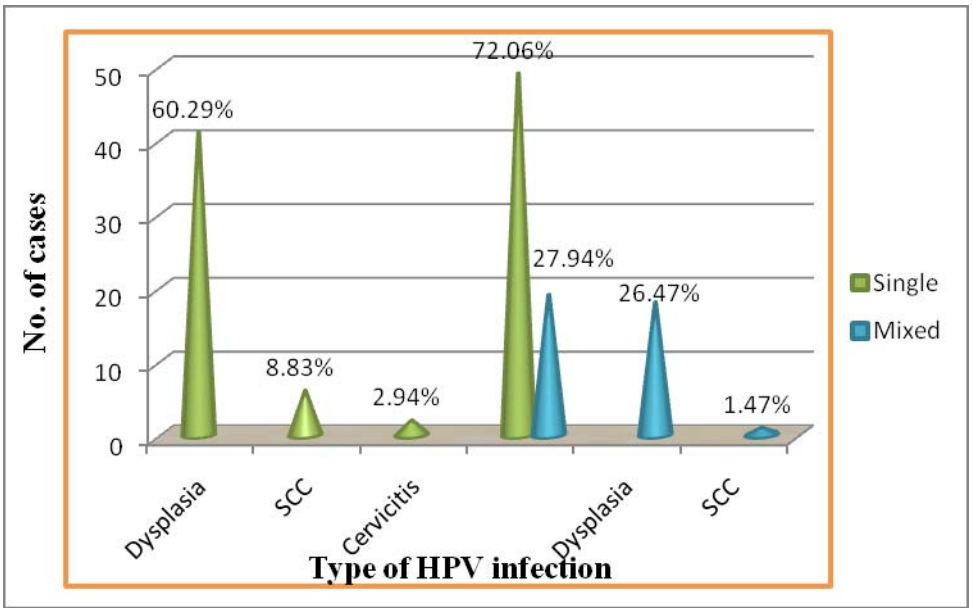


Fig. 1. Distribution Single and Mixed HPV infections according to cytological categories of infected women, term dysplasia indicates women with CIN I, and CIN II/III.

of cervical disease but their effect on SCC pathogenesis is unclear (Rong Sun *et al*., 2010).

In Conclusion: Our results provide evidence the genoarray using for detection was increasing the number of isolates. Since 28% of infected women had HPV-16 and -18, the HPV vaccine is importance to introduction. Moreover, HPV-16, - 45 and -18 were highly associated with increasing severity of the disease, thus the strongest risk factor for persistence of infection was the presence of these types.

## ACKNOWLEDGEMENT

We deeply thank to director Faiza L. Tome/virologist and all staff members of the General viruses Laboratory/National Central Public Health Laboratory for their help.

## REFERENCES

Ahn, WS., Bae, SM. and Kim, TY. 2003. A therapy modality using recombinant IL-12 adenovirus plus E7 protein in a human papillomavirus 16 E6/E7-associated cervical cancer animal model. Human Gene Therapy. 14(15):1389-1399.

Alsbeih, G., Ahmed, R., Al-Harbi, N., Venturina, LA., Tulbah, A. and Balaraj, K. 2011. Prevalence and genotypes distribution of human papillomavirus in invasive cervical cancer in Saudi Arabia. Gynecol. Oncol. 121(3):522-526.

Bosch, FX., Lorincz, A., Munoz, N., Meijer, CJ. and Shah, KV. 2002. Thecausal relation between human papillomavirus and cervical cancer. J. Clin. Pathol. 55:244-265.

Brink, AA., Snijders, PJ. and Meijer, CJ. 2007. HPV detection methods. Dis. Markers. 23(4):273-281.

Clifford, GM., Gallus, S., Herrero, R., *et al*. 2005[a]. HPV Prevalence Surveys Study Group: Worldwide distribution of human papillomavirus types in cytologically normal women in the International Agency for Research on Cancer HPV prevalence surveys: a pooled analysis. Lancet. 366(9490):991-8.

Clifford, GM., Rana, RK., Franceschi, S., Smith, JS., Gough, G. and Pimenta, JM. 2005[b]. HPVs genotype distribution in low-grade cervical lesions: comparison by geographic region and with cervical cancer. Cancer Epidemiol. Biomarkers. 14(5):1157-1164.

Coutlee, F., Trottier, H., Gagnon, S., *et al*. 2009. Low-risk HPV type 6 DNA load and integration in cervical samples from women with Squamous intraepithelial lesion. J. Clin.Virol. 45(2):96-99.

de Villiers, EM., Fauquet, C., Broker, TR., Bernard, HU. and ZurHausen, H. 2004. Classification of papillomaviruses. Virol. 324(1):17-27.

Dursun, P., Senger, SS., Arslan, H., Kuscu, E. and Ayhan, A. 2009. Human papillomavirus (HPV) prevalence and types amoung Turkish women at a gynecology outpatient unit. BMC Infect. Dis. 9:191-195.

García, DA., Cid-Arregui, A., Schmitt, M., Castillo, M., Briceño, I. and Aristizábal, FA. 2011. Highly Sensitive Detection and Genotyping of HPV by PCR Multiplex and Luminex Technology in a Cohort of Colombian Women with Abnormal Cytology. The Open Virol. J. 5:70-79.

Gillison, ML. and Lowy, DR. 2004. A causal role for human papilloma-virus in head and neck cancer. Lancet.363:1488-1489.

Grisaru, D., Avidor, B., Niv, J., *et al*. 2008. Pilot study of prevalence of high-risk papilloma virus genotypes in Israeli Jewish women referred for colposcopic examination. J. Clin. Microbiol. 46(5):1602-1605.

Hildesheim, A. and Wang, SS. 2002. Host and viral genetics and risk of cervical cancer: a review. Virus Res. 89(2):229-40.

Kulmala, SMA., Syrjanen, SM., Gyllensten, UB., *et al*. 2006. Early integration of high copy HPV-16 detectable in women with normal and low grade cervical cytology and histology. J. Clin. Pathol. 59(5):513-517.

Liu, SS., Leung, RC., Chan, KK., Cheung, AN. and Ngan, HY. 2010. Evaluation of a newly developed GenoArray human papillomavirus (HPV) genotyping assay and comparison with the Roche Linear Array HPVgenotyping assay. J. Clin. Microbiol. 48(3):758-764.

Molano, M., Brule, V., Plummer, M., *et al*. 2003. Determinations of clearance of HPV infections in Colombian women with normal cytology: A population-based, 5-years follow up study. Am. J. Epidemiol. 158(5):486-494.

Molijn, A., Kleter, B., Quint, W. and Van Doorn, LJ. 2005. Molecular diagnosis of human papillomavirus (HPV) infections. J. Clin. Virol. 32(Suppl. 1):S43-S51.

Muñoz, N., Bosch, FX., de Sanjosé, S., *et al*. 2003. International Agency for Research on Cancer Multicenter Cervical Cancer Study Group. Epidemiologic classification of human papillomavirus types associated with cervical cancer. N Engl J Med. 348(6):518-527.

Muñoz, N., Castellsague´X., de Gonza´lez, AB. and Gissmann, L. 2006. HPV in the etiology of human cancer. Vaccine. 24(S3):S3/1-S3/10.

RongSun, Z., Ji, YH., Zhou, WQ., Zhang, SL., Jiang, WG. and Ruan, Q. 2010. Characteristics of HPV prevalence among women in Liaoning province, China. Int. J. Gynecol. Obstet. 109(2):105-109.

Sabol, I., Salakova, M., Smahelova, J., *et al*. 2008. Evaluation of different techniques for identification of human papillomavirus types of low prevalence. J. Clin. Microbiol. 46(5):1606–1613.

Schellekens, MC., Dijkman, A., Aziz, MF., *et al*. 2004. Prevalence of single and multiple HPV types in cervical carcinomas in Jakarta, Indonesia. Gynecol. Oncol. 93(1):49-53.

Schiffman, M., Herrero, R., Desalle, R., *et al*. 2005. The carcinogenicity of human papillomavirus types reflects viral evolution. Virol. 20(337):76-84.

Strickler, HD., Palefsky, JM., Shah, KV., *et al*. 2003. HPV type 16 and immune status in human immunodeficiency virus-seropositive women. J. Natl. Cancer Inst. 95(14):1062-1071.

Youngkim, J., Park, S., Nam, BH., *et al*. 2009. Low initial HPV Viral load implicates worse prognosis in patients with uterine cervical cancer treated with radiotherapy. J. Clin. Oncol. 27(30):5088-5093.

Yumin, W., Jie, C., Wenhui, Z., Wangdong, H. and Fangyou, Y. 2012. Study of the prevalence of human Papillomavirus infection in Chinese women with cervical cancer. Afri. J. of Microbiol. Res. 6(5):1048-1053.

ZandiK, E., Ghbali, SS., Hamkar, R., *et al*. 2010. Prevalence of various Human Papillomavirus (HPV) genotypes amoung women who subjected to routine Pap smear test in Bushehr city (South West of Iran) 2008-2009.Virol. J. 7(1):65-68.

Zuna, RE., Allen, RA., Moore, WE., Mattu, R. and Dunn, ST. 2004. Comparison of HPV genotypes in high-grade squamous intraepithelial lesions and invasive cervical carcinoma: evidence for differences in biologic potential of precursor lesions. Mol. Pat hol. 17:1314-1322.

Received: Sept 24, 2013; Accepted: Oct 26, 2013

SENRA Academic Publishers, British Columbia
Vol. 8, No. 1, pp. 2677-2684, February 2014
Online ISSN: 1920-3853; Print ISSN: 1715-9997

Canadian Journal of pure&applied sciences

# BIOMASS, CARBON STOCK AND CARBON DIOXIDE MITIGATION POTENTIAL OF *CEDRUS DEODARA* (DEODAR) UNDER TEMPERATE CONDITIONS OF KASHMIR

Nasir Rashid Wani, Khwaja Naved Qaisar and Parvez Ahmad Khan
Faculty of Forestry, Sher-e-Kashmir University of Agricultural Sciences and Technology of Kashmir
Shalimar (J & K), India

## ABSTRACT

Carbon management in forests is the global concern to mitigate the increased concentration of greenhouse gases. Carbon sequestration through biomass seems to be a cheap and viable option to mitigate the greenhouse gases in the atmosphere. The study attempted to estimate growth, biomass production, carbon stock and carbon dioxide mitigation potential of 19 year old *Cedrus deodara* plantation under different diameter classes. The volume of trees in the stand varied from 0.072 to 0.596$m^3$. The average dry stem biomass varied between 27.60 to 226.67kg, branch dry biomass between 7.88 to 64.14kg, needle dry biomass between 1.57 to18.19kg, total above ground dry biomass between 37.06 to 309.0kg and root dry biomass varied from 8.88 to77.25kg. The stem carbon varied from 12.80 to 105.15kg, branch carbon between 3.62 to 29.53kg, needle carbon between 0.67 to 7.78kg, root carbon between 4.09 to 35.66kg and total carbon between 21.18 to 178.12kg. The stem carbon dioxide mitigation potential varied from 46.83 to 384.84kg, branch from 12.91 to 108.07kg, needle from 2.44 to 28.47kg, root from 14.99 to 130.51kg and total carbon dioxide mitigation varied from 73.92 to 651.91kg.

**Keywords**: *Cedrus deodara*, biomass, carbon stock, carbon dioxide mitigation, growth.

## INTRODUCTION

In India 120.72 million hectare area has been delineated as degraded and wastelands of the country and out of this 1.07 million hectares of demarcated forests has been reported as degraded and wastelands in Jammu and Kashmir (Anonymous, 2010). In order to solve the problems associated with wood supply deficiencies, to reduce pressure on natural forests and to increase carbon stocks for climate change mitigation, trees have been proposed as a vital tool for restoration of these degraded and wastelands by affecting the vegetation structure and soil. Trees are used on degraded sites because they produce abundant leaf litter covering the ground and protecting against soil erosion, promotes atmospheric carbon sequestration and restore biodiversity. Sequestration of biomass carbon is considered as the most promising approach to mitigate climate change (Kimble *et al*., 2002). At global level, trees contribute 80-90% of plant biomass carbon and 30-40% of soil carbon (Harvey, 2000). Therefore trees can play an important role in carbon dioxide sequestration due to several reasons. The first is that the tree component fixes and stores carbon from the atmosphere via photosynthesis. They can function as active carbon for the period of many years and continue to store the carbon until they are harvested or die. The second reason is that trees provide a good surface cover which minimizes the loss of nutrients from the surface soil, improves edaphic conditions, increase biomass production, decrease risk of soil degradation by erosion, leaching and nutrient depletion.

On the global scale, deforestation results in the release of approximately 1000 million tons of carbon to the atmosphere each year in the form of carbon dioxide, an important greenhouse gas. This is about 15 percent of the total human caused carbon emissions and is a significant portion of the global carbon cycle that could contribute to global climate change. The trees play a pivotal role in the global carbon cycle. Tremendous amounts are actively exchanged between vegetation and the atmosphere. Any land use practices that increase vegetation cover or reduce its removal, could have an influence on the global carbon budget by increasing the terrestrial carbon sink. Policy makers could attempt to produce increases in carbon sequestration in a variety of ways. The government could provide subsidies in the form of payments, tax credits or cost sharing to private landowners for adopting practices that are known to increase carbon stocks. Alternatively the government could expand its own tree plantations on public lands. Finally trees are one of the viable alternatives to increase forest cover which will widen the area of carbon sink. In view of the above, a study on the most demanding commercial, valuable timber tree species of Kashmir valley commonly known as Deodar (*Cedrus deodara*) having a rotation of 120 years and is a large evergreen conifer belongs to family Pinaceae. It is well distributed over the western Himalayas from Afghanistan

*Corresponding author email: nasirwani2012@gmail.com

in the west to parts of Nepal in the east (Luna, 2005). Thus an attempt was made to quantify the ability of the tree species to sequester atmospheric carbon.

## MATERIALS AND METHODS

### Site description

The experimental site is located between 74.89$^0$East longitude and 34.08$^0$North latitude at an altitude of about 1600 meters above mean sea level. It is roughly 15km southeast of the Srinagar city and the soil of the site is silty loam and is well drained. The climate is generally temperate with severe winter extending from December to March. The region faces a wide temperature range from a minimum of -4$^0$C in winter to a maximum of 33$^0$C in the summers. The annual precipitation of the area is about 676mm and most of the precipitation is received in the form of snow during winter months. The present study was carried out in *Cedrus deodara* Plantation Block of Faculty of Forestry during the year 2009 and 2010 at Sher-e-Kashmir university of Agricultural sciences and technology of Kashmir ( SKUAST-K),Shalimar.The trees were planted during March, 1990 having 19 years of age during the study.

### Demarcation and enumeration for measurements

After surveying of the experimental site, a quadrate of size 10 x 10m was laid in the area and total 24 trees in a particular quadrate were enumerated according to diameter at breast height (DBH). These trees were then classified into three diameter classes viz. 10-20cm, 20-30cm and 30-40cm for measuring various parameters.

### Estimations

### Volume and tree biomass

Tree biomass was estimated by adopting non-destructive methods for different plant parts viz. stem, branch and leaf.

### Stem biomass

The diameters at breast height (DBH) of the trees falling in the plot of size 10 x 10 m were measured with diameter tape and height with Ravi's multimeter respectively. Form factor and volume was calculated by using the following formula given by Pressler (1865) and Bitlerlich (1984).

$$f = \frac{2h_1}{3h}$$ Where, f is the form factor, $h_1$ = height at which diameter is half of DBH and h is the total height. The volume (V) was calculated by Pressler's formula:

$V = f \times h \times g$ Where, f = form factor, h = total height (m) and g = basal area, $g = \pi r^2$ or $\pi (dbh/2)^2$ Where, r = radius

### Specific gravity

The stem cores were taken to find out the specific gravity of wood, taking into account the variation in different parts of the tree, which was used further to determine the biomass of stem using the maximum moisture method (Smith, 1954).

$$Gf = \frac{1}{\frac{M_n - M_o}{M_o} + \frac{1}{G_{so}}}$$

Where,

$G_f$ = specific gravity based on gross volume

$M_n$ = weight of saturated volume sample

$M_o$ = weight of oven dried sample

$G_{so}$ = Average density of wood substance equal to 1.53

Thus the weight of stem wood = specific gravity × stem volume

Or

Stem biomass = Specific gravity × stem volume

### Branch biomass

The total number of branches irrespective of size was counted on each of the sample tree, then these branches were categorized on the basis of basal diameter into three groups viz. small, medium and large. Fresh weight of two sampled branches from each group was recorded separately. The following formula (Chidumaya, 1990) was used to determine the dry weight of branches:

$$B_{dwi} = B_{fwi} \Big/ 1 + M_{cdbi}$$

Where,

$B_{dwi}$ = oven dry weight of branches

$B_{fwi}$ = Fresh/green weight of branches

$M_{cdbi}$= Moisture content of branches on oven dry weight basis

Total branch biomass (fresh/dry) per sample tree will be determined as given below:

$$B_{bt} = n_1 b_{w1} + n_2 b_{w2} + n_3 b_{w3} ..... = \sum_{i=1}^{n} n_i b_{wi}$$

Where,

$B_{bt}$ = Branch biomass (fresh/dry) per tree

$n_i$ = Number of branches in the $i^{th}$ branch group

$b_{wi}$ = Average weight of branch of $i^{th}$ group

I = 1, 2, 3,.... the branch groups

### Leaf biomass

Leaves from five branches of individual trees were removed. Five trees per plot were taken for observation. The leaves were weighed and oven dried separately to a constant weight at 80±5$^0$C. The average leaf biomass was then arrived at by multiplying the average biomass of the leaves per branch with the number of branches in a single tree and the number of trees in a plot (Koul and Panwar, 2008).

### Tree biomass (Above ground)

The total tree biomass (above ground) was the sum of stem, branch and leaf biomass.

**Root biomass**

The root biomass was determined as per the procedure given by (Dury *et al*., 2002). The aboveground biomass was multiplied by a default ratio of 0.24 for softwood species for estimating root biomass.

**Biomass carbon stock**

Carbon percentage was estimated by the ash content method described by Negi *et al.* (2003). In this method oven dried plant components (bark, leaves, stem wood and root) were burnt in a muffle furnace at $400^0$C. The ash content left after burning was weighed and carbon content was calculated by using the following equation:

Carbon % = 100 – (ash weight + molecular weight of $O_2$ (53.3) in $C_6H_{12}O_6$

The carbon (%) was then multiplied with the biomass to get biomass carbon stock.

Carbon stock = Biomass × carbon (%)

**Carbon dioxide equivalent ($CO_2e$)**

The carbon dioxide equivalent was calculated as per the following equation:

Carbon dioxide equivalent = Carbon stock × 3.66

## STATISTICAL ANALYSIS

The data was statistically analyzed for the computation of standard error (Gomez and Gomez, 1989).

## RESULTS AND DISCUSSION

**Growth characteristics of *Cedrus deodara***

The data pertaining to the growth characteristics of *Cedrus deodara* is presented in (Table 1). Among the different diameter classes, the DBH, height, basal area and volume showed an increasing trend with the increase in diameter class and the maximum DBH (34.12 cm/tree) was recorded in diameter class 30-40cm during 2010 and minimum (15.95 cm/tree) DBH was observed in diameter class 10-20cm during 2009. Similarly, Negi (1997) has reported that DBH increases with the increase in diameter class by virtue of secondary or radial growth which is responsible for the increase in diameter of the tree. The maximum height (20.42m/tree) was registered in diameter class 30-40cm during 2010 and minimum (10.31m/tree) was recorded under diameter class 10-20cm during the year 2009. Enhancement of primary or apical growth in the buds of a tree increases significantly the height with the increase in diameter class (Negi, 1997). The basal area was found to be maximum ($0.091m^2$/tree) in diameter class 30-40 cm during 2010 and minimum ($0.020m^2$/tree) in diameter class 10-20cm during 2009. The increase in basal area with the increase in diameter class is due to increase in diameter which proportionally increases the basal area (Singh and Gupta, 2008). Consequently the stem volume was recorded maximum ($0.596m^3$/tree) under higher diameter class 30-40cm during 2010 and minimum ($0.072m^3$/tree) under lower diameter class 10-20cm during 2009. The increase in stem volume with the increase in DBH and height is attributed to natural and proportionate growth of the trees (Rawat and Kumar, 1989). Singh and Gupta (2008) while studying growth and standing volume estimation of *Cedrus deodara* stands in Himachal Pradesh and reported that the growth parameters like DBH, height, basal area and volume increases with the increase in diameter class. Further current findings are in close conformity with the results of Tewari (1998), Dogra and Sharma (2003) and Roy *et al*. (2006).

**Biomass production of *Cedrus deodara***

The results on above and below ground biomass of *Cedrus deodara* (Table 2) suggests that average dry stem biomass (kg/tree) increased with a corresponding increase in DBH class and it was recorded maximum (226.67kg/tree) in diameter class 30-40 cm during 2010 and minimum (27.60kg/tree) in diameter class 10-20 cm during 2009. The present findings are well in accordance with the observations made by Singh and Puri (1990), Koul and Panwar (2008), Yadava (2010a) and Heryati *et al.* (2011). They reported that biomass production per tree increased with an increase in diameter of trees and biomass allocation is more towards the stem. The branch biomass also showed a steady increase with the increase in diameter of trees and it was recorded maximum (64.14kg/tree) under diameter class 30-40cm during 2010 and minimum (7.88kg/tree) under diameter class 10-20 cm during 2009. The branch biomass depends on the average number of branches on the trees and also the branch biomass increased with an increase in diameter class of trees. The findings are in conformity with that of Tandon *et al.* (1988), Singh and Lodhiyal (2009) and Uma *et al*. (2011). They reported that with the increase in diameter class, the number of branches increases which in turn increases the branch biomass. The needle biomass increased from lower diameter class (10-20cm) to higher diameter class (30-40cm). The reason is due to more number of branches in higher diameter class. Also the needle biomass depend upon the size of the branches and structure of large and small branch sizes in the canopy (Heriansyah *et al*., 2007). The present findings are in line with the observations made by Brenes and Montagnini (2006) and Fonseca *et al*. (2012). The total aboveground biomass was recorded maximum (309kg/tree) in diameter class 30-40cm during 2010 and minimum (37.06kg/tree) in diameter class10-20cm during 2009. A study conducted by Rawat and Tandon (1993) on biomass production in young Chir pine (*Pinus roxburghii*) plantations,16 years old in Himachal Pradesh under different spacing and reported that the total aboveground biomass on dry weight basis was recorded maximum (158.18kg/tree) in higher diameter class and minimum (15.10kg/tree) in lower diameter class. But our values are higher as reported earlier for other conifers because the biomass production

of tree species varies considerably from place to place according to climatic and edaphic factors even for the same species. Another study similar results have also been reported by Swamy and Puri (2005), Singh and Lodhiyal (2009) and Yadava (2010b). The root biomass showed an increasing trend with an increase in diameter class and it was recorded maximum (77.25kg/tree) in diameter class 30-40cm during 2010 and minimum (8.88kg/tree) in diameter class 10-20cm during 2009. Hase and Foeister (1983) observed that trees produce a larger root system that needed for the uptake of soil resources, thus resulting in higher values in higher diameter class. A current result corroborates with the findings of several other workers (Shanmughavel and Ramarathinam, 1993; Yadava, 2010a) who reported that higher the diameter class, more will be the root biomass. The biomass productivity of *Cedrus deodara* trees (19 years old) was observed maximum (9.15 t $ha^{-1}$ $yr^{-1}$) in higher diameter class 30-40cm and minimum (3.26 t $ha^{-1}$ $yr^{-1}$) in lower diameter class 10-20cm. Since the *Cedrus deodara* trees are in juvenile phase, their growth is accelerating exponentially. Rana and Singh (1990) estimated the biomass productivity for central Himalayan Chir pine forest (20 years age) under different diameter classes in the west Almora Division and reported that the biomass productivity increased from lower diameter class to higher diameter class (4.12 to 11.9 t $ha^{-1}$ $yr^{-1}$). Since biomass productivity varies from species to species and also on the age, climatic and edaphic factors. Further our findings are well in accordance with the findings of Brenes and Montagnini (2006) and Heryati *et al*. (2011).

**Production of carbon stock of *Cedrus deodara***

It is evinced from the data in (Table 3) that stem carbon shows an increasing trend with the increase in diameter class and was maximum (105.15 kg/tree) under diameter class 30-40cm during 2010 and minimum (12.80kg/tree) under diameter class 10-20cm during 2009. These values also correspond perfectly to the findings of Kumar *et al.* (2009),Yadava (2010a) and Juwarkar *et al.* (2011) who reported that trees during their initial stages of growth i.e. when their DBH is lower will thus sequester less carbon but gradually as it increases in DBH would accumulate more carbon. Hence, it can be concluded that carbon stock is more in higher diameter class as compared to lower diameter class. Moreover, Ogawa *et al.* (2009) has reported that the component which constitutes a maximum portion of biomass will store the maximum amount of carbon. Since the stem is contributing more biomass as compared to other components hence is storing more carbon in its biomass. The branch carbon is recorded maximum (29.53kg/tree) under diameter class 30-40cm during 2010 and minimum (3.62kg/tree) under diameter class 10-20cm during 2009. The branch carbon depends on the average number of branches on the trees and also it increases with the increase in diameter class. These findings are in conformity with that of Koul and Panwar (2008), Yadava (2010b) and Uma *et al.* (2011). The carbon stock of *Cedrus deodara* needles increased from diameter class 10-20cm to diameter class 30-40cm. The increase in needle carbon stock from lower diameter class to higher diameter class could be due to a more number of branches in higher diameter class and hence more needles and subsequently more carbon stock. The present findings corroborate with the observations made by Losi *et al.* (2003), Singh and Lodhiyal (2009) and Juwarkar *et al.* (2011). The root carbon stock shows an increasing trend with the increase in diameter class and was recorded maximum (35.66kg/tree) under diameter class 30-40cm during 2010 and minimum (4.09kg/tree) under diameter class 10-20cm during 2009. The present findings are well in accordance with the observations made by Jana *et al.* (2009), Yadava (2010a) and Fonseca *et al.* (2012) who reported that root carbon stock is more in higher diameter class as compared to lower diameter class. Finally the total carbon stock was recorded maximum (178.12kg/tree or 89.06 t $ha^{-1}$) under higher diameter class 30-40cm of *Cedrus deodara* during 2010 and minimum (21.18 kg/tree or 27.53 t $ha^{-1}$) under lower diameter class 10-20cm during 2009. Similar results have also been reported by Albrecht and Kandji (2003), Yadava (2010b) and Fonseca *et al.* (2012). The carbon productivity of *Cedrus deodara* was recorded maximum (4.22 t $ha^{-1}$ $yr^{-1}$) under diameter class 30-40cm and minimum (1.50 t $ha^{-1}$ $yr^{-1}$) under diameter class 10-20cm. The present findings are well in accordance with the findings of Brenes and Montagnini (2006), Jana *et al*. (2009) and Yadava (2010a).

**Carbon dioxide mitigation potential of different components of *Cedrus deodara***

The carbon dioxide mitigation ($CO_2$ equivalent) potential of different components of *Cedrus deodara* has been presented in (Table 4). The data reveals that stem $CO_2$ equivalent shows an increasing trend with the increasing diameter class and was recorded maximum (384.84 kg/tree) under diameter class 30-40cm during 2010 and minimum (46.83 kg/tree) under diameter class 10-20cm during 2009.$CO_2$ mitigation by trees is directly related to biomass production of the different plant components. The higher mitigation potential of stem in higher diameter class can be attributed to more biomass (Yadava, 2010a). Similar results were reported earlier by many other workers (Wang and Fenz,1995 and Kursten, 2000). The branch $CO_2$ equivalent was recorded maximum (108.07kg/tree) in diameter class 30-40 cm during 2010 and minimum (12.91kg/tree) under diameter class 10-20cm during 2009. In a recent study Yadava (2010b) has reported that $CO_2$ mitigation potential is more in higher diameter class as compared to lower diameter class because of more biomass in higher diameter class. The results are in conformity with the findings of Lal and Singh (2000) and Albrecht and Kandji (2003). The leaf $CO_2$ equivalent was registered maximum (28.47kg/tree)

Table 1. Growth parameters of *Cedrus deodara* trees under different diameter classes.

| Diameter class (cm) | DBH (cm) | | | Height (m) | | | Basal area ($m^2$/tree) | | | Stem volume ($m^3$/tree) | | |
|---|---|---|---|---|---|---|---|---|---|---|---|---|
| | 2009 | 2010 | Increment | 2009 | 2010 | Increment | 2009 | 2010 | Increment | 2009 | 2010 | Increment |
| 10-20 | 15.95 (±0.73) | 16.56 (±0.80) | 0.61 (±0.07) | 10.31 (±0.30) | 10.84 (±0.34) | 0.53 (±0.04) | 0.020 (±0.001) | 0.022 (±0.002) | 0.002 (±0.001) | 0.072 (±0.007) | 0.082 (±0.010) | 0.010 (±0.008) |
| 20-30 | 21.75 (±0.46) | 22.70 (±0.64) | 0.95 (±0.18) | 13.85 (±0.45) | 14.02 (±0.48) | 0.17 (±0.02) | 0.037 (±0.001) | 0.040 (±0.002) | 0.003 (±0.001) | 0.167 (±0.010) | 0.213 (±0.016) | 0.046 (±0.013) |
| 30-40 | 33.30 (±0.71) | 34.12 (±0.92) | 0.82 (±0.21) | 19.94 (±1.30) | 20.42 (±1.37) | 0.48 (±0.07) | 0.087 (±0.003) | 0.091 (±0.005) | 0.004 (±0.002) | 0.510 (±0.050) | 0.596 (±0.065) | 0.086 (±0.027) |

Figures in parenthesis are standard error of mean

Table 2. Production of above and below ground biomass of *Cedrus deodara* trees under different diameter classes.

| Diameter class (cm) | Stem biomass (kg/tree) | | | Branch biomass (kg/tree) | | | Needle biomass (kg/tree) | | | Total above ground biomass (kg/tree) | | |
|---|---|---|---|---|---|---|---|---|---|---|---|---|
| | 2009 | 2010 | Increment | 2009 | 2010 | Increment | 2009 | 2010 | Increment | 2009 | 2010 | Increment |
| 10-20 | 27.60 (±2.72) | 31.16 (±3.88) | 3.55 (±1.16) | 7.88 (±0.77) | 8.89 (±1.10) | 1.01 (±0.33) | 1.57 (±0.15) | 1.77 (±0.22) | 0.20 (±0.07) | 37.06 (±3.65) | 41.82 (±5.21) | 4.76 (±0.31) |
| 20-30 | 63.73 (±8.26) | 81.20 (±12.71) | 17.47 (±4.45) | 18.20 (±2.01) | 23.19 (±2.37) | 4.99 (±0.36) | 3.63 (±0.29) | 4.63 (±0.36) | 1.0 (±0.12) | 85.56 (±11.04) | 109.03 (±14.92) | 23.47 (±3.88) |
| 30-40 | 193.91 (±18.16) | 226.67 (±24.77) | 32.76 (±6.61) | 55.41 (±6.93) | 64.14 (±8.31) | 8.73 (±1.38) | 15.17 (±1.83) | 18.19 (±1.99) | 3.02 (±0.54) | 264.49 (±26.72) | 309.0 (±33.26) | 44.51 (±6.54) |

| Diameter class (cm) | Root biomass (kg/tree) | | | Total biomass (kg/tree) | | | Total biomass (t $ha^{-1}$) | | Biomass productivity (t $ha^{-1}$ $yr^{-1}$) |
|---|---|---|---|---|---|---|---|---|---|
| | 2009 | 2010 | Increment | 2009 | 2010 | Increment | 2009 | 2010 | |
| 10-20 | 8.88 (±0.87) | 10.03 (±1.25) | 1.15 (±0.38) | 45.95 (±5.83) | 51.85 (±6.46) | 5.90 (±0.81) | 59.73 (±6.91) | 67.40 (± 7.57) | 3.26 (±0.17) |
| 20-30 | 20.53 (±2.21) | 26.16 (±2.61) | 5.63 (±0.40) | 106.09 (±14.13) | 135.2 (±16.39) | 29.11 (±2.87) | 63.65 (±7.02) | 81.12 (±8.21) | 3.71 (±0.36) |
| 30-40 | 63.48 (±6.22) | 77.25 (±7.98) | 13.77 (±1.76) | 327.97 (±35.02) | 386.25 (±41.24) | 58.28 (±7.02) | 163.98 (±18.04) | 193.12 (±17.87) | 9.15 (±0.48) |

Figures in parenthesis are standard error of mean

Table 3. Production of above and below ground carbon stock of *Cedrus deodara* trees under different diameter classes.

| Diameter class (cm) | Stem carbon (kg/tree) | | | Branch carbon (kg/tree) | | | Needle carbon (kg/tree) | | |
|---|---|---|---|---|---|---|---|---|---|
| | 2009 | 2010 | Increment | 2009 | 2010 | Increment | 2009 | 2010 | Increment |
| 10-20 | 12.80 (±1.26) | 14.45 (±1.80) | 1.65 (±0.54) | 3.62 (±0.35) | 4.09 (±0.51) | 0.47 (±0.11) | 0.67 (±0.06) | 0.75 (±0.09) | 0.08 (±0.02) |
| 20-30 | 29.56 (±2.91) | 37.66 (±3.28) | 8.10 (±1.19) | 8.38 (±0.84) | 10.67 (±0.93) | 2.29 (±0.87) | 1.55 (±0.09) | 1.98 (±0.15) | 0.43 (±0.09) |
| 30-40 | 89.96 (±8.89) | 105.15 (±11.49) | 15.19 (±2.07) | 25.51 (±2.52) | 29.53 (±2.89) | 4.02 (±1.10) | 6.49 (±0.61) | 7.78 (±0.73) | 1.29 (±0.47) |

| Diameter class (cm) | Root carbon (kg/tree) | | | Total carbon (kg/tree) | | | Total carbon (t $ha^{-1}$) | | Carbon productivity (t $ha^{-1}$ $yr^{-1}$) |
|---|---|---|---|---|---|---|---|---|---|
| | 2009 | 2010 | Increment | 2009 | 2010 | Increment | 2009 | 2010 | |
| 10-20 | 4.09 (±0.40) | 4.63 (±0.57) | 0.54 (±0.13) | 21.18 (±2.09) | 23.93 (±2.98) | 2.75 (±0.15) | 27.53 (±2.01) | 31.10 (±3.21) | 1.50 (±0.07) |
| 20-30 | 9.47 (±0.89) | 12.07 (±1.01) | 2.60 (±0.91) | 48.96 (±4.62) | 62.40 (±5.23) | 13.44 (±1.12) | 29.37 (±2.74) | 37.44 (±3.88) | 1.71 (±0.19) |
| 30-40 | 29.30 (±2.85) | 35.66 (±3.68) | 6.36 (±1.04) | 151.27 (±15.26) | 178.12 (±17.31) | 26.85 (±1.98) | 75.63 (±7.41) | 89.06 (±8.57) | 4.22 (±0.23) |

Figures in parenthesis are standard error of mean

Table 4. Carbon dioxide mitigation potential of different components of *Cedrus deodara* trees under different diameter classes

| Diameter class (cm) | Stem $CO_2e$ (kg/tree) | | Increment | Branch $CO_2e$ (kg/tree) | | Increment | Needle $CO_2e$ (kg/tree) | | Increment |
|---|---|---|---|---|---|---|---|---|---|
| | 2009 | 2010 | | 2009 | 2010 | | 2009 | 2010 | |
| 10-20 | 46.83 (±4.62) | 52.88 (±6.59) | 6.05 (±1.97) | 12.91 (±1.31) | 14.96 (±1.86) | 2.05 (±0.55) | 2.44 (±0.24) | 2.74 (±0.34) | 0.30 (±0.06) |
| 20-30 | 108.18 (±14.31) | 137.83 (±16.69) | 29.65 (±2.38) | 30.66 (±3.82) | 39.05 (±3.96) | 8.39 (±0.74) | 5.67 (±0.34) | 7.24 (±0.56) | 1.57 (±0.46) |
| 30-40 | 329.26 (±38.71) | 384.84 (±46.98) | 55.58 (±8.27) | 93.36 (±13.20) | 108.07 (±14.26) | 14.71 (±1.06) | 23.76 (±2.72) | 28.47 (±3.68) | 4.71 (±0.31) |

| Diameter class (cm) | Root $CO_2e$ (kg/tree) | | Increment | Total $CO_2e$ (kg/tree) | | Increment | Total $CO_2e$ (t $ha^{-1}$) |
|---|---|---|---|---|---|---|---|
| | 2009 | 2010 | | 2009 | 2010 | | |
| 10-20 | 14.99 (±1.48) | 16.94 (±2.11) | 1.95 (±0.59) | 73.92 (±8.51) | 87.52 (±10.93) | 13.60 (±1.46) | 104.93 (±13.36) |
| 20-30 | 34.66 (±4.01) | 44.17 (±4.51) | 9.51 (±2.14) | 179.18 (±21.87) | 228.29 (±28.56) | 49.11 (±4.69) | 122.23 (±14.15) |
| 30-40 | 107.24 (±14.18) | 130.51 (±15.34) | 23.27 (±6.08) | 553.63 (±55.88) | 651.91 (±62.29) | 98.28 (±13.61) | 301.38 (±36.43) |

Figures in parenthesis are standard error of mean, ($CO_2e$= Carbon dioxide equivalent)

under diameter class 30-40cm during 2010 and minimum (2.44kg/tree) under diameter class 10-20cm during 2009. It also depends upon the biomass production because $CO_2$ mitigation is more in the trees having higher diameter class, so leaf $CO_2$ mitigation potential is more in higher diameter class as compared to lower diameter class (Lal and Singh, 2000). Our results are also well in accordance with the findings of Yadava (2011) and Fonseca (2012). The total $CO_2$ equivalent was registered maximum (301.38 t $ha^{-1}$) under diameter class 30-40cm and minimum (109.93 t $ha^{-1}$) under diameter class 10-20cm. Higher $CO_2$ mitigation potential in higher diameter class can be attributed to more biomass production (Yadava, 2010b). Our results are well supported by many other workers ( Lal and Singh, 2000; Uma *et al*., 2011).

## CONCLUSION

Growth parameters like DBH, height, basal area and volume of *Cedrus deodara* increased with the increase in diameter class and maximum volume was recorded under diameter class 30-40cm. Total biomass was noticed maximum under the higher diameter class 30-40cm but in case of individual contribution of biomass allocation of different components of *Cedrus deodara*, maximum biomass was contributed by stem followed by root, branch and needle respectively. The total carbon stock was recorded maximum in higher diameter class 30-40cm. Among the different components, stem recorded the maximum carbon stock followed by root, branch and needle respectively. The Carbon dioxide mitigation potential was registered maximum under the higher diameter class 30-40cm. But among the different components of *Cedrus deodara*, stem recorded the maximum mitigation potential followed by root, branch and needle respectively. *Cedrus deodara* being a slow growing conifer will provide a long term carbon fixation capacity as compared to fast growing species which provide revenues in the short term. Therefore the use of such trees with higher carbon sequestration capacity could improve carbon stocks thus mitigate the carbon dioxide in the atmosphere.

## REFERENCES

Albrecht, A. and Kandji, ST. 2003. Carbon sequestration in tropical agroforestry systems. Agriculture Ecosystems and Environment. 99:15-27.

Anonymous, 2010. Degraded and wastelands of India, Status and Spatial Distribution. ICAR and NASS, New Delhi, India.

Bitlerlich,W. 1984. The Relaskop Idea Slough : Common Wealth Agricultural Bureause, Farnham Royal, England.

Brenes, AR. and Montagnini, F. 2006. Growth, productivity, aboveground biomass and carbon sequestration of pure and native tree plantations in the Caribbean lowlands of Costa Rica. Forest Ecology and Management. 232:168-178.

Chidumaya, EN. 1990. Above ground woody biomass structure and productivity in a Ambezian woodland. Forest Ecology and Management. 36:33-46.

Dogra, AS. and Sharma, SC. 2003. Volume prediction equations for *Eucalyptus* hybrid in Punjab. Indian Forester. 129:1451-1460.

Dury, SJ., Polglase, PJ. and Vercose, T. 2002. Green house resource kit for private forest growers. Common Wealth Department of Agriculture and Forestry, Canberra, Australia. IV:95.

Fonseca, W., Alice, FE. and Benayas, JMR. 2012. Carbon accumulation and aboveground and belowground biomass and soil of different age native forest plantations in the humid tropical low lands of Costa Rica. New Forests. 43:197-211.

Gomez, KA. and Gomez, AA. 1989. Statistical procedure for agriculture research (2nd edi.). John wiley, New York, USA. pp680.

Hase, H. and Foeister, H. 1983. Impact of plantation forestry with teak (*Tectona grandis*) on the nutrient status of young alluvial soil of West Venezuela. Forest Ecology and Management. 6:33-57.

Hervey, LDD. 2000. Global warming- the hard science. Singapore: Pearson Education. pp336.

Heriansyah, IK., Miyakuni, K., Kato, T., Kiyono, Y. and Kanazawa, Y. 2007. Growth characteristics and biomass accumulation of *Acacia mangium* under different management practices in Indonesia. Journal of Tropical Forest Science. 19:226-235.

Heryati, Y., Belawan, D., Abdu, A. and Mahat, MN. 2011. Growth performance and biomass accumulation of a *Khaya ivorensis* plantation in three soil series of ultisols. American Journal of Agricultural and Biological Sciences. 6:33-44.

Jana, BK., Biswas, S., Majumder, M., Roy, PK. and Mazumdar, A. 2009. Carbon sequestration rate and aboveground biomass carbon potential of four young species. Journal of Ecology and Natural Environment. 1:15-24.

Juwarkar, AA.,Varghese, AO., Singh, SK., Aher, VV. and Thawale, PR. 2011. Carbon sequestration potential in aboveground biomass of natural reserve forest of central India. International Journal of Agriculture Research and Review. 1:80-86.

Kimble, JM., Heath, LS., Birdsey, RA. and Lal, R. 2002. The potential of U.S forest soils to sequester carbon and mitigate the green house effect. Boca Raton, Lewis

Publishers.

Koul, DN and Panwar, P. 2008. Prioritizing land management option for carbon sequestration potential. Current Science. 95:658-663.

Kumar, GP., Ashutosh, A., Gupta, MS. and Singh, SB. 2009. Carbon sequestration with special reference to agroforestry in cold deserts of Ladakh. Current Science. 97:1063-1068.

Kursten, E. 2000. Fuelwood production in agroforestry system for sustainable landuse and carbon dioxide mitigation. Ecology and Environment. 16:569-572.

Lal, M. and Singh, R. 2000. Carbon sequestration potential of Indian forests. Environmental Monitoring and Assessment. 60:315-327.

Losi, J., Siccama, T., Condit, R. and Morales, J. 2003. Analysis of alternative methods for estimating carbon stock in young plantations. Forest Ecology and Management. 184:355-368.

Luna, RK. 2005. Plantation trees. International book distributors, Dehradun, India.

Negi, JDS., Manhas, RK. and Chauhan, PS. 2003. Carbon allocation in different components of some tree species of India: A new approach for carbon estimation. Current Science. 85:1528-1531.

Negi, SS. 1997. Wood Science and Technology. International book distributors, Dehradun, India. pp31.

Ogawa, H., Yoda, K., Ogino, K. and Kira, T. 2009. Comparative ecological studies on three main type of forest vegetation in Thailand. Nature and life in Southeast Asia. 4:49-80.

Pressler, M. 1865. Das Gesetzder Stambildung Leipzig. pp153.

Rana, BS. and Singh, RP. 1990. Plant biomass and productivity estimates for central Himalayan mixed Banj oak (*Quercus leucotrichophora* A.Camus)- Chir pine (*Pinus roxburghii* Sarg.) forest. Indian Forester. 116:220-226.

Rawat, JK and Tandon, VN. 1993. Biomass production and mineral cycling in young chir pine plantations in Himachal Pradesh. Indian Forester. 119:977-985.

Rawat, VRS and Kumar, P. 1989. Ecological studies of some *Cedrus deodara* (Deodar) forests in western Himalayas- India. Indian Journal of Forestry. 12:145-150.

Roy, MM., Pathak, PS., Rai, AK. and Kushwaha, D. 2006. Tree growth and biomass production in *Melia azedarach* on farm boundaries in a semi-arid region. Indian Forester. 132(1):105-110.

Shanmughavel, P. and Ramarathinam, DR. 1993. Biomass and primary productivity of *Tephrosia* in semi-arid vegetation at Perungudi, district Madurai. Indian Forester. 119:326-333.

Singh, A. and Gupta, NK. 2008. Growth and standing volume estimation of *Cedrus deodara* (Roxb.) Loud stands under the present system of management in Himachal Himalayas-a case study. Indian Forester. 13:458-468.

Singh, P. and Lodhiyal, LS. 2009. Biomass and carbon allocation in 8-year old poplar (*Populus deltoides*) plantation in Tarai agroforestry systems of central Himalaya, India. New York Science Journal. 2:49-53.

Singh, V. and Puri, S. 1990. Aboveground biomass and net primary productivity of nine years old poplar plantation in semi-arid region of Haryana. Journal of Tree Science. 9(1):27-32.

Smith, DM. 1954. Maximum moisture content for determining specific gravity of small wood samples. Forest product laboratory. USDA Forest Service Report. pp2014.

Swamy, SL. and Puri, S. 2005. Biomass production and carbon sequestration of *Gmelina arborea* in plantation and agroforestry system in India. Agroforestry Systems. 64:181-195.

Tandon, VN., Pande, MC., Rai, L. and Rawat, HS. 1988. Biomass production and its distribution by *Acacia nilotica* plantations at five different ages in Haryana. Indian Forester. 114:770-775.

Tewari, A. 1998. Tree layer analysis of three major forming species of Kumaun central Himalaya. Journal of Eco-Biology. 11:23-28.

Uma, M., Rajendran, K. and Kuru, S. 2011. Biomass and carbon sequestration potential of *Casuarina equisetifolia* in farm forestry plantation of east coast in southern Tamil Nadu, India. Plant Archives. 119:957-963.

Wang, X. and Fenz, Z. 1995. Atmospheric carbon sequestration through agroforestry in China. Energy. 20:117-121.

Yadava, AK. 2010[a]. Biomass production and carbon sequestration in different agroforestry systems in Tarai region of central Himalaya. Indian Forester.136:234-244.

Yadava, AK. 2010[b]. Carbon sequestration: underexploited environmental benefits of Tarai agroforestry systems. Report and Opinion. 2:35-41.

Yadava, AK. 2011. Potential of agroforestry systems in carbon sequestration for mitigating climate changes in Tarai region of central Himalaya. Nature and Science. 9:72-80.

Received: Sept 30, 2013; Revised: Oct 26, 2013;
Accepted: Oct 28, 2013

SENRA Academic Publishers, British Columbia
Vol. 8, No. 1, pp. 2685-2690, February 2014
Online ISSN: 1920-3853; Print ISSN: 1715-9997

Canadian Journal of pure&applied sciences

# INFECTION DYNAMICS OF *SCHISTOCEPHALUS SOLIDUS* (MULLER, 1776), IN THREE-SPINED STICKLEBACK, *GASTEROSTEUS ACULEATUS* L. IN AIRTHREY LOCH, SCOTLAND

Zafar Iqbal
Department of Zoology, University of the Punjab
New Campus, Lahore 54590, Pakistan

**ABSTRACT**

Infection of *Schistocephalus solidus* in three-spined stickleback, *Gasterosteus aculeatus* was investigated for over a two year period from Airthrey Loch, Scotland. Altogether 1301 fishes were sampled. A total of 1327 *S. solidus* plerocercoid worms were extracted from the visceral cavity of 385 fish. The prevalence was 29.55%, mean intensity (3.44) and abundance (1.01). Monthly prevalence and abundance showed significant difference in two years. Infection in female (14.68%) was higher than male fish (5.99%). The highest infection was recorded in autumn and spring. There are two waves of infection, the first wave operates from July to October and second starts in February and ends in June. The growth of *S. Solidus* in the fish is influenced by a rise in water temperature in summer. In natural environment, probably different biotic and abiotic factors may affect the transmission of *S. solidus* and thus may affect the prevalence and intensity of infection. Such factors could influence the survival of coracidia, or abundance of suitable copepod at a given time. The growth of plerocercoid in the fish host may be influenced by factors both internal and external to the fish host. It is concluded that *S. solidus* was moderately established in second intermediate host *G. aculeatus* in Airthrey Loch

**Keywords:** *Schistocephalus solidus, Gasterosteus aculeatus*, infection dynamics, freshwater loch,

## INTRODUCTION

*Schistocephalus solidus* is a pseudophyllidean tapeworm with three host life cycle. The free swimming coricidea are ingested by freshwater copepod, the first intermediate host. In the copepod, coricidia develops into the infective stage in almost 2 weeks. Then it is ready to be transmitted to second intermediate, the fish *G. aculeatus.* In fish worm grow to large size and mass of plerocercoid may account for sometimes equaling or exceeding host mass (Hopkins and Symth, 1951, Clark, 1954, Arme and Owen, 1967). Nearly 40 species of piscivorous birds (Smyth, 1962), such as gulls and herns and other vertebrates like Baltic ringed seal *Phoca hispida botnica* (Gmelin) are intended definitive host (Chubb *et al*., 1995). In the final host, worm becomes reproductively mature within 2-3 days and in the next 7 days all eggs are produced and the worm dies. The plerocercoids of *S. solidus* are commonly found in the visceral cavity of *G. aculeatus*, in Britain and throughout its geographical range (Barber, 2007).

Heavy infection results in the death or predation of the fish (Pennnycuick, 1971b) and change in the behavior of the host (Holmes and Bethel, 1972). The seasonal variation and occurrence of *S. solidus* in *G. aculeatus* as well its effects on the behavior, pathology and growth of the host have been reported by many researchers (Arme and Owen, 1967; Chappell, 1969a,b; Pennycuick, 1971a; Curtis, 1981). The influence of parasitism on stickleback physiology has been investigated by Pascoe and Cram (1977), Pascoe and Woodworth (1980). Infection of *G. aculeatus* with *S. solidus* (Seed, 1984) and Scanning electron microscopy (SEM) of this parasite from different geographical location has been described by Chubb *et al*. (1995). A significant difference in the infection of three-spined stickleback with *S. solidus* has been reported in two lakes in Alaska (Heins *et al*., 2002). Another study, Dorucu *et al*. (2007) found a significant difference in the relationship between plerocercoid mass and lifetime eggs output of *S. solidus* recovered from singly and multiple infected *G. aculeatus*. *Schistocephalus solidus* has effects on stickleback reproduction (Macnab *et al*., 2009). Epizootic of *S. solidus* appear to depend on particular and at times on, rare set of circumstances (Heins *et al*., 2010). Mortality of the host during winter is a major factor which reduces transmission and influences the population dynamics of *S. solidus* (Heins *et al*., 2011). *Schistocephalus solidus* has been reported for the first time from body cavity of anadromous three-spined stickleback inhabiting Mud Lake, Alaska (Confer *et al*., 2012). While carrying out PhD project on biology of *Proteocephalus filicollis* from *G. aculeatus* (Iqbal, 1998; Iqbal and Wootten, 2013), some interesting observations on infection dynamics of *S. solidus* in *G. aculeatus* from Airthrey Loch, Scotland were obtained and these are compared with earlier studies from Britain.

*Corresponding author email: dr.zafariqbal.pu@gmail.com

Table 1. Composition of various length classes of *Gasteosteus aculeatus* from Airthrey Loch, Scotland.

| Month | LC-I | LC-II | LC-III | LC-IV | LC-V | Month | LC-1 | LC-II | LC-III | LC-IV | LC-V |
|---|---|---|---|---|---|---|---|---|---|---|---|
| A93 | - | 20.96 | 30.64 | 46.77 | 01.61 | - | - | - | - | - | - |
| M | - | 04.87 | 41.46 | 60.97 | 02.43 | - | - | - | - | - | - |
| J | 32.50 | 37.50 | 02.50 | 25.00 | 02.50 | - | - | - | - | - | - |
| **J93** | 27.77 | 44.44 | 01.85 | 22.22 | 03.70 | **J94** | 58.33 | 41.66 | - | - | - |
| A | 02.59 | 64.93 | 27.27 | 03.89 | 01.29 | A | 50.00 | 40.00 | 07.50 | - | 02.50 |
| S | 02.35 | 37.64 | 45.88 | 12.94 | 01.17 | S | 18.86 | 50.94 | 24.52 | 05.66 | - |
| O | 01.53 | 26.15 | 56.92 | 15.38 | - | O | - | 50.00 | 50.00 | - | - |
| N | - | 46.00 | 44.0 | 10.00 | - | N | 01.96 | 49.01 | 39.21 | 05.88 | 01.96 |
| D | - | 50.00 | 39.58 | 10.41 | - | D | - | 37.50 | 50.00 | 08.33 | 04.17 |
| **J94** | - | 50.00 | 40.98 | 08.19 | - | **J95** | - | 35.00 | 55.00 | 10.00 | - |
| F | - | 38.23 | 58.88 | 05.88 | - | F | - | 32.14 | 53.37 | 14.28 | - |
| M | - | 47.97 | 47.97 | 03.37 | 01.36 | M | - | 40.62 | 40.62 | 15.62 | 03.12 |
| A | - | 33.33 | 44.44 | 19.04 | 03.16 | A | - | 15.00 | 35.00 | 50.0 | - |
| M | - | 12.96 | 29.62 | 55.55 | 02.50 | M | - | 08.51 | 40.42 | 48.93 | 02.12 |
| J | - | 02.50 | 40.00 | 55.00 | 02.50 | J | 03.63 | 16.36 | 12.72 | 50.99 | 14.30 |

(Values are in %; - indicates zero value)

Table 2. Infection of *S. solidus* in three samples of *G. aculeatus* in relation to sex of the host.

| Sample | Fish Exam. | Infected fish prevalence, MI | Infected fish | | | Female: male |
|---|---|---|---|---|---|---|
| | | | Sex ? | Female | Male | |
| 1 | 147 | 70 (47.61%) 4.81 | 13(18.57%) | 32(45.71%) | 25(35.57%) | 1.28:1 |
| 2 | 704 | 140 (19.88%) 2.87 | 39(27.85%) | 65(46.42%) | 36(25.71%) | 2.03:1 |
| 3 | 450 | 175 (38.88%) 3.52 | 64(36.57%) | 94(53.71%) | 17(9.71%) | 5.52:1 |
| Total | 1301 | 385(29.59%)3.44 | 116(30.12%) | 191(49.61%) | 78(20.23%) | 2.44:1 |

## MATERIALS AND METHODS

The fish, *G. aculeatus* were sampled from Airthrey Loch, University of Stirling, Scotland (Grid Reference 806965) with the help of hand net on a monthly basis (April 1993 to June 1995). The physicochemical and biological features of the Loch are given by Iqbal, (1998), Iqbal and Wootten (2004). The fishes were brought live in loch water to the Parasitology laboratory, Institute of Aquaculture and maintained in 40liter glass aquarium at ambient water temperature. The fishes weighed were and measured and examined within 2-4 hours. The worms were extracted from the visceral cavity of the fish and relaxed in tap water. The fish collected comprised three samples; sample-1 (April-June 1993); sample-II (July 1993 to June 1994); sample –III (July 1994-June 1995). The fishes were divided into five length classes as under; LC-1 (up to 20mm); LC-II (21-30mm); LC-III (31-40mm); LC-IV (41-50mm) and LC-V (51mm<). Prevalence, abundance and mean intensity were followed after Margolis *et al*. (1981). Pearson correlation analysis was applied to verify the significance between the values of prevalence, mean intensity and abundance.

## RESULTS

A total of 1301 *G. aculeatus* were sampled and examined. These fishes are represented by five length classes (Table 1). Altogether 385 fishes were infected with *S. solidus* hence, prevalence was 29.59%. A total of 1327 *S. solidus* plerocercoid worms were extracted (abundance 1.04 and mean intensity 3.44) from infected fish. Infection and mean intensity of *S. solidus* in three samples of *G. aculeatus*, according to the sex of the host is given in table 2. The female fish population was always high, compared to the male population. Similarly, female fish had higher infection compared to male in all samples.

The monthly prevalence of *S. solidus* in the fish fluctuated over the study period. In sample II and III, there was

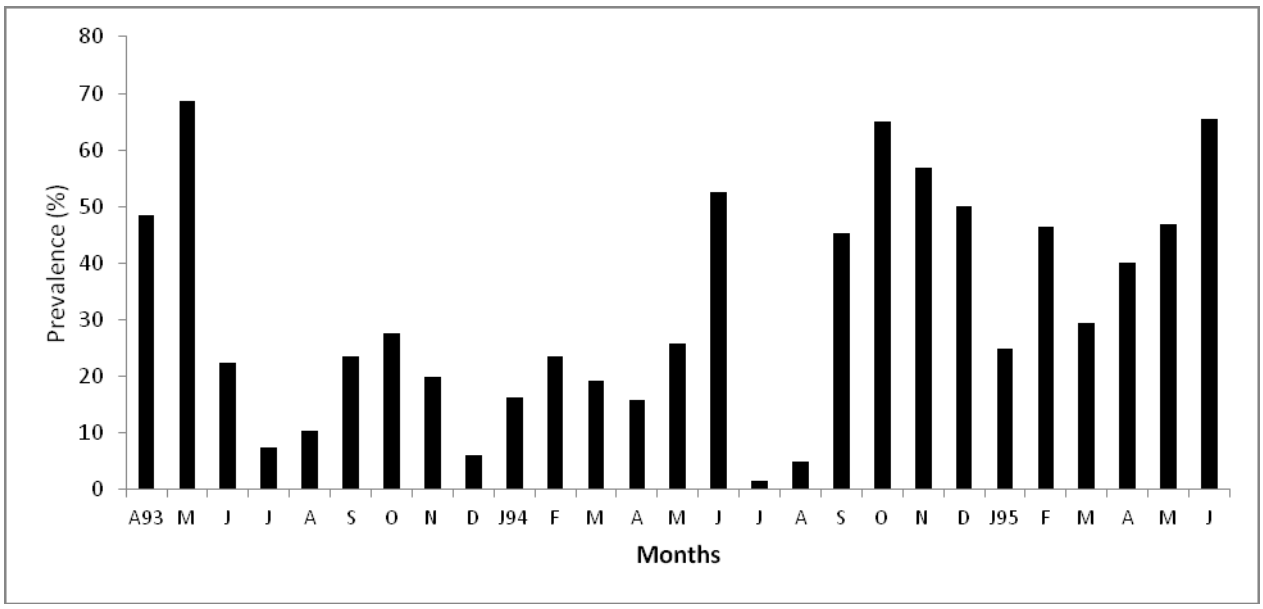


Fig.1A. Prevalence of *S. solidus* in *G. aculeatus* from Airthrey Loch Scotland.

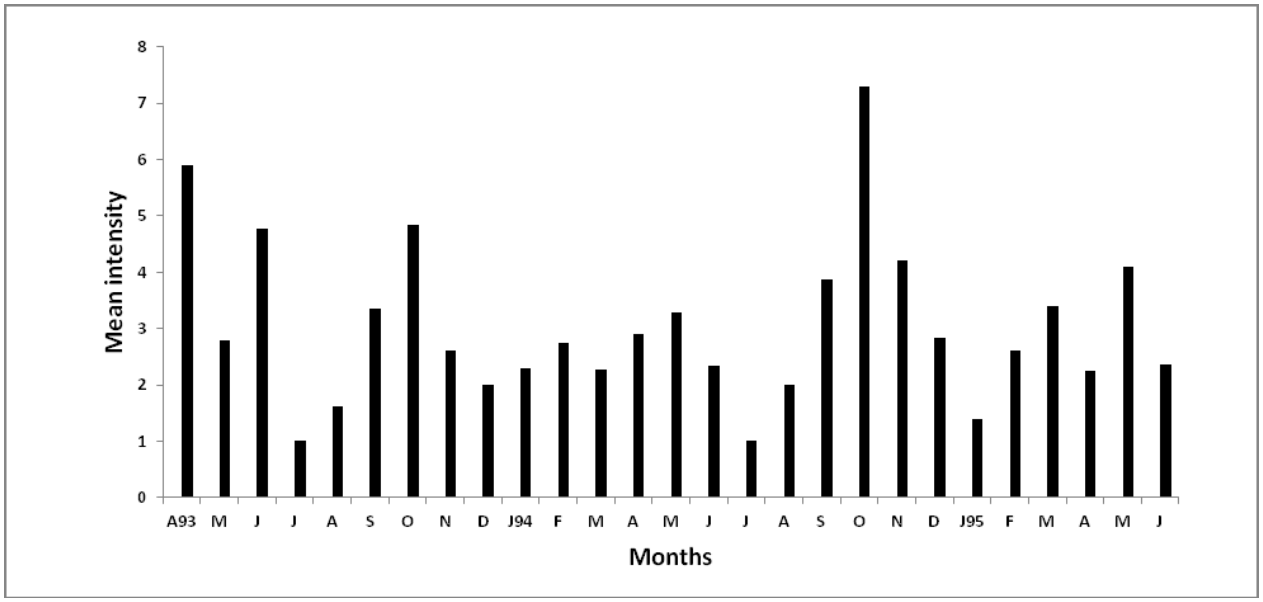


Fig.1B. Mean intensity of *S. solidus* in *G. aculeatus* from Airthrey Loch Scotland.

gradual rise in prevalence from July to October which dropped to the lowest level in December-January and increased gradually through February to May-June with some fluctuation (Fig. 1A). The mean intensity of infection showed rising trend from July to October and then gradually dropping from November to December-January which increased through spring and dropped in June in sample II and III with some fluctuation (Fig.1B). The monthly prevalence and mean intensity was not significantly correlated (P=0.18) in sample II. But was significantly correlated (P=0.02) in sample III.

The prevalence was low in summer followed by a rise in autumn and dropping in winter and high in spring. The mean intensity followed the same pattern of seasonal rise and fall as that of prevalence. Low mean intensity is observed in winter. High mean intensity from late winter to early spring in sample-II and sample-III indicates a second wave of infection. Adult fish showed high infection in the samples I, II and III (April to June). There was no significant correlation between prevalence and mean intensity in adult fish infection cases in three samples (P=0.23). Prevalence in various length classes of fish (Table 3) shows a rising trend from LC-I to LC-V in

Table 3. Prevalence (%) and mean intensity of *S. solidus* in various length classes of *Gasterosteus aculeatus* in Airthrey Loch, Scotland.

| Length Class | Sample-I | | | Sample-II | | | Sample-III | | |
|---|---|---|---|---|---|---|---|---|---|
| | Fish | Prev. | MI | Fish | Prev. | MI | Fish | Prev. | MI |
| LC-I | 13 | 0 | 0 | 20 | 5.0 | 2.0 | 68 | 11.76 | 1.1 |
| LC-II | 30 | 20.0 | 3.3 | 279 | 15.05 | 3.21 | 157 | 38.85 | 3.59 |
| LC-III | 37 | 70.27 | 3.19 | 289 | 22.84 | 2.36 | 130 | 40.79 | 4.96 |
| LC-IV | 64 | 54.68 | 5.62 | 107 | 26.16 | 3.82 | 81 | 54.32 | 2.54 |
| LC-V | 03 | 100 | 2.33 | 9 | 33.33 | 1.0 | 14 | 64.28 | 1.66 |
| Total | 147 | 47.61 | 4.81 | 704 | 19.88 | 2.87 | 450 | 38.88 | 3.52 |

Table 4. *Schistocephalus solidus* infection in different *G. aculeatus* populations in Britain.

| Locality | % population infected | Mean intensity | Max. worm /fish | Authority |
|---|---|---|---|---|
| Hunslet,Yorkshire | 100 | 6.0 | 16 | Hopkins & Smyth (1951) |
| Stourton,Yorkshire | - | | (5)[2] | Clark, (1954) |
| Farnley, Yorkshire<br>1962<br>1963-65 | <br>100<br>36-96 | 46.5 | 138 | Arme & Owen (1967) |
| Baildon, Yorkshire | 27 | 1-1.6 | 4 | Chappell (1969a) |
| Priddy Pool Somerset | 88 | 4.4 | 106 | Pennycuick (1971a) |
| Beaumaris,N.Wales | 79 | 2.9 | 43 | Seed (1984) |
| Stirling, Scotland<br>1993<br>1993-94<br>1994-95 | <br>47.4<br>19.88<br>38.38 | <br>4.81<br>2.87<br>3.52 | <br>66<br>40<br>40 | Present Study |

sample II and sample III. However, this trend was not observed in mean intensity in these length classes. The recruitment continues from July to October as highest number of worms has been recorded in this period.

The mature *G. aculeatus* were observed in April, May and June in three samples. The fish normally mature at the age of one year. But, the fish reach sexual maturity at the age of two years. Healthy fish showed full maturation i.e. ripe ovaries and testes. Whereas, the infected fish at the same time were not mature, either they had suppressed or under developed gonads.

## DISCUSSION

This is another detailed investigation of *S. solidus* infection in *G. aculeatus* from Scotland. The infected female population exceeded the male population in Airthrey Loch. The prevalence of *S. solidus* in *G. aculeatus* was high in sample I and sample III compared to sample II. The earlier studies from Britain (Table 4) reported high prevalence of *S. solidus* in *G. aculeatus* compared to the present study. Mean intensity also followed the same pattern as that of prevalence but showed some fluctuation. In Scotland, infection of *S. solidus* starts in summer and becomes high in autumn which drops to the lowest in winter and gradually rise in summer again. Monthly prevalence and mean intensity in sample II and sample III did not show any significant correlation to abiotic factors (pH, water temperature, conductivity and rain fall) of the Loch, but a significant correlation was observed in prevalence and mean intensity and pH in sample III (P=0.008). The low prevalence and mean intensity in sample II might be due to mortality of larger and heavily infected hosts during winter, as a result of infection stress and long starving winter.

In the Airthrey Loch, three-spined sticklebacks are infected in their first summer. Infection also takes place in fishes of 1 year of age, and multiple infections are common, and this is also reported by Heins *et al.* (1999). Healthy and uninfected fishes live up to 2 or sometime 3 years of age, as observed in the present study. The *S. solidus* may live in the fish host as long as two years until the death of the host and all the growth of the worm occurs during plerocercoid stage in the fish host. The water temperature has been proposed as an explanation for seasonal maturation of *Proteocephalus* sp. in their host (Kennedy, 1977). However, growth is accelerated in spring and summer. There is also fall in the mean intensity of infection during this period. The low mean

intensity of infection may also reduce competition within the parasite infrapopulation at a time when metabolic requirement of individual cestode associated with growth increases.

The eutrophic nature of the Airthrey Loch (Iqbal and Wootten, 2004) may be suggested to increase the large population of infected copepod that may have influenced the high transmission of *S. solidus* in the fish. The high prevalence may be associated with warm late summer and autumn of Year I and Year II (Iqbal and Wootten, 2004) which might have acted indirectly by facilitating the copepod population to multiply. The high water temperature in Year I in Airthrey Loch may have operated by; 1) enhancing the feeding rate of *G. aculeatus*; 2) by facilitating the establishment of worms in the fish; 3) providing high biomass of infected cyclops resulting in higher population of larval worms. The parasite populations fluctuate on year to year basis as reported by Kennedy (1996) and the transmission rate of a parasite may be determined by the size of parasite population (Nie and Kennedy, 1991). The composition and abundance of suitable intermediate host in a locality may contribute to the distribution and infection level of a parasite.

The role of parasites on host reproduction and host death by predation may also be taken into consideration in infection dynamics of *S. solidus* in *G. aculeatus.* The effects of the parasite on the host are most evident when the host reproductive potential is reduced and infection results in mortality of larger host. The larger fish carry bigger parasites which are able to reproduce in the final host (Heins *et al.*, 2002). Our results are in contrast to Heins *et al.* (2010); because in our case low values of metrics for parasite population was in sample II, when the host fish population was high and vice versa in sample III. In nature probably different biotic and abiotic factors may affect the transmission of *S. solidus* at any stage of life cycle and thus could affect the prevalence and intensity of infection. Such factors could influence the survival of coracidia, or abundance of suitable copepod at a given time. Moreover, the growth of plerocercoid in fish host may be influenced by factors both internal and external to the fish host.

## CONCLUSION

It may be concluded that *S. solidus* was moderately established in *G. aculeatus* population in Airthrey Loch as compared to earlier studies in Britain.

## REFERENCES

Arme, C. and Owen, RW. 1967. Infections of the three-spined stickleback, *Gasterosteus aculeatus* L., with the plerocercoid larvae of *Schistocephalus solidus* (Muller, 1776) with special reference to pathological effects. Parasitology. 57:301-314.

Barber, I. 2007. Host-paarasite interaction of the three-spined sticklback. In: Biology of the Three-SpinedSticklback. Eds.Ostlund-Nilsson, S., Mayer, I. and Huntingford, FA. CRC Press. BocaRaton, FL. 271-318.

Chappell, LH. 1969[a]. The Parasites of the three-spined stickleback, *Gasteroseus aculeatus* L. from a Yorkshire pond.1. Seasonal Variation of Parasite Fauna. Journal of Fish Biology. 1:137-152.

Chappell, LH. 1969[b]. The Parasites of the three-spined stickleback, *Gasteroseus aculeatus* L. from a Yorkshire pond.11. Variation of the Parasite Fauna with Sex and Size of the Fish. Journal of Fish Biology. 1:339-347.

Chubb, JC., Valtonen, ET., Mcgeorge, J. and Helle, E. 1995. Characterization of the external features of *Schistocephalus solidus* (Muller, 1776) (Cestoda) from different geographical regions and an assessment of the status of the baltic ringed seal *Phoca hispida botnica* (Gmelin) as a definitive host. Systematic Parasitology. 32:113-123.

Clark, AS. 1954. Studies on the life cycle of pseudophylidean cestode, *Schistocephalus solidus.* Proceedings of oological Society of London. 124B:257-302.

Confer, A., Vu, V., Drevecky, CJ. and Aguirre, WA. 2012. Occurrence of *Schistocephalus solidus* in Anadromous Three spined stickleback. Journal of Parasitology. 98(3):676-678.

Curtis, MA. 1981. Observations on the occurance of *Diplostomum spatheceum* and *Schistocephalus* sp. in nine spined stickleback (*Pungitius pungitius*) from the Belcher Island, Northwest Territories. Canadian Journal of Wildlife Diseases. 17:24-246.

Dorucu, M., Wilson, D. and Barber, I. 2007. Diffference in adult eggs production of *Schistocephalus solidus* (Muller, 1776) in singly-and Multiply-infection Stickleback. Journal of Parasitology. 93:1521-1523. DOI:10.1645/GE-1221.1.

Heins, DC., Singer, SS. and Baker, JA. 1999. Virulence of the cestode *Schistocephalus solidus* and reproduction in infected three spined stickleback, *Gasteerosteus aculeatus*. Canadian Journal of Zoology. 77:1967-1974.

Heins, DC., Baker, JA. and Martin, HC. 2002. The "crowding effect" in cestode *Schistocephalus solidus* density-dependent effects on plerocercoid size and infectivity. Journal of Parasitology. 88:302-307.

Heins, DC., Birden, EL. and Barker, JA. 2010. Host mortality and variability in epizootics of *Schistocephalus solidus* iinfecting the three spined stickleback,

*Gasteerosteus aculeatus*. Parasitology. 94:1-6. DOI:10.1017/S003118201000048X.

Heins, DC., Barker, JA. and Green, DM. 2011. Processes influencing the duration and decline of epizootic in *Schistocephalus solidus.* Journal of Parasitology. 97(3):371-380.

Holmes, JC. and Bethel, WM. 1972. Modification of intermediate host behaviour by parasites. In: Behavioural aspects of parasites transmission. Eds. Canning, EU. and Wright, CA. Academic Press, London. 123-129.

Hopkins, CA. and Symth, JD. 1951. Notes on morphology and life history of *Schistocephalus solidus* (Cestoda: Diphyllobothriidae). Parasitology. 41:281-291.

Iqbal, Z. 1998. Aspects of the biology of the cestode, *Proteocephalus filicollis* (Rudolphi) from *Gasterosteus aculeatus* L. Ph.D. Thesis, Scotland, University of Stilring, Scotland. pp188.

Iqbal, Z. and Wootten, R. 2004. Biological and Physicochemical features of Airthrey Loch. Scotland, UK. Biologia (Pakistan). 50:175-182.

Iqbal, Z. and Wootten, R. 2013. Population Biology of a cestode, *Proteocephalus filicollis* (Rudolphi) from *Gasterosteus aculeatus* L. in Scotland. Canadian Journal of Pure and Applied Sciences. 7(3):2475-2480.

Kennedy, CR. 1977. The Regulations of Fish Parasites Population. In: Regulation of Parasite Population. Ed. Esch, GW. Academic Press, New York. 63-109.

Kennedy, CR. 1996. Establishment, survival and site of selection of the cestode, *Eubothrium crassum* in brown trout *Salmo trutta*. Parasitology. 112:347-355.

Macnab, V., Katsiadaki, I. and Barber, L. 2009. Reproductive potential of *Schistocephalus solidus* - infected male three-spined stickleback *Gasterosteus aculeatus* from two UK Populations. Journal of Fish Biology. 75:2095-2107. DOI:10.1111/j.1095-8649.2009.02411.x

Margolis, L., Esch, GW., Holmes, JC., Kuris, A. and Schad, GA. 1981. The use of Ecological terms in Parasitology (Report of an Adhoc Committee of the American Society of Parasitologists). Journal of Parasitology. 68:131-132.

Nie, P. and Kennedy, CR. 1991. Population Biology of *Proteocephalus macrolepis* (Creplin) in European eel, *Anguilla Anguilla* (Linnaeus) in two small Rivers. Journal of Fish Biology. 38: 921-927.

Pascoe, D. and Cram, P. 1977. The effects of toxicity of cadmium to three-spined stickleback, *Gasterosteus aculeatus* L. Journal of Fish Biology. 10:467-472.

Pascoe, D. and Woodworth, J. 1980. The effects of joint stress on sticklebacks. Zeitschrift far Parasitenkunde. 62:159-163.

Pennycuick, L. 1971[a]. Seasonal variations of parasites infection in a population of the three-spined stickleback, *Gasteroseus aculeatus* L. Parasitology. 63:373-388.

Pennycuick, L. 1971[b].Quantative effects of three species of parasites on a population of the three-spined stickleback, *Gasteroseus aculeatus* L. Journal of Zoology. 165:143-162.

Seed, R. 1984. The occurrence of *Schistocephalus solidus* (Muller) (Cestoda: Diphyllobothriidae) in a population of the three-spined stickleback, *Gasterosteus aculeatus* L. from a disused reservoir in North Wales. Nature in Wales. 3:58-62.

Symth, JD. 1962. Introduction to Animal Parasitology. C.C. Thomas Ltd. Springfield, Illinois, USA.

Received: July 29, 2013; Accepted: Oct 30, 2013

SENRA Academic Publishers, British Columbia
Vol. 8, No. 1, pp. 2691-2697, February 2014
Online ISSN: 1920-3853; Print ISSN: 1715-9997

Canadian Journal of pure&applied sciences

# PSATHYRELLA CANDOLLEANA (FR.) MARIE, A SAPROPHYTIC FUNGUS FORMING ORCHID MYCORRHIZA IN SATYRIUM NEPALENSE D. DON FROM INDIA

*BS Jyothsna[1] and KB Purushothama[2]
[1]Department of Botany, Government Science College, Bangalore 560001
[2]Post Graduate and Research Centre, St. Joseph's College, Langford Road, Bangalore - 560027, India

## ABSTRACT

*Psathyrella candolleana* (Fr.) Marie is a saprophytic fungus which inhabits litter in the forest ecosystem. *Satyrium nepalense var. nepalense*, a rare autotrophic terrestrial orchid was found associated with this fungus forming orchid mycorrhiza. Isolation from root and tuber yielded two different fungi on Potato dextrose agar medium. Molecular identification of the fungal cultures was carried out by sequencing ITS region of nuclear rDNA. The isolate from the root was identified as *Psathyrella candolleana* and the isolate from tuber as *Colletotrichum dematium* .Light microscopic studies of the roots have shown that 60% of the cortical cells contained both digested and intact pelotons. TEM studies of the root have revealed the fine structure of the pelotons with the hyphae observed in the form of fungal cells with thick chitin wall. Pelotons were surrounded by the host cell membrane as an electron dense interfacial matrix suggesting biotrophic relationship. The cortical cells showed shrinkage of protoplasm indicating digestion of the pelotons. An anatomical study of the tuber has not revealed any pelotons. This is the first report of *Psathyrella candolleana* as an orchid mycorrhizal fungus colonizing the roots of *Satyrium nepalense* from the Indian region.

**Keywords**: Orchid mycorrhiza, pelotons, *Psathyrella candolleana*, saprophytic fungus, *Satyrium nepalense*.

## INTRODUCTION

Orchidaceae is the largest family of flowering plants comprising about 17,000-35,000 species which occur as epiphytes or as terrestrial. In nature, all orchids require a suitable fungal partner for their dust sized seeds to germinate and develop into a protocorm. The fungal symbiont invades the embryo and forms intracellular hyphal coils referred to as pelotons. All orchid species are considered to be mycoheterotrophic during this stage of their life cycle (Smith and Read, 2008). Orchid mycorrhizas are found intracellularly in the cortical cells and are generally confined to the roots and persist for a limited period before collapsing and degenerating (Hadley, 1982).

*Satyrium nepalense* is an endangered, ethnobotanically important terrestrial orchid. This species is represented by two varieties namely *S. nepalense* D. Don *var. nepalense* and *S. nepalense var. ciliatum* (Lindl.) Hook., distributed in Western and Eastern Himalayas. It occurs in Jammu and Kashmir, Uttarakand, Bhutan, Sikkim, Assam, Arunachal Pradesh and South India. The plant grows on grass hilly slopes at varying elevations of 600-4600m. It grows to a height of 30-45cm, with tubers which are oblong, leaves are oval to lanceolate, 7-10cm long, small, pink and fragrant flowers occur on an upright spike. The flower has an interesting shape with the lip which is a hood like having a terminal tip called flap. It has two spurs one on each side of the ovary. The indigenous people of upper Nilgiris call this plant as "Ezhtkwehhdr" which means "bullock horns", as the spur of these flowers look like bullock horns. It flowers from July-December. The plant has medicinal value-the tubers are powdered, dried and used as energizing drink, as an aphrodisiac, decoction of tubers, roots and stems are used to cure infectious diseases, as a nutritional supplement, in treating diarrhea, malaria and dysentery (Saklani *et al*., 2012). Review of literature revealed that not much work has been done on the mycorrhizal association of this endangered and ethno-botanically important orchid plant. Hence, the mycorrhizal association of *Satyrium nepalense* has been investigated.

## MATERIALS AND METHODS

### Collection of plant and rhizosphere soil samples

The underground part of the terrestrial orchid along with its rhizosphere soil was collected from Kemmangundi (13°33'N and 75°46'E; 1434m MSL) of Karnataka State, India. The plant was identified as *Satyrium nepalense* D. Don *var. nepalense* (Fig. 1a).

### Isolation, purification and maintenance of mycorrhizal fungi

Pure cultures of the fungi were isolated from roots and

*Corresponding author email: jyothsnaharish2@gmail.com

tubers using Potato dextrose agar medium. The fresh root/tuber samples were cleaned with running tap water, surface sterilized using 0.1% $HgCl_2$, rinsed several times with sterile distilled water, cut into 0.5-1cm pieces, plated aseptically in petriplates containing PDA and inoculated at room temperature (28°C). The plates were observed periodically for the mycelial growth. The fungal mycelium emerging from the cut ends of the roots after suitable growth was selected for purification and further studies. Hyphal tip method was used for purification. Isolated fungi were sub-cultured and maintained on PDA.

**Anatomical studies**

Thin free hand sections of the plant material such as root, tuber were taken and stained with tryphan blue (0.1% in lactophenol) and observed under the light microscope for the presence of fungal hyphae in the cortical cells. Highly coiled hyphae called pelotons (intact and digested) were observed and assessed in each section. Ultrathin sections were taken for Transmission Electron Microscopy. Root bits of 0.5cm were excised and fixed overnight in 3% Glutaraldehyde in 0.1M Cacodylate buffer (pH 7.2).The roots were post fixed in 1% Osmium tetroxide, dehydration was done in a gradient series of ethanol and Propylene oxide, and later embedded in Epon-Araldite (Hoch, 1986). Semi-thin sections (1µm) were stained with 1% Toluidene blue. Ultrathin sections were stained with Uranyl acetate, Lead citrate (Reynolds, 1963) and observed with an FEI Tecnai 12 $G^2$ Electron microscope operating at 80 kV.

**Identification of orchid mycorrhizal fungi using molecular techniques**

Pure cultures of orchid mycorrhizal fungi were used to isolate genomic DNA. Extraction of DNA from fungal mat was performed using CTAB. Electrophoresis was performed in a horizontal submarine apparatus (Genei, Bangalore, India) as outlined by Sambrook and Russel (2001). To amplify the ITS region, PCR was performed using Thermocycler PTC-100 TM to produce multiple copies of a specified DNA. Universal primers (forward and reverse) were used. The DNA was purified using gel extraction kit according to manufacturer's specifications.

**DNA sequencing and Data analysis**

The purified PCR product was sequenced. Sequences were determined by the chain terminal method using ABI 3130 Genetic Analyzer. Sequencing was done in forward and reverse direction. The sequence was generated using data analysis software. Basic local alignment search tool (BLAST) was used to provide rapid searching of nucleotides and protein database. The rDNA gene sequence was used to carry out BLAST with the data base of the NCBI GenBank. Based on maximum identity scores first 10 sequences were selected and aligned using multiple sequence alignment software program Clustal -W.

## RESULTS AND DISCUSSION

**Patterns of fungal colonization**

The transverse section of the root under the light microscope revealed the entry of the fungus through the root hairs. The root hairs lost their straight cylindrical nature and got distorted. After entry through the root epidermis the hypha entered the cortical cells and formed hyphal network called pelotons. Initially colonisation of the cortical cells was noticed in the epidermal cells and subsequently towards the outer and inner cortex. Two patterns of colonization by mycorrhizal fungi were observed. In the first pattern, the pelotons formed in the outer layer of cortical cells remained intact which may serve as a source of inoculum for the recolonization of cells deeper in the root cortex. The second pattern consisted of synchronously formed and degraded patches of pelotons in the inner cortex. Lysis of the pelotons, a characteristic of orchid mycorrhiza was observed in most of the cells and were referred as digestion cells (Fig. 1d,e).

**Transmission Electron microscopy**

Ultra-thin sections of the root revealed that the fungal hyphae were confined to the cortical cells. Epidermal cells were not colonized. The middle and inner cortex showed a multitude of fungal colonization as coils (pelotons) which were not clumped and free in the outer cortex, whereas in the inner cortex clumping of hyphae was observed. TEM revealed that the host cells showed increased cell cytoplasm in the cells colonized by fungal hyphae. The hyphal cells with large number of mitochondria indicates an increased activity of hyphae in the host cells. The hyphae were separated from the host cytoplasm by the host cell membrane as a layer of electron dense interfacial matrix suggesting a biotrophic relationship. No septal types were recognized. Digested and lysed pelotons were observed as typical collapsed hyphae (Figs. 1 f, g, h).

**Colony characteristics**

Two distinct fungal isolates were obtained, one each from the root and tuber of *Satyrium nepalense* on Potato dextrose agar (PDA). Macroscopic observation of the isolate obtained from the root showed white colony with wool like surface (Fig. 1b).The mycelial growth was observed in the range of 2-5cms for 7 days of incubation. The mycelium consisted of hyaline, thin walled, septate hyphae with clamp connections and formed mycelial strands. The other isolate from the tuber showed that the colony was initially white, turning dark gray, with felt like appearance and grew to a diameter of 3cm in 10 days. The mycelium consists of thick walled, closely branched, septate hyphae without clamp connections (Fig. 1c).

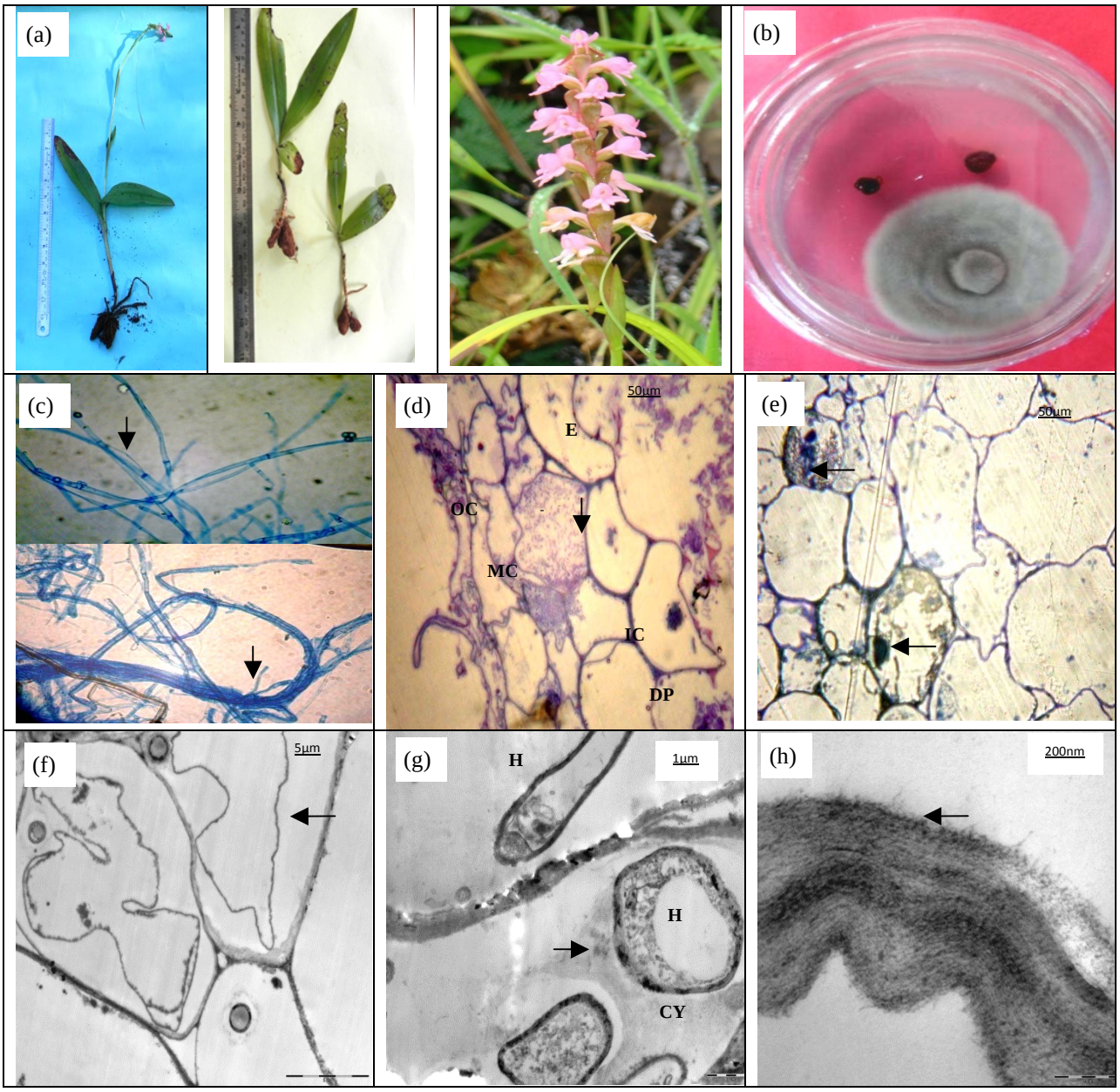


(a) Habit of *Satyrium nepalense* with inflorescence (b) Isolation of the fungus on PDA from the root (c) Mycelium showing septate hyphae and formation of rhizomorph (arrow heads) (d) Light microscopy - TS of root showing colonization of fungal hyphae in epidermal and cortical cells with pelotons (e) Digested pelotons in the cortical cells. (arrow heads) (f) TEM – showing digested peloton separated from the cortical cells (arrow head) (g) Transverse section of fungal hyphae in the cortical root cytoplasm with dense cell wall surrounded by host derived wall material (arrow head) (h) Fungal hyphae surrounded by electron dense layer of the host (arrow head); **CY** – Cytoplasm, **DP** – Digested pelotons, **E-** Epidermis, **H-** Hyphae, **IC**- Inner cortex, **MC** – Middle cortex, **OC**- Outer cortex

**Molecular identification of mycorrhizal fungi**

Two fungal isolates, one each from the root and tuber were identified by sequencing the fungal internal transcribed spacer (ITS) of ribosomal DNA. It revealed that the ground orchid in the root was colonized by *Psathyrella candolleana*, (GenBank Accession No. KC920474) a Basidiomycete. The isolate from the tuber was closely related to *Colletotrichum dematium*, (GenBank Accession No. KC920476) belonging to Deuteromycetes (Figs. 2a,b). Phylogenetic tree of both the fungal isolates showed 98% and 99% resemblance to the above species respectively. The novel aspect of the present work is that two fungi were found to be associated with the same orchid plant. Such dual infection of the

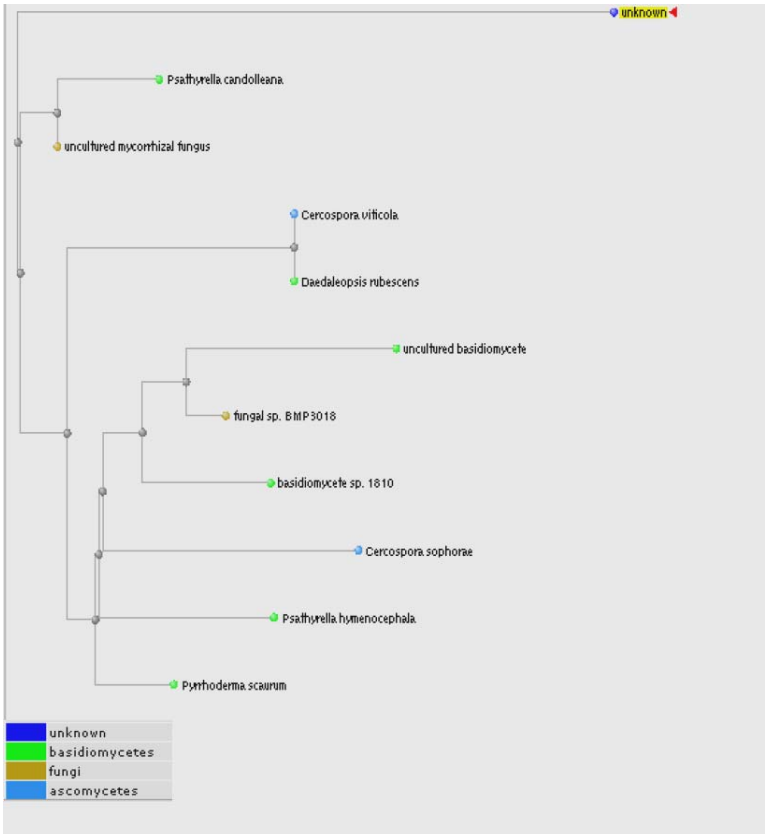


Fig. 2a. Phylogenetic Tree - *Psathyrella candolleana*.

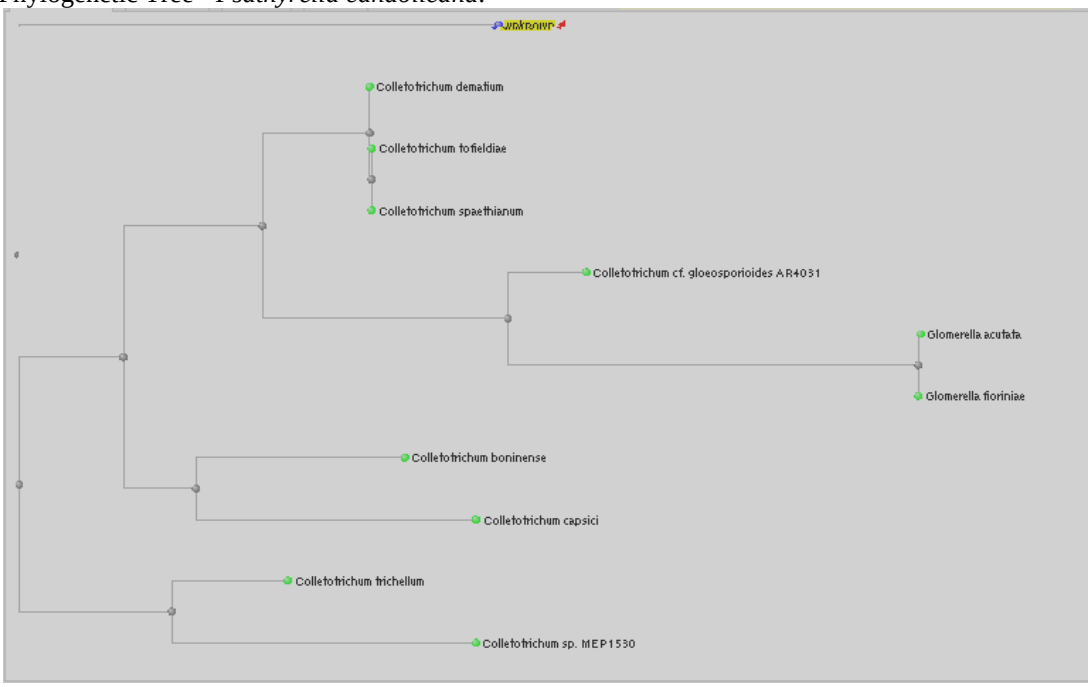


Fig. 2b. Phylogenetic Tree - *Colletotrichum dematium*.

same plant was considered a rare occurrence in orchid-fungal interaction (Kristiansen *et al*., 2001). These two phylogenetically distant taxa shared closely spaced tissues of the orchid. The presence of two different fungi in the same plant does not necessarily play a trophic role of mycorrhizal nature. It may be that the first fungi are the mycorrhizal partner and the second could be an endophyte whose possible role remains to be established.

*Psathyrella candolleana* is a saprophytic fungus growing on decomposing leaves and wood. It occurs in North America, Europe, Africa and many Asian countries like China, India, Japan and Sri Lanka. This is a new report on the mycorrhizal association of a saprophytic fungus with a terrestrial mycoautotrophic orchid. The saprophytic fungus with the flexibility to shift from saprophytism to mutualism is required for an orchid mycobiont (Rasmussen and Rasmussen, 2009). It is probable that due to the non-availability of regular symbionts, the terrestrial orchids may utilize the natively available saprophytic fungi like *Psathyrella* for their mycorrhizal requirements.

## CONCLUSION

Isolation studies on mycobionts of *Satyrium nepalense* revealed the presence of *Psathyrella candolleana* in the root and *Colletotrichum dematium* in the tuber, which suggests that natively available fungal species can form mycorrhizal associations with terrestrial orchids. Interaction between the different fungal isolates and with that of plants would be worth investigating to understand the biology of orchid and mycorrhizal partners.

## ACKNOWLEDGEMENT

The authors are thankful to the Management of St. Joseph's College, Bangalore, for providing laboratory facilities, Dr. K.M. Divakar, Department of Botany, St. Joseph's College, Bangalore, for helping in procuring the plant specimens and to Dr. B.K. Chandrasekhar Sagar, Department of Electron microscopy and Research Laboratory, NIMHANS, Bangalore for providing facilities for TEM studies.

## REFERENCES

Hadley, G. 1982. Orchid mycorrhiza, In: Orchid Biology, Reviews and Perspectives II'. Ed. Arditti, J. Cornell University Press, Ithaca. 84-118.

Hoch, HC. 1986. Freeze-substitution of Fungi. In: Ultrastructure techniques for microorganisms, Eds. Aldrich, HC. and Todd, WJ. Plenum Press, New York, USA. 183-211.

Kristiansen, KA., Taylor, DL., Kjoller, R., Rasmussen, HN. and Rosendahl, S. 2001. Identification of mycorrhizal fungi from single pelotons of *Dactylorhiza majalis (Orchidaceae)* using single strand conformation polymorphism and mitochondrial ribosomal large subunit DNA sequences. Mol. Ecol. 10:2089-2093.

Rasmussen, HN. and Rasmussen, FN. 2009. Orchid mycorrhiza: implications of mycophagous life style. Oikos. 118:334-345.

Reynolds, EW. 1963. The use of lead citrate at high pH as an electron opaque stain in electron microscopy. J. Cell.Biol. 17:208-212.

Saklani, S. and Mishra, AP. 2012. *Satyrium nepalense*: A rare medicinal orchid of Western Himalaya (India); Phytochemical screening, antimicrobial evaluation and conservation studies. Indonesian Journal of Pharmacy. 23(3):162-170.

Sambrook, J. and Russel, DW. 2001. Molecular cloning. A laboratory manual (3rd edi.). CSHL Press, New York, USA.

Smith, SE. and Read, DJ. 2008. Mycorrhizal Symbiosis. Academic Press, London.

Received: June 19, 2013; Revised: Aug 17, 2013;
Accepted: Sept 14, 2013

SENRA Academic Publishers, British Columbia
Vol. 8, No. 1, pp. 2697-2713, February 2014
Online ISSN: 1920-3853; Print ISSN: 1715-9997

Canadian Journal of pure & applied sciences

# DISTRIBUTION, POPULATION STATUS AND CONSERVATION OF THE BIRDS IN KARACHI, SINDH, PAKISTAN

M Zaheer Khan, *Fozia Tabbassum, Syed Ali Ghalib, Afsheen Zehra, Babar Hussain, Saima Siddiqui, Ghazala Yasmeen, Karim Gabol, Nazia Mahmood, Iqbal Saeed Khan, Abdur Razzaq Khan, Darakshan Abbas, Tanveer Jabeen, Naseem Samreen and M Asif Iqbal
Department of Zoology, Faculty of Science, University of Karachi, Karachi-75270, Pakistan

## ABSTRACT

The present study was undertaken during 2008 – 2012 on the birds of Karachi to determine their status and distribution to devise an action plan for their conservation. The sites selected for study included coastal areas, urban areas, wetlands and suburbs. In this study, a total of 172 species of birds were recorded including 71 waterbirds, 46 passerines, 28 birds of prey, 9 game birds and 18 other birds. The important bird areas were identified as Clifton, Manora, Hawkesbay, Sandspit, Hub Dam, Karachi University Campus, and Urban areas. Karachi Coast and Hub Dam were found to be the two most important bird habitats mainly for Waterbirds, while Cape Monze, Hub Dam and Korangi Creek were important areas for Birds of Prey. The common species are Black Kite (*Milvus migrans*), Black-headed Gull (*Larus ridibundus*), Black winged Stilt (*Himantopus himantopus*), Blue Rock Pigeon (*Columba livia*), Cattle Egret (*Bubulcus ibis*), Bank Myna (*Acridotheres ginginianus*), Common Myna (*Acridotheres tristis*), Common Babbler (*Turdoides caudatus*), Common Crow (*Corvus splandens*), House Sparrow (*Passer domesticus*), Little Turn (*Sterna albifrons*), Pied Kingfisher (*Ceryle rudis*), Purple Sunbird (*Nectarinia asiatica*), Red Wattled Lapwing (*Vanellus indicus*), Ring Dove (*Streptopelia decaocto*), Senegal Dove (*Streptopelia senegalensis*), White-throated Kingfisher (*Halcyon smyrnensis*), and White-cheeked Bulbul (*Pycnonotus leucogenys*). The threatened or near-threatened species are Egyptian Vulture (*Neophron percnopterus*) [E], Greater Spotted Eagle (*Aquila clanga*) [V], Imperial Eagle (*Aquila heliaca*) [V], Pallas's Fishing Eagle (*Haliaeetus leucoryphus*) [V], Cinereous Vulture (*Aegypius monachus*) [NT], White Eyed Pochard (*Aytha nyroca*) [NT], Pallid Harrier (*Circus macrourus*) [NT], Lagger Falcon (*Falco jugger*) [NT], and Black-bellied Tern (*Sterna acuticauda*) [NT]. There are no serious threats to the birds. Minor threats include capturing of birds for sale as pet birds and diminishing of birds habitats in most areas. Some measures for the conservation of birds have been proposed such as monitoring of the status of waterbirds and birds of prey, regular waterbird census on Karachi Coast and Hub Dam, and mitigation measures for the impact of urbanization on bird habitats.

**Keywords**: Karachi, waterbirds, distribution, status.

## INTRODUCTION

Pakistan lies at the junction of three zoogeographic regions viz. Oriental, Palaearctic and Ethiopian regions. Wildlife species belonging to the Palaearctic region are found in the Himalayan and Balochistan uplands, those belonging to the Oriental region are found in the Indus Plain including the Thar Desert and Himalayan foot hills, while the dry southwestern region along with the Makran coast has species of Ethiopian origin (GoP, 1992; GoP, 2000a; GoP, 2009).

The province of Sindh forms the lower Indus basin and lies between $23^0$ 35' and $28^0$ 30' northern latitude and $66^0$ 42' and $71^0$ 10' east longitude. There are four major relief elements in the Province: a fringe of hills in the west, a sandy desert in the east, alluvial plains between the hills and the desert, and the delta. The northern section of the western hills is known as the Kirthar Mountains, while the southern half is the Sindh Kohistan. The eastern desert, which is an extension of the Rajasthan Desert, is known as the Thar Desert. The alluvial plains form the lower Indus Valley. The low lying plains south of Thatta and creeks are identified as the Indus Delta. The Province of Sindh is quite rich in terms of abundance and diversity of avian species. As many as 414 species of birds have so far been recorded from its various habitats viz. coastal and marine environment, mangrove forests, swamps and marshes, rivers, riverine forests, inland wetlands, tropical thorn forests, dry sub-tropical semi-evergreen forests and sand dune deserts.

Karachi is the biggest city of Pakistan as well as the capital of the Province of Sindh. It is located in the south of Pakistan, on the coast of the Arabian Sea, north-west of the Indus River Delta. The Karachi coastline stretches over 135km. It is unique due to its ecology and diversity.

*Corresponding author email: ku_zoologist@yahoo.com

Karachi and the adjoining areas have plains, hills, rivers, valleys and coasts as diversified physical features. Karachi stretches from Korangi / Phitti Creek in the east to Cape Monze in the west. The Mehar and Mol mountains lie to the north. The climate of Karachi can be characterized as humid and moderate to hot conditions; however, sometimes it becomes dry when the wind blows from land to sea. There is minor seasonal intervention of a mild winter from mid December to mid-February and a long moderate to hot and humid summer extending from April to September. In July and August, due to cloud cover, the climate is relatively moderate but humid.

Rainfall in Karachi is limited from June to September, and the annual rainfall is at most 500mm. About 50 to 65 percent of the total annual rainfall occurs during July and August when the southwest monsoon is on; another 15 to 25 percent of the annual rainfall occurs during NE monsoon during the winter months (December - February). The rest of the rainfall occurs in the form of occasional cloud bursts. The mean relative humidity in summer is 60 - 70 % while the mean relative humidity during winter is 23 – 30%. The rainfall in the Karachi coastal zone is extremely low and erratic; therefore, this region falls in the semi-arid climate zone.

Due to the proximity with the sea, humidity levels in Karachi usually remain high throughout the year, with a humidity of 50% during December, the driest month, and 85% during August, the moistest month. The mean monthly maximum temperature in Karachi is about 36$^{o}$C from April to June and in October, and about 27$^{o}$C in January at the minimum. The mean monthly minimum temperature is about 29$^{o}$C, in June at maximum and about 12$^{o}$C in January.

Pakistan has 668 bird species including 29 Globally threatened species, 5 Critically Endangered, 6 Endangered, 18 Vulnerable, 19 Near Threatened, and 554 Least Concern Species, while 55 Important Bird Areas (BirdLife International, 2013).

A lot of work on the avifauna of Sindh has been done by Roberts *et al*. (1986), Khanum and Ahmed (1988), Roberts (1991-92), Ghalib and Hasnain (1994, 1997, 1997a), Hasnain and Ghalib (1997), Ahmed *et al*. (1999), Ghalib *et al.* (2000), Siddiqui *et al.* (2001), Khan (2005), Mirza (2007), Durranee *et al.* (2008), Grimmett *et al.* (2008), Ghalib and Nawaz (2008), Ghalib *et al*. (2009), Abbas *et al.* (2010), Hassan and Javed (2011), Khan *et al.* (2012). The Ministry of Climate Changes Pakistan Wetland Program (2012), Ahmed (2013) and Begum *et al*. (2013). The current study was conducted to assess the distribution, population status and conservation of the Birds in Karachi, which will help in further development of conservation and management plans.

## MATERIALS AND METHODS

The following methods of bird counting were used to record and estimate bird population:
For bird surveying, there are two types of transects commonly used, line transects and point transects.

### Line Transacts

A line transect involves traveling a predetermined route and recording birds on either side of the observer.

### Point Transects

Point transects differ from the line transect in that the observers travel along the transect and stop at predefined spots, allow the birds time to settle. Records of all the birds seen or heard for a predefined time, ranging, at the extremes, from 2 to 20 minutes are then taken.

### Capture Techniques

Capture methods can be time consuming and require substantial training to develop the skills necessary to catch, handle, and mark birds. The safety and welfare of the birds are always of paramount importance. Mist netting is a relatively poor method for surveying birds.

### Counting Water Birds

Counts of different water bird species give information on the usage of the site by those birds. It is very important to collect this basic data in order to be able to formulate management plans for the avifauna and/or their wetland/habitats.

### Accurate Counts or Estimates

The evaluation of water bird numbers requires methods to accurately count or estimate. There are many factors which influence the decision as to which count or estimate is more applicable. Among these we must consider.

1. The time period available to evaluate the numbers.
2. The site conditions i.e. are the birds a long distance from the observer? Are the birds partially hidden by obstacles (reed beds, banks)?
3. The size of the site. Should the count area be divided into smaller sub-sites?
4. The behavior of the birds i.e. Are they flying? Are there any disturbances which may disrupt a count?
5. Weather conditions i.e. is there a heat haze, strong winds or rain?
6. The overall number of birds present, i.e. if there are less than 3000 birds, they can usually all be counted in a short space of time, and conversely, large flocks (3000+) may have to be estimated. This decision will depend on the observer's own experience. Either binoculars or telescopes, or more ideally a combination of the two are necessary for assessing the number of water birds or identifying species present.

In the majority of cases, the most practical method for evaluating waterbird numbers will be by accurately estimating them. This is achieved by using the Block method. The block method is used for a distant flock in flight, very large flocks or densely packed flocks on the ground. This method involves 'counting or estimating a "block" of for example 10, 100 or 1000 birds within the flock (depending on the flock size, for larger flocks use larger blocks).

During the estimation, using the block method, the dominant species within the flock can be noted by the observer. Later, in order to collect data on the numbers of the individual species present, the observer can again scan through the flock and count the dominant species, then the second most abundant species and so on until all species have been counted or proportions estimated.

Table 1. Locations and coordinates of Study Sites.

| S. No. | Sites | Coordinates |
|---|---|---|
| 1 | Clifton Beach | 24.805086 N 67.021863 E |
| 2 | Hawke's Bay /Sandspit Beach | 24.840401 N 66.909821 E |
| 3 | Cape Monze | 24.832304 N 66.661556 E |
| 4 | Manora Island | 24.804299 N 66.97040 E |
| 5 | Gizri Creek | 24.8024038 N 67.078679 E |
| 6 | Korangi Creek | 24.786045 N 67.145173 E |
| 7 | Phitti Creek | 24.698242 N 67.196931 E |
| 8 | Hub Dam | 25.248535 N 67.108689 E |
| 9 | Super Highway | 24.953792 N 67.097150 E |
| 10 | Malir Area | 24.906600 N 67.183172 E |
| 11 | Safari Park | 24.924954 N 67.110627 E |
| 12 | Karachi Zoological Garden (Gandhi Garden) | 24.875488 N 67.023155 E |
| 13 | Karachi University Campus | 24.940015 N 67.120931 E |

## RESULTS

During the study from 2008-2012, a total of 172 species of birds were recorded from the study area comprising of 17 orders, and 50 families (see Table 2). For the sake of convenience, the birds were classified into the five groups (Table 3).

### Important Bird Habitats in Karachi

In order to record the species of birds and their status, field surveys were made in 13 selected bird habitats (see Table 1, Fig. 1). However, the following vital bird sites have been identified:

### Hub Dam

Hub Dam has been declared a Wildlife Sanctuary since 1972 for the preservation of waterbirds and the fish Mahsher. This site is an important staging and wintering area for Grebes, Pelicans, Anatids and Cranes. It used to regularly support over 45,000 water birds including Black-necked Grebe, Little Cormorant, Tufted Duck, Common Pochard, Dalmatian and White Pelicans, Coot, and Little Tern.

### Karachi Harbor

There are three small sandstones islands (Oyster Rocks) on the eastern side at the entrance to Karachi Harbor. The Lyari River flows out at the Karachi Harbor through the Manora Channel and its runoff increases in the monsoon season causing the water to become highly polluted. Keamari spits are made up of very fine sand which has been carried west of the Indus Delta, from here onwards, a series of barrier spits and barrier bars are extended southeast along the edge of the Indus Delta.

### Sandspit

Sandspit is a 14.5 km long barrier bar which connects the rocky head end of Manora with the mainland. The beach on the seaward side of the bar is backed by low dunes. Behind the bar there is an 8km long tidal lagoon (Backwaters) with clumps of mangroves (*Avicennia marina*). The lagoon has been greatly altered due to development activities.

### Hawkesbay

Hawkesbay is located on the coast south west of the city. There is a gently sloping sand beach on the eastern part of Hawkesbay while the western part has some rocky areas. There are extensive, intertidal mudflats and some mangrove swamps behind the beach. The beach consists of fine to medium grained sands and sand dunes which are susceptible to wind. The back waters at Hawkesbay extend to the area behind Sandspit and reach up to the Naval Officers housing society. A major area of the backwater supports mangrove vegetation comprising of *Avicennia marina.* The mudflats are barren except for some stunted bushes of mangroves along with a high salinity indicator plant *Arthrocnemum indicum.* In the east of the Karachi coast, mangroves can also be seen in the area from Keamari to Hawkesbay, Boat Basin, and Gizri creek through Korangi Pitthi creek system which is the beginning of the vast mangrove complex of the Indus Delta.

Table 2. List of Birds of Karachi recorded.

| S. No. | Order | Family | Scientific name | Common name | Status |
|---|---|---|---|---|---|
| 1 | Podicipediformes | Podicipedidae | *Tachybaptes ruflcollis* | Little Grebe | R |
| 2 | Pelecaniformes | Pelecanidae | *Pelecanus onocrotalus* | White Pelican | WV |
| 3 | Pelecaniformes | Phalacrocoracidae | *Phalacrocorax carbo* | Large Cormorant | WV |
| 4 | Pelecaniformes | Phalacrocoracidae | *Phalacrocorax niger* | Little Cormorant | R |
| 5 | Ciconiiformes | Ardeidae | *Ardea cinerea* | Grey Heron | WV |
| 6 | Ciconiiformes | Ardeidae | *Ardea purpurea* | Purple Heron | R |
| 7 | Ciconiiformes | Ardeidae | *Ardeola grayii* | Indian Pond Heron | R |
| 8 | Ciconiiformes | Ardeidae | *Bubulcus ibis* | Cattle Egret | R |
| 9 | Ciconiiformes | Ardeidae | *Egretta alba* | Large Egret | WV |
| 10 | Ciconiiformes | Ardeidae | *Egretta intermedia* | Intermediate Egret | R |
| 11 | Ciconiiformes | Ardeidae | *Egretta garzetta* | Little Egret | R |
| 12 | Ciconiiformes | Ardeidae | *Egretta gularis* | Indian Reef Heron | R |
| 13 | Ciconiiformes | Threskiornithidae | *Plegadis falcinellus* | Glossy Ibis | R |
| 14 | Ciconiiformes | Phoenicopteridae | *Phoenicopterus roseus* | Flamingo | WV |
| 15 | Anseriformes | Anatidae | *Tadorna tadorna* | Common Shelduck | WV |
| 16 | Anseriformes | Anatidae | *Anas acuta* | Pintail | WV |
| 17 | Anseriformes | Anatidae | *Anas crecca* | Common Teal | WV |
| 18 | Anseriformes | Anatidae | *Anas platyrhynchos* | Mallard | WV |
| 19 | Anseriformes | Anatidae | *Anas strepera* | Gadwall | WV |
| 20 | Anseriformes | Anatidae | *Anas penelope* | Wigeon | WV |
| 21 | Anseriformes | Anatidae | *Anas clypeata* | Shoveller | WV |
| 22 | Anseriformes | Anatidae | *Aytha ferina* | Common Pochard | WV |
| 23 | Anseriformes | Anatidae | *Aytha nyroca* | Ferruginous Pochard | WV |
| 24 | Falconiformes | Accipitridae | *Elanus caeruleus* | Black-winged Kite | R |
| 25 | Falconiformes | Accipitridae | *Milvus migrans* | Black Kite | R |
| 26 | Falconiformes | Accipitridae | *Haliastur indus* | Brahminy Kite | R |
| 27 | Falconiformes | Accipitridae | *Accipiter badius* | Shikra | R |
| 28 | Falconiformes | Accipitridae | *Buteo buteo* | Common Buzzard | WV |
| 29 | Falconiformes | Accipitridae | *Buteo rufinus* | Longlegged Buzzard | WV |
| 30 | Falconiformes | Accipitridae | *Hieraetus pennatus* | Booted Hawk Eagle | WV |
| 31 | Falconiformes | Accipitridae | *Aquila heliaca* | Imperial Eagle | WV |
| 32 | Falconiformes | Accipitridae | *Aquila rapax* | Tawny Eagle | R |
| 33 | Falconiformes | Accipitridae | *Aquila nipalensis* | Steppe Eagle | WV |
| 34 | Falconiformes | Accipitridae | *Aquila clanga* | Greater Spotted Eagle | WV |
| 35 | Falconiformes | Accipitridae | *Haliaeetus leucoryphus* | Pallas's Fishing Eagle | R |
| 36 | Falconiformes | Accipitridae | *Aegypius monachus* | Cinereous Vulture | R |
| 37 | Falconiformes | Accipitridae | *Gyps fulvus* | Griffon Vulture | R |
| 38 | Falconiformes | Accipitridae | *Neophron percnopterus* | Egyptian Vulture | R |
| 39 | Falconiformes | Accipitridae | *Circus macrourus* | Pallid Harrier | WV |
| 40 | Falconiformes | Accipitridae | *Circus pygargus* | Montagu's Harrier | WV |
| 41 | Falconiformes | Accipitridae | *Circus aeruginosus* | Marsh Harrier | WV |
| 42 | Falconiformes | Accipitridae | *Circaetus gallicus* | Short-toed Eagle | R |

*Continued…*

Table 2 continued

| S. No. | Order | Family | Scientific name | Common name | Status |
|---|---|---|---|---|---|
| 43 | Falconiformes | Pandionidae | *Pandion haliaetus* | Osprey | WV |
| 44 | Falconiformes | Falconidae | *Falco jugger* | Laggar Falcon | R |
| 45 | Falconiformes | Falconidae | *Falco columbarius* | Pallid Merlin | WV |
| 46 | Falconiformes | Falconidae | *Falco tinnunculus* | Common Kestrel | WV |
| 47 | Galliformes | Phasianidae | *Francolinus francolinus* | Black Partridge | R |
| 48 | Galliformes | Phasianidae | *Francolinus pondicerianus* | Grey Partridge | R |
| 49 | Galliformes | Phasianidae | *Conturnix conturnix* | Grey Quail | WV |
| 50 | Gruiformes | Gruidae | *Grus grus* | Common Crane | DPM |
| 51 | Gruiformes | Rallidae | *Amaurornis phoenicurus* | White-breasted Water Hen | R |
| 52 | Gruiformes | Rallidae | *Gallinula chloropus* | Indian Moorhen | R |
| 53 | Gruiformes | Rallidae | *Porphyrio porphyrio* | Indian Purple Moorhen | R |
| 54 | Gruiformes | Rallidae | *Fulica atra* | Coot | WV |
| 55 | Charadriiformes | Haematopodidae | *Haematopus ostralegus* | Oyster Catcher | WV |
| 56 | Charadriiformes | Charadriidae | *Vanellus leucurus* | White-tailed Lapwing | WV |
| 57 | Charadriiformes | Charadriidae | *Vanellus indicus* | Red Wattled Lapwing | R |
| 58 | Charadriiformes | Charadriidae | *Pluvialis squatarola* | Grey Plover | WV |
| 59 | Charadriiformes | Charadriidae | *Charadrius hiaticula* | Ringed Plover | WV |
| 60 | Charadriiformes | Charadriidae | *Charadrius dubius* | Little Ringed Plover | R |
| 61 | Charadriiformes | Charadriidae | *Charadrius alexandrinus* | Kentish Plover | R |
| 62 | Charadriiformes | Charadriidae | *Charadrius mongolus* | Lesser Sand Plover | WV |
| 63 | Charadriiformes | Scolopacidae | *Numenius phaeopus* | Whimbrel | WV |
| 64 | Charadriiformes | Scolopacidae | *Numenius arquata* | Curlew | WV |
| 65 | Charadriiformes | Scolopacidae | *Limosa limosa* | Black-tailed Godwit | WV |
| 66 | Charadriiformes | Scolopacidae | *Limosa lapponica* | Bartailed Godwit | WV |
| 67 | Charadriiformes | Scolopacidae | *Tringa totanus* | Common Redshank | WV |
| 68 | Charadriiformes | Scolopacidae | *Tringa stagnatilis* | Marsh Sandpiper | WV |
| 69 | Charadriiformes | Scolopacidae | *Tringa nebularia* | Greenshank | WV |
| 70 | Charadriiformes | Scolopacidae | *Tringa terek* | Terek Sandpiper | WV |
| 71 | Charadriiformes | Scolopacidae | *Tringa hypoleucos* | Common Sandpiper | WV |
| 72 | Charadriiformes | Scolopacidae | *Capella gallinago* | Common or Fantail Snipe | WV |
| 73 | Charadriiformes | Scolopacidae | *Calidris alba* | Sanderling | WV |
| 74 | Charadriiformes | Scolopacidae | *Calidris minutus* | Little Stint | WV |
| 75 | Charadriiformes | Scolopacidae | *Calidris temminckii* | Temminck's Stint | WV |
| 76 | Charadriiformes | Scolopacidae | *Calidris alpinus* | Dunlin | WV |
| 77 | Charadriiformes | Scolopacidae | *Calidris testaceus* | Curlew Sandpiper | WV |
| 78 | Charadriiformes | Scolopacidae | *Philomachus pugnax* | Ruff | WV |
| 79 | Charadriiformes | Rostratulidae | *Rostratula benghalensis* | Painted Snipe | R |
| 80 | Charadriiformes | Recurvirostridae | *Himantopus himantopus* | Black-winged Stilt | R |
| 81 | Charadriiformes | Recurvirostridae | *Recurvirostra avosetta* | Avocet | WV |
| 82 | Charadriiformes | Burhinidae | *Burhinus oedicnemus* | Stone Curlew | R |
| 83 | Charadriiformes | Burhinidae | *Esacus magnirostris* | Great Stone Plover | R |
| 84 | Charadriiformes | Laridae | *Larus argentatus* | Herring Gull | WV |
| 85 | Charadriiformes | Laridae | *Larus brunnicephalus* | Brown-headed Gull | WV |
| 86 | Charadriiformes | Laridae | *Larus ridibundus* | Black-headed Gull | WV |

*Continued…*

Table 2 continued

| S. No. | Order | Family | Scientific name | Common name | Status |
|---|---|---|---|---|---|
| 87 | Charadriiformes | Laridae | *Larus genei* | Slenderbilled Gull | R |
| 88 | Charadriiformes | Sternidae | *Chlidonias hybrida* | Indian Whiskered Tern | DPM |
| 89 | Charadriiformes | Sternidae | *Gelochelidon nilotica* | Gullbilled Tern | WV |
| 90 | Charadriiformes | Sternidae | *Hydroprogne caspia* | Caspian Tern | WV |
| 91 | Charadriiformes | Sternidae | *Sterna aurantia* | Indian River Tern | R |
| 92 | Charadriiformes | Sternidae | *Sterna hirundo* | Common Tern | SV |
| 93 | Charadriiformes | Sternidae | *Sterna repressa* | White-cheecked Tern | SV |
| 94 | Charadriiformes | Sternidae | *Sterna acuticauda* | Black-bellied Tern | R |
| 95 | Charadriiformes | Sternidae | *Sterna albifrons* | Little Tern | R |
| 96 | Charadriiformes | Sternidae | *Sterna sandvicensis* | Sandwich Tern | M |
| 97 | Columbiformes | Pteroclididae | *Pterocles exustus* | Chestnut-bellied or Common or Indian Sandgrouse | R |
| 98 | Columbiformes | Pteroclididae | *Pterocles alchata* | Pintailed Sandgrouse | R |
| 99 | Columbiformes | Columbidae | *Columba livia* | Blue Rock Pigeon | R |
| 100 | Columbiformes | Columbidae | *Streptopelia decaocto* | Ring Dove | R |
| 101 | Columbiformes | Columbidae | *Streptopelia tranquebarica* | Red Turtle Dove | R |
| 102 | Columbiformes | Columbidae | *Streptopelia senegalensis* | Little Brown or Senegal Dove | R |
| 103 | Psittaciformes | Psittacidae | *Psittacula krameri* | Rose-ringed Parakeet | R |
| 104 | Cuculiformes | Cuculidae | *Eudynamys scolopacea* | Indian Koel | R |
| 105 | Cuculiformes | Cuculidae | *Centropus sinensis* | Greater Coucal | R |
| 106 | Strigiformes | Tytonidae | *Tyto alba* | Indian Barn Owl | R |
| 107 | Strigiformes | Strigidae | *Bubo bubo* | Indian Great Horned or Eagle Owl | R |
| 108 | Strigiformes | Strigidae | *Bubo coromandus* | Dusky Horned Owl | R |
| 109 | Strigiformes | Strigidae | *Athene brama* | Spotted Owlet | R |
| 110 | Strigiformes | Strigidae | *Asio otus* | Longeared Owl | WV |
| 111 | Caprimulgiformes | Caprimulgidae | *Caprimulgus europaeus* | Euasian Nightjar | SBV |
| 112 | Caprimulgiformes | Caprimulgidae | *Caprimulgus mahrattensis* | Syke's or Sind Nightjar | R |
| 113 | Caprimulgiformes | Caprimulgidae | *Caprimulgus asiaticus* | Indian Nightjar | R |
| 114 | Apodiformes | Apodidae | *Apus pallidus* | Pallid Swift | WV |
| 115 | Apodiformes | Apodidae | *Apus melba* | Alpine Swift | SBV |
| 116 | Apodiformes | Apodidae | *Apus affinis* | House Swift | R |
| 117 | Coraciiformes | Alcedinidae | *Ceryle rudis* | Indian Pied Kingfisher | R |
| 118 | Coraciiformes | Alcedinidae | *Alcedo atthis* | Indian Small Blue Kingfisher | R |
| 119 | Coraciiformes | Alcedinidae | *Halcyon smyrnensis* | White-breasted Kingfisher | R |
| 120 | Coraciiformes | Meropidae | *Merops superciliosus* | Blue-cheeked Bee-eater | SV |
| 121 | Coraciiformes | Meropidae | *Merops orientalis* | Green Bee-eater | R |
| 122 | Coraciiformes | Coraciidae | *Coracias benghalensis* | Indian Roller | R |
| 123 | Coraciiformes | Upupidae | *Upupa epops* | Hoopoe | WV |
| 124 | Piciformes | Picidae | *Jynx torquilla* | European Wryneck | DPM |
| 125 | Piciformes | Picidae | *Dinopium benghalensis* | Sind Goldenbacked Woodpecker | R |

*Continued…*

Table 2 continued

| S. No. | Order | Family | Scientific name | Common name | Status |
|---|---|---|---|---|---|
| 126 | Piciformes | Picidae | *Picoides assimilis* | Sind Pied Woodpecker | R |
| 127 | Passeriformes | Alaudidae | *Eremopterix grisea* | Ashycrowned Finch-Lark | R |
| 128 | Passeriformes | Alaudidae | *Eremopterix nigriceps* | Blackcrowned Finch-Lark | R |
| 129 | Passeriformes | Alaudidae | *Ammomanes deserti* | Desert Finch-Lark | R |
| 130 | Passeriformes | Alaudidae | *Galerida cristata* | Crested Lark | R |
| 131 | Passeriformes | Hirundinidae | *Riparia riparia* | Collared Sand Martin | WV |
| 132 | Passeriformes | Hirundinidae | *Riparia paludicola* | Grey-throated Indian Sand Martin | R |
| 133 | Passeriformes | Hirundinidae | *Ptyonoprogne fuligula* | Rock Martin | R |
| 134 | Passeriformes | Hirundinidae | *Hirundo smithi* | Wire-tailed Swallow | R |
| 135 | Passeriformes | Hirundinidae | *Hirundo rustica* | Common Swallow | WV |
| 136 | Passeriformes | Laniidae | *Lanius isabellinus* | Rufous-tailed or lsabelline Shrike | WV |
| 137 | Passeriformes | Laniidae | *Lanius meridionalis* | Southern Grey Shrike | R |
| 138 | Passeriformes | Lanidae | *Lanius vittatus* | Baybacked Shrike | R |
| 139 | Passeriformes | Lanidae | *Lanius schach* | Rufous-backed Shrike | R |
| 140 | Passeriformes | Dicruridae | *Dicrurus adsimilis* | Black Drongo or King Crow | R |
| 141 | Passeriformes | Sturnidae | *Sturnus roseus* | Rosy Starling or Rosy Pastor | DPM |
| 142 | Passeriformes | Sturnidae | *Acridotheres ginginianus* | Bank Myna | R |
| 143 | Passeriformes | Sturnidae | *Acridotheres tristis* | Common Myna | R |
| 144 | Passeriformes | Corvidae | *Dendrocitta vagabunda* | Tree Pie | R |
| 145 | Passeriformes | Corvidae | *Corvus splendens* | Sind House Crow | R |
| 146 | Passeriformes | Bombycillidae | *Hypocolius ampelinus* | Grey Hypocolius or Shrike Bulbul | WV |
| 147 | Passeriformes | Pycnonotidae | *Pycnonotus leucogenys* | White-cheeked Bulbul | R |
| 148 | Passeriformes | Pycnonotidae | *Pycnonotus cafer* | Red-vented Bulbul | R |
| 149 | Passeriformes | Timaliidae | *Turdoides caudatus* | Common Babbler | R |
| 150 | Passeriformes | Timaliidae | *Turdoides striatus* | Sind Jungle Babbler | R |
| 151 | Passeriformes | Sylviidae | *Acrocephalus stentoreus* | Great Reed Warbler | WV |
| 152 | Passeriformes | Sylviidae | *Prinia burnesii* | Long -tailed Grass Warbler | R |
| 153 | Passeriformes | Sylviidae | *Orthotomus sutorius* | Tailor Bird | R |
| 154 | Passeriformes | Sylviidae | *Sylvia curruca* | Lesser White throat | WV |
| 155 | Passeriformes | Sylviidae | *Sylvia nana* | Desert Warbler | WV |
| 156 | Passeriformes | Sylviidae | *Phylloscopus sindianus* | Sind Chiffchaff | WV |
| 157 | Passeriformes | Turdidae | *Luscinia svecicus* | Bluethroat | WV |
| 158 | Passeriformes | Turdidae | *Phoenicurus ochruros* | Black Redstart | WV |
| 159 | Passeriformes | Turdidae | *Saxicola caprata* | Pied Bush Chat | R |
| 160 | Passeriformes | Turdidae | *Oenanthe isabellina* | Isabelline Wheatear | WV |
| 161 | Passeriformes | Turdidae | *Oenanthe deserti* | Desert Wheatear | WV |
| 162 | Passeriformes | Turdidae | *Oenanthe alboniger* | Hume's Chat or Wheatear | R |
| 163 | Passeriformes | Turdidae | *Saxicoloides fulicata* | Indian Robin | R |
| 164 | Passeriformes | Motacillidae | *Motacilla flava* | Yellow Wagtail | DPM |
| 165 | Passeriformes | Motacillidae | *Motacilla citereola* | Citrine Wagtail | WV |

Table 2 continued

| S. No. | Order | Family | Scientific name | Common name | Status |
|---|---|---|---|---|---|
| 166 | Passeriformes | Motacillidae | *Motacilla alba* | White or Pied Wagtail | WV |
| 167 | Passeriformes | Motacillidae | *Motacilla cinerea* | Grey Wagtail | WV |
| 168 | Passeriformes | Nectariniidae | *Nectarinia asiatica* | Purple Sunbird | R |
| 169 | Passeriformes | Passeridae | *Zosterops palpebrosa* | White Eye | R |
| 170 | Passeriformes | Passeridae | *Passer domesticus* | House Sparrow | R |
| 171 | Passeriformes | Estrildidae | *Lonchura malabarica* | White-throated Munia | R |
| 172 | Passeriformes | Emberizidae | *Emberiza melanocephala* | Blackheaded Bunting | DPM |

Legend: PM: Passage migrant, R: Resident, SBV: Summer breeding visitor, SV: Summer visitor, WV: Winter visitor, M: Migrant, DPM: Double Passage Migrant.

**Cape Monze**

It is located on the extreme south west of Karachi. It was once an estuarine area of Hub River. There are small rocky hills adjacent to the beach which rise about 20 – 25m above the mean sea level. Some rocky head islands near the mouth of the river give partial protection from the southwest monsoon waves.

Table 3. Groups of bird species.

| S. No. | Groups | Number of Species |
|---|---|---|
| 1 | Water birds | 71 |
| 2 | Passerines | 46 |
| 3 | Birds of Prey | 28 |
| 4 | Game Birds | 09 |
| 5 | Others (Parrot, Roller, Greater Coucal, Hoopoe, Nightjars, Swifts, Kingfisher, Bee-eaters, Roller, Hoopoe and Woodpeckers.) | 18 |

**Common and Widespread Species**

The common and widespread species recorded during the study include: Bank Myna, Common Babbler, Black Kite, Black-winged Stilt, Black-headed Gull, Blue Rock Pigeon, Common Crow, Cattle Egret, Common Myna, Green Bee-eater, House Sparrow, Collared Dove, Little Tern, Laughing Dove, Purple Sunbird, Pied Kingfisher, Redwattled Lapwing, White-throated Kingfisher and White-cheeked Bulbul.

**Status of the various migrant species**

As many as 87 species were recorded as resident, while 85 species were recorded as migrants. The categories of the migrants are given in the table 4.

Table 4. The Categories of the Migrant's Species.

| S. No. | Categories of the migrants | Number of Species |
|---|---|---|
| 1 | **Winter Visitors** | 73 (see Table 1) |
| 2 | **Double Passage Migrants** Black headed Bunting, Common Crane, Eurasian Wryneck, Rosy Starling, Whiskered Tern and Yellow Wagtail. | 06 |
| 3 | **Summer Breeding Visitors** Alpine Swift and Eurasian Nightjar. | 02 |
| 4 | **Summer Visitors** Common Tern (recorded mainly in summer months); white-cheeked Tern (recorded from March - June) and Blue cheeked Bee-eater (recorded as Passage Migrant in summer). | 03 |
| 5 | **Year-round Migrant** Sandwich Tern was recorded from October – June. | 01 |

**Status of the Vagrants**

Single recordings of seven species of stragglers have been reported in the Karachi area, out of which two are quite old records of occurrence of White-bellied Minivet, (*Pericrocotus erthropugius*) in 1919, Orange – breasted Green Pigeon (*Treron bicincta*) in 1938, and Bohemian Waxwing (*Bombycilla garrulus*) in 1969. The other four records are for Black-necked Monarch (*Hypothymus azurea*) in 1980, Eurasian Dotterel (*Charadrius morinellus*) in 1998, Black-capped Kingfisher (*Halcyon pileata*) in 1998 and Woodchat Shrike (*Lanius senator*) in 2002 (Grimmett *et al*., 2008). None of these vagrants were recorded in the present study from Karachi and the adjoining areas.

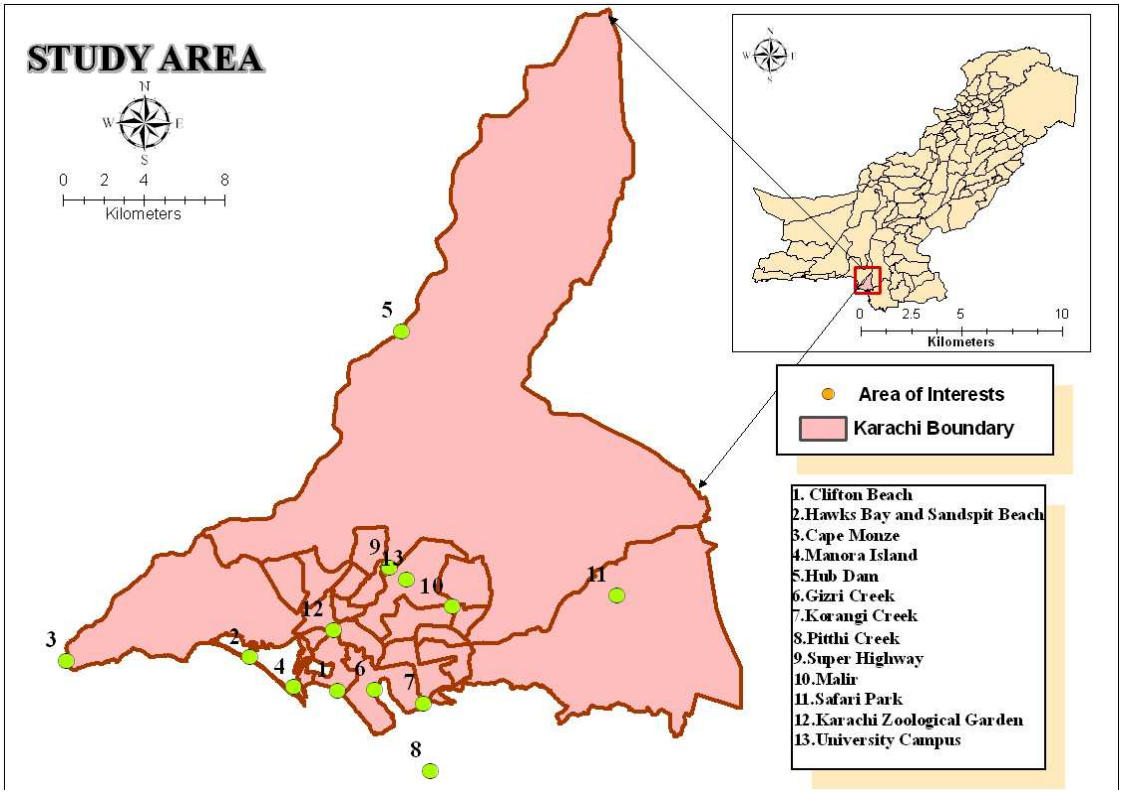


Fig. 1. Map of important Bird Habitats in Karachi.

**Threats to Birds**

There are no severe threats to the birds and their habitats in the study area. The minor threats to the birds are:

Trapping of Birds

The following species of birds are trapped by bird trappers for sale to the public on roads or brought to the weekly markets for sale as cage birds.

1. Rose ringed Parakeet
2. House Sparrow
3. Bank Myna
4. Common Myna
5. Blue Rock Pigeon
6. Blackheaded Bunting
7. Red Munia

Trapping of Quails

Grey Quail (*Coturnix coturnix*), is a double passage migrant in Pakistan. The autumn passage starts from late August and the return spring passage starts in late April. It is a highly relished delicacy throughout its overall range as hundreds of thousands are netted all along the migration route annually. The birds are kept for fattening and sold in local markets in large numbers. It is also prized as a fighting bird.

Human Impact

Due to increase in human population and urbanization of the area, birds habitats are disturbed.

Collection of firewood/ loss of vegetation

Collection of firewood by the locals in the villages and slum areas for use in their houses and mostly on roadside hotels is a potential threat to the forest cover of most of the area. A lot of mangrove forests which provide substantial habitat for the birds have been disappearing which has negatively affected the bird populations on the Karachi Coast.

**DISCUSSION**

Karachi city and adjoining areas provides suitable habitat for a variety of birds. The area consists of coasts, islands, wetlands, forests, safari park, zoos and creeks. These areas are important for water birds, migratory birds and birds of prey in particular (refer photographs of some birds of Karachi, Figs. 1-30).

PHOTOGRAPHS OF SOME BIRDS OF KARACHI

Fig. 1. Little Grebe

Fig. 2. Gadwall (Source: animalphotos.info)

Fig. 3. Purple Moorhen

Fig. 4. Red Wattled Lapwing

Fig. 5. Black Winged Stilt

Fig. 6. Southern Grey Shrike

Fig. 7. Rufous Backed Shrike

Fig. 8. Black Drongo

Fig. 9. Bank Myna (Source: http://ibc.lynxeds.com)

Fig. 10. Tree Pie

Fig. 11. White-Cheeked Bulbul

Fig. 12. Pied Bush Chat

Fig. 13. White Wagtail

Fig. 14. Purple Sunbird

Fig. 15. Black Winged Kite

Fig. 16. Brahminy Kite

Fig. 17. Shikra

Fig. 18. Longlegged Buzzard

Fig. 19. Imperial Eagle

Fig. 20. Tawny Eagle

Fig. 21. Egyptian Vulture

Fig. 22. Marsh Harrier
(source: newswatch.nationalgeographic.com)

Fig. 23. Kestrel
(source: radioactivebirdwatcher.blogspot.com)

Fig. 24. Grey Partridge

Fig. 25. Rose Ringed Parakeet (source: zooskopje.com)

Fig. 26. Indian Pied Kingfisher

Fig. 27. Blue Cheeked Bee Eater

Fig. 28. Green Bee Eater

Fig. 29. Indian Roller (source: Trek nature.com)

Fig. 30. Golden Backed Woodpecker

The threatened and Near-threatened species recorded are Egyptian Vulture (E), Greater Spotted Eagle (V), Imperial Eagle (V), Pallas's Fishing Eagle (V), White-eyed Pochard (NT), Black-bellied Tern (NT) and Cinereous Vulture (NT).

There are no serious threats to the birds or their habitats. Hunting of wildlife has been controlled to a great extent. The minor threats to the birds and their habitats include trapping of birds and the impact of human population etc. Karachi provides very favorable habitats for the birds, in particular, waterbirds. The overall population of the birds in Karachi is fluctuating but there is no noticeable decline.

The overall populations of certain birds are on the rise due to the favourable environment for them.This includes species such as pigeons, doves, crows, mynas, and kites around the urban areas. The Common Kite is also very abundant in the coastal areas, particularly near coastal villages such as Chashma Goth and Rehri Goth area. Gulls and terns are also observed in fairly large numbers near Korangi, Rehri and Phitti Creek area. Flamingos are regularly sighted in Gizri creek area.

The declining species include the waders on the Karachi Coast in particular Sanderling, Large Sand Plover and Curlew Sandpiper due to disturbance, loss of habitat and shrinkage of feeding grounds. Oystercatchers have nearly been wiped out from the coastal areas. Similarly the Vultures (Egyptian, Griffon and Cinereous) have almost disappeared from the coastal / creek areas.

There is a new record of Scaly-breasted Munia (*Lonchura punctulata*) from Karachi University Campus (Abbas *et al*., 2010). It has previously been recorded from KPK and Punjab but not from Sindh.

The most notable sites for the birds in Karachi now remain the coastal areas (Sandspit/ Hawkesbay, Korangi / Phitti / Rehri / Gizri Creek Area). Hub Dam area (Hub Dam Reservoir plus Khar Centre Area) and the Karachi University Campus.

It is necessary to undertake the monitoring of the population of the key species of birds of Karachi. There are very bright prospects for ecotourism in the area on account of its scenic beauty, water birds and beautiful coastal areas and wetlands.

**CONSERVATION OF THE BIRDS IN KARACHI**

Although there are no serious threats to the birds and their habitats in Karachi yet for their long term management, the following plan of action is suggested:

1. In order to record the trends of populations in the waterbirds which are an integral part of the most important ecosystem of Karachi, regular waterbird census may be undertaken in January consistent with the AWC each year.
2. Regular monitoring of the populations of key species of birds such as Pelicans, Flamingos, Falcons and Vultures may be undertaken.
3. Collaborative avifaunal research may be initiated with the Academia and the NGO's particularly with reference to migratory species such as Quails, Waterbirds and Birds of Prey.
4. Pakistan has ratified various conventions related to biodiversity for the safeguard of the fauna and flora and their habitats. The provisions of these conventions may be taking into account for the purpose.

(i) The Convention on Biological Diversity requires that the government should take action to resuscitate degraded ecosystems and establish conservation facilities. It should establish training and research programs for sustainable use of biodiversity. It may be made imperative to carry out an Environmental Impact Assessment (EIA) prior to any proposed project that may reduce biodiversity.

(ii) The Convention on International Trade in Endangered Species of Wild Fauna and Flora (CITES) aims to ensure that international trade in specimens of wild animals and plants does not threaten their survival. Trade in species listed in Appendix 1 of the CITES is not allowed, while the trade in species of Appendix 2 is allowed only under a special permit. The following species of birds in Pakistan are included in Appendix 1 of the CITES: Dalmatian Pelican, Houbara Bustard, Imperial Eagle, Laggar Falcon, Peregrine Falcon , Cheer Pheasant, Himalayan Monal, Siberian Crane, Western Tragopan, Red-Capped Falcon, while the birds included in Appendix 2 are: Black Stork, Flamingo, Spoonbill, Rose-ringed Parakeet, Lesser Flamingo and White-headed Duck.

(iii) The Convention on Migratory Species (CMS) aims to conserve the migratory (avian, marine and terrestrial) species over the whole of their range. Appendix 1 of the Convention lists all migratory species which have been categorized as being in danger of extinction and for which strict protection measures are required. The following species of birds in Pakistan have been included in Appendix 1: Dalmatian Pelican, Imperial Eagle, Kestrel. Sociable Plover, Pallas's Fishing Eagle, White Pelican, Baikal Teal, Greater Spotted Eagle, Lesser White Fronted Goose, Siberian Crane, Marbled Teal, White-eyed Pochard, White-headed Duck, and White-tailed Sea Eagle.

Appendix 2 of the CMS lists migratory species which have an unfavorable conservation status and which require international agreements for their conservation and management. The following species of birds in Pakistan are included in Appendix 2:

Dalmatian Pelican, Black Stork, White Stork, Spoonbill, Osprey, Common Quail, Houbara Bustard, Crab Plover, Eurasian Thick-Knee, Slenderbilled Gull, Lesser Crested Tern, Little Tern, Red-necked Grebe, Pygmy Cormorant, Glossy Ibis, Little Crake, Bailion's Crake,Watercock, Collared Pratincole, Greater Crested Tern, Saunders Little Tern, White-cheeked Tern, Eastern Turtle Dove and European Bee-eater.

(iv) Under the Ramsar Conservation on Wetlands, there is a general obligation for the contracting Pakistan to include wetland conservation in their national land use planning. They are expected to encourage research regarding wetlands and their fauna and flora and to endeavor through management to increase waterbird populations on appropriate wetlands. And to promote the training of personnel competent in the field of wetland research, management and wardening.

**RECOMMENDATIONS**

1. Action may be taken to control pollution on the Karachi Coast as it is one of the main habitats for birds in Karachi.
2. Regular Annual Waterbird Census on Hub Dam and the Karachi Coast may be undertaken in January each year to record the trends in waterbird populations and to identify the threatened wetlands for their wardening. Regular monitoring of bird population on Karachi Coast and at the Hub Dam Wildlife Sanctuary/Ramsar Site may be undertaken.
3. Public awareness may be created through the material about wildlife, protected areas, wetlands, water birds, game birds and environmental protection.
4. City master plans may be built up to make expansion of cities in a premeditated manner to avoid severe damage to wildlife and its habitats.

**REFERENCES**

Abbass, D., Rais, M., Ghalib, SA. and Khan, MZ. 2010. First Record of Spotted Munia (*Lonchura punctulata*) from Karachi. Pakistan J. Zool. 42(4): 503-505.

Ahmad, MF., Ghalib, SA., Iffat, F. and Hasnain, SA. 1999. Vertebrate biodiversity of mangroves of Pakistan. In: Proceedings of the National Seminar on Mangroves Ecosystem Dynamic of the Indus Delta. 148-169.

Ahmed, SI. 2013. Raptors of Pakistan. A Field Guide. Zoological Survey of Pakistan, Islamabad. pp92.

Begum, A., Zubair, A., Hussain, SE. and Khan, AR. 2013. Water birds diversity and conservation at Hub Dam, Lasbela, Karachi, Pakistan. African J. Science and Research. 2(3):22-26.

BirdLife International. 2013. Country profile: Pakistan. Available from: http://www.birdlife.org/datazone/country/pakistan.

Durranee, J., Hasnain, SA. and Ahmed, E. 2008. Observation on the Birds of Sandspit/ Hawkesbay Coastal Wetland Complex, Karachi Coast. Pakistan. J. Zool. 40 (4):229-237.

Ghalib, SA. and Hasnain, SA. 1994. The Waterfowl of the Karachi Coast. Records. Zool. Surv.Pak. 11:39- 61.

Ghalib, SA. and Hasnain, SA. 1997. Observation of waterbirds of Clifton Beach, Karachi. Records. Zool. Surv. Pak. 13:23-29.

Ghalib, SA. and Hasnain, SA. 1997[a]. Observations on the birds of Cape Monze (Mouth of Flab river and Sonehri Area), Karachi. Pakistan J. Zool. 29(3):287-291.

Ghalib, SA., Hasnain, SA. and Khursheed, SN. 2000. Observations on the avifauna of Hub Dam. Pakistan J. Zool. 32(1):27-32.

Ghalib, SA. and Nawaz, R. 2008. Field guide to the birds of the Indus Eco-region. WWFP. Karachi.

Ghalib, SA, Rais, M., Abbas, D., Tabbassum, F., Begum, A. and Jabeen, T. 2009. An overview of the status of shorebirds and internationally important sites in Pakistan. Pak J. Zool. 41(3):165-172.

Government of Pakistan (GoP) 1992. The Pakistan National Conservation Strategy. Environment and Urban Affairs Division, Government of Pakistan and IUCN-Pakistan. pp378.

Government of Pakistan (GoP). 2000[a]. Biodiversity action plan for Pakistan. Ministry of Environment, Pakistan, WWFP and IUCNP. pp78.

Government of Pakistan (GoP). 2009. Fourth National Report. Convention on Biological Diversity. Ministry of Environment, Government of Pakistan. Xii+ pp97.

Grimmett, R., Roberts, T. and Inskipp, T. 2008. Birds of Pakistan Christopher Helm, London. pp258.

Hasnain, SA. and Ghalib, SA. 1997. The Waders of Karachi Coast. In: Marine Sciences of Arabian Sea. Eds. Thompson, F. and Tirmizi, NM. American Institute of Biological Science, Washington, DC, USA.

Hassan, A. and Javed, HI. 2011. Effects of Tasman Spirit oil spill on coastal birds at Clifton, Karachi Coast, Pakistan. J. Animal and Plant Sciences. 21(2 Suppl.):33

Khan, MZ. 2005. Wetlands of Sindh with reference to Ramsar Sites in 2005. J. nat. his. Wildl. 4(2):141-145.

Khan, MZ., Begum, A., Ghalib, SA., Khan, AR., Yasmeen, R., Siddiqui, TF., Zehra, A., Abbas, D., Tabbassum, F., Siddiqui, S., Jabeen,T. and Hussain, B. 2012. Effects of Environmental Pollutions on Aquatic

Vertebrate Biodiversity and inventory of Hub Dam: Ramsar Site. Canadian Journal of Pure and Applied Sciences. 6(2):1913-1935.

Khanum, Z. and Ahmed, M. 1988. Resident and Migratory Birds of the Karachi Coast Proceeding of the International Conference- Marine Science of the Arabian Sea- 1986. American Institute of Biological Sciences, Washington, DC, USA. 467-469.

Mirza, ZB. 2007. A field guide to the birds of Pakistan. Bookland. pp366.

Roberts, TJ., Passburg, R. and Zalinge, NPV. 1986. A Checklist of birds of Karachi and lower Sindh, Pakistan. WWF Pakistan.

Roberts, TJ. 1991. The Birds of Pakistan (vol. 1), (Non-Passeriformes). Oxford University Press. pp527.

Roberts, TJ. 1992. The Birds of Pakistan (vol. 2), (Passeriformes). Oxford University Press. pp541.

Siddiqui, PA., Saqib, TA. and Kazmi, MA. 2001. Birds Population in Different Coastal Areas of Sindh. Pakistan Journal of Marines Science. 10(1):49-60.

The Ministry of Climate Change's Pakistan Wetland Program. 2012. Pakistan National Wetland Policy. The Ministry of Climate Change. Islamabad.

Received: Aug 29, 2013; Revised: Sept 30, 2013; Accepted: Oct 4, 2013

SENRA Academic Publishers, British Columbia
Vol. 8, No. 1, pp. 2715-2720, February 2014
Online ISSN: 1920-3853; Print ISSN: 1715-9997

Canadian Journal of pure&applied sciences

# DETERMINATION OF HEAVY METALS IN TOMATO (*SOLANUM LYCOPERSICUM*) LEAVES, FRUITS AND SOIL SAMPLES COLLECTED FROM ASABA METROPOLIS, SOUTHERN NIGERIA

*Gabriel CC Ndinwa, Anislt Mirsm[1], CO Chukumah, Mens Mirsm[1], KI Obarakpor[2], EA Edafe[2] and WE Morka[3]
[1]Department of Industrial Safety and Environmental Management Technology
Delta State School of Marine Technology, Burutu
[2]Department of Science Laboratory Technology, Delta State School of Marine Technology, Burutu
[3]General Unit Studies, Delta State School of Marine Technology, Burutu, Nigeria

## ABSTRACT

Soil, tomato leaves and tomato fruits collected from Asaba metropolis were digested and analyzed for metals such as lead, copper, cadmium, nickel, zinc, chromium, manganese, arsenic, iron, selenium and cobalt. The aforementioned metals were determined using atomic absorption spectrophotometry (AAS). The results obtained revealed that all the metals were detected and there were metal variations. Metal concentration in soil samples exceeded those of tomato leaves. Also, tomato leaves metals were higher than those values obtained in tomato fruits. This is an indication that the soil was pollution to the tomato leaves and fruits. The highest concentrations were found to lead and iron.

**Keyword**: Heavy metal, contamination, concentration, environment, vegetation, bioaccumulation.

## INTRODUCTION

The environment is a natural system that encompasses the relationship between relief, vegetation, plant, animal, man and the physical world (Robinson, 1998). Another study, Konz-Lisi and Friebele (1998) discussed that the environment is constantly being spoiled and rendered very unsafe for human habitation and other organism. This unhealthy environment is brought about through the various activities of man such as mineral exploitation, agricultural practice, industrial production, food processing, social, domestic and commercial activities. All these lead to pressure on the commercial environment. However, the misleading of these activities result in environmental pollution. Heavy metal as defined by Yang and Zhang (2003) are metals having a density greater than 5g/cm$^3$. They are inorganic element found in plant and animal growth in trace or very minute quantities, toxic and poisonous in relatively higher concentration, biologically undegradeable but easily assimilable and bioaccumulated in the protoplasm of living organism. Advance in technology has led to high levels of industrialization and urban migration leading to the discharge of effluents containing heavy metals in our environment. The various activities of man in recent years have increased the quantity and distribution of heavy metals in the atmosphere, land and water bodies (Zurera-cosano, 2008).

Heavy metals are usually present at level as low as ppb in a polluted or moderately polluted natural source but biological system accumulate these metals by factor as high as 1000 times more (Ademorati, 1996). This accumulation is passed on to the food chain in ppm (part per million) or higher concentration in soil, consumed by man in very much accumulated amounts and will continue to build up. The most dangerous and serious implication of these bioaccumulation is that symptoms of heavy metals poisoning may not appear or may not be identified until several years of continuous exposures and intake (Edward and Kuo, 2006). On appearance of these symptoms, they will not easily be traced back to the correct and original cause or source. The said source may have been a regular and delicious diet such as vegetables, fish or drinking water. Therefore, communities relying greatly on a contaminated diet become particularly exposed to the danger of long term chronic heavy metal poisoning.

Vegetables constitute an essential dietary component by contributing protein, vitamins, iron, calcium and other nutrients, which are usually in short supply (Thompson and Kelly, 2000). They also act as buffering agents for acidic substances produced during the digestion process. However, they contain both essential and toxic elements over a wide range of concentrations. Metal accumulation in vegetables may pose a direct threat to human health (Turkdogan *et al*., 2003; Damek-porawa and Sawicka-kapusta, 2003). Vegetables take up metals by absorbing them from contaminated soils, as well as from deposits on different parts of the vegetables exposed to the air from polluted environments (Zurera-cosano *et al*., 2008). It has been reported that nearly half of the mean ingestion of lead, cadmium and mercury through food is due to plant

*Corresponding author email: gndinwa@yahoo.com

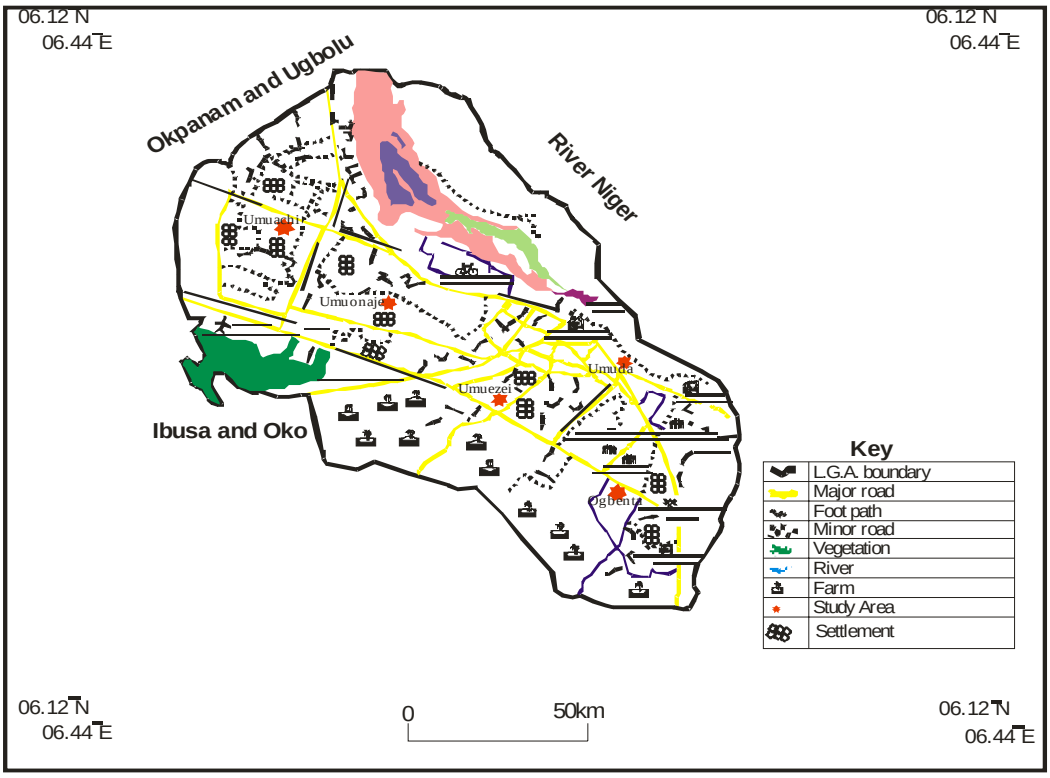


Fig. 1. Map of Asaba showing the study area.

origin. Moreover, some population groups seem to be more exposed, especially vegetarians, since they absorb more frequently "tolerable daily doses".

This study aims to (i) determine the levels of metals in tomato fruit, leaves and soil (ii) determine the sources of heavy metals in tomato fruit, leaves and soil and (iii) determine the pollution status, if any.

## MATERIALS AND METHODS

### Materials

Soil, tomato leaves and fruit were collected in Asaba metropolis from three different farms along Asaba-Benin expressway. The soil samples were stored in polyethylene bags and taken to Mail–In Laboratory in Warri Metropolis. The wet soil samples were dried under sunlight and later kept at room temperature at 25°C free from moisture. The tomato leaves and fruit samples were collected from the same site at 10m, 50m and 100m. Samples were air dried, grinded and sieved.

### Study site

Asaba is a town in Oshimili South Local Government Area and also the capital territory of Delta State situated in the Niger Delta region of the Southern part of Nigeria (Fig. 1). It lies between latitude $6^0$12'N and longitude $6^0$44'E of the equator. It is bounded on the east by Onitsha, in Anambra State, on the west by Ibusa, on the north by Asako and Ugbolu, while on the south by Oko. The town also has a lot of registered and unregistered small and large industries. This includes block industry, Asaba Aluminium Company, borehole, sales of cements/depot, bakeries, Eternite roofing sheet company, sales of timber, plywood industry, commercial banks and poultry/animal farms.

### Apparatus

The apparatus used in this study included: measuring cylinder (100ml), funnel, volumetric flask (500ml), pyrex bottom flask (25ml) hot plate, beam balance (electrical digital), wattman's filter paper, masking tape, sampling bottles (plastics) and atomic absorption spectrophotometer (AAS).

### Determination of Metal in Soil Sample

The loamy sand texture was 99% sand and 1% silt and clay. Soil samples were taken at the three randomly replicated plots in three different quarters. 20g of soil was weighed into acid washed platinum crucible. 20ml of concentrated $HNO_3$ was added and left for 20 minutes (it is imperative that this step be carried out before the

Table 1. Heavy metal in soil obtained from Asaba metropolis.

| Sample Code | Metals in mg/kg dry weight | | | | | | | | | | |
|---|---|---|---|---|---|---|---|---|---|---|---|
| | Pb | Cu | Cd | Ni | Zn | Cr | Mn | As | Fe | Se | Co |
| SSA ($O_1$) | 10.14 | 2.28 | 0.01 | 3.96 | 7.88 | 0.15 | 14.53 | 0.01 | 66.00 | 0.01 | 0.01 |
| SSB ($O_2$) | 7.01 | 2.01 | 0.01 | 2.03 | 5.53 | 0.16 | 12.15 | 0.01 | 70.12 | 0.01 | 0.01 |
| SSC ($O_3$) | 9.12 | 2.24 | 0.01 | 3.01 | 4.35 | 0.01 | 11.52 | 0.01 | 61.22 | 0.01 | 0.01 |

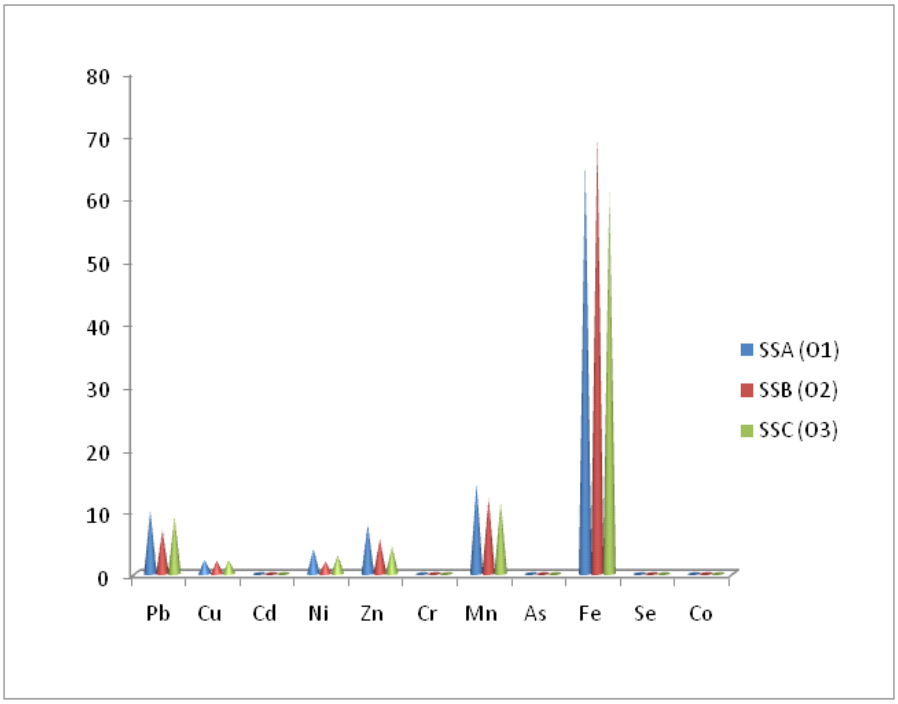


Fig. 2. The concentration of heavy metals in soil collected from Asaba metropolis.

addition of perchloric acid otherwise, explosion may occur). 2ml each of $HClO_4$ and HCl in the ratio of 10:1 was added and left for about 10 minutes. Heat the sample in the crucible in a hot plate from 135–180$^0$C and evaporate the content almost to dryness. 10ml of deionised water was added and boil gently to dissolve the residue. Cool and filter through No. 42 wattman filter paper into 100ml volumetric flask and make to mark with deionised water. The soil extracts and the standard solutions were aspirated into the air-acetylene flame of Varian 220 (*fast sequential*) Atomic Absorption Spectrometer. A blank sample was also prepared and analyzed along the sample.

**Determination of Metal in Tomato Leaves and Fruits Samples**

20g each of tomato leaves and fruits were weighed into two acid washed platinum crucible. 20ml of concentrated $HNO_3$ was added to each of the containers and leave for 20 minutes (it is imperative that this step be carried out before the addition of perchloric acid otherwise, explosion may occur). 2ml each of $HClO_4$ and HCl in the ratio of 10:1 was added and left for about 10 minutes. The samples were heated in the crucible in a hot plate from 135–180$^0$c and evaporate the content almost to dryness. 10ml of deionised water was added and boil gently to dissolve the residue. Cool and filter through No. 42 wattman filter paper into 100ml volumetric flask and make to mark with deionised water. The tomato leaves and fruits extract and the standard solutions were aspirated into the air-acetylene flame of Varian 220 (*fast sequential*) Atomic Absorption Spectrometer. A blank sample was also prepared and analyzed along the sample.

**Determination of plant biomass**

The weight of the vegetables or plant species was determined in two phases (the wet weight WW and the dry weight DW) at the end of the study by the method of Edwin-wosu and Kinako (2004). The wet weights were obtained using a weighing balance. The entire plant leaves and fruits of known fresh weights were dried under the sun for 10 days to constant weight. The dried plants were reweighed to obtain the dry weight.

Table 2. Heavy metal in tomato leaves obtained from Asaba metropolis.

| Sample Code | Metals in mg/kg dry weight | | | | | | | | | | |
|---|---|---|---|---|---|---|---|---|---|---|---|
| | Pb | Cu | Cd | Ni | Zn | Cr | Mn | As | Fe | Se | Co |
| TLSA ($O_1$) | 4.01 | 1.19 | 0.01 | 1.83 | 4.89 | 0.16 | 4.51 | 0.01 | 7.13 | 0.01 | 0.15 |
| TLSB ($O_2$) | 3.84 | 1.56 | 0.01 | 2.07 | 4.00 | 0.41 | 4.48 | 0.01 | 8.15 | 0.01 | 0.4 |
| TLSC ($O_3$) | 4.03 | 1.75 | 0.01 | 2.01 | 4.52 | 0.01 | 4.42 | 0.01 | 8.11 | 0.01 | 0.01 |

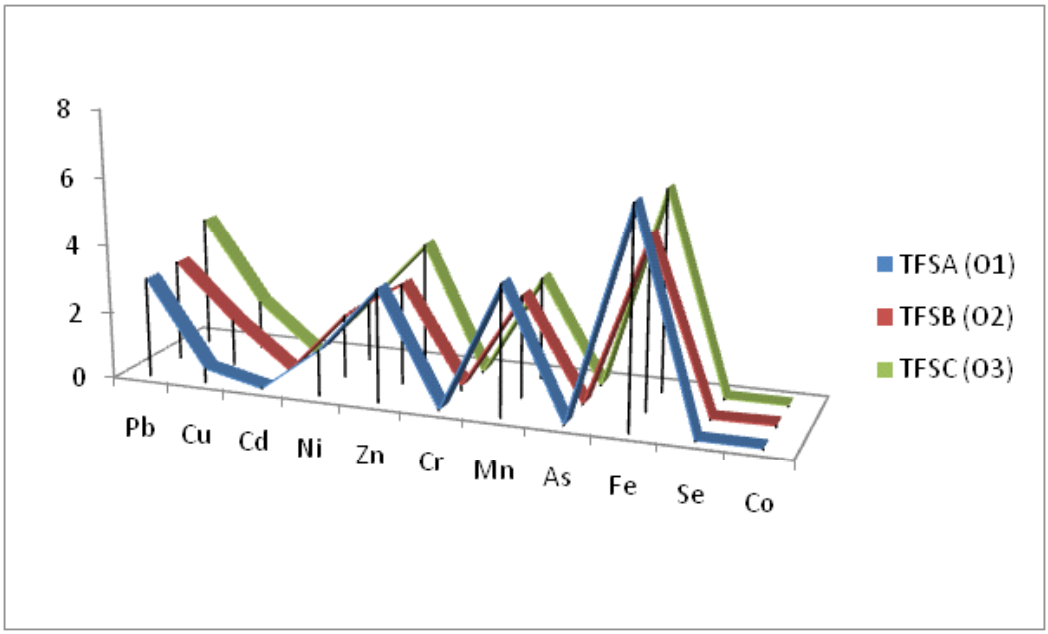


Fig. 3. The concentration of heavy metals in tomato leaves obtained from Asaba metropolis.

**Quality Control**

Quality control was assumed from the use of analytical blank and spike. The blank were prepared in a similar manner like the same. All instrument reading was corrected with the blank. A recovery test of the entire procedure was carried out by a spike and already analyzed with known standard of the metal of interest. An acceptable recovery of 92% and 93.4% was achieved for chromium and nickel.

$$\frac{\text{Concentration of the spike} - \text{Concentration of the unspiked}}{\text{Concentration of the unspiked sample}} \times \frac{100}{1}$$

## RESULTS AND DISCUSSION

Soil, tomato fruits and tomato leaves collected in Asaba metropolis were digested and analyzed for heavy metals. The results obtained revealed that all the metals analyzed were detected and there were variation in the values obtained in soil, tomato fruits and tomato leaves respectively. The metal concentrations obtained in the aforementioned samples are presented in table 1, 2, and 3 respectively.

The results of the analysis as displayed in the various tables and figures show the concentrations of heavy metals in the samples. Table 1 and figure 2 shows the concentration of heavy metals in the soil sample. Table 2 and figure 3 show the concentration of heavy metals in tomato leaves samples and table 3 and figure 4 shows the concentration of heavy metals in tomato fruit samples. A look at the three soil samples location revealed that metal concentrations in samples $SSO_1$, $SSO_2$ and $SSO_3$ were higher than those values obtained in samples $TLSO_1$, $TLSO_2$ and $TLSO_3$ (tomato leaves). Also, the tomato leaves metal values exceeded those of $TFSO_1$, $TFSO_2$ and $TFSO_3$ (tomato fruits). Although, metals such as copper, nickel, zinc, manganese and cobalt, concentrations in this study are not considered dangerous when compared with other studies with similar areas. Whereas metals such as lead, cadmium, chromium, arsenic, iron and selenium are considered to be dangerous on long-term basis. The contamination of the tomato leaves and tomato fruits is an indication that the soil is polluting the vegetables. The elevated concentrations of metals in soil samples are traceable to the activities of various industries in Asaba

Table 3. Heavy metal in tomato fruits obtained from Asaba metropolis.

| Sample Code | Metals in mg/kg dry weight | | | | | | | | | | |
|---|---|---|---|---|---|---|---|---|---|---|---|
| | Pb | Cu | Cd | Ni | Zn | Cr | Mn | As | Fe | Se | Co |
| TFSA ($O_1$) | 2.96 | 0.41 | 0.01 | 1.35 | 3.33 | 0.01 | 3.83 | 0.01 | 6.38 | 0.01 | 0.01 |
| TFSB ($O_2$) | 3.01 | 1.35 | 0.01 | 1.88 | 2.98 | 0.15 | 3.01 | 0.01 | 5.09 | 0.01 | 0.05 |
| TFSC ($O_3$) | 3.92 | 1.44 | 0.01 | 1.82 | 3.73 | 0.01 | 3.05 | 0.01 | 6.00 | 0.01 | 0.01 |

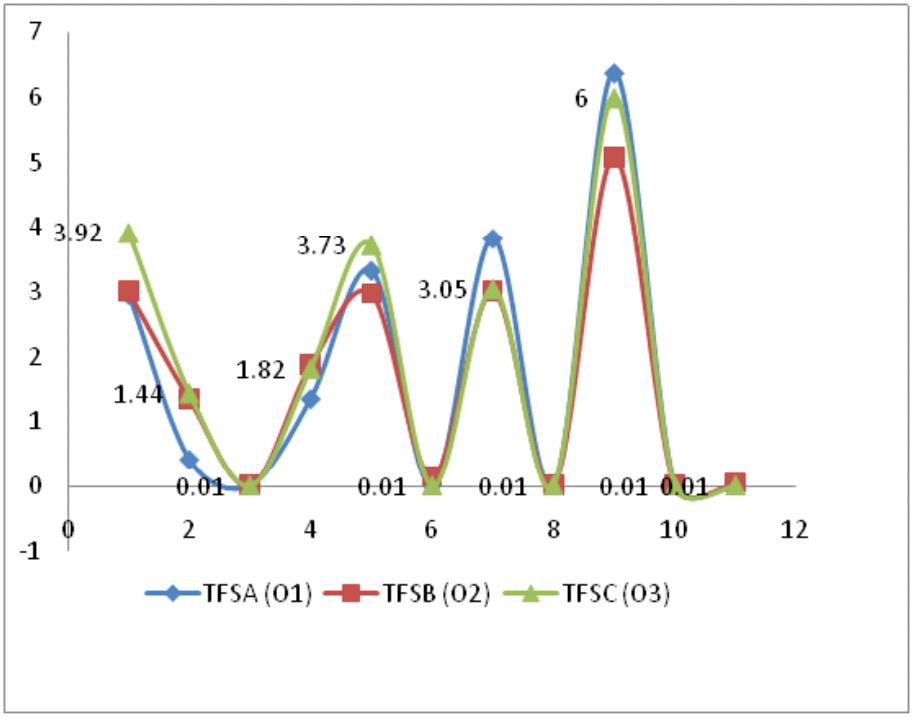


Fig. 4. The concentration of heavy metals in tomato fruits obtained from Asaba metropolis.

and its environs. Lead and iron concentrations in this study are highly elevated. Especially, lead values in all the sample can lead to health problems on long-term basis. Mental retardation and brain damage especially in children could occur, if no urgent measure is taken.

This study had revealed that metal concentrations in tomato leaves are higher than those of the fruits indicating that it is safer to consume the tomato fruits. The increase in metal values in leaves of tomato plants is as a result of the uptake rate of the soil nutrient.

Metal such as cadmium, arsenic, selenium and cobalt in soil, tomato leaves and tomato fruits did not indicate variations in terms of metal values. However, the presence of the aforementioned trace metals in tomato fruits could lead to metal poison. Urbanization and anthropogenic wastes normally found in urban towns could account for vegetable contamination via the soil.

## CONCLUSION

Soil, tomato leaves and tomato fruits were collected in Asaba metropolis. These samples were analyzed for metals such as lead, copper, cadmium, nickel, zinc, chromium, manganese, arsenic, iron, selenium and cobalt respectively. Metal levels in soils were considered to be higher than those of the tomato leaves and tomato fruits. This is an indication that the contamination of the vegetables was through the soil. These elevated concentrations of metals were attributed to the activities of industries and anthropogenic wastes around Asaba and its environs. Lead and iron concentrations in all the samples determined were highly elevated indicating pollution.

## RECOMMENDATIONS

This study has some recommendations towards reducing the level of environmental pollution in the study area.

- The Delta State Environmental Protection Agency (DELSEPA) should live up to their expectation in monitoring environmental pollution in the state.
- DELSEPA should set up a guideline and published same to the public for proper monitoring of pollution in urban and rural area of the state
- A central laboratory should be established in the major cities of the state for effective monitoring of soil pollution
- Any company which gaseous emission and/or discharged effluent are detected to be above the set limit for air and water should be penalized for non-compliance by paying any applicable fine.

**REFERENCES**

Ademorati, CMA. 1996. Environmental chemistry and toxicology, Benin: Foludex Press Ltd. pp49.

Damek-Poprawna, M. and Sawicka-Kapusta, K. 2003. Damage to liver, kidney and teats with reference to burden of heavy metals in tomato fruits from areas around steelworks and zinc smelters in Poland. Toxicology. 186(2):1-10.

Edward, G. and Kuo, JL. 2006. Heavy metals in vegetables grown in Netherlands and in domestic and imported fruits. Z. Lebensm Unters Forsch. 190(1):34-39.

Edwin-wosu, NL. and Kinako, PDS. 2004. Biomass loss as an index of pollution in various gradients of a crude oil polluted terrestrial environment. Global J. Pure Applied Sci. 10:623-625

Konz-Lisi, T. and Friebele, OI. 1998. Chemistry, environmental impact and health effects. Oxford Parhamin Press. 382-399.

Robinson, GO. 1998. Environmental Science ($2^{nd}$ edi.). John Wiley and Son Incorporated. Canada. pp471.

Thompson, BC. and Kelly, R. 2000. Buffering agents for acidic substances produced in the digestion of Chinese cabbage, winter green and tomato. Bulletin on Agriculture. 3:16-22.

Turkdogan, OS., Perkins, DL. and Tyler, HE. 2003. Vegetable uptake of heavy metal and absorption in contaminated soil. Asia Pollution Bulletin. 4(2):146-155.

Yang, ET. and Zhang, O. 2003. Heavy metal on plant growth. Journal of Environmental Pollution and Management. 3(2):12-25.

Zurera-Cosano, LB. 2008. Man as a contributory factor to pollution. Article on Global Pollution. 5:56-64.

Received: April 23, 2012; Accepted: Nov 22, 2013

SENRA Academic Publishers, British Columbia
Vol. 8, No. 1, pp. 2721-2726, February 2014
Online ISSN: 1920-3853; Print ISSN: 1715-9997

Canadian Journal of pure&applied sciences

# THE SEX RATIO, GONADOSOMATIC INDEX AND STAGES OF GONADAL DEVELOPMENT OF SADDLE GRUNT FISH, *POMADASYS MACULATUM* (BLOCH, 1793) OF KARACHI COAST

*Amtyaz[1], M Atiqullah Khan[2], M Zaheer Khan[2] and M Usman Ali Hashmi[3]
[1]Department of Zoology, Sir Syed Govt. Girls College Nazimabad, Karachi-74600
[2]Department of Zoology, University of Karachi, Karachi-75270
[3]Department of Zoology, Dehli Govt. Science College, Karachi, Pakistan

## ABSTRACT

The sex ratio, gonadosomatic index, stages of gonadal development and fecundity of saddle grunt fish, *Pomadasys maculatum* (Block, 1793) of the Karachi coast were investigated. *Pomadasys maculatum* had a sex ratio of 1: 1.36 (male to female). The difference in sex ratio was not significantly different ($p > 0.05$) from the expected theoretically 1: 1 distribution except June, September and December. Gonadosomatic index value in males during August – November were 3.109 to 5.630, while in females the high values during August – December were found to be 3.542 to 6.679, which suggested the spawning period. The highest GSI value in males was 5.967 in stage VI and the lowest GSI value was 1.256 recorded during VII stage. GSI values in males increased slowly reaching for maximum in 5.967 in (stage VI), while in females at high value was 6.630 during stage VI and the lowest GSI values were 1.625 and 1.124 during stages I & II respectively. Seven stages of gonadal development were observed in male and female fish. *Pomadasys maculatum* is found in coastal waters over sand near reefs or muddy bottoms. The results will increase our knowledge of reproductive biology of *Pomadasys maculatum* which is relevant for fisheries and aquaculture management as well as breeding programs.

**Keywords**: *Pomadasys maculatum,* sex ratio, gonadosomatic index, gonadal development.

## INTRODUCTION

Commercial quantities of large numbers of finfish and shellfish are present in the coastal waters of Pakistan (Hoda, 1985). The saddle grunt, *Pomadasys maculatum* is an economically important fish, it belongs to the family Haemulidae and can be found at depths between 20 - 110m in soft, sandy and muddy bottoms of the Indo-west pacific and western pacific areas. Gonadosomatic index which is an index of gonad size relative to fish size is a good indicator of gonadal development in fish (Dadzie and Wangila, 1980). The percentage of body weight of fish that is used for production of eggs is determined by the gonadosomatic index. Sex ratio studies provide information on the representation of male and female fish present in a population. It states the proportion of male to female fish in a population and indicates the dominance of sex of fish species in a given population. Sex ratio also constitutes basic information necessary for the assessment of the potential of fish reproduction and stock size estimation in fish population (Vicentini and Araujo, 2003). In estimating the reproductive potential of fish, information on sex ratio of fish can be included to determine female spawning biomass.

*Corresponding author email: imtiazsafi76@gmail.com

Information on the reproductive biology of some economically important fish species which include *Pomadasys kaakan*, *Velamugil cunnesius, Drepane longimana, Pomadasys hasta* and *Euryglossa orientalis* of the Karachi coast has been reported by some authors (Iqbal, 1989; Hoda and Qureshi, 1993; Hoda and Iqbal, 1994; Deshmukh, 1973; Khan and Hoda, 1993). There is a paucity of information on the study of reproductive biology of the grunts in the Karachi coast. The reproductive biology of *Pomadasys maculatum* has not been widely reported in literature. The aim of this study was to investigate the sex ratio, gonadosomatic index and stages of gonadal development which are some aspects of the reproductive biology of *Pomadasys maculatum* of the Karachi coast. It is hoped that the information obtained from this study will contribute to our knowledge of the reproductive biology of *Pomadasys maculatum* and will be useful for fisheries and aquaculture production for the future.

## MATERIALS AND METHODS

### Study area

The Karachi coast was the study area for this research. The Karachi coastline is between latitude 24°53'N and longitude 67°00'E and lies in the Northern boundary of Arabian Sea.

**Collection of specimens and sampling**

Samples of *Pomadasys maculatum* were collected fortnightly (A total of 32 collections) from fish harbors of West Wharf and Korangi Creek of Karachi coast. The specimens were collected from January to December. The fish was identified by using the Bianchi (1985) and Fisher and Bianchi (1984) [FAO Fish Identification Manuals]. The simple random sampling technique was used (Cochran, 2007). A total of 408 samples collected during the study period. The samples were transported to the laboratory and preserved in a deep freezer at -20°C until examination and analysis.

**Body measurements**

The specimens were brought out of the deep freezer and allowed to thaw and the body length and weight were measured. Total and standard lengths were measured using a one-meter measuring board graduated in cm. The fish was wiped with a dry napkin before weighing and body weight and ovary weight were measured using a weighing balance (Sartorius model).

**Sex ratio**

Each specimen was dissected and the gonads were removed. The sex of each specimen was identified by examination of the gonads. The proportion of the two sexes relative to one another was used to calculate the sex ratio.

**Gonadosomatic index**

The Gonadosomatic index was calculated by following formula:

$$GSI = \frac{\text{Weight of gonad}}{\text{Weight of fish}} \times 100$$

**Stages of Gonadal Development**

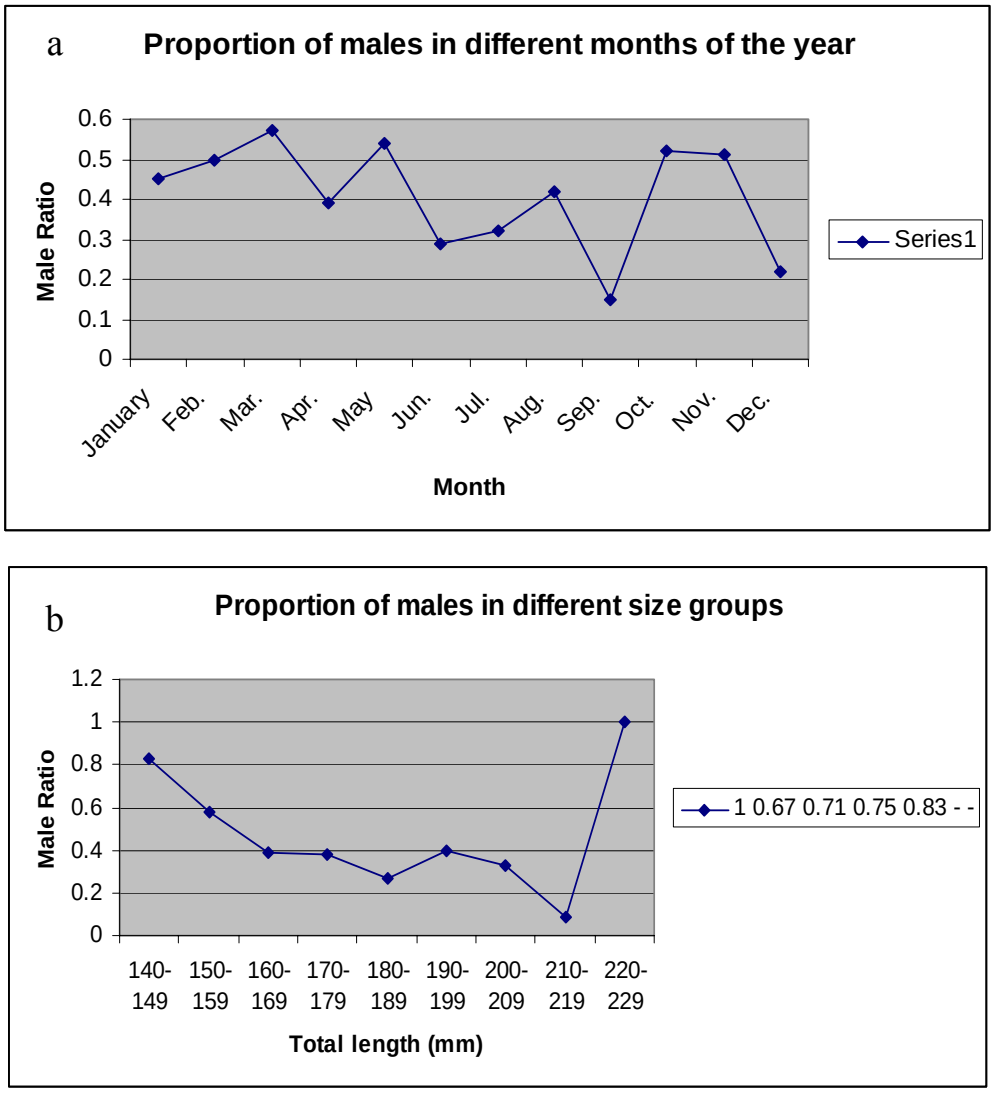


Fig. 1. Proportion of male in different (a) Months and (b) Different size groups.

Gonadal stages were examined microscopically and classified according to Nikolsky (1963) as follows:

Stage I- immature, Stage II- Developing, Stage III- Developing, Stage IV- Maturing, Stage V- mature, Stage VI- Ripe(Running) and Stage VII- spent.

The number of males and females in the different stages of Gonadal development was counted and recorded.

## RESULTS

A total of 173 males and 235 females were observed out of 408 samples examined. The sex ratio was 1:1.36 (male to female). The difference in sex ratio was not significant ($p > 0.05$) (Fig. 1). The GSI values in males during August – November were 3.109 to 5.630 after which the values decreased slowly reaching to minimum in July (1.072), while in females the high values during August – December were found to be 3.542 to 6.679. This suggests that male and female gonads mature during August – December, the peak value being in October (Table 1 and Fig. 2).

The highest gonadosomatic index value in males were 5.967 (Stage VI) and the lowest GSI value 1.256 were recorded during stage VII, GSI values increased slowly reaching to maximum in stage VI (5.967) and then suddenly dropped to 1.256 in stage VII, while in females the high value was 6.63 during stage VI and the lowest GSI value were 1.625 and 1.124 stages I and II respectively (Table 2 and Fig. 3).

In this study, seven stages of gonadal development were observed in male and female *P. maculatum.* These stages were:

**Ovarian stages**

**Stage I-** (immature virgin): Small, transparent, a bit asymmetrical, somewhat cylindrical, ova transparent and devoid of yolk deposition, Occupying less than half the length of the body.

**Stage II-** (Developing virgin): Slightly creamy to pale, a bit asymmetrical, half or a little more than half the length of the body.

**Stage III-** (Developing): Oviduct much reduced, granular appearance, occupying less than $1/3^{rd}$ of body cavity.

**Stage IV-** (Maturing): Yellow, oviduct further reduced, occupying nearly $2/3^{rd}$ of body cavities, ova still in the follicle.

**Stage V-** (Mature): Yellow, occupying $2/3^{rd}$ to $3/4^{th}$ of the body cavity, blood vessels ramifies over the surface.

**Stage VI-** (Ripe, Running): Occupy almost the whole of the body cavity, deep yellow in colour.

**Stage VII-** (Spent): Ovaries spent, bag like with some residual ova.

**Testicular stages**

**Stage I-** (Immature): Small, thin, whitish, a bit asymmetrical.

**Stage II-** (Developing): Whitish, elongated, about half of the body cavity.

**Stage III-** (Developing): More elongated, Vas difference widens but reduced.

**Stage IV-** (Maturing): Quite massive, pale whitish, blood capillaries visible.

**Stage V-** (Mature): Pale white, with seldom transverse grooves, viscous fluid oozes out from the cut surface.

**Stage VI-** (Ripe, Running): More elongated, the outer margins slightly wrinkles, milt expression

Table 1. GSI of *P. maculatum* in different months.

| Month | No. of males | ♂GSI % | No. of females | ♀GSI % |
|---|---|---|---|---|
| Jan. | 21 | 1.877 | 25 | 1.950 |
| Feb. | 30 | 1.970 | 29 | 2.316 |
| Mar. | 28 | 2.192 | 21 | 3.384 |
| Apr. | 21 | 1.854 | 32 | 1.597 |
| May | 6 | 1.569 | 5 | 1.249 |
| Jun. | 8 | 1.134 | 20 | 1.188 |
| Jul. | 6 | 1.072 | 13 | 1.401 |
| Aug. | 13 | 3.109 | 18 | 4.474 |
| Sep. | 3 | 3.315 | 17 | 3.542 |
| Oct. | 11 | 5.630 | 10 | 6.679 |
| Nov. | 18 | 4.964 | 17 | 5.146 |
| Dec. | 8 | 1.668 | 28 | 3.129 |
| Total | 173 | - | 235 | - |

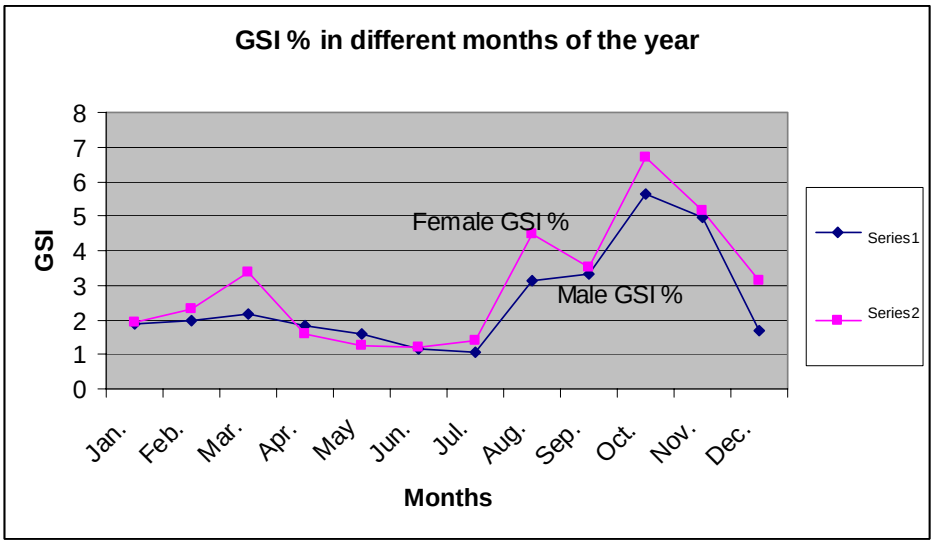


Fig. 2. GSI % of Male and Female in different Months.

Table 2. GSI values of male and female *P. maculatum* in different Gonadal developmental stages.

| Male Testicular Stages | No. of males | ♂GSI % | Female Ovarian Stages | No. of females | ♀GSI % |
|---|---|---|---|---|---|
| I | 59 | 2.017 | I | 39 | 1.625 |
| II | 32 | 1.483 | II | 50 | 1.124 |
| III | 26 | 1.783 | III | 43 | 1.943 |
| IV | 24 | 2.852 | IV | 53 | 2.819 |
| V | 13 | 4.391 | V | 18 | 3.909 |
| VI | 15 | 5.967 | VI | 23 | 6.63 |
| VII | 4 | 1.256 | VII | 9 | 2.647 |
| Total Male | 173 | | Total Female | 235 | |

by a moderate pressure.

**Stage VII-** (Spent): Testes shrunken, flaccid, grayish, no milt expression.

## DISCUSSION

The females were more than the males. However, the difference in sex ratio was not significantly different (P> 0.05) from the expected 1:1 distribution. Adebiyi (2013) reported the sex ratio of Sompat Grunt, *Pomadasys jubelini* of Lagos coast, Nigeria, which was in contrast to the result obtained in this study; the males were more than the females. However, the sex ratio of big eye grunt, *Brachydeuterus auritus* of Cape coast Ghana was reported by Asabere-Ameyaw (2001), in which females were more than males. This was similar to the sex ratio of *Pomadasys maculatum* in this study with no significant difference (P> 0.05) in the expected 1: 1 distribution. A sex ratio of 1:1.09 (Males to Females) was reported by Al-Ogaily and Hussain (1990) for the trout sweetlip grunt, *Plectorhynchus pictus*. The difference in sex ratio was not significantly different (P> 0.05) from the expected 1:1 distribution, which was similar to the sex ratio of *Pomadasys maculatum* observed in this study. In this study the sex ratio of *Pomadasys maculatum* was in favour of female dominance and there was no significant difference (P> 0.05) in the sex ratio. On the West coast of United Arab Emirates, striped piggy grunt, *Pomadasys stridens* had a sex ratio of 1:2.5 (Male to Female) (Al-Ghais, 1995). There were more females than male fish in the population, which was similar to the sex ratio of *Pomadasys maculatum* observed in this study from Karachi coast.

High gonadosomatic indices were recorded for both male and female *Pomadasys maculatum* in this study from August to December, which suggested that the spawning period of *Pomadasys maculatum* was August to December, the peak value being in October. The gonadosomatic index of *Pomadasys commersonnii* ranged from 0.4 – 5.5 % for both sexes and was high in July to November (Al-Nahdi *et al*., 2010). This was about similar

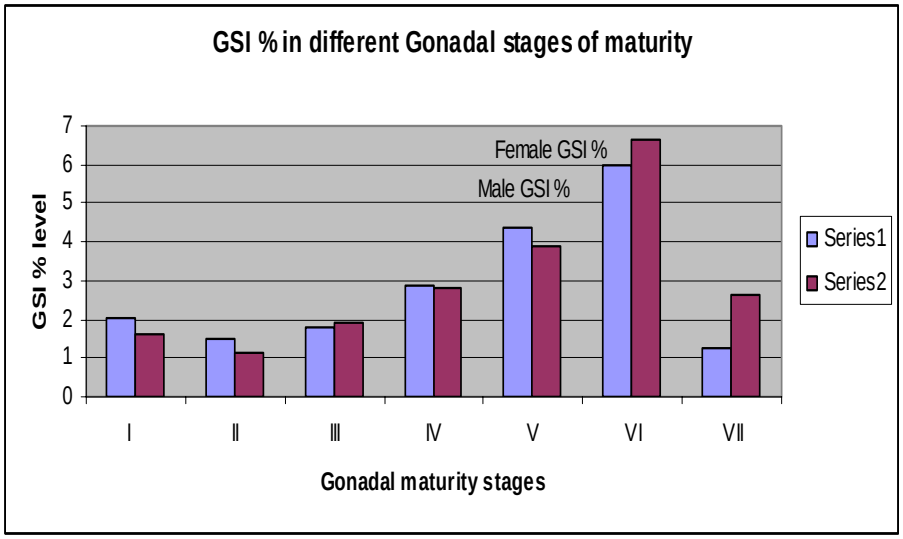


Fig. 3. GSI % of Male and Female in different Gonadal developmental stages.

to the results of the gonadosomatic index of *P. maculatum* observed in this study. Whereas in this study, the gonadosomatic index of *P. maculatum* was higher than that of *Pomadasys commersonnii*. High gonadosomatic indices were recorded for *P. jubelini* in July to September (Adebiyi, 2013). Bastard grunt *Pomadasys incisus* had a gonadosomatic index range of 0.159 - 7.880 and high gonadosomatic indices were observed in July to September (Fehri-Bedoui and Gharbi, 2008). According to Al-Ogaily and Hussain (1990) high GSI was recorded for trout sweet lip grunt, *Plectorhynchus pictus* from March to May. This was in contrast to the results obtained in this study. GSI of silver grunt, *Pomadasys argenteus* was highest in March and an additional small peak was observed in October in the females. High GSI values were observed in February to May in the males. The spawning periods of *Pomadasys argenteus* were February, April and October (Abu-Hakima, 1984). This was in contrast with the results of this study. Spawning occurred throughout the year in bastard grunt, *Pomadsys incisus* (Pajuelo *et al*., 2003). This was unlike the spawning period of *Pomadasys maculatum* observed in this study which was from August to December.

The stages of gonadal development observed in both male and female *Pomadasys maculatum* in this study were according to Nikolsky (1963) as stage I- immature, stage II- Developing, stage III- Developing, stage IV- Maturing, Stage V- mature, Stage VI- Ripe(Running) and stage VII- spent. In *Pomadasys jubileni* only three stages (Quiescent, Maturing and Mature stages) were observed (Adebiyi, 2013). This was unlike the stages of gonadal development observed in *Pomadasys maculatum* in this study. In *Pomadasys commersonnii* all the stages gonadal developments were observed in both male and female fish except the ripe running stage which was not encountered (Al-Nahadi *et al*., 2010). Fehri-Bedoui and Gharbi (2008) observed immature, resting, maturing, mature, spawning and spent stages of gonadal development in bastard grunt, *Pomadsys incisus.* Eight stages of gonadal development were observed in silver grunt, *Pomadasys argenteus* (Abu-Hakima, 1984). This study will be contribute valuable knowledge needed for fisheries management and aquaculture of *Pomadasys maculatum* by increasing the knowledge of reproductive biology of *Pomadasys maculatum.*

## ACKNOWLEDGMENTS

My sincere gratitude is extended to the staff members and fellow colleagues of the Centre (MRC & RC), Department of Zoology, University of Karachi and Department of Zoology, Sir Syed Govt. Girls College, Nazimabad, Karachi.

## REFERENCES

Abu-Hakima, R. 1984. Comparison of aspects of the reproductive biology of *Pomadasys otolithes* and *Pampus Sp*. In Kuwaiti water. Fish. Res. 2:177-200.

Adebiye, FA. 2013. The sex ratio, gonadosomatic index, stages of gonadal development and fecundity of Sompatgrunt. *Pomadasys jubelini* (Cuvier, 1830), Pakistan J. Zool. 45(1):41-46.

Al-Ghais, SM. 1995. Aspects of the biology of *Pomadasys stridens* Forskaal 1775 from the West coast of the United Arab Emirates. Arab Gulf J. Sci. Res. 13:401-419.

Al-Nahdi, A., Almarzouqi, Jayabalan, N. and Al-Habsi, S. 2010. Maturation and spawning of the small spotted grunt *Pomadasys commersonnii* (Lacepede, 1801) in the

Arabian Sea of Oman. Thalassas. 27:67-79.

Al-Ogaily, SM and Hussain, A. 1990. Biology of grunt *Plectorhynchus pictus* (Thunberg, 1972) (Haemulidae, Teleostei, Percoidei) from the red sea (Jizan area). Fish Res. 9:119-130.

Asabere-Ameyaw, A. 2001. Observations on the reproductive biology and recruitment of the big eye grunt *Brachydeuterus auritus* (Pisces: Haemulidae), in Ghana. J. Ghana Sci. Assoc. 3:14-21.

Bianchi, G. 1985. Field guide to the Commercial marine and brackish water species of Pakistan. FAO, Rome. pp22.

Cochran, WG. 2007. Sampling techniques. John Wiley and Sons, New York, USA.

Dadzie, S. and Wangila, BCC. 1980. Reproductive biology, length-weight relationship and relative condition of pond raised *Tilapia zilli* (Gervais). J. Fish Biol. 17:243-253.

Deshmukh, VM. 1973. Fishery and biology of *Pomadasys hasta* (Bloch). Indian Journal of fisheries. 20(2):497-522.

Fehri-Bedoui, R. and Gharbi, H. 2008. Sex ratio, reproduction and feeding habits of *Pomadasys incisus* (Haemulidae) in the Gulf of Tunis (Tunisia). Acta Adriat. 49:5-19.

Fisher, W. and Bianchi, SG. 1984. FAO species identification sheets for fishery purpose. Western Indian Ocean (vol. 2). FAO, Rome.

Hoda, SMS. 1985. Fishes from the Coast of Pakistan. Pakistan Aquaculture. **7**:38-44.

Hoda, SMS. and Iqbal, M. 1994. Some aspects of the reproductive biology of *Drepane longimana* (Family; Drapanidae) from Sindh coast. Pakistan Marine Research. 3(2):47-55.

Hoda, SMS. and Qureshi, N. 1993. Aspect of the reproductive biology of the mullet *Valamugil cunnesius* in Karachi, Sindh waters. J. Mar. Bio. Ass. India. 35:123-130.

Iqbal, M. 1989. A note on the population dynamics of *Pomadasys kaakan* (Haemulidae) from Pakistan. Fish byte. 7(3):4-5.

Khan, MA. and Hoda, SMS. 1993. Sex ratio of the sole, *Euryglossa orientalis* (Bal and Schneider) (Family: Soleidae) from Karachi coast. Pakistan Jr. Mar. Sc. 2(2):157-159.

Nikolsky, GV. 1963. The ecology of fishes. Academy Press, London and New York.

Pajuelo, JG., Lorenzo, JM., Gregoire, M. and Dominguez-Seoane, R. 2003. Life history of the *Pomadasys incisus* (Osteichthyes: Haemulidae) of the Canarian archipelago. Sci. Mar. 67:241-248.

Vicentini, RN. and Araujo, FG. 2003. Sex ratio and size structure of *Micropogonias furnieri* (Desmarest, 1823) (Perciformes, Sciaenidae) in Sepetiba bay, Rio de Janeiro. Brazil. Braz. J. Biol. 3:559-566.

Received: July 30, 2013; Revised: Sept 25, 2013;
Accepted: Sept 26, 2013

SENRA Academic Publishers, British Columbia
Vol. 8, No. 1, pp. 2727-2731, February 2014
Online ISSN: 1920-3853; Print ISSN: 1715-9997

Canadian Journal of pure&applied sciences

# OCCURRENCE OF BLACK SPOT DISEASE IN *LABEO ROHITA* (HAMILTON) FRY IN CARP FISH HATCHERY LAHORE, PAKISTAN

*Zafar Iqbal[1], Sonia A Shukerova[2] and Imtiaz K Minhas[3]
[1]Department of Zoology, University of the Punjab, Quaid-E-Azam Campus, Lahore
[2]Department of Ecology and Protection of Environment
Agricultural University, Plovdiv, Mendeleev 12, 4000 Plovdiv, Bulgaria
[3]Fisheries Department, Sanda Road Lahore, Pakistan

## ABSTRACT

Two hundred fry of *Labeo rohita* were obtained from Central Fish Seed Hatchery Lahore. The mean total length of fry was 20.47 mm. The fry were examined to be infected with metacercaria of a digenetic fluke *Posthodiplostomum cuticola*. The infection resulted in the formation of black spots on the skin of fry. This infection is commonly called as a Black spot disease or Posthodiplostomasis in fish. The prevalence of *P. cuticola* was 100% and mean intensity of infection was 4.495. The size of metacercaria varied from 0.70 - 0.98 mm. A moderate significant relationship existed between the total length of the fry and number of black spots ($r^2 = 0.15$). The black spots were randomly distributed on the body of fry. The ventral side of the fry (Section-I); was having a significantly higher number of the black spots than the dorsal side (Section II) ($\chi^2 = 3.75$; P = 0.05). No skeletal deformation was observed in the infected fry. The black spot disease in *L. rohita* fry, its relationship to pond management and control is discussed.

**Keywords**: *Posthodiplostomum cuticola*, black spot disease, *Labeo rohita*, fry, control.

## INTRODUCTION

*Posthodiplostomum cuticola* is a digenetic fluke. Adult *P. cuticola* lives in the intestine of piscivorous birds of family Ardeidae, such as common heron, *Ardea cinerea* L. purple heron *Ardea purpurea* L. squacco heron *Ardeola ralloides* (Mierzejewska *et al*., 2004). The eggs of *P. Cuticola* are released into the water with bird's feces and hatch into free living larvae, miracidia. The miracidia enters into aquatic snail *Planorbis planorbis* and *Planorbis carinatus* the first intermediate host of this fluke. In the snail miracidia produce numerous sporocysts, which develop into furcocercaria. Furcocercaria leaves the snail and burrows into the skin and fins of the fish, the second intermediate host. The infection in fish by metacercaria results in the formation of black spots on the skin and fins of fry. Hence, this infection is commonly called as a Black spot disease or Posthodiplostomasis in fish. It is common disease in earthen bottom ponds and lakes. Once the infected fish is eaten by bird, the metacercariae develops into an adult fluke in the intestine of the bird (Anon, 2010).

The black spot or the cyst accumulates black pigment cells (Mierzejewska *et al*., 2004). Juvinle and young fish are more susceptible to infection. The black spot disease is not deadly to fish in general. However, the disease easily spread throughout the pond quickly. The *P. cuticola* infection is common in many species of fish, primarily cyprinids (Bauer *et al.,* 1973; Mierzejewska *et al.,* 2004; Rolbiecki, 2004; Zrnici *et al,.* 2009). Infected fish show symptoms like; weight reduction, pathological changes in the blood, backbone and musculature deformation, kidney and liver dystrophy, appetite of fish is poor and it often die (Williams and Jones, 1994; Rolbiecki, 2004). The aim of this study was to investigate *P. cuticola* infection in *L. rohita* fry and to evaluate parasitological indices such as prevalence and mean intensity of infection and suggest control measures for this infection.

## MATERIALS AND METHODS

The infected *L. rohita* fry were collected from a fry rearing cemented tank (earthen bottom) located at Central Fish Seed Hatchery, Lahore, during October 2001. The fry were brought live in polyethylene bag in pond water to the Fish Pathology Laboratory, Fisheries Research and Training Institute, Lahore (FR&TI) and kept in 40 liters glass aquaria in aerated water. Two water samples were taken and analyzed at Water quality Laboratory at FR&TI, according to APHA (1992) protocol. The snails were also collected from the pond bottom and identified according to Huet (1974). The water plants present in the pond were also collected for identification. Total length of fry ranged from 15 to 27mm, mean 20.47mm.

In order to better visualize the parasite distribution and to

*Corresponding author email: dr.zafariqbal.pu@gmail.com

improve statistical treatment the body of fry was divided into two sections. Section-I covered the area from the middle of the fry upwards. Section-II covered area from middle of the fry downwards (Fig. 1). The number of black spots was counted from Section-I and Section-II of the fry on both left and right side.

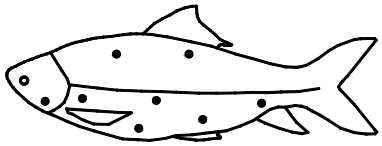

Fig. 1. Location of black spots on *Labeo rohita.*

The cysts were removed from the fish with the help of scalpel and opened with needles to expose the metacercaria. The metacercaria were fixed in 4% hot formalin, and preserved in 70% ethanol and stained with iron acetocarmine dehydrated in an alcohol series, cleared in eugenol and mounted in Canada balsam (Bauer *et al*., 1973; Moravec *et al*., 1991). The mounted worm were measured with the help of eye piece graticule fitted in the microscope and were photographed. Two cattle egret (*Bubulcus ibis* L.), from the fish hatchery complex were obtained and dissected. One mature *P. cuticola* worm was recorded from the intestine of one bird. The prevalence and mean intensity of infection was calculated according to Margolis *et al*. (1982). The differences between numbers of black spots in Section-I and Section-II of the body of fry were tested for statistical significance with the Chi square test. The relationship between the number of black spot/cyst and total length of fry was calculated by regression analysis.

## RESULTS

### 1. Management of Infected pond

The infected fry sampling tank measured 62 x 31 x 1.40m. The pond has earthen bottom and cemented vertical walls. Organic manure (cow dung) and inorganic fertilizer (Urea) are added to the pond to maintain productivity in the pond before and after stocking of fry. The pond was supplied with ground water through electric tube-well. The water quality parameters of the pond water (water temperature, dissolved oxygen, pH, total hardness and total alkalinity) are given in table 1. The pond had thick vegetation of aquatic plants; *Hydrilla* sp. and *Vallisneria* sp. spread throughout the pond. The visibility through water was 30.5-35.5cm in various parts of the pond. The snails, *Planorbis* sp. and *Lymnaea* sp. were also obtained from the pond. However, the snail population could not be estimated due to sampling difficulties at the pond bottom.

### Infection of *Labeo rohita* with *Posthodiplostomum cuticola*

In total 200 fry were examined and all were infected. The prevalence was 100% mean total length of fry was 20.47mm. The total length of the fry ranged from 15 to 27mm. The fry with total length 17, 18, 23, 24 and 25mm were not present in the sample (Table 2). A total of 899 black spots were recorded on 200 fry. The mean number of black spots per fry was 4.49 ± 1.53. The mean number of black spots increased with the rise in the total length of the fry (Table 2). The fry were divided into three groups with different length range, to observe the infection pattern of *P. cuticola* (Table 3). Second length group (19-22mm) was the most prominent as it comprised 60% of all the fry examined (Table 2). There was a statistically significant difference in the mean intensity with the existing length groups of the fry. A positive correlation between number of black spots and total length of the fry existed. The regression equation can be expressed as under;

No. of black spots =1.18143 + 0.161874 Length ($r^2$ = 0.15)

The length of metacercaria ranged from 0.70 – 0.98mm (Fig. 2) and diameter of the black spot/cyst was 0.79-1.01mm. The mature worm obtained from egret was 3.50mm in length (Fig. 3). No abnormality in the body shape of any fry was observed. However, the fry with

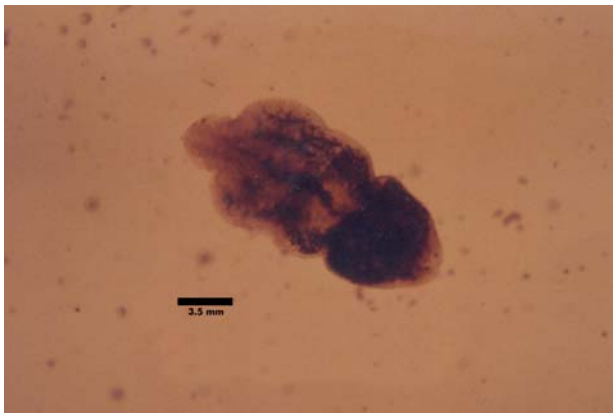


Fig. 2. A metacercaria of *Posthodiplostomum cuticola* from *Labeo rohita* fry.


Fig. 3. A mature *Posthodiplostomum cuticola* from *Bubulcus ibis.*

Table 1. Water quality parameters of infected fry rearing pond.

| Transparency of water (cm) | Temp. °C | Dissolved oxygen mg/l | pH | Alkalinity mg/l | Total hardness mg/l |
|---|---|---|---|---|---|
| 30.5-35.5 | 21.5 | 6.95 | 8.60 | 287 | 1560 |

Table 2. Occurrence of black spots in *Labeo rohita* fry.

| S. No. | Total Length (mm) | No. of Fry | Total no. of black spots | Mean No. Black spots/fry | Black spots on Section-I | Black spots on Section-II |
|---|---|---|---|---|---|---|
| 1 | 15 | 30 | 97 | 3.23±0.858 | 30 | 67 |
| 2 | 16 | 10 | 37 | 3.70±0.483 | 13 | 24 |
| 3 | 19 | 40 | 172 | 4.30±1.264 | 49 | 123 |
| 4 | 20 | 40 | 190 | 4.75±1.970 | 58 | 132 |
| 5 | 21 | 12 | 58 | 4.83±1.585 | 15 | 43 |
| 6 | 22 | 28 | 138 | 4.93±1.864 | 47 | 91 |
| 7 | 26 | 24 | 122 | 5.08±0.829 | 37 | 85 |
| 8 | 27 | 16 | 85 | 5.31±0.793 | 27 | 58 |
| Total | | 200 | 899 | 4.495±1.533 | 276(30.70%) | 623(69.30%) |

Table 3. Mean intensity of *P. cuticola* in three length groups of *L. rohita* fry.

| Length Group | No. of fry | Mean total length (mm) | No. and range of black spots | Mean Intensity | Black spots on Section-1 | Black spots on Section-II |
|---|---|---|---|---|---|---|
| 1(15-16mm) | 40 | 15.25±0.438 | 134(1-4) | 3.350 | 43 | 91 |
| 2(19-22mm) | 120 | 20.23±1.150 | 558(2-8) | 4.650 | 69 | 389 |
| 3(26-27mm) | 40 | 26.40±0.496 | 207(4-6) | 5.175 | 64 | 143 |
| Total | 200 | 20.47±3.668 | 899(1-8) | 4.495 | 276 | 623 |

higher number of black spots on the body were more conspicuous and showed slow swimming movement and looked lethargic. The black spots were present randomly on both left and right side of the body of the fry. Section-I and Section–II of the body of the fry had 30.70% and 69.30% black spots respectively and it was significantly different ($\chi^2$=3.75; P = 0.05) (Table 3).

## DISCUSSION

Black spot disease was investigated in *L. rohita* fry. The causative agent of this disease is *P. cuticola*, which is commonly found in many freshwater fish families like, Cyprinadae, Percidae, Ecocidae, Acipenseridae. Siluridae (Bykhovskaya-Pavlovskaya *et al.*, 1964). *Posthodiplostomum cuticola* is widely distributed in Europe and over 50 fish species are thought to be potential hosts (Hoole *et al*., 2001). The infection level was 100% and mean intensity 4.495. Whereas, Shukerova (2005) reported low prevalence and mean intensity (8.33%, 0.39) of *P. cuticola* in *Carassius gibelio*. Shukerova *et al*. (2010) observed low prevalence (0.6%) of *P. cuticola* in perch, *Perca fluvitalis.* In another study Shukerova and Kirin (2008) reported high prevalence and mean intensity (92.22%, 8.58 ±7.80) of *P. cuticola* from rudd, *Scardinius erythrophthalmus.* Our results are comparable to Zrncic *et al.* (2009) who reported 47.83-100% infection of *P. cuticola* in some freshwater fishes.

The present study is first documented report of *P.cuticola* infection in *L. rohita* from Pakistan. Shukerova (2005) reported *P. cuticola* in prusian carp, *C. gibelio* for the first time in Bulgaria. *Posthodiplostomum cuticola* infection in eight freshwater fishes was reported by Zrncic *et al.* (2009). Infection of *Abramis brama*, *Rutilus rutilus* and *Cyprinus capio* fry with *P. cuticola* in rearing ponds has also been reported. However, the susceptibility of *P. cuticola* infection decreases with age of the fish (Bauer *et al*, 1973). Infection of *P. cuticola* in commercial fishes like *Catla catla* (Ganapati and Rao, 1962) silver carp, *Hypophthalmichthys molitrix,* grass carp *Ctenopharyngodon idella* (Bauer *et al*., 1973) and now in *L. rohita* can cause losses in fish farms. *Labeo rohita* is a popular food fish in Pakistan. This fish has high fecundity and Gondosometic index (Iqbal and Batool, 2013) and grow fast in polyculture system in ponds. Being a highly commercial fish, its health status is of great concern to the fish farmers and hatchery managers. Khan *et al*. (2011) and Iqbal *et al*. (2013) has reported that some commercially important fishes like *L. rohita* are

declining in natural waters of the Province of Punjab, Pakistan; due to high population of invasive exotic species and other factors. The infection such as lernaeasis, abdominal dropsy and aspergillomycosis has been reported in *L. rohita* from fish ponds (Iqbal *et al*., 2001; Minhas *et al*., 2001; Iqbal *et al*., 2012).

No skeletal abnormality was observed in the infected fry, which indicates that, the infection was recent. However, the black spots can be quite pathogenic if they are located in sensitive areas like gills. Gill infection leads to respiratory problems (Hoole *et al*., 2001) and the fish with eye infection may be blinded. Heavily infected fry experience retarded growth, physiological stress and even death. The disturbed coordination of infected fry reduces its mobility and makes it easy prey for the birds the final host of *P. cuticola* (Bauer *et al*., 1973). This mechanism, hence facilitate transmission of parasite from fish to bird. This view has also been discussed by Ondrackova *et al*. (2006) and Zrncic *et al*. (2009).

The pond water was alkaline and within the normal range required for carp culture (Boyd and Tucker, 1998; Ali *et al*., 2001). High prevalence of *P. cuticola* in *L. rohita* fry may be associated to the snails and egrets populations in and around the pond. The rich organic sediment of pond, abundance of decomposers and aquatic plants probably made the pond environment suitable for snail to multiply and facilitated the completion of digeneans life cycle (Garg *et al*., 2009). Habitat degradation increases the incidence of black spot disease (Steedman, 1991) and high prevalence and abundance of *P. cuticola* infection in fish in water bodies is associated with thick vegetation (Ondrackova *et al*., 1999). Hence, the environmental conditions observed in infected pond were important factors which supported high parasitic infection in fry. The control of snails and fish eating birds is essential to minimize black spot disease. The eradication of snails is difficult because they can escape themselves from chemicals by burrowing into substrate (Brown, 1991). However, birds can be driven off. These steps can prevent further infection, but it takes years for black spot to eliminate from the fish (Lane and Morris, 2000). It may be concluded that the infection of *P. cuticola* in *L. rohita* fry may be linked to the organically rich pond bottom, decomposers and aquatic plants, snail and egrets populations in and around the pond.

## ACKNOWLEDGEMENT

We are grateful to Nasreen Ijaz for helping in water analysis, Tariq Rashid for identification of aquatic plants, Ishfaq Ahmad for drawing the figure of infected *L. rohita* and Mr. A. Rehman for assistance in coloured figures (CMYK work).

## REFERENCES

Anon. 2010. Black spot. National Fisheries Technical Team Fish Health, Aging and Species. Environment Agency Bromholme Lane, Brampton. Huntingdon. UK. pp1-2.

APHA. 1992. American Public Health Association. Standard Methods for Examination of Water and Waste water (18th edi.). Washington DC, USA.

Ali, A., Ali, A., Ayub, M., Abidi, SZA. and Khan, MN. 2001. Water quality profile of fish farms in various ecological zones of Punjab. Pak. J. Fish. 1(1):89-94.

Bauer, ON., Musselius, V. and Stsrelvok, YUA. 1973. Diseases of Pond Fishes. Israel Program for Scientific Translation. Keter Press Jerusalem, Israel.

Boyd, CE. and Tucker, CS. 1998. Pond Aquaculture water quality Management (2nd edi.). Rashtriya Printers. New Delhi, India. 1-130.

Brown, KM. 1991. Mollusca: Gastropoda. In: Ecology and classification of North American freshwater invertebrate. Eds. Thorp, JH. and Covich, AP. Academic Press. California, USA. 285-314.

Bykhoskaya-Pavlovskaya, IE., Gusev, AV., Dubinina, MN., Izyumova, NA., Smimova, TS., Sokolovskaya, IL., Shietin, GA., Shulman, SS. and Epstein, VM. 1964. Key to Parasites of freshwater Fish of USSR. Academy of Sciences USSR. Zoology Institute. 239-245.

Ganapati, PN and Rao, KM. 1962. Ecological and life history studies on strigeid metacercaria (Trematode Diplostomatidae) from freshwater fishes of Andhra Pradesh. Parasitology. 52:519-525.

Garg, RK., Rao, RJ. and Saksena, DN. 2009. Correlations of Molluscan diversity with physico-chemical characteristics of water of Ramsagar reservoir, India. Int. J. Biotechnol. Conservation. 1(6):202-207.

Hoole, D., Bucke, D., Burgess, P. and Wellby, I. 2001. *Diseases of Carps and other Cyprinid Fishes*. Fishing News Books, Oxford. England. pp264.

Huet, M. 1974. Text Book of Fish Culture, Breeding and cultivation. Fishing News Books, Oxford, England. pp 470.

Iqbal, Z., Minhas, IK. and Khan, MN. 2001. Seasonal Occurrence of Lernaeasis in pond Aquaculture in Punjab. Proc. of 21st Pakistan Cong. Zool. 21:159-168.

Iqbal, Z., Sheikh, U. and Mughal. R. 2012. Fungal Infections in some Economically Important Freshwater Fishes. Pakistan Vet. J. 32(3):422-426.

Iqbal, Z., Pervaiz, K. and Javid, MN. 2013. Population Dynamics of *Tor macrolepis* (Teleostei: Cyprinidae) and

other Fishes of Attock, Region Pakistan. Canadian Journal of Pure and Applied. Sciences. 7(1):2195-2201.

Iqbal, Z. and Batool, A. 2013. Fecundity of *Labeo rohita* (Teleostei: cyprinidae) reared in earthen pond in Lahore. Canadian Journal of Pure and Applied Sciences. 7(2): 2391- 95.

Khan, AM., Ali, Z., Shelly, SY. and Mirza, MR. 2011. Aliens: a catastrophe for native freshwater fish diversity in Pakistan. J. Anim. Plant. Sciences. 21:435-440.

Lane, RL. and Morris, JE. 2000. Biology, prevention and effects of common grebs (digenetic trematodes) in freshwater fish. Tech. Bull. Series Iowa State University. 5:1-6.

Margolis, L., Esch, GW., Holmes, JC., Kuris, AM. and Schad, GA. 1982. The use of Ecological terms in Parasitology (Report of an Adhoc Committee of the American Society of Parasitologists). J. Parasit. 68(1):131-132.

Mierzejewska, K., Wlasow, T., Anita, K. and Szymanczyk, K. 2004. Fish digeneans from seven Islands Ornithological reserve at Oswin lake Poland. Part1. *Posthodiplodtomum cuticola* van Nordmann, 1832. Acta Ichthyologica Et. Piscatoria. 34(1):73-84.

Minhas, IK., Iqbal, Z. and Khan, MN. 2001. Occurrence of Abdominal dropsy in culturable fish species in Punjab. Proc. of 21st Pakistan Cong. Zool. 21:169-174.

Moravec, F., Nasincova, V. and Scholz, T. 1991. Methods for Investigations of Endoparasitic Helminths. Training Course on Fish Parasites. Institute of Parasitology, Czechoslovak Academy of Sciences. Ceske Budvjovice. 30th Sept.-13th Oct. 1991. pp1-27.

Ondrackova, M., Dykova, I. and Jurajda, P. 1999. Posthdiplostomatosis of cyprinidae. Helminthologia. 36:125-132.

Ondrackova, M., Davidova, M., Gelnar, M. and Jurajda, P. 2006. Susceptibility of Prussian carp infected by metacercariae of *Posthdiplostomum cuticola* (v. Nordmann, 1832) to fish predation. Eco. Res. 21:526-529.

Rolbiecki, L. 2004. Distribution of *Posthodiplostomum cuticola* (Nordmann, 1832) metacercaria in cyprinids of the Vistula Lagon, Poland. Arch. Polish Fish. 12(1):93-98.

Shukerova, S. 2005. Helminth fauna of the Prussian carp, *Crassius gibelio* (Bloch, 1782) from the Srebarna Bioshere Reserve. Trakia J. Sci. 3(6):36-40.

Shukerova, S. and Kirin, D. 2008. Helminth communities of the rudd, *Scardinius erythrophthalmus* (Cypriniformes, Cyprinidae) from Srebarna Biosphere Reserve, Bulgaria. J. Helminth. 82:319-323.

Shukerova, S., Kirin, D. and Hanzelová, KV. 2010. Endohelminth communities of the perch, *Perca fluviatilis* (Perciformes, Percidae) from Srebarna Biosphere Reserve, Bulgaria. Helminthologia. 47(2):99-104.

Steedman, RJ. 1991. Occurrence and environmental correlates of black spot disease in stream fishes near Toronto, Ontario, Trans. Am. Fish. Soc. 120:494-4999.

Williams, H. and Jones, A. 1994. Parasitic worms of Fish. Taylor and Francis, London. pp593.

Zrncic, S., D. Oraic, D., Mihaljevic, Z., Caleta, M., Zanell, D., Jelic, D. and Jelic, M. 2009. First observation of *Posthodiplostomum cuticola* (Nordmann, 1832) metacercaria in Cypriniformes from Crotia. Helminthologia. 46(2):112-116.

Received: June 3, 2013; Accepted: Sept 25, 2013

SENRA Academic Publishers, British Columbia
Vol. 8, No. 1, pp. 2733-2738, February 2014
Online ISSN: 1920-3853; Print ISSN: 1715-9997

Canadian Journal of pure&applied sciences

**Short communication**

# SOYBEAN FORTIFICATION OF MAASA: A GHANAIAN FERMENTED MILLET-BASED CAKE

*James Owusu-Kwarteng and Fortune Akabanda
Department of Applied Biology, Faculty of Applied Sciences, University for Development Studies
PO. Box 24, Navrongo Ghana

## ABSTRACT

Fortification of commonly consumed cereals with inexpensive plant protein sources such as soybeans has been exploited to improve the protein quality of staple foods through a mutual complementation of their limiting amino acids. In Ghana and other parts of West Africa, millet is used for the processing of many traditional fermented foods including maasa. The purpose of this study was to assess the effect of soybean fortification on the fermentation characteristics and proximate composition of fermented millet dough as well as consumer acceptability of maasa produced from different soy-millet blends. Maasa samples were prepared from a blend of steeped pearl millet grains and pre-soaked, blanched, hand dehulled soybean added at 0, 10, 20, 30 and 40% replacement levels. The millet-soybean blends were wet-milled, formulated into a dough, spontaneously fermented for 14 h and fried into cake known as maasa. During spontaneous fermentation, samples were analyzed for pH, total titratable acidity, microbial counts and proximate composition. Finally, maasa prepared from the fermented millet-soybean blends were assessed for consumer acceptability using a nine point hedonic scale. There was a general decrease in pH from 5.4-5.5 to 3.9-4.1 pH units and an increase in titratable acidity from 0.10-0.30 to 0.58-1.26 (%lactic acid) during the 14 h fermentation period. Lactic acid bacteria and yeast counts reached 9.7 and 8.0 logcfu/g respectively. Crude protein and fat contents increased with the addition of soybeans whereas carbohydrate content reduced. Consumer sensory evaluation showed that fortification with 20% soybean positively affected taste, colour, texture and the overall acceptability of maasa. Therefore, soybean can be used to fortify the Ghanaian millet-based maasa to improve nutrient quality and acceptability of maasa by replacing 20% of the millet with soybeans prior to milling and fermentation.

**Keywords**: Millet, soybeans, fortification, fermentation, maasa.

## INTRODUCTION

Cereal grains serve as an important source of dietary proteins, carbohydrates, vitamins, minerals and fiber. Millet grains, one of such important cereal crops, remains a major source of calories and forms a vital component of the food security in the developing world (FAO, 1996). Throughout Africa, millet is processed into many different staples through fermentation. In Ghana, millet grains serve as the raw material for the processing of various fermented foods such as koko (Lei and Jakobsen, 2004), fura (Owusu-Kwarteng *et al*., 2012), and maasa (Owusu-Kwarteng and Akabanda, 2013). Maasa is processed and consumed throughout the country, especially in communities of northern Ghana extraction and Muslim dominated areas. Maasa is popularly consumed as an adjunct to breakfast porridges or may be consumed alone as food (Owusu-Kwarteng and Akabanda, 2013).

Despite the widespread use and dependence on millet and other cereals in tropical Africa, they are considered to be of lower nutritive value due to their low protein content and limitations in certain essential amino acids such as lysine, and also the presence of some antinutritional factors (Chavan and Kadam, 1989).This has therefore necessitated the need to investigate various methods of processing aimed at improving the nutritional quality and acceptability of traditional cereal-based foods. In this light, fortification ofthe cereals with soybeans (which is high in both proteins and lysine) is one method which has been exploited in many developing countries over the years. During such cereal-legume blends, protein quality of the staple is complimentary enhanced through the contribution of high protein and lysine by the legume and methionine by the cereal (Afoakwa*et al*., 2002). Several cereal-legume blends for staples foods have been developed with varying degrees of success. Fortification of the Ghanaian fermented maize dough with soybeans has been investigated (Plahar *et al*., 1997). It was found that the addition of boiled whole soybeans to soaked maize grains before milling and fermentation was the most appropriate and cost-effective technique for household, small-scale and medium scale operations

*Corresponding author email: jowusukwarteng@yahoo.co.uk

(Plahar *et al*., 1997).

The purpose of this investigation was to assess the influence of soybean fortification on the fermentation characteristics and proximate composition of spontaneously fermented millet dough. Maasa produced from different soy-millet blends at different fortification levels were also evaluated for consumer acceptability. This is geared towards improving nutritional value maasa and therefore the nutritional security of consumers.

## MATERIALS AND METHODS

*Cereal and legume grains*

The local variety of pearl millet (*Pennisetumglaucum*) and *Salinatum* variety of soybeans were both purchased from a local retail outlet in Navrongo market, Ghana. They were cleaned and stored at ambient temperature (29±1°C) until they were used.

*Preparation of traditional unfortified and soy-fortified maasa*

The processing of unfortified and soy-fortified maasa is shown in figure 1. The processing of traditional unfortified maasa involved steeping 2 kg of cleaned millet grains in 3L de-mineralized water for 12 h. After steeping, the millet grains were washed and excess water drained off. After draining, the millet grains were milled using a plate attrition mill (model: No 2A – Amuda grinding mill) to obtain a wet milled dough. The dough samples were then divided into two portions of two-thirds (⅔) and one-third (⅓). The ⅓ portion was used to prepare a 30% (w/v) slurry, cooked into a pre-gelatinized meal and mixed with the ⅔ portion to obtain a thick paste. The mixture was then allowed to spontaneously ferment for 14 h. The fermented paste was fried (in portions of about 100 g) in oil for approximately 5 min to obtain maasa. For soybean fortification, portions of millet grains were replaced with separately weighed soybeans at 0, 10, 20, 30 and 40 % replacement levels. The soybeans were pre-soaked in de-mineralized water for 2 hours and boiled for 20 min to inactivate trypsin inhibitor activity and reduce be any flavor (Plahar *et al*., 1997). The boiled beans were hand dehulled by rubbing in cold water. The dehulled soybeans were then mixed with the decanted soaked millet grains prior to milling and fermentation (Fig. 1).

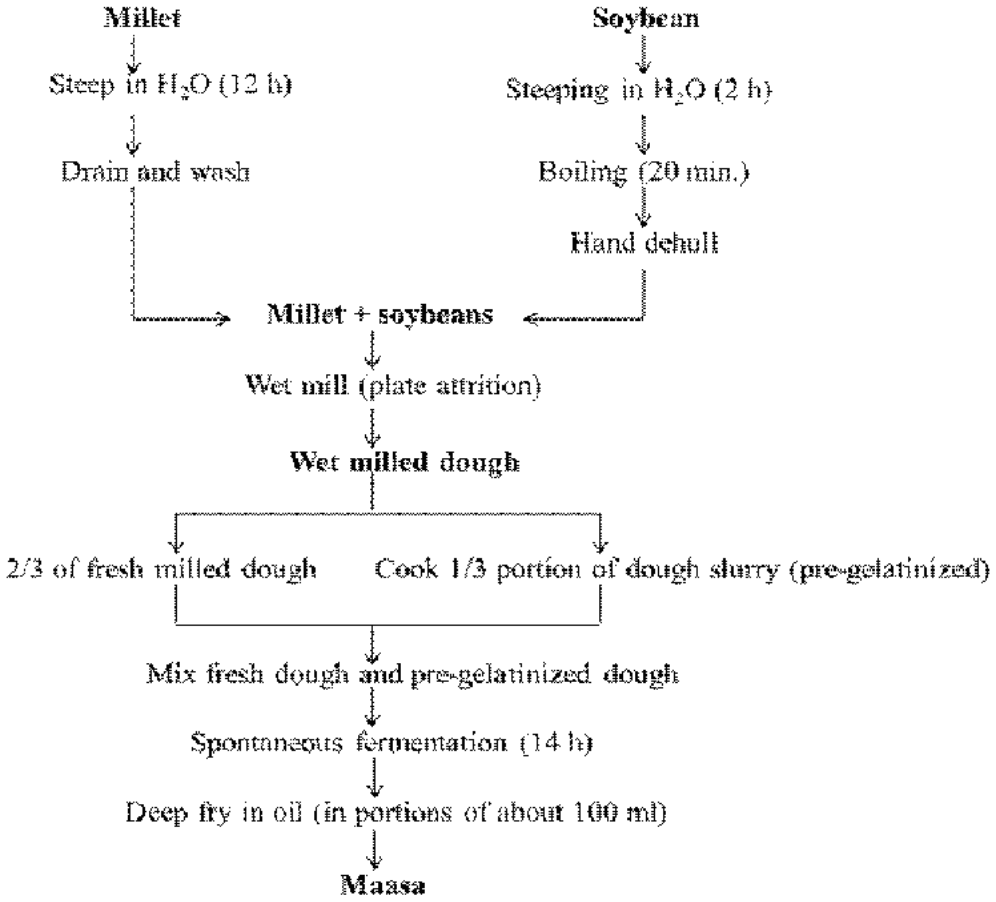


Fig. 1. Processing of soybean fortified maasa.

*Determination of dough acidity*

Titratable acidity and pH of unfortified and soy-fortified millet were determined in 10% (w/v) slurry of dough samples. Particles in the slurry were kept in suspension by stirring for 15 min and filtered. Ten milliliter aliquots of the filtrate were then titrated 0.1 N NaOH standard solution to determine the total titratable acidity, while pH was measured using a pH meter (CrisonBasic, model 20) calibrated with standard buffers. Acidity was expressed as lactic acid based on the conversion of 1 ml of 0.1 N NaOH being equivalent to 9.008 x $10^{-3}$ g lactic acid (Annan *et al*., 2005).

*Microbiological analysis*

Duplicate 10 g samples of fermenting dough were homogenized with 90ml sterile peptone physiologicalsaline solution (5g bactopeptone, 8.5g NaCl, 1000ml distilled water, pH 7.0 ± 0.2). The homogenate wasserially diluted in the $10^{-9}$ concentration and 0.1ml aliquots of the dilutions directly inoculated by surface plating on different isolation media. Lactic acid bacteria were isolated on MRS agar (Merck, Darmstadt, Germany). Plates were incubated anaerobically (BBL gas pack, Anaerocult A, Merck) at 30°C for 48h. Aerobic mesophilic bacteria were enumerated on Plate count agar (PCA) (Oxoid Ltd, Basingstoke, Hampshire, England), pH 7.0 and incubated at a temperature of 32°C for 48 h. Sabour and Dextrose Agar (Merck), supplemented with250mg/100ml chloramphenicol (selective supplement, Oxoid) with pH adjusted to 3.5 with tartaric acid was used for the isolation and enumeration of yeasts. Inoculated plates were incubated at 25°C for 5 days. Following incubation, the number of colony forming units (cfu) per gram of sample was determined using a digital colony counter and recorded.

*Proximate analysis of unfortifiedand soybean-fortified fermented millet dough*

Proximate composition on dry matter basis was determined according to the AOAC (2000) methods. Crude protein content was determined using the Kjeldahl method (Method 960.52) (N × 5.83). Crude lipid content was determined using the Soxhlet extraction method (Method 920.39C). Ash content was determined by heating the dried sample in a furnace at 550°C (Method 923.03). Carbohydrate content was calculated by difference.

*Consumer sensory evaluation of maasa samples*

The final products (maasa) prepared from millet with different levels of soybean fortification were served to a 35member panel of judges (drawn from the Faculty of Applied Sciences of the University for Development Studies) who are familiarwith maasa. The panel evaluated the products for sensory qualities (taste, colour, odour, texture andoverall acceptability) using a nine-point hedonic scale (1 and 9 representing extremely dislike and extremely likerespectively). The judges were made to wash their mouths with clean water before and after evaluating each product.

*Statistical analysis*

All analyses were carried out in duplicates in two independent fermentation trials. Data obtained were subjected to one-way analysis of variance (ANOVA) and means were separated by Tukey's family error rate multiple comparison test ($P<0.05$).

## RESULTS AND DISCUSSION

*Dough acidity and microbial changes*

Changes in acidity and microbial counts of unfortified and soybean-fortified millet dough is presented in table 1. Differences in pH between unfortified and soybean-fortified millet dough samples were not significant ($p<0.05$). However, there were significantly higher levels of total acids expressed as percent lactic acid observed in soybean-fortified dough than in the unfortified dough samples. Similar observations of high titratable acidity in soybean fortified cereals have been observed for fermented millet and maize (Owusu-Kwarteng *et al*., 2010; Annan *et al*., 2005, Plahar*et al*., 1997). This observation has been attributed to a buffering effect from the higher content of soluble proteins and amino acids contributed by the beans in such soy-cereal blends (Annan *et al*., 2005; Nche *et al*., 1994; Plahar *et al*., 1997, 1983; Zamora and Fields, 1979). Thus, free fatty acids from soybeans may contribute significantly to soybean-fortified fermented millet dough as observed in table 1, where higher levels of total titratable acids were recorded in soybean-fortified millet than unfortified millet dough samples, even at time zero (0h), when fermentation had not started. In general, similar trends of acidification with fermentation time have been associated with several African fermented cereal-based foods (Owusu-Kwarteng *et al*., 2012; Sawadogo-Lingani*et al*., 2007; Vieira-Dalodé *et al*., 2007; Lei and Jakobsen, 2004; Muyanja *et al*., 2002; Hounhouigan *et al*., 1994).

Yeasts counts during millet dough fermentation increased from 4.9-54 to 7.6-8.0 log cfu/g after 14 h fermentation period. Counts were similar for both unfortified and soybean-fortified millet dough samples. Lactic acid bacteria counts however, significantly increased with the addition of soybeans (Table 1). An accelerated growth of lactic acid bacteria in fermenting cereals in the presence of amino acids has been reported (Gobetti *et al*., 1994; Spicher and Schroeder, 1978). Thus, the increased protein content of fermented millet as a result of soybean fortification may have contributed additional amino acids and thereby accelerating the growth of lactic acid bacteria. Additionally, interactions between yeasts and lactic acid bacteria during the production of fermented foods are suggested to involve a 'symbiotic' association due to a mutual growth stimulation based on their amino

Table 1. Acidity and microbial counts during spontaneous fermentation of unfortified and soybean fortified millet dough.*

| Acidity and microbial count | Fermentation time (h) | Level of soybean addition (%), by replacement | | | | |
|---|---|---|---|---|---|---|
| | | 0 | 10 | 20 | 30 | 40 |
| pH | 0 | 5.56±0.05[a] | 5.50±0.04[a] | 5.61±0.09[a] | 5.44±0.13[a] | 5.58±0.12[a] |
| | 14 | 4.08±0.07[a] | 4.01±0.04[a] | 3.91±0.15[a] | 3.88±0.11[a] | 4.03±0.17[a] |
| TTA (% lactic acid) | 0 | 0.10±0.02[a] | 0.17±0.04[b] | 0.21±0.04[c] | 0.24±0.03[d] | 0.30±0.04[e] |
| | 14 | 0.58±0.06[a] | 0.64±0.05[b] | 0.85±0.09[c] | 0.98±0.11[d] | 1.26±0.08[e] |
| LAB (logcfu/g) | 0 | 6.9±1.2[a] | 7.0±1.9[a] | 6.7±1.4[a] | 6.9±0.9[a] | 6.8±1.3[a] |
| | 14 | 8.0±0.7[a] | 8.9±1.3[b] | 9.2±1.9[bd] | 9.4±1.4[d] | 9.7±1.0[e] |
| yeast (logcfu/g) | 0 | 5.2±2.3[a] | 5.0±1.7[a] | 4.9±1.0[a] | 5.2±2.1[a] | 5.4±1.3[a] |
| | 14 | 7.8±1.5[a] | 7.6±0.9[a] | 8.0±1.7[a] | 7.6±1.3[a] | 7.7±1.6[a] |

*Values are means of duplicate determinations from two independent fermentation trials. Means with the same superscript in a row are not significantly different ($P< 0.05$)

Table 2. Proximate composition of unfortified and soybean fortified spontaneously fermented millet dough (dry matter basis)*

| Soybean addition (%), by replacement | Protein | Fat | Ash | Fiber | Carbohydrates |
|---|---|---|---|---|---|
| 0 | 11.2±0.4 | 4.9±0.7 | 1.6±0.2 | 4.2±0.5 | 77.8±0.7 |
| 10 | 14.6±0.6 | 5.2±1.2 | 2.1±0.1 | 3.6±0.3 | 74.5±0.6 |
| 20 | 18.4±0.5 | 5.7±0.4 | 2.4±0.3 | 3.1±0.3 | 70.3±0.8 |
| 30 | 22.0±1.1 | 6.1±0.4 | 2.6±0.2 | 2.5±0.6 | 66.8±0.8 |
| 40 | 25.5±0.9 | 6.2±0.2 | 2.9±0.2 | 2.1±0.4 | 63.4±0.5 |

*Values are means of duplicate determinations from two independent fermentation trials.

acids and carbohydrate metabolisms (Martinez-Anaya *et al*., 1990; Wood and Hodges, 1985). Thus, in a co-metabolism between yeasts and lactic acid bacteria, the bacteria provide the rapid acidic environment, which selects for the growth of yeasts, whereas the yeasts provide essential metabolites such as pyruvates, vitamins and amino acids to the bacteria (Gadaga *et al*., 2001; Steinkraus, 1996; Gobbetti *et al*., 1994; Leroi and Pidoux, 1993) and thereby accelerating the growth of the lactic acid bacteria. The faster growth of microorganisms and the accelerated acid production could be important in reducing fermentation time as well as positively affect safety and shelf stability of the product.

*Proximate analysis*

Crude proteins, fats and ash contents increased with the addition of soybeans whilst carbohydrates decreased (Table 2). The addition of 20% soybeans by replacement resulted in about 60.8% increase in protein content whilst the addition 30% soybeans by replacement resulted in a 100 % increase in the protein content of soybean-millet blends for maasa production.

Several studies have previously reported increased protein content in soybean fortified cereals and tubers, which make a very significant contribution towards the alleviation of protein-energy malnutrition (Kolapo and Sanni, 2005; Plahar *et al*., 1997, 1983; Sanni and Sobamiwa, 1994; Nout, 1993). Although soybean is known to contain some anti-nutritional factors which inhibit the availability of the desirable elements such as protein, these anti-nutritional factors can be destroyed through boiling and other processing methods (Loo, 1978; Enwere, 1998; Osho and Dashiell, 1998). Therefore,the incorporation of soybeans in the processing of maasa a cereal-based food of the rural poor and underprivileged communities in Ghana, will greatly contribute towards efforts aimed at alleviating protein-energy malnutrition, as animal protein is beyond the reach of many of these people.

*Consumer sensory analysis of maasa samples*

Consumer sensory evaluation of maasa produced from different soybean- millet blends is shown in Table 3. The addition of boiled whole soybeans to millet for maasa preparation did not significantly taste, texture and overall acceptability at 10 and 20% fortification levels but were significantly and negatively affected beyond 20% soybean fortification level.

The odor was negatively affected whereas color improved with the addition of soybeans. Legumes such as soybeans

Table 3. Consumer sensory evaluation of unfortified and soy-fortified millet based maasa.

| Soybean addition(%) by replacement | Taste | Odour | Colour | Texture | Overall acceptability |
|---|---|---|---|---|---|
| 0 | 5.8±1.6[a] | 7.1±1.5[a] | 3.8±2.2[a] | 5.1±1.2[a] | 5.8±0.8[a] |
| 10 | 5.5±1.4[a] | 6.0±1.2[b] | 4.5±1.6[b] | 5.3±1.9[a] | 6.1±1.3[a] |
| 20 | 5.7±1.6[a] | 6.3±0.9[b] | 5.2±2.0[c] | 5.0±1.7[a] | 5.9±1.0[a] |
| 30 | 3.3±1.1[b] | 3.5±1.7[c] | 5.1±1.5[c] | 4.3±1.2[c] | 4.1±1.5[b] |
| 40 | 2.8±1.8[b] | 2.9±1.2[c] | 5.5±1.1[c] | 3.5±2.0[d] | 3.3±0.7[c] |

Means with same superscript in a column are not significantly ($p< 0.05$).

used in foods to enhance nutritional and functional qualities have often been found to alter the organoleptic qualities of the food. However, the addition of boiled whole soybeans at 20% fortification level prior to milling and fermentation was found to be appropriate for maasa processing and accepted by consumers.

## CONCLUSION

Soybean fortification accelerates the production of total acids and the growth of lactic acid bacteria during the fermentation of millet dough to produce maasa. This is significant in safety and stability since accelerated acid production contributes to the inhibition of pathogens and spoilage microorganisms. Again, protein quality of soy-millet blends improved with the addition of soybeans, and maasa produced by fortification of millet with 20% soybeans replacement level, prior to milling and fermentation was found to be most acceptable to consumers.

## ACKNOWLEDGEMENT

The work was carried out at the University for Development Studies (UDS)/DANIDA microbiology laboratory, Navrongo Ghana. Mr. Samuel Amponim Boadi is acknowledged for contribution to primary data collection.

## REFERENCES

Afoakwa, EO.,Sefa-Dedeh, S. and Cornelius, B. 2002. Optimization of the Nutritional Quality Characteristics of Cowpea-fortified Nixtamalized Maize using Computer-generated Response Surface Models. South African Journal of Clinical Nutrition. 15:17-19.

Annan, NT., Plahar, WA., Poll, L. and Jakobsen, M. 2005. Effect of soybean fortification on Ghanaian fermented maize dough aroma. International Journal of Food Science and Nutrition. 56(6):315-326.

AOAC. 2000. Official Methods of Analysis of AOAC International (17th edi.). AOAC. Gaithersburg, MD, USA.

Chavan, JK. and Kadam, SS. 1989. Nutritional improvement of cereals by sprouting. Critical Reviews in Food Science and Nutrition. 28(5):401-437.

Enwere, NJ. 1998. Foods of plant origin: Processing and utilization with recipes and technology profiles. Afro-Orbis Publications Ltd., Nsukka. pp301.

FAO. 1996. Sorghum and millet in human nutrition. FAO Food and Nutrition Series. Trends and Outlook. Patencheru, Andhra Pradesh, India.

Gadaga, TH., Mutukumira, AN. and Narvhus, JA. 2001. The growth and interaction of yeasts and lactic acid bacteria isolated from Zimbabwean naturally fermented milk in UHT milk. International Journal of Food Microbiology. 68:21–32.

Gobbetti, M., Corsetti, A. and Rossi, J. 1994. The sourdough microflora. Interactions between lactic acid bacteria and yeasts: metabolism of amino acids. World Journal of Microbiology and Biotechnology. 10:275-279.

Hounhouigan, DJ., Nout, MJR., Nago, CM., Houben, JH. and Rombouts, FM.1994. Microbiological changes in mawè during natural fermentation. World Journal of Microbiology and Biotechnology.10:410-413.

Kolapo, A. and Sanni, MO. 2005. Processing and characteristics of soybean- fortified tapioca. Journal of Women in Technology Education. 4:59-66.

Lei, V. and Jakobsen, M. 2004. Microbiological characterization and probiotic potential of koko and koko sour water, African spontaneously fermented millet porridge and drink. Journal of Applied Microbiology. 96:384-397.

Leroi, F. and Pidoux, M. 1993. Detection of interactions between yeasts and lactic acid bacteria isolated from sugary kefir grains. Applied Bacteriology. 74:48-53.

Loo, TG. 1978. Small-scale and home processing of soybeans with applications and recipes (Communication 64a). Department of Agricultural Research of the Tropical Institutite, Amsterdam. pp59.

Martinez-Anaya, MA., Pitarch, B., Bayarri, P. and Benedito de Barber, C. 1990. Micro flora of the sourdoughs of wheat flour bread. X. Interactions between

yeasts and lactic acid bacteria in wheat doughs and their effects on bread quality. Cereal Chemistry. 67:85-91.

Muyanja, CMBK., Narvhus, JA.,Treimo, J. and Langsrud, T. 2002. Isolation, characterization and identification of lactic acid bacteria from *bushera*: a Ugandan traditional fermented beverage. International Journal of Food Microbiology. 80:201-210.

Nche, PF., Odamtten, GT., Nout, MJR. and Roumbout, FM. 1994. Dry milling and accelerated fermentation of maize for industrial production of kenkey, a Ghanaian cereal food. Journal of Cereal Science. 20:291-298.

Nout, MJR. 1993. Processing weaning foods for tropical climates. International Journal of Food Science and Nutrition. 43:213-221.

Osho, O. and Dashiell, KE. 1998. Expanding soyabean production, processing and utilization in Nigeria. In: Post harvest Technology and Commodity Marketing. Proceedings of a Post Harvest Conference. Ed. RSB. Ferris. Accra, Ghana. 151-156.

Owusu-Kwarteng, J., Tano-Debrah, K., Glover, RLK. and Akabanda, F. 2010. Process characteristics and microbiology of fura processed in northern Ghana. Nature and Science. 8(8):41-51.

Owusu-Kwarteng, J., Akabanda, F., Nielsen, DS.,Tano-Debrah, K., Glover, RLK. and Jespersen, L. 2012. Identification of lactic acid bacteria isolated during traditional fura processing in Ghana. Food Microbiology. 32:72-78.

Owusu-Kwarteng, J. and Akabanda, F. 2013. Applicability of nixtamalization in the processing of millet-based maasa, a fermented food in Ghana. Journal of Food Research. 2(1):59-65.

Plahar, WA., Nti, CA. and Annan, NT. 1997. Effects of soy- fortification method on the fermentation characteristics and nutritional quality of fermented maize meal. Plant Foods for Human Nutrition. 51:365-380.

Plahar, WA., Leung, HK. and Coon, CN. 1983. Effects of dehydration and soy- fortification on physico- chemical, nutritional and sensory properties of Ghanaian fermented maize meal. Journal of Food Science. 48:1225-1259.

Sanni, MO. and Sobamiwa, AO. 1994. Processing and characteristic of soybean-fortified gari. World Journal of Microbiology and Biotechnology. 10:268-270.

Sawadogo-Lingani, H., Lei, V., Diawara, B., Nielsen, DS., Moller, PL., Traore, AS. and Jakobsen, M. 2007. The biodiversity of predominant lactic acid bacteria in dolo and pitowort for the production of sorghum beer. Journal of Applied Microbiology. 103:765-777.

Spicher, G. and Schroeder, R. 1978. The microflora of sourdough. IV. Bacterial composition of sourdough starters genus. Lactobacillus beijerinck Z LebensmUntersForsch. 167:342-354.

Steinkraus, KH. 1996. Hand book of indigenous fermented foods (2nd edi.). Marcel Dekker, New York, USA.

Vieira-Dalodé, G., Jespersen, L., Hounhouigan, J., Moller, PL., Nago, CM. and Jakobsen, M. 2007. Lactic acid bacteria and yeasts associated with *gowé* production from sorghum in Bénin. Journal of Applied Microbiology. 103(2):342-349.

Wood, BJB. and Hodge, MH. 1985. Yeast-lactic acid bacteria Interactions and their contribution to fermented foodstuffs. In: microbiology of Fermented Foods, Ed. Wood, BJB. Elsevier Applied Science Publishers.

Zamora, AF. and Fields, ML. 1979. Nutritive value of fermented cowpea (*Vignasinensis*) and chickpea (*Cicerarietinum*). Journal of Food Science. 44:234-238.

Received: Sept 25, 2013; Accepted: Oct 28, 2013

SENRA Academic Publishers, British Columbia
Vol. 8, No. 1, pp. 2739-2741, February 2014
Online ISSN: 1920-3853; Print ISSN: 1715-9997

Canadian Journal of pure&applied sciences

**Short Communication**

# EVALUATION OF SOME MICRONUTRIENT PATTERNS IN BLOOD SAMPLE OF TYPE 1 DIABETIC PATIENTS

*GS George[1], AA Uwakwe[2] and F Ogbotobo[3]
[1]Department of Medical Laboratory Science, Niger Delta University, Wilberforce Island Bayelsa State
[2]Department of Biochemistry, University of Port Harcourt, Nigeria
[3]Department of Chemical Pathology, Federal Medical Center, Yenagoa

## ABSTRACT

To investigate the relationship of micronutrients concentration in Type 1 Diabetic Patients and how their interactions affect the homeostasis in this hyperglycemic state, we evaluated the concentration of calcium, magnesium, zinc and glucose. We observed a concomitant increase in calcium with raised glucose level while magnesium and zinc levels where decreased. Using only Samples with plasma glucose above threshold (≥10.0mmol/L) the micronutrients were measured at time intervals of 0 to 30 mins, 60 mins, 120 minutes, 180 mins and 240 mins. It was observed that raised glucose induced significant ($P< 0.05$) elevation of calcium from 20.2 ± 1.4 mmol/L to 60.4 ± 21 mmol/L while reduction of magnesium and zinc were in the order 180 ± 7 to 58.4 ± 3 Φmol/L and 15.4 ± 0.5 to 4.3 ± 0.4 Φmol/L respectively. We conclude that variations in concentration of micronutrients may elicit clinical expression of common abnormal homeostatic environment expressed partly by the reduced levels of magnesium and zinc that complicates the diabetic process.

**Keywords**: Micronutrients, blood sample, type 1 diabetic patients.

## INTRODUCTION

Studies on the relationship between diabetic conditions and micronutrient concentration have been carried out by other workers as shown by Lawrence *et al*. (2001). Our knowledge of the role ions play to effect cells response and the dynamics surrounding this relationship will require further scrutiny over time. Calcium, magnesium and zinc are known to contribute towards the maintenance of the intracellular ion homeostasis. Magnesium is known to play a key role in the process by serving as an important co-factor for activation of calcium and sodium pumps (Guillemett, 1991; Anetor *et al*. 2002). Moreover magnesium and calcium both play a significant role to stimulate the B – cell of pancrease to produce insulin. As shown (Boyd *et al*., 1989; Zureil *et al*., 2004) reduced magnesium level is a catalyst for induction of hyperinsulnism. This gives credence to the underlying fact that some of the sequelae of magnesium deficiency may be partly accountable for the inbalance of competition between calcium and magnesium along with other ions as they move into the cells.

Calcium is essentially known to play vital role in the intracellular transduction mechanism for insulin secretion from pancreatic B – cells, modulation in one of two ways as a regulator or as a signaling system for cellular enzyme activities.

*Corresponding author email: docgeogborie@yahoo.com

Serum Zinc is known to exert strong antioxidant behaviour as shown by Powel (2000). Being an important component of biomembranes and essential cofactor in a variety of enzymes (Bettger *et al*., 1981), zinc plays an important role in the synthesis and functions of insulin as well as membrane – stabilizing properties.

## MATERIALS AND METHODS

At the Federal Medical Center Yenagoa, Nigeria, blood Samples were collected from known type 1 diabetic patients (n = 50) all having glucose levels above threshold (10.0 mmol/L), minimum 15.0mmol/L. The second group were non-diabetics (n = 50) whose fasting plasma glucose level ranged between 3.5mmol/L – 6.0mmol/L. Measurements of the micronutrients for the diabetic patients were compared with those of non-diabetic patients whose glucose concentration were varied by the addition of 5.0mmol/L, 10mmol/L, 20mmol/L and 30 mmol/L and a coordinated measurement taken at a time interval of t = o, t = 30, t = 60, t = 180 and t = 240 minutes.

Spectrophotometric method was used for the determination of glucose (oxidase method). Calcium was measured by the O-cresolphthalein complexone (CPC) method while the calgamite and Methylthymol method was used for magnesium. Zinc level was determined by Atomic absorption spectroscopy.

Table 1. Measured concentration of $Ca^{2+}$, $Mg^{2+}$ and $Zn^{2+}$ .

| Time Min | 0 | 30 | 60 | 120 | 180 | 240 |
|---|---|---|---|---|---|---|
| $Ca^{2+}$ (mmol/L) | 2.2 | 2.8 | 3.6 | 4.8 | 6.7 | 6.2 |
| Mg2+ (Φmol/L) | 210 | 200 | 180 | 132 | 58.4 | 53.3 |
| $Zn^{2+}$ (Φmol/L) | 15.4 | 14.6 | 13.2 | 12.3 | 10.1 | 8.6 |

Table shows time course of effects of elevated glucose 20 mmol/L on $Ca^{2+}$, $Mg^{2+}$, $Zn^{2+}$ for the different ions demonstrated.

## RESULTS

The sustained effects of raised glucose concentration on $Ca^{2+}$, $Mg^{2+}$ and $Zn^{2+}$ at glucose levels greater than 10.0 mmol/L over the course of 4 hours are recorded (Table 1).

Glucose was observed to elicit a co-ordinated elevation of calcium in which peak values was approximately 3 times higher than at base line 2.2mmol/L to 6.2 mmol/L (P=0.05 at t = 30, 60, 120, 180 and 240mins) as shown in table 1.

We equally observed concurrent suppression of $mg^{2+}$ in which values dropped from a baseline of 210 **Φ**mol/L to 53.3 **Φ**mol/L almost representing a three fold decrease. Zinc values also show a moderate decrease in concentration over the four hours period under study (Table 2).

Table 2. Effects of varied glucose concentration Vs Time.

| $Ca^{2+}$ (mmol/L) | $Mg^{2+}$ 2+ (Φmol/L) | $Zn^{2+}$ (Φmol/L) |
|---|---|---|
| $t_0 = 2.8$ | $t_0 = 220$ | $t_0 = 15.4$ |
| $t_{30} = 3.5$ | $t_{30} = 180$ | $t_{30} = 14.6$ |
| $t_{60} = 6.8$ | $t_{60} = 155$ | $t_{60} = 13.2$ |
| $t_{120} = 7.3$ | $t_{120} = 140$ | $t_{120} = 12.3$ |
| $t_{180} = 6.0$ | $t_{180} = 147$ | $t_{180} = 10.1$ |
| $t_{240} = 5.8$ | $t_{240} = 140$ | $t_{240} = 8.6$ |

The elevated glucose induced changes persisted over the period of observation. We however observed calcium level elicited a return close to the normal baseline value as shown in the table 3.

Table 3. Measured value of calcium vs glucose in 30 mins.

| $Ca^{2+}$ (mmol/L) | Glucose (mmol/L) |
|---|---|
| 2.6 | 5.0 |
| 3.3 | 7.5 |
| 4.0 | 10.0 |
| 4.5 | 15.0 |
| 3.5 | 20.0 |
| 3.0 | 30.0 |

Effects of various extracellular glucose concentration in vitro (n = 6 for respective concentration on calcium in normal red cells samples incubated with glucose for 30 mins P = 0.05 Vs basal (5mmol/L) repeated measures analysis of variance.

## STATISTICAL ANALYSIS

Values obtained for the response of each micronutrient (ion specie) to glucose were analyzed for statistical significance with the repeated measures of analysis of variance for both the effect of glucose over time at t = 0, 60, 120, 180, 240 mins over the range of concentrations tested at 5.0, 7.5, 10, 15, 20, 25 **Φ**mol/L. All values are reported as mean of ±SEM.

## DISCUSSION

The clinical association of micronutrients in diabetic abnormalities related to insulin has been established according to Sigh *et al*. (1998).

Our present findings suggest that glucose itself may be a factor contributing both to cellular ion homeostasis and (cellular ion inbalance) and also to the risk of pathophysiology of hyperglycemic stress state. Glucose induced micronutrient effects were found to be existing effects that are both time and concentration dependent as shown in table 2 which corresponds to the renal glucose threshold for glucose excretion. Recent evidence suggests that inhibitory effect of glucose on membrane calcium Atpase has seen reported at concentrations similar to those associated here with elevated cystolic free calcium levels. Moreover, there is evidence to suggest an interaction of glucose with membrane bound phosphoinositide system. In skin microvascular and adipose tissue, glucose stimulated diacetyl and protein kinase activity in an insulin dependent manner (Guilemette *et al.*, 1991).

Both intracellular and extracellular calcium are increased in most tissues. The activities of the ATpase associated cation pumps which determined intracellular calcium level i.e calcium ATpase and (sodium + potassium) ATpase, are also altered. The nature of alteration is often tissue specific and may depend on the level of blood glucose.

Diabetics often have low concentrations of $Ca^{2+}$. There is a consistent association of low level $Ca^{2+}$ level and risk and incidence of diabetes mellitus. Calcium is necessary for intracellular communication between the hormone insulin and tissues that utilizes insulin including sketetal muscle and fat tissues. Only a small amount of calcium is

needed for optimal insulin-related functions, but being a little bit off can cause serious health consequences including resistance and impaired insulin signaling. It is known that calcium supplementation on blood sugar level when properly regulated can elucidate the comparative effect like using the diabetes drug metformin (Joseph, 2007; Danit and Sharhar, 2007).

There is growing body of evidence to suggest that $Mg^{2+}$ play play a pivotal role in reducing cardiovascular risk and may be involved in the pathogenesis of Diabetes mellitus. It is known that magnesium supplementation improved insulin sensitivity. Magnesium depletion may play a role in delaying the complications associated with type 1 diabetes mellitus onset and potentially reduce its devastating complication; cardiovascular disease, retinopathy and nephropathy. Both mean plasma and intracellular free $mg^{2+}$ are lower in diabetes mellitus. Magnesium is a crucial co-factor involved in many enzymatic reactions involved in the metabolic process. Plasma levels were seen to be lower in normal persons. Levels of serum ionized $Mg^{2+}$ and erythrocyte intracullar free $Mg^{2+}$ are strong predisposing factors for development of the excess cardiovascular morbidity. Plasma $Mg^{2+}$ as shown by Paolisso *et al*. (1989) declined and erythrocyte $Mg^{2+}$ level rose significantly ($P<0.05$) in response to insulin in fasting healthy adults with no family history of diabetes. Reasons for low magnesium is adduced to the high renal excretory state, the effect imposed on it by its insensitivity to insulin and $Mg^{2+}$ deficiency is associated with insulin resistance and increased platelets reactivity. Sasakis *et al*. (2009) and other colleagues have confirmed that magnesium deficiency decrease insulin mediated glucose disposal in non diabetic subjects, which is consistent with insulin resistance. Diabetes is known to effect zinc homeostasis since zinc plays a role in the synthesis and activation of insulin. Deficiency of $Zn^{2+}$ results in oxidative stress which may damage the cells irreversibly exacerbating some of the classical complications of Diabetes. The current study was undertaken to understand the roles of some micronutrients in the diabetic process and has shown parts played by $Ca^{2+}$, $mg^{2+}$ and $Zn^{2+}$ in this hyperglycemic condition. The results strongly suggested that a well co-ordinated combination of these micronutrient could exhibit beneficial effect in managing diabetes mellitus.

## REFERENCES

Anetor, J., Seujobi, A., Ajose, O. and Agbedana, E. 2002. Decreased Serum magnesium and zinc levels: atherogenic implications in type 2 diabetes mellitus in Nigeria. Nutr Health. 16:291-300.

Boyd, III AE., Rajan, AS. and Gaines, KL. 1989. Regulation of insulin Release by Calcium In: Insulin Secretion: Molecular and Cellular Biology of Diabetes Mellitus. (1):93:105.

Bettger, W. and O' Dell, B. 1981. A Critical Physiological role of Zinc in the Structure and Function of Biomembrane. Life Science. 28:1425-1438.

Danit, R. and Sharhar, S. 2007. Does Daily Calcium intake enhance weight loss among over weight Diabetic patients? Diabetes care. 3(3):485-493.

Guillemett, C., Poitras, M. and Boulay, G. 1991. Two Calcium System as distinguished on the basis of their $my^{2+}$ dependency in a post nuclear particulate fraction of bovine adrenal cortex. Cell Calcium. 8:51-60.

Joseph, L. 2007. Diabetes Mealitus, A Disease of Abnormal Cellular Calcium Metabolism. American Journal of Medicine. 34:293-307.

Powell, S. 2000. The antioxidant Properties of Zinc. J Nutr. 130:14475-14545.

Paolisso, G., Sgambato, P. and Pissarielon, G. 1989. Improved insulin response and action by chronic magnesium administration in aged NIDDM Subjects. Diabetes Care. 12:262-269.

Sasaki, S., Oshime, T. and Matsura, H. 2009. Abnormal magnesium status in patient with cardiovascular disease. Clin Sci. (Colch). 98:175-181.

Sigh, R., Niar, M., Rastogi, S., Bajaj, S., Gaoli, Z. and Shoumin, Z. 1998. Current Zinc intake and risk of diabetes and coronary attery disease and factors associated with insulin resistance in rural and urban population of North India. J. AM. Coll. Nutr. 17:564-570.

Zureil, M., Galan, P., Bertrais, S., Mennen, L., Czeruichow, S., Blacher, J., Ducimetiere, P. and Henberge, S. 2004. Effects of long-term daily low dose supplementation with antioxidant, vitamins and mineral, on structure and function of large arteries. Arterioscler Thromb Vasc Biol. 24:1485-1495.

Received: July 12, 2013; Oct 18, 2013; Accepted: Oct 29, 2013

SENRA Academic Publishers, British Columbia
Vol. 8, No. 1, pp. 2743-2749, February 2014
Online ISSN: 1920-3853; Print ISSN: 1715-9997

Canadian Journal of pure&applied sciences

# APPLICATION OF X-RAY COMPUTED TOMOGRAPHY FOR ANALYZING CLEATS AND PORES FOR COALBED METHANE IN COAL FROM THAR COALFIELD

*Imdadullah Siddiqui[1],Sarfraz H Solangi[1], Aftab Ahmed Soomro[2], Mashooque Ali Warar[1], Muhammad Kashif Samoon[1]and Sohail Ajmal[1]
[1]Centre for Pure and Applied Geology, University of Sindh, Jamshoro
[2]Liaquat University of Medical & Health Sciences, Jamshoro, Pakistan

## ABSTRACT

The computed tomography (CT) is a non-destructive technique that can provide information of internal structure of coal in 2D, this technology is now widely used in geoscientific research. This technique is used for the measuring cleat dimension and pore width of the coal. The slicing study of Thar coal shows that the length of cleats in various seams ranges from 0.5mm to 5mm and the aperture of these cleats vary between 0.1mm to0.5mm. The porosity also plays an important role in storage and production of coalbed methane, the size or width of pores in coal under investigation ranges between 0.1mm to 0.7mm. The present investigation shows that seam III and V of the Thar coalfield can be considered as viable as hold a potential for CBM resources, however, the coal samples from these seams need to be analyzed for the presence of methane.

**Keywords**: X-ray Computed Tomography, Cleats, Picker-IQ, CT slices.

## INTRODUCTION

Computed tomography (CT) is a technique that provides information about the internal structure of coal by an X-ray source detector that in turn produces the cross-sectional images of slices of interior of coal in 2 directions. This technique is now widely used in geoscientific research (Duliu, 1999; Mess *et al*., 2003). Computed tomography technique is also useful for the coal petrological and petrophysical research. Another study Verhelst *et al*. (1995); Van Geet *et al*. (2001) had carried out extensive research on coal with CT techniques.

The coal is composed of three basic components, i.e., the cleat fracture, coal matrix, pores and mineral. The network of cleat fractures in coal plays an important role in the production of methane from coalbeds. The major characteristics of cleats include cleat length, cleat aperture and extent of mineral filling (Close and Mavor, 1991). Micropores are responsible for most of the porosity in coal and size or width of pore also plays an important role. Computed tomography (CT scan) technique enables us to study the cleat aperture and length as well as the width or size of pores.

The Thar coalfield is the largest coalfield of Pakistan, with proven reserves of 175 billion tons of coal. At present efforts are being made to produce coalbed methane and underground coal gasification from this coal, but there is need of geoscientific research on coal for clean coal utilization of Thar coalfield.

## GEOLOGY OF THE STUDIED AREA

The Thar coalfield is located between latitudes 24$^{o}$15'N and 25$^{o}$ 45'N and longitudes 69$^{o}$ 45'E and 70$^{o}$ 45'E (Fig.1, Survey of Pakistan topographic sheet Nos. 40 L/2, L/5 and L/6) situated in District Tharparkar of south-eastern Sindh. It is the largest coalfield of Pakistan having an area of about 9100 square kilometres. It has north-south length of 140km and east-west width of 65km. The resource potential of this single coalfield is about 175 billion tonnes (Jaleel *et al*., 1999). Thar coalfield is the largest coalfield of Pakistan, located on the Indus Platform, in the Thar desert in southeastern corner of Pakistan.

The coal samples were obtained from block-XI of Thar coal field. Geologically this block is covered with sand dunes, and coal bearing Bara formation is encountered at 180 to 206m, which comprises of Clay stone, carbonaceous claystone, coal, sandstone. siltstone, silty claystone, clayey sandstone and sandy claystone (Table 1). Sub-Recent deposits consist of variegated colored sandstone, siltstone claystone and sometimes clayey sandstone and silty sandstone. Maximum 10 coal seams are encountered in this block while the thickest coal seam of this block is about 9.18m. Megascopically the coal is

*Corresponding author email: siddiqui57@gmail.com

Table 1. General stratigraphic sequence of Thar coalfield (Jaleel *et al.*, 1999).

| Formation | Age | Thickness | Lithology |
|---|---|---|---|
| Dune Sand | Recent | 14m to 93m | Sand, Silt and Clay |
| …… | ……Unconformity | ……. | …… |
| Alluvial Deposits | Sub Recent | 11m to 209m (variable) | Sandstone, Siltstone, Clay stone, mottled |
| …… | ..……Unconformity | ……. | …… |
| Bara Formation | Palaeocene to Early Eocene | +52m (variable) | Clay stone, shale, sandstone, coal, carbonaceous clay stone |
| …… | …. Unconformity | …….. | …… |
| Basement Complex | Pre-Cambrian | ---- | Granite, quartz and diorite |

Table 2. Seam-wise distribution of cleat length and width and their types in Thar coal.

| Seam No. | Interval (m) | CT Scan Slice No. | Type of cleat fracture identified | Cleat dimension (mm) | Seam No. | Interval (m) | CT Scan Slice No. | Type of cleat fracture identified | Cleat dimension (mm) |
|---|---|---|---|---|---|---|---|---|---|
| II | 188.24-192.86 | S #23 | Isolated 'S' | *L: 1.5 - 3<br>**W: 0.1 – 0.3 | | III | S #40 | Face & Butt | L: 2<br>W: 0.2-0.3 |
| | | S #25 | Butt & Isolated 'S' | L: 1.5 - 3<br>W: 0.1 - 0.5 | | | S #42 | Butt | L: 2<br>W: 0.2 |
| | | S #26 | Butt & Isolated 'S' | L: 2.1 - 2.2<br>W: 0.1 - 0.3 | | | S #46 | **Butt | Nil |
| | | S #28 | Butt | L: 0.5 - 3<br>W: 0.1 - 0.3 | | | S #51 | Butt | L: 2-4<br>W:0.2- 0.3 |
| III | 242.85-247.92 | S #29 | Butt | L: 1 - 2<br>W: 0.2 - 0.3 | | | S #58 | Nil | Nil |
| | | S #30 | Butt | L: 2.6 - 2.7<br>W: 0.2 - 0.3 | V | 248.74-257.92 | S #59 | Nil | Nil |
| | | S #31 | Butt | L: 1.3 - 2.7<br>W: 0.2 - 0.3 | | | S #60 | Nil | Nil |
| | | S #34 | Nil | Nil | | | S #63 | Butt | L: 1.5<br>W: 0.3 |
| | | S #35 | Butt | L: 3 - 5<br>W: 0.3 - 0.5 | | | S #97 | ***Butt | Nil |
| | | S #36 | Butt | L: 3 - 5<br>W: 0.3 - 0.5 | | | S #101 | Butt | L: 3<br>W: 0.2 |
| | | S #37 | Butt | L: 4-5<br>W: 0.2 - 0.3 | | | S #105 | Butt & Face | L: 1.5-2.7<br>W:0.1- 0.2 |
| | | S #39 | Face | L: 3<br>W: 0.1 | | | | | |

*L: length of cleat, **W: width of cleat, ***Mineralized/pyritized pores

brownish black and grayish black in color, the coals from Thar coal basin are slightly banded and poorly to well cleated and compacted. It contains scattered resin of brown and greenish yellow color. Coal contains very fine to fine grained pyrite in patches upto one sq. cm size. The rank of coal is lignite 'A' to lignite 'B' (Pakistan Energy yearbook, 2010). The thickness of coal beds in the investigated block varies from 4.5m to 19 meters.

## MATERIALS AND METHODS

Three representative coal seam samples of Block-XI were obtained from the Sindh coal authority. The samples obtained were from seam II (sample No. BP-10), seam III (sample No. BP-30) and seam V (sample No. BP-5) the depth of these seam samples are 188.24 to 192.86, 242.85 to 247.92 and 248.74 to 257.92 meters (Figs. 2 and 3). For the X-ray CT scanning, Picker-IQ X-ray scanner equipment was used for the cleat study (Fig. 1). The scanner operated at 130kV and 85mA and it produced a series of 2D images known as 'slices' as it looks that object has been sliced along the scan plane. The scanning time was 4sec per slice, the X-ray source was 0.8 x 0.9mm spot size. Slice thickness of 2mm and 5mm have been used, the reconstruction matrix each consists of pixel 512x512 pixels, in the XY plane (Mazumder *et al*., 2006). The images are usually seen as monochromatic, with various shades of grey color (Figs. 4-7).

Table 3. Showing toal pore, Open and Closed pores in Thar coal.

| Seam No. | CT Scan Slice No. | Total Pores | Open Pores | Closed Pores | Seam No. | CT Scan Slice No. | Total Pores | Open Pores | Closed Pores | Seam No. | CT Scan Slice No. | Total Pores | Open Pores | Closed Pores |
|---|---|---|---|---|---|---|---|---|---|---|---|---|---|---|
| II | S #23 | Nil | Nil | Nil | III | S #51 | 18 | 11 | 07 | V | S #76 | 11 | 06 | 05 |
| II | S #25 | Nil | Nil | Nil | III | S #52 | 18 | 08 | 10 | V | S #77 | 08 | 05 | 03 |
| II | S #26 | Nil | Nil | Nil | III | S #53 | 15 | 10 | 05 | V | S #78 | 14 | 06 | 08 |
| II | S #28 | 01 | 01 | Nil | III | S #54 | 13 | 01 | 12 | V | S #79 | 10 | 05 | 05 |
| III | S #29 | 06 | Nil | 06 | III | S #55 | 12 | 02 | 10 | V | S #80 | 16 | 10 | 06 |
| III | S #30 | 09 | Nil | 09 | III | S #56 | 18 | 12 | 06 | V | S #81 | 14 | 06 | 08 |
| III | S #31 | 08 | Nil | 08 | III | S #57 | 15 | 08 | 07 | V | S #82 | 14 | 08 | 06 |
| III | S #32 | 14 | Nil | 14 | III | S #58 | 18 | 11 | 07 | V | S #83 | 16 | 10 | 06 |
| III | S #33 | 14 | Nil | 14 | V | S #59 | 16 | 06 | 10 | V | S #84 | 12 | 03 | 09 |
| III | S #35 | 06 | Nil | 06 | V | S #60 | 24 | 14 | 10 | V | S #85 | 04 | 02 | 02 |
| III | S #36 | 06 | 02 | 04 | V | S #61 | 10 | 06 | 04 | V | S #86 | 08 | 04 | 04 |
| III | S #37 | 04 | 02 | 04 | V | S #62 | 18 | 12 | 06 | V | S #87 | 10 | 06 | 04 |
| III | S #38 | 10 | 05 | 05 | V | S #63 | 16 | 08 | 08 | V | S #89 | 14 | 08 | 06 |
| III | S #39 | 06 | 03 | 03 | V | S #64 | 16 | 05 | 11 | V | S #90 | 16 | 07 | 09 |
| III | S #40 | 08 | 03 | 05 | V | S #65 | 24 | 16 | 08 | V | S #91 | 14 | 10 | 04 |
| III | S #41 | 22 | 08 | 14 | V | S #66 | 23 | 15 | 08 | V | S #92 | 14 | 05 | 08 |
| III | S #42 | 10 | 03 | 07 | V | S #67 | 02 | 01 | 01 | V | S #93 | 09 | 05 | 04 |
| III | S #43 | 06 | 03 | 03 | V | S #69 | 01 | Nil | 01 | V | S #95 | 14 | 08 | 06 |
| III | S #44 | 12 | 05 | 07 | V | S #70 | 21 | 13 | 08 | V | S #96 | 04 | 04 | Nil |
| III | S #45 | 12 | 07 | 05 | V | S #71 | 07 | Nil | 07 | V | S #97 | 20 | 10 | 10 |
| III | S #46 | 09 | 03 | 06 | V | S #72 | 11 | 05 | 06 | V | S #100 | 05 | 03 | 02 |
| III | S #47 | 18 | 09 | 09 | V | S #73 | 12 | 08 | 04 | V | S #101 | 11 | 07 | 04 |
| III | S #49 | 11 | 08 | 03 | V | S #74 | 12 | 04 | 08 | V | S #102 | 03 | 02 | 01 |
| III | S #50 | 22 | 14 | 08 | V | S #75 | 11 | 05 | 06 | V | S #104 | 04 | 02 | 02 |
| | | | | | | | | | | V | S #105 | 11 | 06 | 05 |

## RESULTS AND DISCUSSION

For generation and production of coalbed methane, coal must have porosity through which desorption of gas from coal surface may occur. The micropores must have considerable size or width so that diffusion of gas may occur and the coal also must have network of cleats with considerable aperture for the flow of gas. The study of cleats provides important information about the possibility of the occurrence of CBM. Computed Tomography technique provides quantitative images showing cleat dimension and porosity in coal. Comprehensive CT scan study was conducted on samples of three coal seams, from the depth of 188.24 to 192.86, 242.85 to 247.92 and 248.74 to 257.92 meters.

The details of slices or sample are given in table 2. The CT images, identifies network of cleat fractures i.e. face, butt and isolated 'S' cleats. The face cleats are the primary continuous micro fractures having wide aperture, giving a directional permeability. While butt cleats are the secondary cleats and are discontinuous, shorter in extent and localized between adjacent cleats. And isolated 'S' cleats are developed in coal due to tectonic activity.

The X-ray view of slices of sample No. BP-10 (Figs. 4 and 5) show cleats of isolated 'S' type, with the length of 2.1mm and aperture or width of 0.3 to 0.1mm. These types of cleats are produced due to tectonic activity and enhance reservoir porosity and permeability in coal.

Slices of CT images (Fig. 5) shows the prominent isolated 'S' type cleats in seam-II in the hole core BP-10 at the depth of 188.24 to 192.86m. In seam-III, figure 4, the X-ray view of slice sample No. BP-30, shows well developed butt and isolated 'S' cleats, with the length of 0.3 mm to 2.7mm and aperture of 0.2-03mm.

An indistinct network of primary continuous face cleats and secondary localized butt cleats have been observed in the X-ray view of slices in figure 5 (hole/core No. 5 and seam-V) is identified, displaying butt and face cleats with the length of 1.8 to 2mm, and aperture width of 0.2-0.3mm. However, post or syn diagenetic mineralization of pyrite has blocked these cleats.

The porosity has direct impact on coalbed methane, the volume occupied by pores between cleats fractures in coal is known as porosity and these cleats in coal have the capacity of storing less than 10% of the in place gas (Allen, 1997).

Table 3 shows that in seam II, out of four pores one pore (1% of all of these pores) is open there is no closed pore. While in seam –III, out of total 639 pores 46% are open pores and 54% are closed pores and in block-V out of 500 pores 53% are open pores and 47% are closed pores. Table 3 shows that in seam-III; slice (S. # 46) out of 13 cleats 7.69% of the cleats are blocked due pyrite mineralization, at the depth of 242.85-247.92m. While the among the cleats, out of 12 cleats 25% of the cleats are

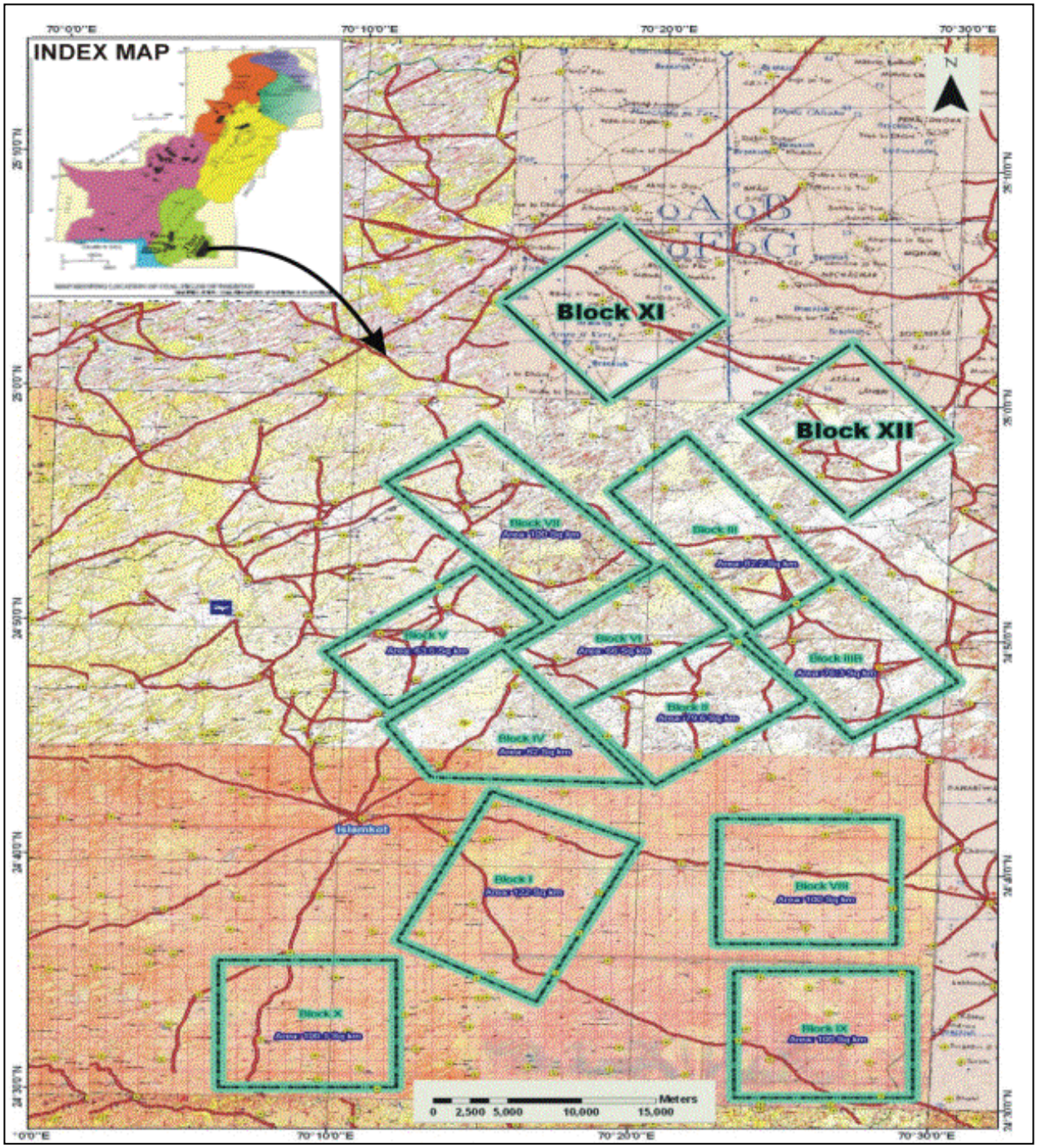


Fig. 1. Map showing various coal blocks (in topographic sheet Nos. 40 L/2, L/5 and L/6) in Thar coalfield of Pakistan.

heavy blocked due to pyritization (Siddiqui *et al*., 2011). Generally it is found that in Thar majority of the coal have closed pores.

The absorbability and flowability of coalbed methane in coal depends upon the pores. According to International Union of Pure and Applied Chemistry (1982) classification, pores having < 0.002 mm width are known as micropores, while mesopores are those having between 0.000002 and 0.00005 mm width and macropores are those having with of > 0.00005 mm (IUPAC, 1982). The X-ray view of slice of sample No. BP-10 shows random pores with the width of 0.1 mm. The size of pores in sample No. BP-30 (seam III) is less than 0.1mm. The size


Fig. 2. Showing X-ray Computed Tomographic Scanning machine used in this study.

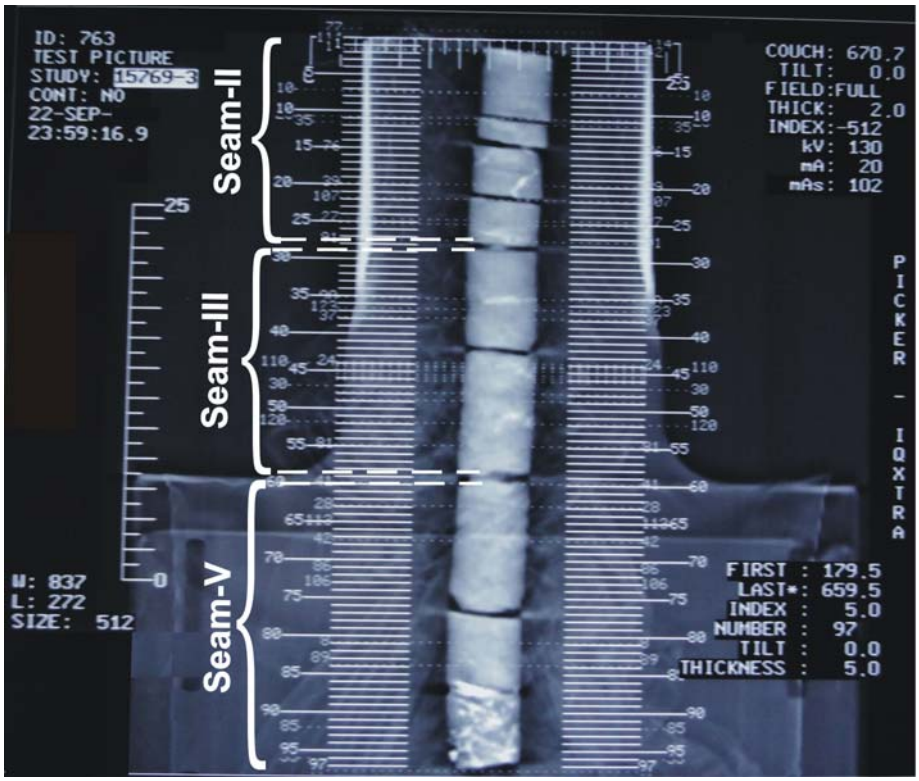


Fig. 3. X-ray view of the sample (collected II, III and V, the lines with figure shows slicing data of the samples.

of pores in sample No. BP-5 (seam-V), ranges between 0.1mm to 0.2mm. However, these pores and cleats are filled in with syn or post deposited pyrite minerals (Fig. 6).

The table 2 displays that Thar coal possess macro-pores, and because of its maceral composition i.e. Huminite group; the coal may possess little or no methane gas. Beside that as Thar coal possess macro-pores which serve as transport pathways, and in these pores little gas is stored in the adsorbed state.

The pore volume distribution may be used to predict the methane adsorption capacity in coal. Siddiqui *et al.*

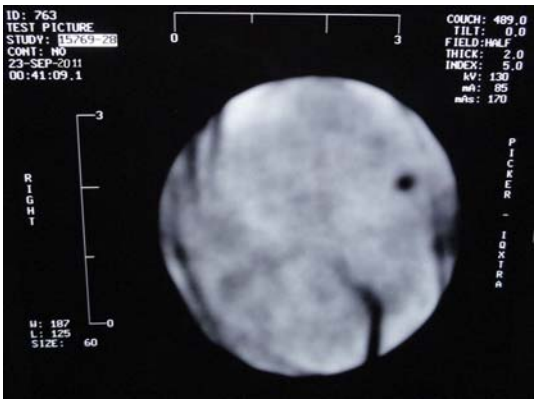


Fig. 4. X-ray view of slice, showing isolated 'S' cleats and pores.

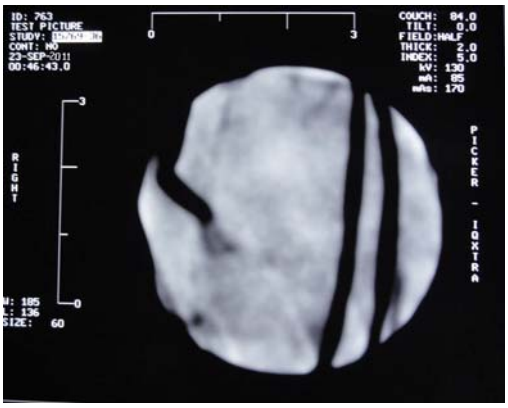


Fig. 5. X-ray view of slice, showing butt cleats and isolated 'S' cleat.


Fig. 6. X-ray view of slice, showing mineralization (pyritization) in cleats and pores.

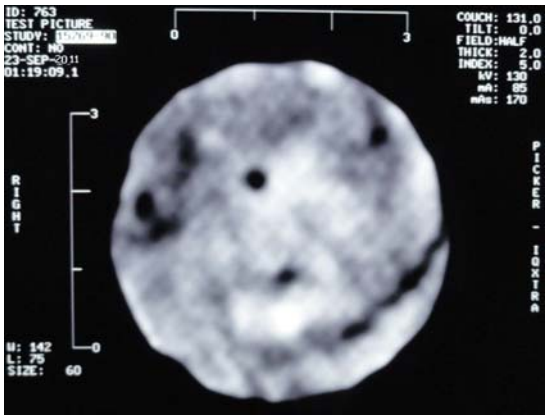


Fig. 7. X-ray view of slice showing porosity in coal.

(2012) had studied the porosity in Thar coal and as per his study the pore volume ranges from 0.06 to 2.36 cc/g and pore diameter in Thar coal ranges from 34.81 to 121.51Å, that is termed as meso-pore and macro-pore. These meso and macro-pores serve as transport pathways, and little methane is stored in these pores in the adsorbed state.

In the present study, it is evident from the table 2 that high porosity values are due to the presence of cleat fracture networks, which are identified by CT scanned images as shown in figures 5 and 6. Based on the research on coal sample from Saun Juan basin, Zonguldak-Turkish basin and Jharia-Indian coal basin (Close and Mover, 1991; Karacan and Okandan 2000; Mandal *et al.*, 2004, Mahajan and Walker, 1978) it has been observed that permeability of coal if affected by network of cleat fractures in coal. The frequency of cleats fractures, their interconnections along with aperture size, may affect permeability in coal that plays important role in coalbed methane production. Face and butt cleats are primary contributors for coal permeability while the third set of cleats that formed latter in geologic time i.e. tertiary cleats oriented differently and terminates against either but or face cleats and plays an important role in producing cleat permeability.

## CONCLUSION

Based on the present research following conclusion can be made:

1. The slicing analyses identifies extensive cleat network in the coal seam-III and IV, at the depth of 242.85 to 247.92m and 248.74-257.92m.
2. In studied samples cleat length ranges from 0.5mm to 5mm.
3. With the help of Computed Tomograpy technique cleat aperture measured ranges from 0.1mm to 0.5mm.
4. The pores identified by Computed Tomography technique show that the size or width of pores range from 0.1mm to 0.7mm.
5. The slicing analyses also show that seam II and V are promising seams for producing coalbed methane as these seams have network of cleats and good porosity.

6. There is possibility that pyrite mineralization within the cleats and pores may block the flow of CBM in coal.
7. Thar coal posses macro-pores, and it is thought that little methane gas may had stored in coal as macro-pores serve as transport pathways, and in these pores little gas is stored in the adsorbed state.

**ACKNOWLEDGEMENTS**

The authors are highly thankful to Mr. Hidayatullah Kakakheal and Tariq Ali Khan of National MRI, CT scan and Diagnostic center, for extending their CT scanning facilities for CT scanning Thar coal samples.

**REFERENCES**

Allen, T. 1997. Particle size measurement (5th edi., vol. 2): Surface area and Porosity determination. Chapman & Hall, London, UK. pp256.

Close, JC. and Mavor, MJ. 1991. Influence of coal composition and rank on fracture development in fruitland coal gas reservoirs of San Juan Basin: Proceeding of Coalbed Methane of Western North American Rocky Mountain Association Geologist. Field. Conference. Eds. Schwochow, S., Murray, DK. and Fahy, MF. 109-121.

Duliu, OG. 1999. Computer axial tomography in geosciences: an overview. Earth-science reviews. 48:265-281.

IUPAC, 1982. Manual of symbols and terminology. Appendix 2: Part1. Colloidal and surface chemistry. J. Pure Appl. Chem. 52:2201.

Jaleel, A., Alam, GS. and Shah, SAA. 1999. Coal Resources of Thar, Sindh, Pakistan. Geological Survey of Pakistan, Rec.110:59.

Karacan, CÖ. and Okandan, E. 2000. Fracture/Cleat analysis of coals from Zonguldak Basin (northwestern Turkey) relative to the potential of coalbed methane production. Int. Journal of Coal Geology. 44:109-125.

Mandal, D., Tewari, DC. and Rautela, MS. 2004. Methane Exploitation in Jharia coal field. In: Proc. 5th Conference on Exposition on Petroleum Geophysics. Ed. Pandy, IN. 904-909.

Mahajan, OP. and Walker, PL. 1978. Porosity of Coals and Coal Products. US DOE Technical report. FE-2030-TR7. United States Department of Energy, Pennsylvania, USA.

Mazumder, S., Wolf, KHAA., Elewaut, K. and Ephraim, R. 2006. Application of X-ray computed tomography for analyzing cleat spacing and cleat aperture in coal samples. Int. J. Coal Geology. 68:205-222.

Mees, F., Swennen, R., Van Geet, M. and Jacobs, P. 2003. Applications of X-ray computed tomography in Geosciences. In: Applications of X-ray computed tomography in Geosciences. Eds. Mess, F., Swennen, R., Geet, M. and Jocobs, P. Geol. Soc. (London) Special Publication No. 215:1-6.

Pakistan Energy Year Book. 2010. Hydrocarbon Development Institute of Pakistan. Ministry of Petroleum and Natural Resources.

Siddiqui, I., Sarfraz, HS. and Kashif, MS. 2011. Preliminary studies of Cleat fractures and Matrix porosity in Lakhra and Thar coals, Sindh, Pakistan. J. Himalayan Earth Sciences. 44(2):25-32.

Siddiqui, I. Sarfraz, HS. and Mashooque, AW. 2012. Characterization of Pores and its efforts on Probable Occurrence of Coalbed methane in Thar Coalfield-Pakistan. September 10-12, 2012. 9th Eurapean Conference on Coal Research & its implications: ECCRIA-9 University of Nottingham-UK. (Abstract).

Verhelst, F., Vervoort, A., De Boscher, PH. and Marchal, G. 1995. X-ray computerized tomography: determination of heterogeneities in rock samples. Proceedings of the 8th International Congress on Soil and Rock Mechanics. Ed. Fujii, T. 105-108.

Van Geet, M. and Swennen, R. 2001. Quantitative 3D-frature analysis by means of microfocus X-ray computer tomography (μ CT): an example from coal. Geophysical Research Letters. 28:3333-3336.

Received: July 1, 2013; Revised: Aug 19, 2013;
Accepted: Sept 16, 2013

SENRA Academic Publishers, British Columbia
Vol. 8, No. 1, pp. 2751-2760, February 2014
Online ISSN: 1920-3853; Print ISSN: 1715-9997

Canadian Journal of pure&applied sciences

# QUALITY IMPROVEMENT OF FOUNDRY OPERATION IN NIGERIA USING SIX SIGMA TECHNIQUE

*Abidakun OA, Leramo RO, Ohunakin OS, Babarinde TO and Ekundayo-Osunkoya AO
Department of Mechanical Engineering, Covenant University, Ota, Nigeria

## ABSTRACT

In this paper Six Sigma DMAIC analysis was applied in an aluminium mill in order to identify sources and causes of waste with the intention of providing veritable solutions. The foundry section was the segment under scrutiny. Re-work or defects in this firm was found to be on the average of about 37.05% of total production for the twenty-three months under study (January 2009- December 2010). Defect reduction was therefore chosen as the Critical-to-Quality (CTQ) factor. The sigma level of 1.87 in the firm indicated the existence of opportunities for improvement. Analysis was carried out using SPSS, SPC for Excel to perform regression analysis, process capability analysis, generate descriptive statistics, histograms and run charts. The results of these analyses identified three major defects and some of their behaviours. Based on the analysis, solutions were proffered in the Improve and Control phases of this project. Implementation of the proffered solutions resulted in noticeable improvement and led to the firm operating with near- perfect processes thus proving the applicability of Six Sigma.

**Keywords**: Six sigma DMAIC, critical-to-quality, composition error, profile error, trimming error.

## INTRODUCTION

Generally, it is typical of manufacturing processes to produce up to 69.1% as waste since production processes normally function at 1-2 sigma (Kaushik *et al*., 2008). It could be worse in many production firms where little attention is paid to quality control and improvement. This lack of quality may be in terms of customers' dissatisfaction, delay in delivery, defective products and services or waste of resources. Manufacturing firms of the current age are faced with stringent economic conditions, stifling competition and increasing customer awareness among other factors. All these places high demand on manufacturers to constantly produce high quality products in the best way possible. Also, manufacturing industry occupies the central stage in nations' development and in the world economy. The well-being of a nation is thus determined by its capability to convert raw materials to desirable finished goods. One of such processes involved in manufacturing is the foundry operation.

Foundry operation which involves the melting of billets and/or scrap metals is a highly energy and labour intensive operation (Su and Chou, 2008). Waste generation and lack of quality is however a serious issue militating against the efficient performance in foundry operation. Since profit making remains a major objective of every business, value addition and quality improvement have to be given due attention in order to save money and increase revenue. Achieving this objective requires the implementation of such techniques as Six Sigma. Presently, many foundries are interested in implementing Six Sigma to improve the quality of their products (Su and Chou, 2008).

Six Sigma is the application of scientific method to the design and operation of management systems and business processes which enable employees to deliver the greatest value to customers and owners (Pyzdek, 2003; Pantano *et al*., 2006). It is a disciplined, systematic, data-driven approach to process improvement that targets the near-elimination of defects from every product, process and transaction (Evans and Lindsay, 2005; Aggogeri and Gentili 2008; Kaushik *et al*., 2008). Although, it involves measuring and analyzing an organization's business processes, Six Sigma is not merely a quality initiative; it is a business initiative (Pande and Holpp, 2002; Lee-Mortimer, 2006).

The effectiveness of Six Sigma in improving quality and reducing waste has been proved in various sectors by both scholars and practitioners (Treichler *et al*., 2002; Goffnett, 2004; Banuelas *et al*., 2005; Kwak and Anbari, 2006; Aksoy and Orbak, 2009; Ung *et al*., 2007; Gijo and Scaria, 2010; Falcón *et al*., 2012). It has, as a numeric goal; the reduction of errors in output to an outrageous but possible and much desired 3.4 parts per million (Antony and Banuelas, 2002). It also has a business goal of improving customers' satisfaction, reducing cycle time and defects (Antony and Banuelas, 2002; Rajagopalan *et al*., 2004; Evans and Lindsay, 2005; Parast, 2011). A process functioning at 6 sigma level is expected to produce satisfactory outputs 99.99966% of the time (Antony and Banuelas, 2002). The main benefit of a Six

*Corresponding author email: olayinka.ohunakin@covenantuniversity.edu.ng

Sigma program is the elimination of subjectivity in decision making, by creating a system where everyone in the organization collects, analyzes, and displays data in a consistent way (Maleyeff and Kaminsky, 2002).

Implementing the Six Sigma as a defect reduction technique in the Nigeria manufacturing firm is key to national growth. Hence, the objective of this work is to reduce defects in foundry operation by applying the principal Six Sigma methodology known as DMAIC (Define, Measure, Analyze, Improve, and Control). Details of DMAIC methodology applied in this work are comprehensively discussed in Pyzdek (2003) and De Koning and De Mast (2006). The charge preparation, melting and casting operations of the foundry under study remain the focus.

## PROCESS DESCRIPTION

The factory engages in secondary production of aluminium i.e. scrap processing rather than smelting or extracting aluminium from its major ore which is Bauxite. Hence the process includes scrap acquisition, sorting, bailing, weighing, charge mixing, melting and holding, casting, cold rolling, embossing and slitting; and weighing and sales. The process flowchart of the foundry is shown in figure 1. However, the processes of concern in this paper are limited to charging preparation, melting and casting operations.

### Charge preparation/mixing

Pure aluminium ingots are mixed in proportion to the scrap by trained metallurgists to produce the desired class. The charge content is determined by the series of aluminium to be produced.

### Melting and Holding

Charge melted in the melting furnace at roughly 850$^{o}$C is fluxed, degassed and dross removed manually by the use of fork lift. The molten aluminium is then poured into the holding furnace which is held at about 750$^{o}$C whereas the melting temperature of pure aluminium is 660$^{o}$C. Spectroscopic analysis of the molten aluminium is done to determine the composition. In the event of variation from the desired content, necessary amounts of the constituents are added into the holding furnace to neutralize the variation. The melt correction continues until the desired composition is attained after which the holding furnace is tilted to feed the caster.

### Casting

Casting which is the continuous type is done by hot rolling at temperatures ranging from 680 to 700$^{o}$C. The melt flows from the holding furnace through a channel and it is deposited right in between the upper and lower rollers of the caster through a nozzle. The rollers give shape to the melt by compression and slight cooling. The rollers are sprayed with graphite which serve as lubricant and also prevent direct contact with the metal. Contact between the metal and the roller usually leads to the formation of serious defects. The cast is coiled around an iron core and allowed to cool in air thus ensuring slow cooling and homogenization of the microstructure.

## MATERIALS AND METHODS

The key steps followed in using the DMAIC methodology and the tools used in each phase of the study are as shown in table 1 (De Koning and De Mast, 2006). The project goals and customer requirement were defined in the first phase. Second phase measures the process to determine current performance; analysis and determination of the critical input variables for process improvement were done in the third phase. The fourth phase improves the process by eliminating sources of defects while the fifth phase controls the improved process performance.

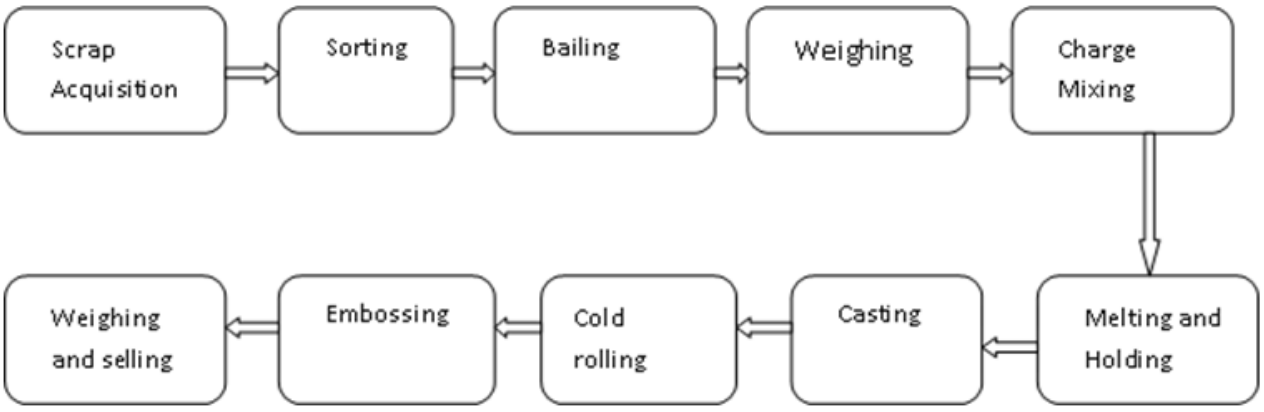


Fig. 1. Process flow chart for the foundry.

## DISCUSSION

### 1. Define Phase

At this phase, the problems concerning (i) who the customers are and (ii) what the customers require were defined. The top management and the quality control department were considered as the customers in this case. Defect reduction was the selected Critical To Quality (CTQ) measure due to the pronounced problem of defects in the Aluminium rolling mill. Tools such as Voice of the Customer (VOC) and Voice of the Process (VOP) were used to make this selection. The Voice of Customer was obtained by direct interaction in the form of interviews and discussions with top officers of the Quality Control department. The responses showed that rework is the major concern within the scope of production.

The voice of the process was obtained from multiple first-hand observations and guided tours of the entire production line. The factors of the process observed were the people, technique, equipment, input material and environment. Observation of the process showed that defect reduction remains the primary target as the delay was not a critical problem; defective products are never sold since the final customers will be dissatisfied with the product. This further supports the selection of defect

Table 1. Phases of Six Sigma DMAIC methodology.

| Phase | Items | Tools |
|---|---|---|
| Phase 1: Define | Who the customers are<br>What the customer require<br>The Critical To Quality<br>Analysis of the ability to process improvement | Voice of customer (VOC)<br>Voice of process (VOP)<br>Supplier Input Process Output Customer (SIPOC) |
| Phase 2: Measurement | Determine the sigma level of the process<br>Identify inputs<br>Non-conforming products,<br>Defect type and probable cause | Statistical Process Control (SPC) |
| Phase 3: Analysis | Exploratory analysis<br>Identity potential critical inputs<br>Description analysis<br>Analysis of the ability to process improvement | Process capability analysis<br>Descriptive statistical analysis<br>Run charts<br>Regression analysis<br>Ishikawa (Fishbone) Diagram |
| Phase 4: Improvement | Analysis of improve of the process | |
| Phase 5:: Control | Implement control plan<br>Verify long term capability<br>Continuously improve process | |

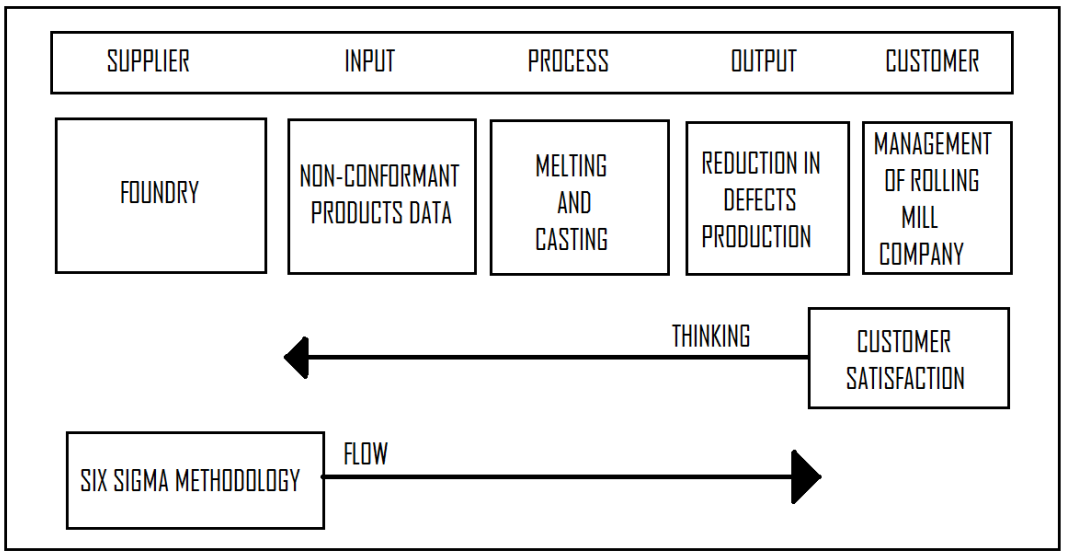


Fig. 2. SIPOC diagram for defects and waste generation.

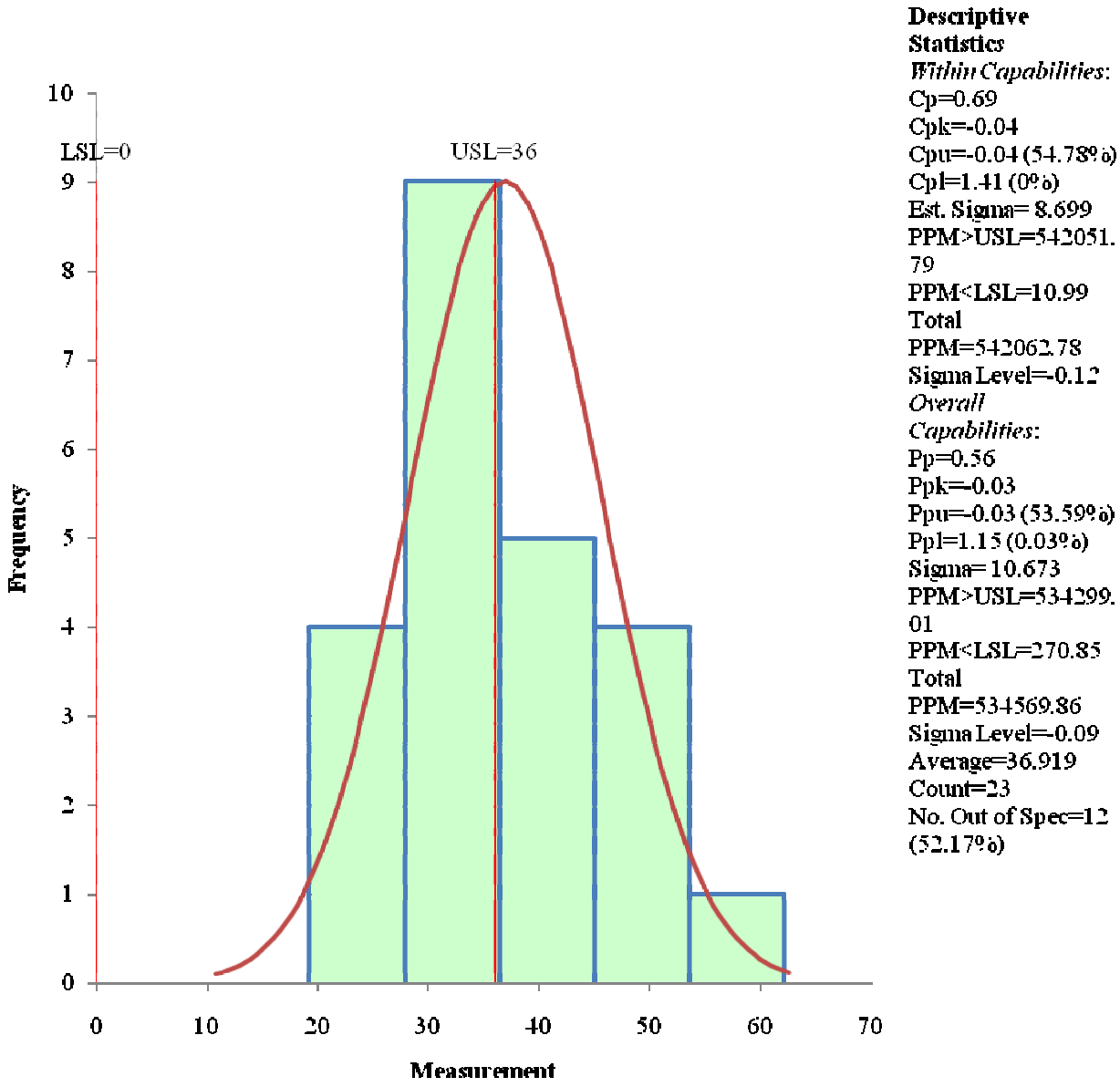


Fig. 3. SPC process capability analysis.

reduction as the CTQ measure for this project.

A high level Supplier Input Process Output Customer (SIPOC) diagram for defects and waste production at the mill is shown in figure 2.

**2. Measurement Phase**

Data related to defects which were required for the CTQ measure were collected from the factory under study. The collected data span January 2009 to December 2010. This record contained information on (i) the tonnage of aluminium products produced, (ii) non-conforming products, (iii) defect types and (iv) probable causes. The analysis in this project shall be done in kilograms and as a percentage of defects to the total production run since aluminium products are measured by mass (in kilograms). The Sigma level of the process was calculated based on the data collected and this showed that the casting section functioned at an average level of 1.84 sigma. This indicated an abundant room for improvement in this section.

**3. Analysis Phase**

**Process capability analysis**

Process Capability analysis of the data (Fig. 3) was done by using Statistical Process Control (SPC) for Excel

Table 2. Statistical analysis of the three main defects.

| | Composition Error | Profile Error | Trimming Error |
|---|---|---|---|
| MEAN | 10.662 | 13.389 | 10.396 |
| MEDIAN | 10.017 | 12.007 | 8.081 |
| MIN | 1.711 | 2.880 | 0.664 |
| MAX | 30.653 | 32.185 | 27.837 |
| Q1 | 5.239 | 9.219 | 3.6325 |
| Q3 | 14.14 | 17.492 | 13.6565 |
| Std dev | 7.009994906 | 6.784028516 | 8.639155773 |

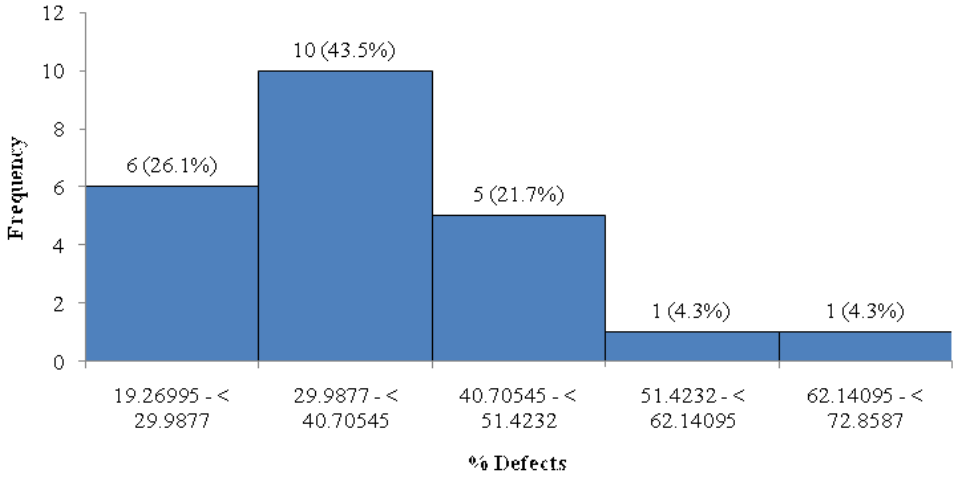


Fig. 4. Histogram of the percentage defects generated.

(Version 4.0). The result also showed the existence of opportunity for massive improvement, since Cp of 0.69 and Cpk of -0.04 are less than 1 and 1.09 respectively.

**4. Statistical Analysis**

Data collected were further analyzed and an overall percentage mean defect of 37.049% with wide standard deviation of 10.7018871 was obtained. This shows the need for further improvement in the foundry as it reflects excessive wastage. The analysis further showed that three defects contribute mainly to the overall non-conformant percentage. These defects include: composition errors, profile and dimension errors and trimming errors; in all, profile error was found to be the chief contributor. Other defects identified include poorly fluxed melts and line marks. Statistical analysis of the three main defects which form the focus of the analysis is shown in table 2.

Histogram showing the percentage defects generated is shown in Figure 4. The plot was normalized by the application of Sturges' rule (Nabi, 2007) expressed as:

$$k = 1 + 3.3 \log10 (n)$$

where k is the number of class intervals or "bins" to be used, and n is the number of data items to classify.

**Run charts**

Run charts for each of the identified main defects were generated by using the SPC for Excel software. These charts show the values of percentage composition defects, percentage profile defects and percentage trimming defects with respect to months of the year 2009 and 2010 (Figures 5 - 9). The lines of best fit and corresponding regression equations were generated to know the level of relationship between the plotted data.

**Composition error**

Figure 5 depicts the complete run chart for percentage composition error. Continuous increase in trend of percentage composition error with time is noticed within the study period (2009 to 2010). The percentage composition error was also observed to be minimum at the beginning of each year; the process for composition control is also veering off steadily and unless mitigated, most products would have compromised content.

**Profile error**

The run chart for percentage profile and dimension error gave irregular trend as shown in figure 6. The drop observed between December 2009 and January 2010 is a reflection of the major maintenance activity performed on

the caster; turn around maintenance is always performed every December. Maintenance activities should be routine so as to improve process performance. The lines of best fit indicate an increase in percentage profile error with time for the plot of constituent years (Figs. 7 and 8). Better trend is found with the two plots when compared with the combined plot for the two study years (Fig. 6). It can be observed from the plots that the process is more controlled in 2010 than 2009 due to the turn around maintenance carried out on the plant in 2009.

**Trimming error**

The run chart for percentage trimming error for the period 2009-2010 is shown in figure 9. Investigations carried out

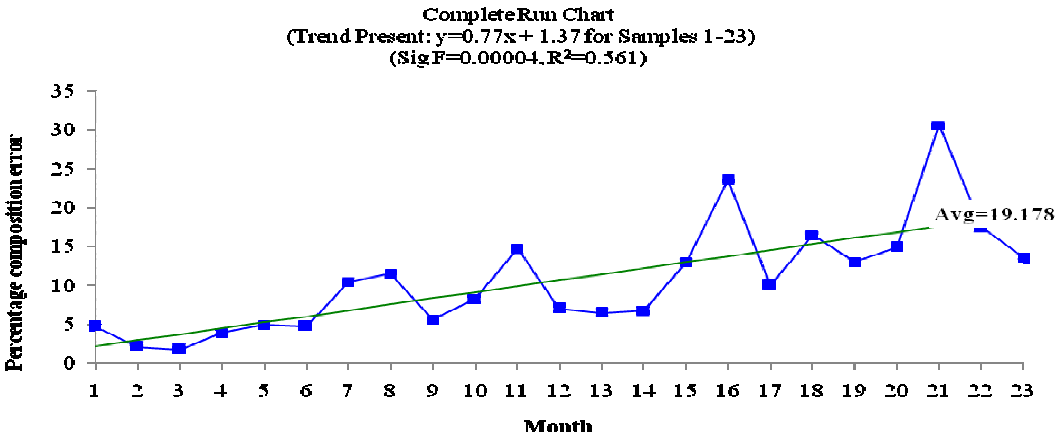


Fig. 5. Complete run chart for percentage composition error.

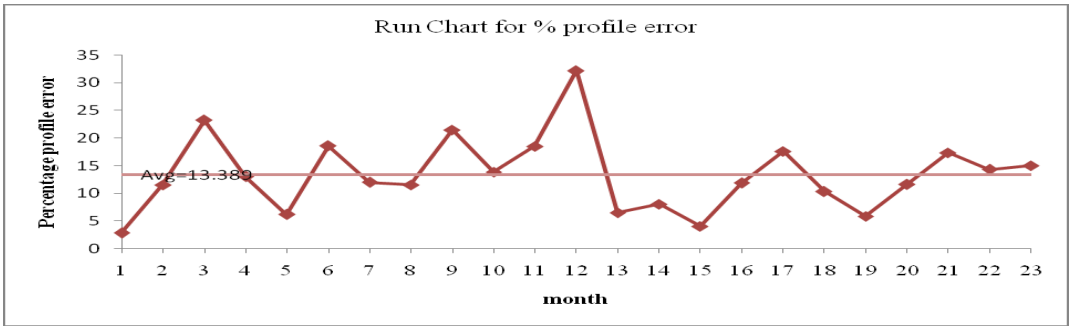


Fig. 6. Complete run chart for percentage profile error.

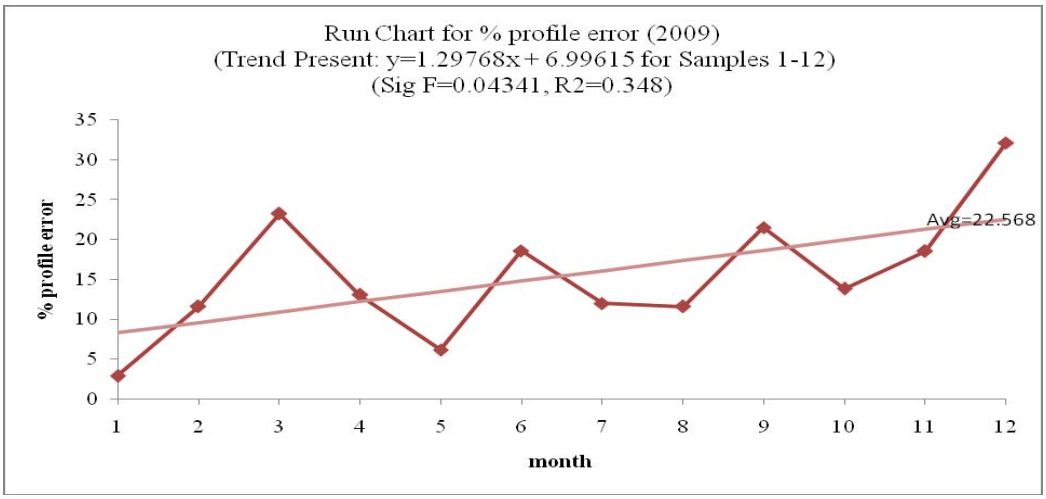


Fig. 7. Run chart of percentage profile error for 2009.

on the system showed that trimming errors were caused primarily by the failure of the edge millers' lubrication pumps. This failure is responsible for the rapid rises in the percentage trimming error; repairs were very effective in bringing down the trimming error percentage.

**Regression Analysis**

Relationships were established between percentage of the various defects and time for each year under study through regression analyses that were carried out between percentage defectives and the total mass produced per month as shown in table 3. This was done to find out if the mass produced had any effect on the proportion that was non-conformant.

**Composition error per month**

The value of the multiple correlation coefficient (R) of 0.749, shows strong correlation between proportion of products with composition errors to months from datum. The $R^2$ value which is 0.561 implies that the model explains only 56.1% of the total variation about the average proportion that is non-conformant. This value also indicates that there are other variables responsible for the other 43.9%, these variables must be unearthed. With the ANOVA analysis, there are less than 0.00004% that this variation can be caused by chance alone. This model is expressed in Equation (1):

$$1.370695652 + 0.77425M = CE \quad (1)$$

where M is the month from datum and CE is percentage containing composition error

**Profile / dimension error per month**

The relationship between percentage profile errors and the month from 2009 to 2010 is negligible (Table 3). There is a 99.71% of obtaining these variations by chance only. This model is therefore not a suitable representation of this scenario. The value of multiple correlation R for the year 2009 is 0.5901 thereby indicating moderate relationship between percentage profile errors and month with the model accounting for about 34.8% of the total variation. Also, 4.34% exist that these variations were produced by chance alone. For 2010, the variations in the analysis have a 3.9% probability of being caused by chance only (Table 3); the variables under study have moderate strength of relationship and this model explains 39.21% of the total variation for 2010. This shows the presence of other variables. The regression models for the years 2009 and 2010 are given as shown in Equations (2) and (3) respectively;

$$6.996151515 + 1.297681818M = PE \quad (2)$$

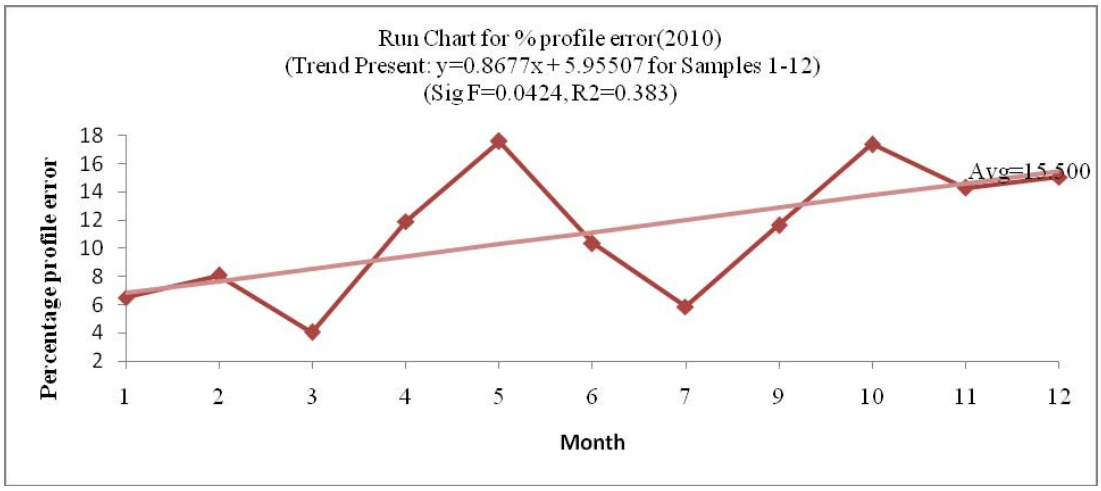


Fig. 8. Run chart of percentage profile error for 2010.

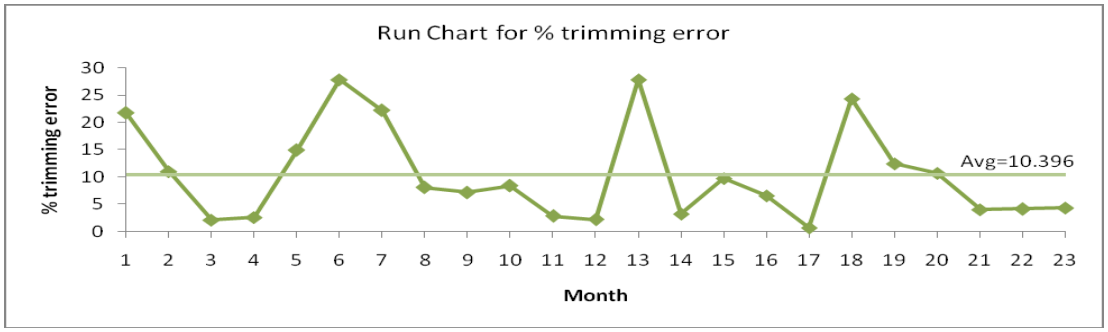


Fig. 9. Complete run chart for percentage trimming error.

Table 3. Analysis for the defects.

| | | Regression Statistics | | ANOVA | |
|---|---|---|---|---|---|
| | Years | Multiple R | $R^2$ | Significance F | Observations |
| Composition error per month | 2009 | - | - | - | - |
| | 2010 | - | - | - | - |
| | 2009 - 2010 | 0.749104537 | 0.561157608 | $3.90475 \times 10^{-5}$ | 23 |
| Profile/ Dimension error per month | 2009 | 0.590097462 | 0.348215015 | 0.043405208 | 12 |
| | 2010 | 0.626236898 | 0.392172652 | 0.039265901 | |
| | 2009 - 2010 | 0.000782413 | $6.1217 \times 10^{-7}$ | 0.99717306 | 23 |
| Trimming error per month | 2009 | 0.3525915 | 0.124321 | 0.260962681 | 12 |
| | 2010 | 0.38443242 | 0.14778829 | 0.243067593 | 11 |
| | 2009 - 2010 | 0.237901388 | 0.05659707 | 0.274350822 | 23 |
| Composition Error (total cast tonnage) | 2009 - 2010 | 0.116913826 | 0.013668843 | 0.595239601 | 23 |
| Profile/ Dimension Error (total cast tonnage) | 2009 - 2010 | 0.085283243 | 0.007273232 | 0.698829118 | 23 |
| Trimming Error (total cast tonnage) | 2009 - 2010 | 0.193772243 | 0.037547682 | 0.375663614 | 23 |

$$6.21715938 + 0.77692995M = PE \quad (3)$$

where M is month and PE is the percentage profile error.

**Trimming error**

It can be seen from the Multiple R, $R^2$ and Sig F values (Table 3) that there exists a weak relationship between time and percentage containing trimming errors. The model explains only 5.7% of the variation and there are 27.4% that these variations are caused by chance. The yearly regression models also show this weak relationship as provided in Equations (4), (5) and (6).

$$14.03265217 – 0.303032609M = TE \quad (4)$$

$$16.53429 – 0.86384M = TE \quad (5)$$

$$15.57689 – 0.9037684M = TE \quad (6)$$

**Ishikawa (Fishbone) Diagrams**

Figures 10a, b and c show the fishbone diagram for obtaining causes of the effects in the boxes. The effects in this case are composition error, profile error and trimming error. All the causes as reflected in the fishbone diagrams were obtained through several discussions with the in-house experts and brainstorming with other company technical personnels after observation of the process.

**Improvement Phase**

Solutions were proffered to several areas of improvement identified in the analysis phase. Among the solutions identified for the foundry include:

- Investments into scrap sorting to improve the effectiveness of sorting process to reduce sorting time.
- Continuous availability of ingots to prevent the adverse effects of ingot shortage on the product grade.
- Proper hot cleaning of the furnaces at least once in a week.
- Monitoring the state of the edge miller on a daily basis so as to reduce trimming problems.
- Condition of the nozzle should be regularly monitored and serviced.
- Installing online profile monitoring device to alert operators of immediate change in profile and/or dimension.
- Revising and following strictly the roll replacement and charging schedule.
- Automating the method of fluxing, degassing and dross removal.
- Proper lubrication of rollers which prevent coil sticking that results in cracks.
- Regular and proper servicing of the pumps, cooling tower and its constituents, to prevent improper cooling which will lead to sticking and cracking.

**Control Phase**

The next stage in Six Sigma deployment (after the implementation of improvement efforts) is the institutionalization of the improvement. It is aimed at locking in the benefits of the optimization and preventing the system from returning to its former state. The gains can be secured by following the following control mechanisms viz:

- Conversion of the quality control department to a Six Sigma department and to train staffs accordingly. This will serve as a take off point and guarantee high

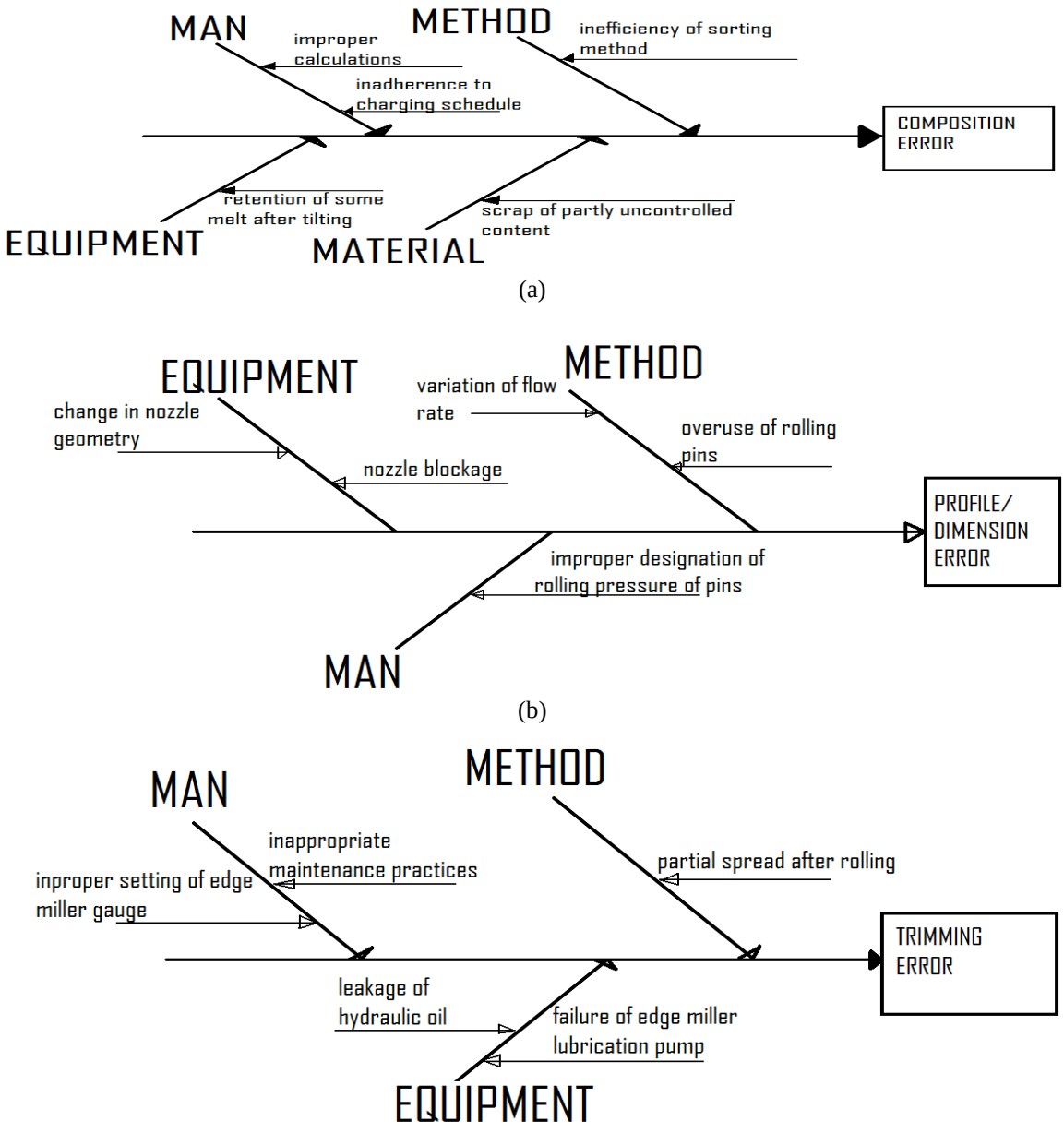


Fig. 10. Ishikawa (fishbone) diagrams for (a) composition error (b) profile error and (c) trimming error.

quality and continuous improvement in the manufacturing processes.

- Transforming the entire company into a Six Sigma company by training every staffs the philosophy and practices of Six Sigma. This will set everybody thinking in the direction of continuous improvement such that every sphere of company activities will be geared towards increased efficiency. This will invariably increase customers' satisfaction and provide positive bottom-line impact.
- Acquisition of the latest compatible equipment and testing devices for improved efficiency.
- Carrying out monthly process audits and statistical analysis of data from each component or machine. This will provide better understanding of the process, its components and their interactions.
- Giving higher priority to staff welfare as this affects dedication, attention and also improves the performance of their various jobs.
- Provision of conducive working conditions within the factory by improving ventilation to reduce discomfort and fatigue caused by high temperatures in the factory.

- Continous revision and strict adherence to the general maintenance schedule so as to prevent failure of machines.

## CONCLUSION

In this study, it has been found that Six Sigma is a veritable methodology for improving the performance of a manufacturing firm, particularly in Nigeria. In the firm studied, it was discovered that production of non-conforming or defective products was the major problem. The main defects were identified as composition errors, profile/ dimension errors and trimming errors. The causes of these errors were identified as operator skill, raw material content, operating procedures, available technology, and maintenance practices. Solutions have been documented in line with Six Sigma methodology. Implementation of these solutions will result in noticeable improvement and firm operating with near-perfect processes, hence, guaranteeing customer satisfaction.

## REFERENCES

Aggogeri, F. and Gentili, E. 2008. Six-Sigma methodology: an effective tool for quality management. International Journal of Manufacturing Technology and Management. 14(3-4):289-298.

Aksoy, B. and Orbak, AY. 2009. Reducing the quantity of reworked parts in a robotic arc welding process. Quality and Reliability Engineering International. 25(4):495-512.

Antony, J. and Banuelas, R. 2002. Key ingredients for the effective implementation of Six Sigma program. Measuring Business Excellence. 6(4):20-27.

Banuelas, R. Antony, J. and Brace, M. 2005. An application of Six Sigma to reduce waste. Quality and Reliability Engineering International. 21(6):553-570.

De Koning, H. and De Mast, J. 2006. A rational reconstruction of Six Sigma's Break-through Cookbook. International Journal of Quality and Reliability Management. 23(7):766-787.

Evans, JR. and Lindsay, WM. 2005. The Management and Control of Quality ($6^{th}$ edi.). South-Western, Mason, OH.

Falcón, RG., Alonso, DV., Fernández, LMG. and Pérez-Lombard, L. 2012. Improving energy efficiency in a naphtha reforming plant using Six Sigma methodology. Fuel Processing Technology. 103:110-116.

Gijo, EV. and Scaria, J. 2010. Reducing rejection and rework by application of Six Sigma methodology in manufacturing process. International Journal of Six Sigma and Competitive Advantage. 6(1/2):77-90.

Goffnett, SP. 2004. Understanding Six Sigma: Implications for Industry and Education. Journal of Industrial Technology. 20(4):1-10.

Kaushik, P., Grewal, CS., Singh, BP. and Khanduja, D. 2008. Utilising Six Sigma for energy conservation: a process industry case study. International Journal of Six Sigma and Competitive Advantage. 4(1):18-34.

Kwak, YH. and Anbari, FT. 2006. Benefits, obstacles, and future of six sigma approach. Technovation. 26:708-715.

Lee-Mortimer, A. 2006. Six Sigma: a vital improvement approach when applied to the right problems, in the right environment. Assembly Automation. 26(1):10-18.

Maleyeff, J. and Kaminsky, FC. 2002. Six Sigma and introductory statistics education. Education & Training. 44:82-89.

Nabi, K. 2007. The Implementation of the Six Sigma Program: Department of Mechanical and Industrial Engineering, University of Toronto, Canada.

Pande, P. and Holpp, L. 2002. What is Six Sigma? McGraw-Hill, New York, USA.

Pantano, V., O'Kane, P. and Smith, K. 2006. Cluster-based six sigma development in small and medium sized enterprises. In: Proceedings of 2006 IEEE International Conference on Management of Innovation and Technology, Singapore. 21-23.

Parast, MM. 2011. The effect of Six Sigma projects on innovation and firm performance. International Journal of Project Management. 29:45-55.

Pyzdek T. 2003. The Six Sigma Handbook: A Complete Guide for Green Belts, Black Belts, and Managers at All Levels. McGraw-Hill, New York, USA.

Rajagopalan, R., Francis, M. and Suarez, W. 2004. Developing novel catalysts with Six Sigma. Research—Technology Management. 47:13-16.

Su, CT. and Chou, CJ. 2008. A systematic methodology for the creation of Six Sigma projects: A case study of semiconductor foundry. Expert Systems with Applications. 34:2693-2703.

Treichler, D., Carmichael, R., Kusmanoff, A., Lewis, J. and Berthiez, G. 2002. Design for Six Sigma: 15 lessons learned. Quality Progress. 35(1):33-42.

Ung, ST., Bonsall, S., Williams, V., Wall, A. and Wang, J. The application of the Six Sigma concept to port security process quality control. Quality and Reliability Engineering International. 23(5):631-639.

Received: July 25, 2013; Accepted: Oct 8, 2013

SENRA Academic Publishers, British Columbia
Vol. 8, No. 1, pp. 2761-2767, February 2014
Online ISSN: 1920-3853; Print ISSN: 1715-9997

Canadian Journal of pure&applied sciences

# REDUCTION OF THE SPARK IGNITION ENGINE EMISSIONS USING LIMESTONE FILTER

Wail Adaileh and *Ali Alahmer
Department of Mechanical Engineering, Tafila Technical University
PO. Box 179, 66110 Tafila, Jordan

## ABSTRACT

This paper presents an experimental study to reduce of a spark ignition engine (SI) emissions using a low cost limestone filter. The limestone filter was constructed and tested on a four cylinder, four stroke spark ignition Nissan Sunny sedan engine (1.6 L) model 2008. The limestone filter was placed in a cast iron housing through the exhaust gas passes. The concentration of pollutant emissions of hydrocarbon (HC), carbon monoxide (CO), carbon dioxide ($CO_2$) and nitrogen monoxide (NO) was measured with and without using limestone filter. The experimental results showed that the pollutant emissions were decreased dramatically after using limestone filter.

**Keywords**: SI engine, emission, limestone, filter, pollutants.

## INTRODUCTION

Emissions from SI engines contribute to a number of serious air pollution and it will lead to adverse health and welfare effects associated with ozone. These emissions also cause significant public welfare harm, such as damage to crops, eutrophication, and regional haze. Today, the major gaseous pollutants emitted include (Turns, 2000; Alkemade and Schumann, 2006): (i) carbon monoxide (CO) which is a poisonous gas, colorless, tasteless and odorless gas. It is formed during incomplete combustion; (ii) oxides of nitrogen ($NO_X$) contributes to smog and acid rain, and it also causes irritation to human mucus membranes, and (iii) Hydrocarbons (HC) consists of unburned hydrocarbons and products of combustion reactions, these can further react to form ground level Ozone ($O_3$), a major component of smog.

There are different technologies to control air pollutant emissions from internal combustion engine (ICEs) can be categorized as process and post combustion controls (Canfield, 1999). Process controls include engine modification or improvements to the combustion. While the post combustion controls include oxidation catalysts in the exhaust system and other technologies applied to react with combustion exhaust constituents including NOx, CO, HCs, and particulate. Also, adjusting the fuel injection timing is an effective method for decreasing NOx emissions.

This paper has a new approach to investigate the effectiveness of using limestone filters to reduce the pollutant emissions from SI engine. Limestone is a very common sedimentary rock composed the minerals calcite and aragonite.

The structure of this paper starts by discussing the different technologies to control pollutant emissions from internal combustion engine in section one. The section two introduces the related researches from the body of literature in section two. The experimental approach and setup was presented in section three. Section four shows the result and discussion of exhaust emission concentrations with and without using limestone filter. Finally, section five summarizes the study findings through the conclusion.

Recently, the emphasis on reduced pollutant emissions from vehicular exhaust has been increasing and becoming one of the competitive technologies and main features in the automobile design. Several researchers have proposed different method to reduce the main pollutant emissions. Wu *et al*. (2004) investigated the effect of air fuel ratio on engine performance and pollutant emission from spark ignition engine using ethanol-gasoline-blended fuels. He found that CO and HC emissions were reduced with the increase of ethanol content in the blended fuel. Another study Alahmer (2013) and Alahmer *et al*. (2010) studied the effect of using the emulsified diesel fuel on pollutant emissions from diesel engines. The study was found that at high amount of water addition, the nitrogen oxide decreases. Canfield *et al*. (1997) described a filter cart designed to capture of NOx, CO, VOCs, and particulate from the A/M32A-86 diesel generator. Shehata and Abdel (2008) installed catalyst converter in the exhaust manifold which provided significant reduction HC and CO concentrations. Musmar and Al-Rousan (2011) studied the effect of HHO gas on combustion emissions in gasoline engines. They showed that a mixture of HHO

*Corresponding author email: A.alahmer@ttu.edu.jo

and gasoline cause a reduction in the concentration of emission pollutant in terms of NO, NOx and CO with improvement in engine efficiency. Sim *et al*. (2001) made a successful reduction of HC and CO emissions by injecting secondary air intermittently into the exhaust port. Tanaka *et al*. (2001) proposed an intelligent catalyst to oxidize HC and CO emissions during cold start by storing HC and CO on-board and then release them into the catalyst once light off. Several researchers have used limestone to reduce exhaust gas emissions. Sakhrieh (2012) designed and tested a limestone filter on a four cylinder direct injection diesel engine. He found the pollutants in terms of $CO_2$ and NOx were decreased significantly with no increase in the fuel consumption rate. In order to reduce the emission of particulate matter in a coal fired circulating fluidized bed combustor the kaolin and limestone addition were added to coal by Chen *et al*. (2011). The reduction was occurring due to kaolin has the capability to capture Na and K vapors, whereas limestone reacts with sulfur effectively. A limestone or kaolin was used by Bafver *et al*. (2009) to reduce the particle emission from combustion of oat grain.

After surveying the published papers, there is a positive trend in the amount of published papers about the using the limestone to reduce the emission. According to the author's knowledge this is the first trial to investigate the effect of using limestone filters to reduce the emission from the spark ignition engine.

## MATERIALS AND METHODS

### Experimental Methodology

Several experiments were carried out to study the effect of using limestone filters on exhaust gas emissions in Tafila Technical University automotive laboratories. In order to reduce the emissions such as CO, NOx, $CO_2$ and HC emitted from SI engine, a limestone was used which is a very common sedimentary rock of biochemical origin. The limestone filter was constructed and tested on a four cylinders, four stroke spark ignition 2008 Nissan Sunny sedan with an engine capacity of 1.6 L. The engine specifications are listed in table 1. The exhaust emission was measured using a Kane automotive gas analyzer by mounting gas analyzer probe on the pipe of gas. The gas analyzer specifications are presented in table 2. The experimental work is set according to the following protocol; First experimental preparation which includes: (i) One kilogram of limestone was brought from the Jordanian chalk manufacturing company, which has a chemical composition as follows: $CO_2$+ CaCl + $H_2O$→ $CaCO_3$+ HCl, and during its preparation gets an impurities like Al, Mg and Si; (ii) The limestone was placed inside a house box to prevent a high pressure drop. The cast iron housing box was installed at the end of the exhaust system tailpipe by a clamp, and keeps the exhaust gas to pass through the limestone filter freely; the housing cylinder dimensions were 40cm long, 10cm diameter and thickness 0.2cm; (iii) The two suggested prototypes of limestone housing being depicted in figure 1. The first suggested prototype consists of main cylinder, a diffuser, and a nozzle. The main cylinder has two grooves with a width of 5 cm, each. And it has three ways to exhaust stream and has some restrictions to increase the contact area with exhaust gas, while the second suggested prototype has low exhaust gas restrictions. The first suggested prototype was chosen due to have an enough time for completing a chemical reaction. The next step on the protocol was experimental operation which includes: (i) The engine was started until it reaches the operating temperature; (ii) the gas analyzer probe was mounted on the pipe of gas exhaust to measure exhaust emissions in terms of gases CO, $CO_2$, $O_2$ and HC; (iii) the emission concentration was measured with limestone filter and without at each specified speed started from 700rpm each step increase 200rpm till reach 3200rpm.

First suggested prototype of limestone house

Second suggested prototype of limestone house

Fig. 1. Two prototypes of the limestone house were suggested.

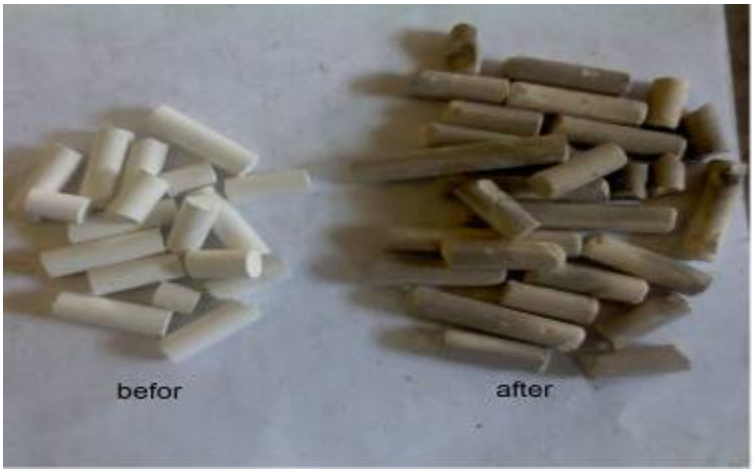


Fig. 2. Limestone color before and after doing the experiments.

## RESULTS AND DISCUSSION

The exhaust emission of CO, $CO_2$, HC and $O_2$ concentration are measured with and without using limestone filter. Figure 2 displays the color of the limestone before and after doing the experiments. The color was changed from white to the darkened as indicated the limestone filter absorbed the harmful gases.

### Carbon Monoxide (CO) Emission

In general, CO is produced during combustion as the engine is running in rich mixtures due to deficiency of oxygen which unable to oxide all carbon atoms of fuel into $CO_2$ , and the exhaust will contain large amount of CO. So, the air fuel equivalence ratio will play a crucial factor in produce CO emission. Other sources of CO formation are: Slow kinetics during expansion, Wall and crevice effects and Partial HC oxidation. The concentration of CO emission variation with engine speed with and without using limestone filter is shown in figure 3. As shown in the figure, CO increases with engine speed due to decrease the time required to oxidize the CO, increase the turbulence intensity, mixing process of burned and unburned gases and non-uniform mixture distribution within the cylinder. After using the limestone filter the amount of CO has been decreased obviously. The average reduction of CO after using limestone filter was 44.4%. The reduction of CO is due to the ability of limestone filter absorbing the CO from the exhaust gas to produce calcium oxide as the following reaction:

$$CaCO_3(s) + 2CO(g) \rightarrow CaO(s) + 2CO_2(g)$$

### Carbon Dioxide ($CO_2$) Emission

It is a product of complete and incomplete combustion. Figure 4 shows the concentration of $CO_2$ emission variation with and without using limestone filter. The chemical reaction of gasoline at a complete combustion was occurred according to

$$C_8H_{18} + 12.5(O_2 + 3.76N_2) \rightarrow 8CO_2 + 9H_2O + 47N_2$$

And the percent of $CO_2$ at dry analysis is $\frac{8}{8+47} \times 100\% = 14.55\%$

At engine speed 2400rpm, the concentration of $CO_2$ with and without using limestone filter are 15.84 and 16.51% respectively. The average reduction of $CO_2$ after using limestone filter was 4.6%. The reduction of $CO_2$ was occurred when calcium carbonate reacts with water that is saturated with carbon dioxide to form the soluble calcium bicarbonate, according to the following chemical reaction which

$$CaCO_3(s) + CO_2(g) + H_2O\ (l) \rightarrow Ca(HCO_3)_2(aq)$$

### Unburned Hydrocarbon (HC) Emission

Unburned hydrocarbon concentration in the exhaust is measured by flame ionization analyzer, which is mainly a carbon atom counter. The total hydrocarbon concentration is measured by this method is specified in parts per million as methane or C1. In order to produce an unburned hydrocarbon there are sixth ways, which mainly are (i) Misfired combustion, which occurs in highly rich or lean situation; (b) Flame quenching on the cylinder walls or in crevices (c) Absorption and desorption in oil film on cylinder walls or in carbon deposits in the chamber; (d) Liquid fuel in the cylinder; (e) Exhaust valve leakage, and (f) Crankcase blow by gases. The concentration of HC emission variation with engine speed with and without using limestone filter is depicted in figure 5. It can be found that the amount of HC has been decreased dramatically after using the limestone filter. And the average reduction of CO after using limestone filter was 26.8%.

### NO emission

Nitrogen and oxygen under high pressure and temperature during combustion react to form nitrogen oxide (NO) and

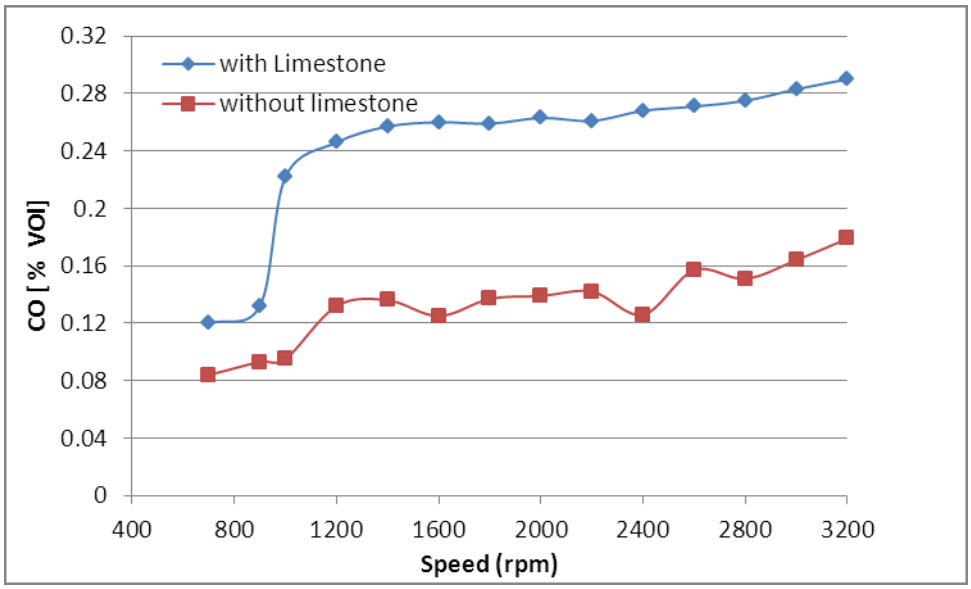


Fig. 4. CO concentration variation with and without using limestone due to engine speed.

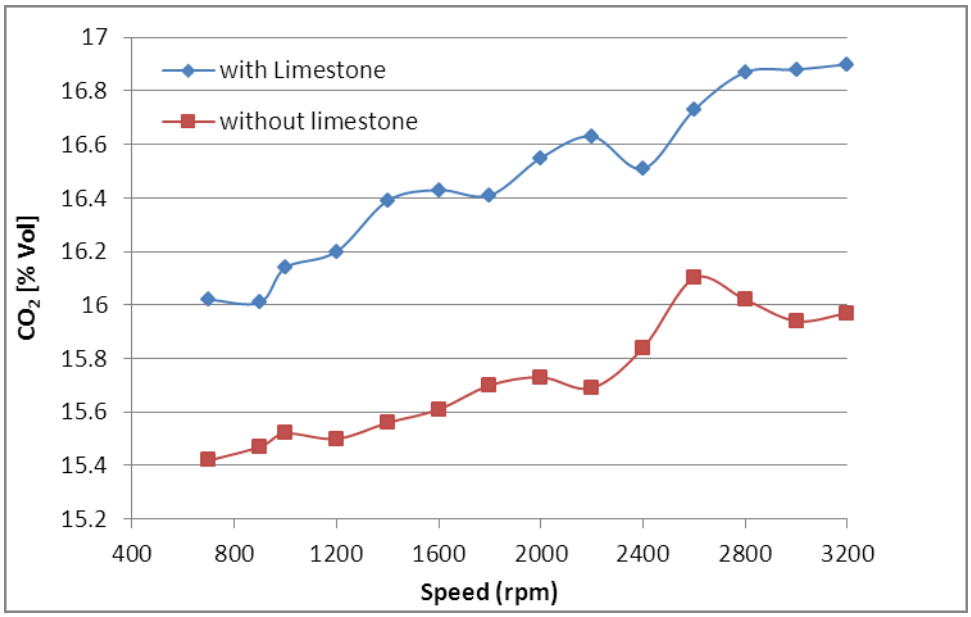


Fig. 4. $CO_2$ concentration variation with and without using limestone due to engine speed.

nitrogen dioxide ($NO_2$). The rate of NO formation is related to temperature. Figure 6 summarizes the effect of using limestone filters on NO. From this graph, the following observations can be seen; the first observation is the combustion by using limestone filter produced significantly less amounts of NO as compared to without using limestone filter. So after installing the limestone filter the nitrogen monoxide reduced by 40.2% on average. This reduction was occurring because the limestone reacts with NO to produce calcium nitrite Ca ($NO_2$):

$$CaCO_3(s) + 2NO(g) + \frac{1}{2}O_2(g) \rightarrow Ca(NO_2)_2(s) + CO_2(g)$$

$$Ca(OH)_2(s) + 2NO(g) + \frac{1}{2}O_2(g) \rightarrow Ca(NO_2)_2(s) + H_2O\ (l)$$

The second observation is the high combustion temperature due to increase of engine speed is directly influenced on NO formation during the reduction in chemical reaction rates. This can be shown from Zeldorich mechanism reactions (Turns, 2000; Miller and Bowman, 1989):

$$O + N_2 \xrightarrow{k1} NO + N$$

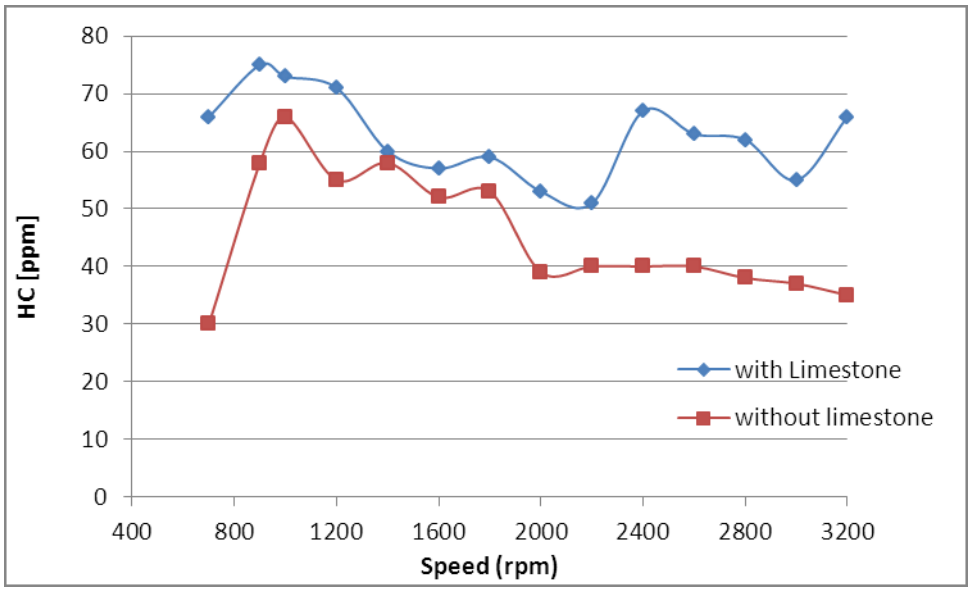


Fig. 6. HC concentration variation with and without using limestone due to engine speed.

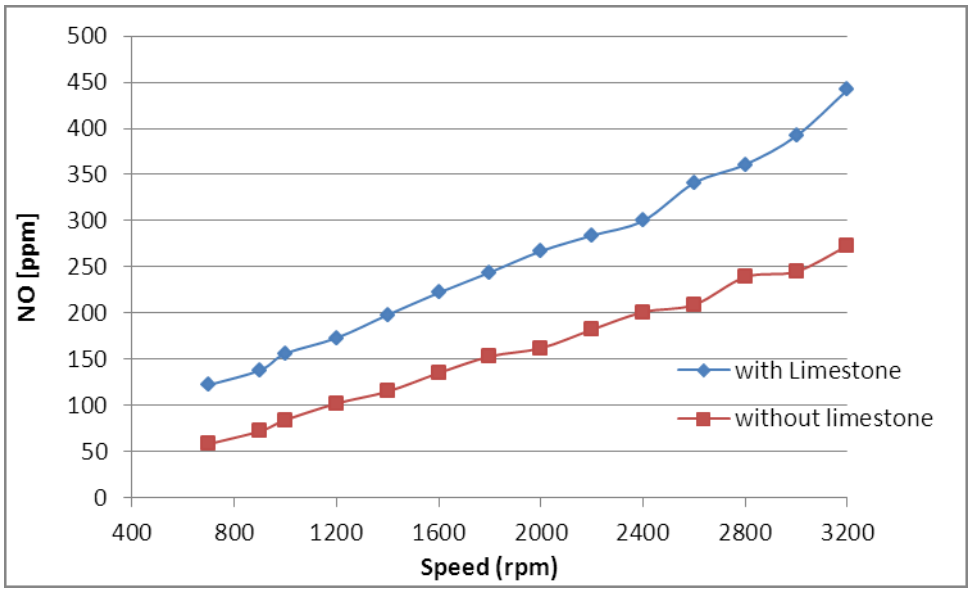


Fig. 6. NO concentration variation with and without using limestone due to engine speed.

$$k1 = 1.8 \times 10^{12} \exp(-319 kJmol^{-1}/RT)$$

$$N + O_2 \xrightarrow{k2} NO + O$$

$$k2 = 6.4 \times 10^{9} \exp(-26 kJmol^{-1}/RT)$$

$$N + OH \xrightarrow{k3} NO + H$$

$$k3 = 3.0 \times 10^{13}$$

## CONCLUSION

This manuscript investigated the effect of using limestone filter as a main agent to reduce emissions such as CO, unburned HC, $CO_2$ and NO caused by spark ignition engine. The limestone filter was installed on a four cylinders, four stroke spark ignition 2008 Nissan Sunny sedan with an engine capacity of 1.6L. The results of this study can be summarized as the pollutant emissions were decreased dramatically after using limestone filter. The average reduction of CO, unburned HC, $CO_2$ and NO after using limestone filter was 44.4, 26.8, 4.6 and 40.2% respectively.

Table 2. Nissan Sumnny engine specifications.

| Type | Data |
|---|---|
| Engine code | MR16DDT |
| No. of cylinders, configuration | 4, in line |
| Valves per cylinder | 4 |
| Air intake system | Turbocharger + Intercooler |
| Engine displacement | 1618 cm³ |
| Bore x stroke | Ø79.7 x 81.1 mm |
| Max. engine power | 140 (190) @ 5600 kW(ps)/min-1 |
| Max. torque | 240Nm @ 2400-5200 Nm/min-1 |
| Compression ratio | 9.5 : 1 |
| Cam type | DOHC led by chain |
| Fuel type | Unleaded Petrol (RON95) |
| Ignition system / Intake system | Individual coils / Knock control |
| Fuel Supply | Sequential High-pressure Direct Injection |

Table 2. Kane automotive gas analyzer Specifications.

| Parameter | Resolution | Accuracy | Range |
|---|---|---|---|
| Carbon Monoxide (Infrared) | 0.01 % | +/- 5 % of reading<br>+/- 0.5 % volume | 0-10 %<br>Over-range 20 % |
| Oxygen (fuel cell) | 0.01 % | +/- 5 % of reading<br>+/- 0.1 % volume | 0-21 %<br>Over-range 48 % |
| Hydrocarbon (Infrared) | 1 ppm | +/- 5 % of reading<br>+/- 12 ppm volume | 0-5000 ppm<br>Over-range: 10,000 ppm |
| Carbon Dioxide (Infrared)) | 0.1 % | +/- 5 % of reading<br>+/- 0.5 % volume | 0-16 %<br>Over-range: 25% |
| Nitric Oxide (fuel cell) | 1 ppm | 0-4000ppm +/-4% or<br>25ppm; 4000-5000 ppm +/-5% | 0-5000ppm |

**REFERENCES**


Alahmer, A. 2013. Influence of using emulsified diesel fuel on the performance and pollutants emitted from diesel engine. Energy Conversion and Management. 73:361-369.

Alahmer, A., Yamin, J., Sakhrieh, A. and Hamdan, MA. 2010. Engine performance using emulsified diesel fuel. Energy Conversion and Management. 51(8):1708-1713.

Alkemade, U. and Schumann, B. 2006. Engines and exhaust after treatment systems for future automotive applications. Solid State Ionics. 177(26-32):2291-2296.

Bäfver, L., Rönnbäck, M., Leckner, B., Claesson, F. and Tullin, C. 2009. Particle Emission from Combustion of Oat Grain and its Potential Reduction by Addition of Limestone or Kaolin. Fuel Processing Technology. 90(3):353-359.

Canfield, C. 1999. Effects of diesel-water emulsion combustion on diesel engine NOx emissions, Master dissertation, Mechanical engineering department, University of Florida, USA.

Canfield, C., Babyak, R. and Wander, J. 1997. Demonstration of a filter cart for NOx removal from ground support equipment, Technical Report No. AL/EQ-TP-1997-0001, US Air Force Research Laboratory, Tyndall AFB, FL, USA.

Chen, J., Yao, H., Zhang, P., Xiao, L., Luo, G. and Xu, M. 2011. Control of PM1 by kaolin or limestone during O2/CO2 pulverized coal combustion. Proceedings of the Combustion Institute. 33(2):2837-2843.

Miller, JA. and Bowman, CT. 1989. Mechanism and modeling of nitrogen chemistry in combustion. Progress in Energy and Combustion Science. 15:287-338.

Musmar, S. and Al-Rousan, A. 2011. Effect of HHO gas on combustion emissions in gasoline engines. Fuel. 90(10):3066-3070.

Sakhrieh, A. 2012. Experimental study on exhaust gas after treatment using limestone. Thermal Science. 17(1):49-56.

Shehata, M. and Abdel Razek, A. 2008. Engine performance parameters and emissions reduction methods for spark ignition engine. Engineering Research Journal. 120, M32- M57.

Sim, H., Min, K. and Chung, S. 2001. Effect of synchronized secondary air injection on exhaust hydrocarbon emission in a spark ignition engine. Journal of Automobile Engineering. 215(4):557-566.

Tanaka, H., Uenishi, M., Tan, I., Kimura, M., Mizuki, J. and Nishihata, Y. 2001. An intelligent catalyst. SAE Technical Paper 2001-01-1301.

Turns, S. 2000. An introduction to combustion concepts and applications (2nd edi.). McGraw-Hill.

Wu, C., Chen, R., Pu, J. and Lin, T. 2004. The influence of air–fuel ratio on engine performance and pollutant emission of an SI engine using ethanol–gasoline-blended fuels. Atmospheric Environment. 38(40):7093-7100.

Received: Sept 30, 2013; Accepted: Oct 26, 2013

SENRA Academic Publishers, British Columbia
Vol. 8, No. 1, pp. 2769-2774, February 2014
Online ISSN: 1920-3853; Print ISSN: 1715-9997

Canadian Journal of pure&applied sciences

# BEARING CAPACITY AND SETTLEMENT RESPONSE OF RAFT FOUNDATION ON SAND USING STANDARD PENETRATION TEST METHOD

Akpila, S B
Department of Civil Engineering
Rivers State University of Science and Technology, PMB. 5080, PortHarcourt

## ABSTRACT

Bearing capacity and settlement response of raft foundations placed on sand was carried out using standard penetration test on soil lithology consisting of loose, silty to slightly silty SAND, overlying medium-dense slightly silty SAND. Results showed that allowable bearing capacity, $q_a$, had a decreasing trend with an increase in raft foundation breadth whereas for a given foundation breadth, $q_a$ increased with foundation depth. Allowable bearing capacity also decreased as the ratio of foundation depth, $D_f$, to breadth, B ratio ($D_f$/B) decreased. Immediate and consolidation settlement increased with foundation breadth, bearing pressure and foundation depth. Comparatively, Burland and Burbidge approach had a higher total settlement against those of Harr. The predictive models can be useful for preliminary design purposes on sites with similar conditions.

**Keywords**: Immediate settlement, poisson ratio, modulus of elasticity, models.

## INTRODUCTION

Bearing capacity and settlement requirements are two basic criteria to be satisfied in the analysis and design of shallow foundations. The criterion on bearing capacity ensures that the foundation does not undergo shear failure under loading, while settlement requirement ensures that settlement of the structure is within the tolerance limit of the superstructure. Three types of shear failures have been identified to occur under foundation induced loading; general shear failure, punching shear failure and local shear failure. Details of these failures and their mechanisms have been reported by Singh (1992), Caquot (1934), Terzaghi (1943), De Beer and Vesic (1958) and Vesic (1967). The use of standard penetration test in the analysis of bearing capacity and settlement has also received numerous attentions (Craig, 1987; Bowles, 1997; Som and Das, 2006; Tomlinson, 2001). In the Niger Delta region of Nigeria, recent studies on bearing capacity and settlement of shallow foundations have been reported by Akpila (2007a), Akpila (2007b), Akpila and ThankGod (2008) and Akpila *et al*. (2008). Details of the field application of Standard Penetration Test are specified in BS 1377. This paper attempts to report on bearing capacity and settlement of raft foundations placed on sand using methods based on the standard penetration test.

## MATERIALS AND METHODS

### *Data Acquisition*

Information on subsurface conditions at the site was studied through ground borings to depths of 24m each using a percussion boring rig. Both disturbed and undisturbed samples were collected for visual examination, laboratory testing and classification. Standard Penetration Tests (SPT) were conducted to determine the penetration resistance values of cohessionless soils at specific depths within the bore holes. Requisite laboratory tests were also carried out on soil samples to obtain input parameters for bearing capacity and settlement assessment. The water table at the site was observed to vary from about 1.0 - 1.1m below the existing ground level.

### Bearing Capacity Analysis on sand

A bearing capacity analysis of raft foundation has been necessitated by the soil stratigraphy at the site which generally consists of loose, silty to slightly silty SAND, overlying medium-dense, slightly silty SAND formation. The proposed foundation was to be placed at 1.6m below the sand formation which had previously been reclaimed with hydraulically dredged sand to meet desired grade level existing between the highway pavement and the project location (Fig. 1). The modified Meyerhof (1956) correlation for bearing capacity using Standard Penetration Resistance presented by Bowles (1997) for an allowable settlement of 50.8mm was used. The choice of using modified Meyerhof method is based on the middle bound values associated with the model compared to that of Parry (1977) which gives higher bound value and Meyerhof (1956) with lower bound values of bearing capacity (Akpila, 2013). The modified Meyerhof

Corresponding author email: sakpilab@yahoo.com

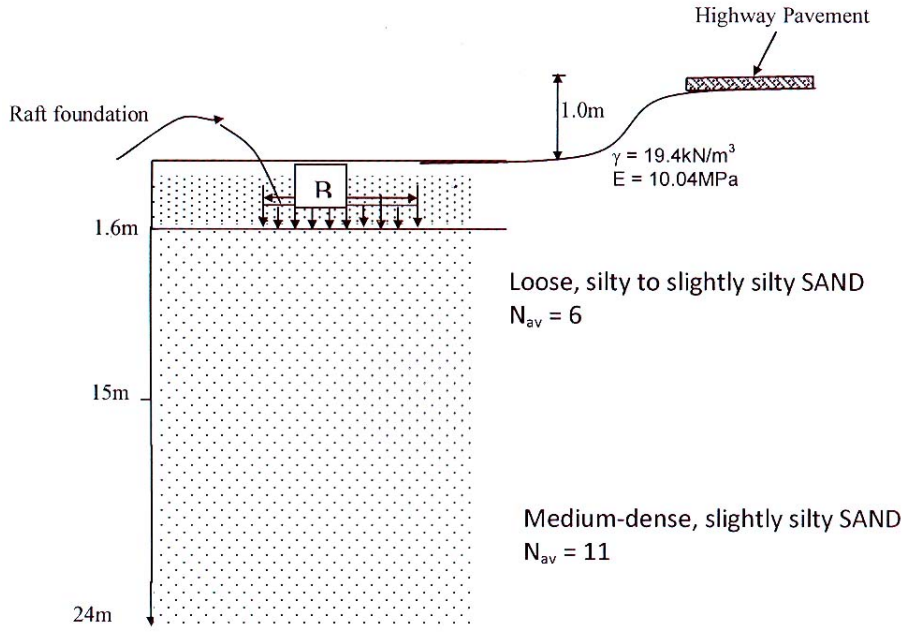


Fig. 1. Raft foundation on Sand formation.

expressions are given by;

$$q_{n(a)} = 19.16NF_d\left(\frac{s}{25.4}\right) \text{ for } B \leq 1.2m \quad (1)$$

$$q_{n(a)} = 11.98N\left(\frac{3.28B+1}{3.28B}\right)^2 F_d\left(\frac{s}{25.4}\right) \text{ for } B > 1.2m \quad (2)$$

where $F_d$ = depth factor = $1+ 0.33\ (D_f/ B) \leq 1.33$

s = tolerable settlement
N = average penetration number

**Settlement Analysis on Sand:**

***Immediate Settlement***

Immediate foundation settlement at a corner of a rigid foundation of breadth B ranging from 8-12m is respectively obtained using the expression proposed by Harr (1966) and reported in Braja (1999) as follows;

$$s_i = \frac{q_n B}{E_o}(1-\mu^2)\alpha_r \quad (3)$$

Where $S_i$ is immediate settlement, B is the breadth of foundation at a corner, $q_n$ is net foundation pressure, $E_o$ is modulus of elasticity, μ is Poisson ratio, $\alpha_r$ is influence factor for rigid foundation. To obtain the settlement at the centre of a square foundation, usually requires the principle of superposition and settlement value is four times the settlement at any corner.

The values of E and μ are obtained from the expressions;

$$E_o = 0.478N + 7.17MPa \quad (4)$$

$$\mu = \frac{1-\sin\Sigma}{2-\sin\Sigma} \quad (5)$$

Where □ is angle of internal friction of sand and N is the average SPT blow count for sand stratum. Values of influence factor, $\alpha_r$, for various lengths to breadth (L/B) ratios were obtained from standard curves presented in Braja (1999). In Burland and Burbidge (1985) approach, they proposed that for normally consolidated sand, the average settlement is expressed as;

$$s_i = \frac{q_n B^{0.7}}{3}\left(\frac{1.71}{N^{1.4}}\right) \quad (6)$$

Where $q_n$ is the net foundation pressure, B is foundation breadth and N is the average value of standard penetration resistance

**Consolidation Settlement:**

Although settlement of sand is generally treated as immediate, the consolidation settlement was attempted adopting Equations (4, 5, 7 and 8). The coefficient of volumetric compressibility, $m_v$, is obtained from the following expression;

$$m_v = \frac{(1+\mu)(1-2\mu)}{E_o(1-\mu)} \quad (7)$$

Where $E_o$ and μ and are as defined in Equations (4 and 5). Consolidation settlement was evaluated from the expression proposed by Skempton and Bjerrum (1957) as follows:

$$\rho_c = \frac{\Delta_e}{1+e_o}\left(\frac{1}{\Delta p}\right)\Delta\sigma_z H$$

$$= 0.55\left\{\frac{\Delta e}{1+e_o}\left(\frac{1}{\Delta p}\right) q_n x 1.5B\right\}$$

$$= 0.55 m_v q_n x 1.5B \quad (8)$$

Where $\rho_c$ is consolidation settlement, $q_n$ is net foundation pressure, B is foundation breadth, Δp is change in pressure, Δe is change in void ratio, $e_o$ is initial void ratio,

$\Delta\sigma_z$ is induced vertical stress and $\frac{\Delta\varepsilon}{1+\varepsilon_o}\left(\frac{1}{\Delta p}\right)$ is coefficient of volume compressibility, $m_v$.

Substituting Equation (7) into Equation (8) yields;

$$\rho_c = 0.55\frac{(1+\mu)(1-2\mu)}{E_o(1-\mu)}q_n x1.5B \quad (9)$$

The total settlement from the Raft foundation can then be expressed as;

$$\rho_t = \frac{q_n B}{E_o}(1-\mu^2)\alpha_r + 0.55\frac{(1+\mu)(1-2\mu)}{E_o(1-\mu)}q_n x1.5B \quad (10)$$

If immediate settlement is considered based on Equation (6), then for normally consolidated sand, total settlement can be expressed as;

$$\rho_t = \frac{q_n B^{0.7}}{3}\left(\frac{1.71}{N^{1.4}}\right) + 0.55\frac{(1+\mu)(1-2\mu)}{E_o(1-\mu)}q_n x1.5B \quad (11)$$

Limiting values for allowable settlement of different structures founded on either clay or sand have been presented by scholars including Skempton and MacDonald (1956), Polshin and Tokar (1957) and Wahls (1981). The vertical deformation of the raft foundation was assessed based on the stipulated limiting values.

## RESULTS AND DISCUSSION

### *Soil Classification/Stratigraphy*

This is obtained from boring records and laboratory tests. The soil profile generally consists of loose, silty to slightly silty SAND overlying medium-dense, slightly silty SAND formation up to the 24m depth of exploration.

### Bearing Capacity

The allowable bearing capacity values of raft foundation with B, ranging from 8-15m and placed at varying foundation depth, $D_f$, are shown in table 1. Generally, allowable bearing capacity, $q_a$, showed a decreasing trend with an increase in raft foundation breadth whereas for a given foundation breadth, $q_a$ increased with foundation depth (Fig. 2). For cases of variation of $q_a$ and $D_f/B$ ratio, it was noticed that $q_a$ values increased with increase in $D_f/B$ ratio. The respective predictive models relating allowable bearing capacity and foundation breadth for varying foundation depths are presented as follows;

$$q_{a(1.0)} = -0.02B^3 + 0.839B^2 - 12.44B + 221.3,\ R^2 = 0.999 \quad (12)$$

$$q_{a(1.2)} = -0.007B^3 + 0.381B^2 - 7.046B + 199.4,\ R^2 = 0.998 \quad (13)$$

$$q_{a(1.4)} = -0.012B^3 + 0.538B^2 - 8.698B + 208.7,\ R^2 = 0.999 \quad (14)$$

$$q_{a(1.6)} = -0.010B^3 + 0.475B^2 - 7.809B + 198.6,\ R^2 = 0.999 \quad (15)$$

### Settlement Analysis on Sand:

### *Immediate Settlement on Raft Foundation*

In Equation (3), immediate settlement values were analyzed for net foundation pressures varying from 161-152kN/m$^2$, the modulus of elasticity was obtained from Equation (4) as 10.04MPa while Poisson's ratio of 0.35 was obtained from Equation (5). Also, the coefficient of volumetric compressibility, $m_v$, of 0.062m$^2$/MN was evaluated from Equation (7). The results of immediate settlement using methods of Burland and Burbidge (1985) and Harr (1966) are presented in table 2 and figure 3. Immediate settlement values for foundation breadth varying from 8-15mm were found to increase with footing size, bearing pressure and foundation depth. Immediate settlement vary from 32 - 47mm for a bearing pressure varying from 161-152kN/m$^2$ and foundation depth varying from 1-1.6m depth respectively for Burland and Burbidge approach. Harr's model gave immediate settlement values of 19.8-35.2mm for bearing pressure range of 161-152kN/m$^2$ respectively. Comparatively, Harr's approach gave conservative values of immediate settlement compared to that of Burland and Burbidge approach. The models describing Burland and Burbidge, and Harr's models are presented in Equations (16) and (17).

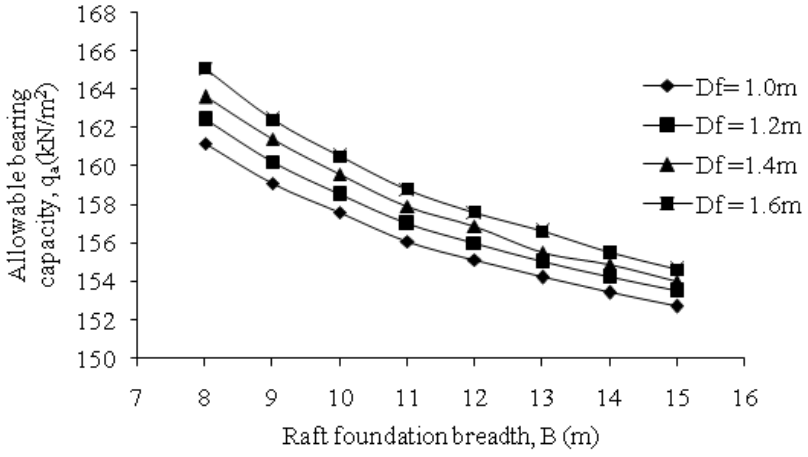


Fig. 2. Variation of allowable bearing capacity with Raft foundation breadth.

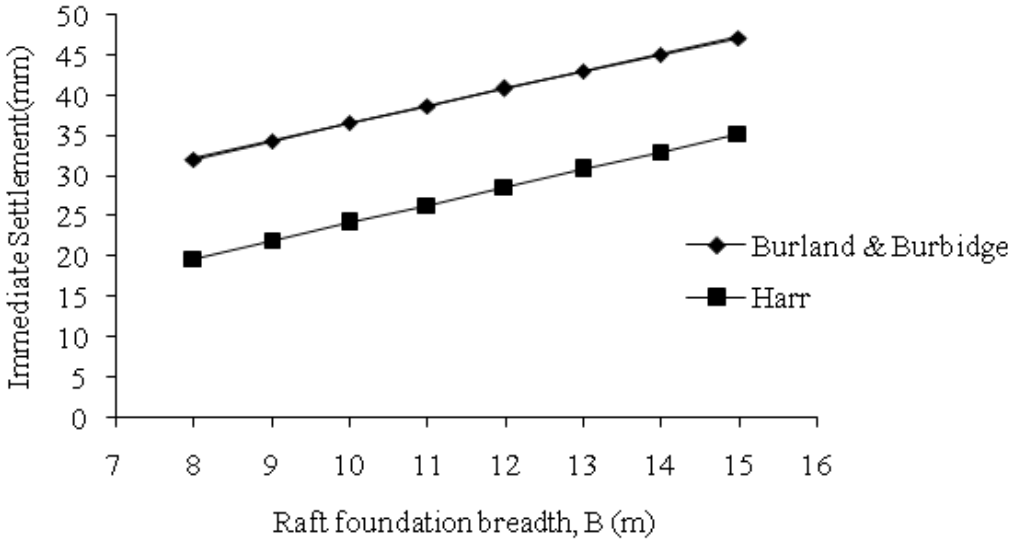


Fig. 3. Variation of Immediate settlement with Raft foundation breadth.

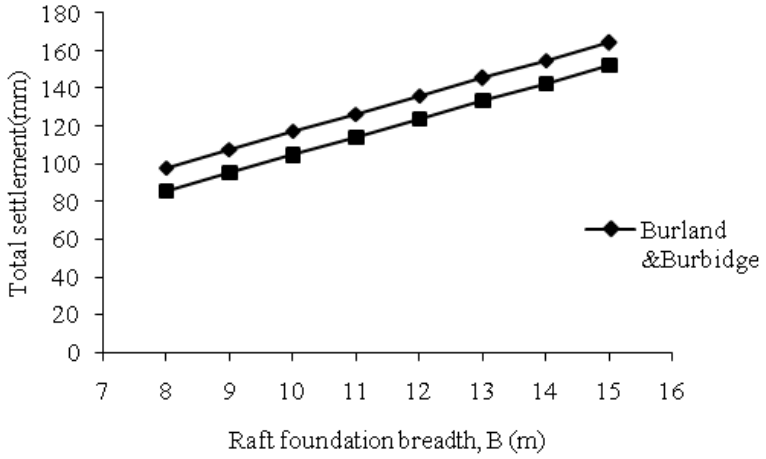


Fig. 4. Variation of total settlement and Raft foundation breadth.

$$s_i = 2.156B + 14.91,\ R^2 = 0.999 \quad (16)$$

$$s_i = 2.2B + 2.2,\ R^2 = 0.999 \quad (17)$$

***Total Settlement on Raft Foundation***

Consolidation settlement values for the Raft foundation of breadth, B, varying from 8-12m were found to increase with footing size. The relationship between foundation breadth and total settlement is shown in figure 4, where Burland and Burbidge approach had higher total settlement compared to those obtained from Harr's approach. The models describing Burland and Burbidge, and Harr's total settlement are presented in Equations (18) and (19).

$$\rho_t = 9.471B + 22.30,\ R^2 = 0.999 \quad (18)$$

$$\rho_t = 9.533B + 9.441,\ R^2 = 0.999 \quad (19)$$

Critical foundation breadth for deformation requirement of Raft placed on sand can be determined using Equation (18). Maximum allowable total settlement values suggested by Skempton and MacDonald (1956) may be adopted.

## CONCLUSION AND RECOMMENDATIONS

Based on the findings, the following conclusions can be drawn;

i. The allowable bearing capacity, $q_a$, had a decreasing trend with an increase in raft foundation breadth whereas for a given foundation breadth, $q_a$ increased with foundation depth.

Table 1. Bearing Capacity of Raft Foundation.

| Depth of Foundation (m) | Foundation Breadth B (m) | $D_f$ / B | SPT value N | Depth Factor $F_d$ | Allowable bearing capacity,$q_a$ (kN/m$^2$) |
|---|---|---|---|---|---|
| 1.0 | 8 | 0.125 | 6 | 1.041 | 161.2 |
| | 9 | 0.111 | | 1.036 | 159.1 |
| | 10 | 0.100 | | 1.033 | 157.6 |
| | 11 | 0.090 | | 1.029 | 156.1 |
| | 12 | 0.083 | | 1.027 | 155.1 |
| | 13 | 0.076 | | 1.025 | 154.2 |
| | 14 | 0.071 | | 1.023 | 153.4 |
| | 15 | 0.066 | | 1.021 | 152.7 |
| 1.2 | 8 | 0.150 | 6 | 1.049 | 162.4 |
| | 9 | 0.133 | | 1.043 | 160.2 |
| | 10 | 0.120 | | 1.039 | 158.5 |
| | 11 | 0.109 | | 1.035 | 157.0 |
| | 12 | 0.100 | | 1.033 | 156.0 |
| | 13 | 0.092 | | 1.030 | 155.0 |
| | 14 | 0.085 | | 1.028 | 154.2 |
| | 15 | 0.080 | | 1.026 | 153.5 |
| 1.4 | 8 | 0.175 | 6 | 1.057 | 163.6 |
| | 9 | 0.155 | | 1.051 | 161.4 |
| | 10 | 0.140 | | 1.046 | 159.6 |
| | 11 | 0.127 | | 1.041 | 157.9 |
| | 12 | 0.116 | | 1.038 | 156.9 |
| | 13 | 0.107 | | 1.035 | 155.5 |
| | 14 | 0.100 | | 1.033 | 154.9 |
| | 15 | 0.093 | | 1.030 | 154.0 |
| 1.6 | 8 | 0.200 | 6 | 1.066 | 165.1 |
| | 9 | 0.177 | | 1.058 | 162.4 |
| | 10 | 0.160 | | 1.052 | 160.5 |
| | 11 | 0.145 | | 1.047 | 158.8 |
| | 12 | 0.133 | | 1.043 | 157.6 |
| | 13 | 0.123 | | 1.040 | 156.6 |
| | 14 | 0.114 | | 1.037 | 155.5 |
| | 15 | 0.106 | | 1.034 | 154.6 |

Table 2. Settlement Analysis on Raft Foundation.

| Analytical Approach | Foundation Breadth B(m) | SPT value N | Poisson ratio, μ | Angle of friction (φ) | Elastic Modulus E(Mpa) | Coefficient of vol. compressibility $m_v$ (m$^2$/MN) | Immediate settlement $s_i$ (mm) | Consolidation settlement, $\rho_c$ (mm) |
|---|---|---|---|---|---|---|---|---|
| Burland & Burbidge | 8 | 6 | 0.35 | 28 | 10.04 | 0.062 | 32.0 | 65.9 |
| | 9 | | | | | | 34.3 | 73.2 |
| | 10 | | | | | | 36.6 | 80.6 |
| | 11 | | | | | | 38.7 | 87.8 |
| | 12 | | | | | | 40.9 | 95.2 |
| | 13 | | | | | | 43.0 | 102.5 |
| | 14 | | | | | | 45.1 | 109.8 |
| | 15 | | | | | | 47.1 | 117.1 |
| Harr | 8 | 6 | 0.35 | 28 | 10.04 | 0.062 | 19.8 | 65.9 |
| | 9 | | | | | | 22.0 | 73.2 |
| | 10 | | | | | | 24.2 | 80.6 |
| | 11 | | | | | | 26.4 | 87.8 |
| | 12 | | | | | | 28.6 | 95.2 |
| | 13 | | | | | | 30.8 | 102.5 |
| | 14 | | | | | | 33.0 | 109.8 |
| | 15 | | | | | | 35.2 | 117.1 |

ii. Allowable bearing capacity also decreased as the ratio of foundation depth, $D_f$, to breadth, B ratio ($D_f$/B) decreased.
iii. Immediate settlement values for foundation breadth varying from 8-15mm were found to increase with footing size, bearing pressure and foundation depth.
iv. Immediate settlement vary from 32 - 47mm for a bearing pressure varying from 161-152kN/$m^2$ and foundation depth varying from 1-1.6m depth respectively for Burland and Burbidge approach.
v. Harr's model gave immediate settlement values of 19.8-35.2mm for a bearing pressure range of 161-152kN/$m^2$ respectively.
vi. The predictive models can be useful for preliminary design purposes on sites having similar conditions.

**REFERENCES**


Akpila, SB. 2007. The Design of a Shallow Foundation on Sand Overlying Soft Clay. Inter-World Journal of Science and Technology. 3(3):200-205.

Akpila, SB. 2007. Stability and Deformation Assessment of Crude Oil Tank Foundation in the Niger Delta: A case Study. Inter-World Journal of Science and Technology. 3(4):600-607.

Akpila, SB. and ThankGod, O. 2008. Comparison of Stability and Deformation Characteristics of Two Crude Oil Tank Foundation in the Niger Delta: A case Study. International Journal of Physical Sciences. 3(1):51-58.

Akpila, SB., ThankGod, O. and Igwe, A. 2008. Bearing Capacity and Settlement Analysis of a Shallow Foundation on Reclaimed Sand Overlying Soft Clay. Journal of Scientific and Industrial Studies. 6(9):84-89.

Akpila, SB. 2013. Comparison of Standard Penetration Test Methods on Bearing Capacity of Shallow Foundations on Sand. Scientific Journal of Pure and Applied Sciences. 2(2):72-78.

Bowles, JE. 1997. Foundation Analysis and Design (5th edi.). McGraw-Hill, New York, USA. 263-266.

Braja, MD. 1999. Principle of Foundation Engineering (4th edi.). PWE Publishing Company, USA. pp243.

British Standard Institution, BS 1377. 1977. Methods of Test for Soils for Civil Engineering Purposes.

Burland, J. B. and Burbidge, MC. 1985. Settlement of Foundations on Sand and Gravel. Proceedings of Institution of Civil Engineers. 78(1):1325-1381.

Craig, RF. 1987. Soil Mechanics (4th edi.). ELBS Edition, Great Britain.

Caquot, A. 1934., Equilibrium des Massifs a frottement Interne. Gauthier-Villars, Paris, France. 1-91.

DeBeer, EE. and Vesic, A. 1958. Etude experimental de la capacitie Portante du sable sous des foundations directes etablies en surface Annale des Travaux publics de Belqique. 59(3):5-58.

Harr, ME. 1966. Fundamentals of Theoretical Soil Mechanics. McGrey-Hill, New York, USA.

Meyerhof, GG. 1956. Penetration Test and Bearing Capacity of Cohesionless Soils. Journal of the Soil Mechanics and Foundation Division, ASCE. 82(1):1-19.

Parry, RHG. 1977. Estimating Bearing Capacity in Sand from SPT Values. Journal of Geotechnical Engineering Division, ASCE. 103(9):1014-1019.

Polshin, DE. and Tokar, RA. 1957. Maximum Non Uniform Settlement of Structures. Proc. of the 4th International Conference of Soil Mechanics and Foundation Engineering, London. 1:402-405.

Skempton, AW. and Bjeruum, L. 1957. A Contribution to the Settlement Analysis of Foundation on Clays. Geotechnique 7:168-178.

Skempton, AW. and MacDonald. 1956. The Allowable Settlement of Buildings," Proceedings, Institute of Civil Engineers. 5(III):727-784.

Singh, A. 1992. A Modern Geotechnical Engineering (3rd edi.). CBS Publishers Delhi, India.

Som, NN. and Das, SS. 2006. Theory and Practice of Foundation Design, Prentice- Hall of India, New Delhi, India.

Terzaghi, K. 1943. Theoretical Soil Mechanics, John Wiley and Sons Inc. New York, USA.

Tomlinson, MJ. 2001. Foundation Design and Construction (7th edi.). Pearson Education Ltd. 73-74.

Vesic, AS. 1967. A study of Bearing Capacity of Deep Foundations. Final Report, Project B-119, Georgia Inst. Techn., Atlanta Georgia, USA.

Wahls, HE. 1981. Tolerable Settlement of Buildings. Journal of the Geotechnical Division, ASCE. 107(11):1489-1504.


Received: April 21, 2013; Revised and Accepted: Aug 15, 2013

SENRA Academic Publishers, British Columbia
Vol. 8, No. 1, pp. 2775-2782, February 2014
Online ISSN: 1920-3853; Print ISSN: 1715-9997

Canadian Journal of pure&applied sciences

# DESIGN OF GENERIC ANTIVIRUS SYSTEM

Osaghae OE, *Egbokhare, FA and Chiemeke SC
Department of Computer Science, University of Benin, Benin City, Edo State, Nigeria

**ABSTRACT**

Antivirus software developers are advocating for sophisticated antivirus designs to implement their antivirus systems. However, the current antivirus systems heavily rely on updating of their malicious signature databases to detect malicious codes in executable programs. The problem with frequent update of malicious signatures databases is that it is not scalable; it cannot detect malicious code whose signature is not in the malicious signature database. Consequently, we designed a generic antivirus system that does not contain malicious database but rather, malicious codes are detected by the type of operating system functions used by the executable program. The proposed generic antivirus system uses deterministic finite automata, Naïve Bayes and Chi square techniques to detect malicious codes in executable programs. When the generic antivirus system is deployed to any operating system environment, malicious codes can be accurately detected in executable programs without a need to update its malicious signature database.

**Keywords**: Antivirus scanners; Malicious Software; Malicious Signatures.

## INTRODUCTION

**A**ntivirus (AV) scanners are used in an attempt to directly protect computer systems from damages. AV scanners detect a specific type of unauthorized activity in the form of malicious code, collectively known as malware. A recent study shows that 81% of all computer users have antivirus software installed on their computer (Feng, 2008). Malicious code is a computer program that modifies a system call or the functioning of a program without the consent of the user of the system. Malicious codes can be classified as virus, worm or a Trojan horse (Devara and Murali, 2012). A virus is a computer program that does not have the capability to replicate on their own, and rely on using other computer programs as a host in order to spread (Microsoft, 2004). A worm can be defined as malicious code which is either requires human intervention or not in order to propagates through a network. The release of worms on computer networks has cost billions of dollars in wasted time and resources. Trojan horse is a non-replicated malicious code designed to cause damage to computer systems, by masquerading as benign programs. A Trojan horse is also regarded as a computer program that appears to have a useful function, but also has a hidden and potentially malicious function. A benign program is an executable program that does not contain any malicious code (Harley and Lee, 2009; Greensmith and Aickelin, 2005; Tikkanen, 2010).

The most common approach developed in anti-virus software products and tools to identify the viruses and malwares is signature-based scanning. It makes use of small strings, named as signatures, which are the results of manual analysis of viral codes. A signature must only be a sign of a specific virus and not the other viruses and normal programs. Accordingly, a virus would be discovered, if the virus related signatures were found Babak *et al*. (2011).

Antivirus definitions are databases that contain information used to identify viruses. Antivirus scanning engines are designed to identify specific viruses using the aforementioned definitions and by recognizing characterized behaviour. Antivirus software vendors release a new virus definition (databases) for their software products when they find new viruses. These vendor-specific database definitions are used by antivirus software to identify known viruses and/or virus-like behaviour. When information about a specific virus is included in a virus definition, it is said to be a known virus NetApp (2006).

Computer malwares can be classified according to their infection mechanism. The mechanism can be in the form of Encryption, oligomorphism, polymorphism and metamorphism. Encrypted virus changes its body binary code with some encryption algorithms to hide it from simple view and make it more difficult to analyze and detect. Oligomorphic virus substitute decryptor code in new offspring, which makes the detection process more difficult for signature based technique. A polymorphic virus is a malicious code that when it decides to infect a new victim program, it modifies some pieces of its body to look dissimilar. Polymorphic virus has capability to create infinite new decryptors. Metamorphic virus mutates all of its body and it also changes the code of decryption loop (Babak *et al*., 2011).

*Corresponding author email: fegbokhare@yahoo.com

The first generation of antivirus products was purely based on signature detection technique. The second generation made attempt to identify and stop network worms based on packet signatures. It also has the ability to disinfect and restore the Operating System from spyware or Trojan backdoor infection. The third generation was developed to effectively block zero-day malware proactively without any dependency on viral signatures. It uses behavioural analysis and behavioural blocking. Behaviour analysis is process to intercept API calls made by an executable program to determine if these API calls are used for malicious intent or not. To prevent malicious attacks generically, it is cost-effective to use behavioural blocking technique to restrict the actions that authorized executable programs can perform in the system when it is noticed that it contains malicious API calls Kumar and Spafford (1992).

The specific objectives of this study are to review the extent of improvements made to the antivirus systems and design a generic antivirus system that detects malicious codes in executable program based on how its uses operating system functions.

Kumar and Spafford (1992) described a virus detection tool called a generic virus scanner. This tool is completely general and is structured in such a way that it can easily be augmented to recognize viruses across different system platforms with varied file types. The implementation defines virus features common to all scannable viruses. The approach used to develop this tool is easy to understand. By combining string sets, it is believed that the coverage may be obtained in a manner superior to most commercial scanners currently available. The tool uses a pattern matching technique to identify malicious signatures in an executable program (Kumar and Spafford, 1992) and this can be evaded by sophisticated malware codes.

Roberto *et al*. (2004) proposed a WHIPS prototype also known as a Reference Monitor (RM) for the detection and prevention of Windows dangerous system calls invocation. WHIPS was designed and implemented to stop common exploits that use the buffer overflow technique to carry out privilege escalation on a system. If a malicious user wants to execute a shell in a context of the exploited service, WHIPS will prevent the attack by stopping the execution of the dangerous system call that invokes the shell. WHIPS is implemented as a kernel driver, also called kernel module, using the undocumented structure of the Windows kernel and the routines typically employed for driver development. The problem with WHIPS is that it was considered to be more efficient if it were implemented directly into the Windows kernel, instead of as a kernel driver Roberto *et al*. (2004).

Antivirus scanners of first generation employed non-complicated techniques in order to find known computer viruses. These set of scanners typically looked for certain patterns or sequences of bytes called string signatures. Antivirus scanners of the second generation was introduced when the earlier scanners lost their efficiency by using simple pattern scanning techniques to detect newer and more complicated viruses appropriately. Then the second generation of scanners introduce almost exact recognition that caused the antivirus scanners became more trustable. Antivirus scanners of the third generation use virus specific detection algorithm. This type of detection algorithm denotes any special method that is specifically designed for a given particular virus. This technique may bring about many problems such as portability of the scanner on different platforms and stability of code. To overcome these problems, virus-scanning languages have been developed that in scanned objects are allowed. Antivirus scanners of the fourth generation simulates the computer central processor, main memory, storage resources and some necessary functions of operating system by a virtual machine to run the malware virtually and investigate its behaviour and performance. The malicious code does not execute on actual machine and it is controlled by the virtual machine precisely, therefore there is no risk for unintentionally propagation of malware. These set of antivirus scanners can detect encrypted, polymorphic, metamorphic and oligomorphic viruses (Babak *et al*., 2011).

A packer is a software tool that can modify and compress an executable file by encrypting and changing its form from its original format. The final result is a modified executable which, when executed, does exactly the same thing as the original code, but from the outside has a completely different form and therefore evades signature-based unless either the engine has the specific unpacking algorithm or it is able to unpack it generically (Pedro *et al*., 2012; Guo *et al*., 2012).

The most important piece in any antivirus infrastructure is the virus definition file. Antivirus product clients keep their protection current by regularly updating virus definition files. These files contain the signatures of all the known viruses and are used by the scan engine. When a new virus comes out, the definition files need to be updated so that client software can detect the new virus. The definition files also give the client instructions on how to clean viruses from a file. Updating virus definition files quickly and efficiently is crucial in any business, especially in a virus situation. In a well-designed antivirus architecture, the clients will automatically update virus definition files on a regular basis (Speice, 2003; Morton, 2010).

## MATERIALS AND METHODS

### METHODOLOGY

In this section, we describe the design of the proposed antivirus system shown in figures 1, 2 and 3. One way to begin the design of any program is to describe the behaviour of the program by a Conceptualized Diagram. In an operating system, an executable program makes a set of system function calls $S_1$, $S_2$, $S_3$... $S_n$. The system functions take various numbers of parameters $S_1(P_1, P_2, P_3, \ldots, P_{c1})$, $S_2(P_1, P_2, P_3, \ldots P_{c2})$, $S_3(P_1, P_2, P_3, \ldots P_{c3})$, ..., $S_n(P_1, P_2, P_3, \ldots, P_{ct})$. Where $n$ is the number of system function calls made by the executable program, and $c1$, $c2$, $c3$ and $ct$ are the number of parameters used by the system functions. The purpose of this design is to define how the proposed antivirus system will detect the set of malicious system function calls made by an executable program. Figure 1 shows the behaviour of the feature extraction phase of Detection system. An executable program can contain executable *statement_1*($S_1$), *statement_2*($S_2$), *statements_3*($S_3$),..., and *statement_n*($S_n$). Each of these executable statements can either be code or data. If it is code, it can be converted to

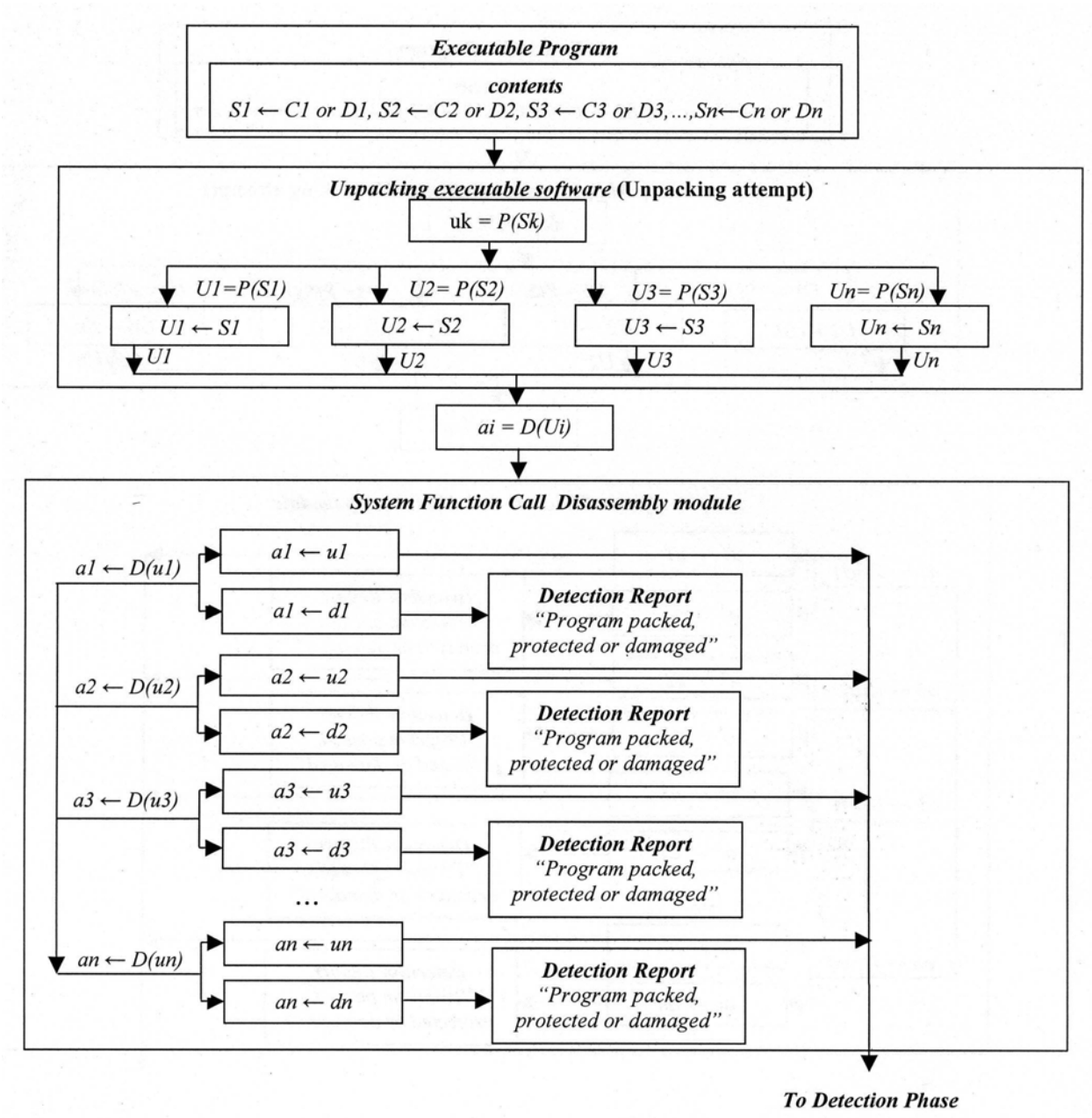


Fig. 1. Feature Extraction Phase of Detection System.

assembly code using a disassembler but if it is data then, it has been packed. The content of the program is sent to the Unpacking section which will attempt to convert an identified executable data statement back to its equivalent executable code. The unpacking executable software section uses a procedure called P(Sk). *P(Sk)* procedure takes one argument at a time called *statement (Sk)* and attempts to covert it to its equivalent executable code using a procedure called *unpacked (Uk)*. When the unpacking section has finished its function, it will pass the processed content of the executable program to the disassembly section. The System Call Disassembly module takes the responsibility of converting the sequences of executable statements to equivalent assembly code statements. This module has a procedure called *D(ui)* which takes unpacked executable code *ui* as argument and produces an equivalent assembly code statement *ai*. It disassembles each of the unpacked executable statement and produces their assembly code equivalent *ai* in the form of $a1 \leftarrow D(u1)$, $a2 \leftarrow D(u2)$, $a3 \leftarrow D(u3)$,…, $an \leftarrow D(un)$. When unpacked executable code *ui* is successfully converted to assembly code equivalent *ai*, the virus detector expresses it in the form of $a1 \leftarrow u1$, $a2 \leftarrow u2$, $a3 \leftarrow u3$,…, $an \leftarrow un$.

When the System Function Call Disassembly module is unable to convert the unpacking executable code *ui* into its equivalent assembly code, then there is a problem. The problem is the Unpacking Executable software module was not able to unpack the program content s*1, s2, s3,..., sn*. The implication of this is that the virus detector expresses the program in the form of $a1 \leftarrow d1$, $a2 \leftarrow d2$, $a3 \leftarrow d3$,…, $an \leftarrow dn$. The found components *d1*, *d2*, *d3*,…, *dn* were not successfully convert to their equivalent unpacked executable codes by the Unpacking Executable Software used. As it is done in conventional antivirus software systems, when a packed executable program cannot be unpacked by series of unpacking software tools, the program is reported as a malicious infected program.

In the Detection Phase, the arrays to store the total number of malicious attributes found, *self-modification*, *self-referential*, *self-replication*, malicious system functions for worms and Trojan are initialized to null. The array names for malicious attributes found are general malicious category, *self-modification*, *self-referential*, *self-replication*, malicious system functions for Trojan and worm are mal, *VDSM, VDSR1, VDSR2, MST* and *MSW* respectively.

When control reaches the Detection phase, these arrays are initialized to null and control is passed to the procedure named *SearchSystemFunc(ak)*. The *SearchSystemFunc(ak)* is a procedure which takes one argument *ak*; assembly code derived by the disassembly module. The responsibility of the *SearchSystemFunc(ak)* is to search and collect the set of system functions in the assembly code presented. When a system function is found, it is stored in a variable called *sfk*. The variable *sfk* is passed as an argument to another procedure called *MalSystemFunction(sfk)*.

The *MalSystemFunction(sfk)* is responsible for identifying the set of malicious system functions by interacting with the set of definition given in the system call behaviour storage. When the procedure finds a malicious system function, it is stored in a variable called *mfk*. As soon as the procedure *MalSystemFunction(sfk)* finds a malicious system function, it is added to the array *mal*. This addition is cumulative until all the malicious system functions are collected. When the array *mal* is empty after the *MalSystemFunction(sfk)* has been called, the detector declares the executable program being examined as benign. When the array *mal* is not empty, the set of malicious system function collected are sent to the virus identification module.

The system call intelligent section uses the multinomial technique of Naïve Bayes classifier to extract the virus attributes (*self-modification*, *self-referential* and *self-replication* attributes) from the malicious attributes. Let C denote the set of class labels, that is:

$$C = \{C_1, C_2, C_3\} \quad (1).$$

Equation 1 is the set of malicious classes and the total number of classes is 3. Let GSF denote the Groups of System Functions(GSF), where

$$GSF = \{ GSF_1, GSF_2, GSF_3\} \quad (2)$$

Equation 2 is the set of GSF that can be got from the malicious classes.

In a virus identification section, when malicious system functions for the definitions for *self-modification (DSM)*, *self-referential (DSR1)* and *self-modification (DSR2)* are found, they are added to their various arrays *VDSM*, *VDSR1* and *VDSR2* respectively. The virus identification section has six procedures they are I*nVSM(DSM), OutVSM(DSM), InVSR1(DSR1), OutVSR1(DSR1), InVSR2(DSR2) and OutVSR2(DSR2)*.

The procedure *InVSM(DSM)* takes one argument DSM and is responsible for accumulating the set of self-modification system functions found in a program. The procedure *OutVSM(DSM)* takes one argument DSM and is responsible for notifying the procedure InVSM(DSM) that the all identified self-modification system functions used by the executable program has been found and collected. Another procedure called *InVSR1(DSR1)* takes one argument DSR1 and is responsible for accumulating the set of self-referential system functions found in a program. The procedure *OutVSR1(DSR1)* takes one argument DSR1 and is responsible for notifying the procedure InVSR1(DSR1) that all identified self-

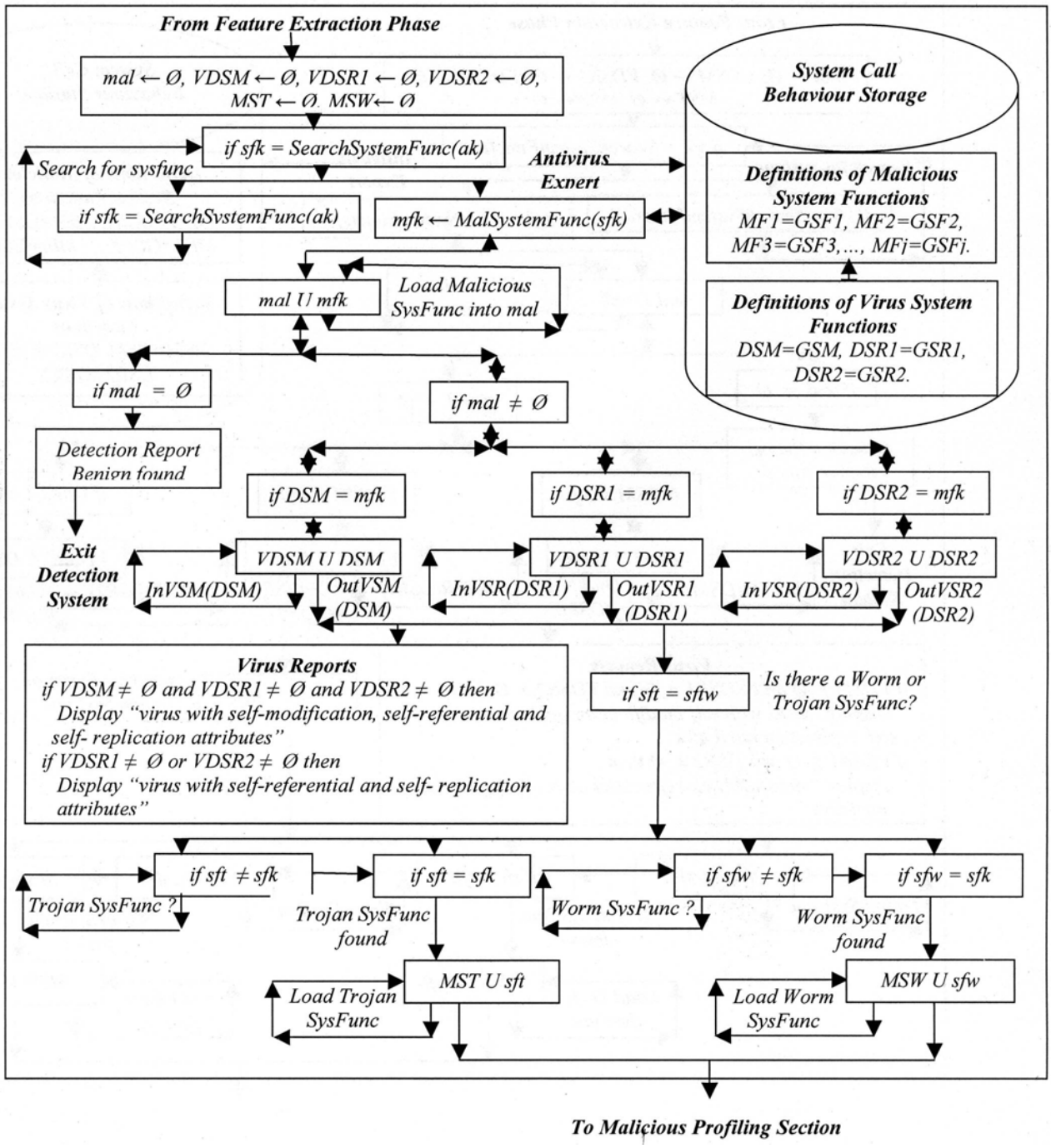


Fig. 2. Detection Phase of Detection System.

referential system functions used by the executable program has been found and collected.

Another procedure called *InVSR2(DSR2)* take one argument *DSR2* and is responsible for accumulating the set of self-replication system functions found in a program. The procedure *OutVSR2(DSR2)* take one argument *DSR2* and is responsible for notifying the procedure *InVSR2(DSR2)* that all identified self-replication system functions used by the executable program has been found and collected. When the virus identification section has finished examining the executable program for the three attributes of a virus, it will send the detection results to a virus report section. In the virus report section, when the arrays for *self-modification(VDSM)*, *self-referential(VDSR1)* and *self-replication(VDSR2)* attributes are not empty, then the following comparisons are carried out. When an

executable program contains *self-modification*, *self-referential* and *self-replication* system function attributes, then it is a virus program with these three attributes. After the virus detector has finished examining the executable program for evidence of possible virus infection, then the set of system functions used by the program are passed to the separator module.

In the separator module, there is an attempt to accumulate the set of system functions used by Trojan and the ones not used by worm. This will enable the virus detector to examine the executable program for Trojan and worm behaviour using chi square technique.

The detector check if the system function *sfk* belongs to the set of system functions *sftw* commonly used by Trojan *sft* and the ones not worm *sfw*. The total number of system functions used by Trojan and the ones not used by worm are store in variables *MST* and *MSW* respectively. After the separator module has finished examine the system functions of an executable program, the set of identified system functions for Trojan and the ones not used by a worm are passed to the Malicious Profiling section of the virus detector. The model for Chi square computation that the Malicious Profiling section will used to detect Trojan horses and worms, are presented in the form of a pseudocode below:

Begin

1) Define $P_i = (P_1, P_2)$ to be the set of profiles of samples in the malicious attribute where Trojan and worm system function has been identified from the classes $C_1$,(classes for Trojan) and $C_2$(classes for worm).
   Define $T = (T_1, T_2, T_3, ..., T_n)$ to be tested samples of a generalized malicious attributes belonging to the classes $C_1$, and $C_2$.
   Define Tr to be the set of system function calls used to identify a Trojan program.
   Define Wo to be the set of system function used to identify a worm program.
2) Get the program system function calls which belong to Tand W extracted by the separator section.
3) Compute chi-square for each attribute class for
   i = 1 to 2 do
   $$X_i^2 = \frac{(A_i - V_i)^2}{V_i}$$
   $A_i$ is the number of observed malicious attribute and i is 2; trojan and worm.
   $V_i$ is number of expected worm or Trojan attribute is suppose to have.
4) Compute degree of membership $\sigma_i = \sum X_i^2$.
5) Compute the degree of freedom = number_ of_ attributes – 1 Degree of freedom = 2 – 1=1
6) Compute threshold value $\sigma_{1,}$ where the null hypothesis judgment would be based upon, by reading the degree of freedom from probability level of *d* from the Chi square table.

A significant level of 0.z based on the degree of freedom, will be selected. This means that z% of the time, $X^2$ is expected to be less than or equal to $\sigma_{1.}$
$X^2_{.z} \leq \sigma_1$.

7) Compute the classification strategy:

If
$$\exists\ i,\ 1 \leq i \leq 2,\ \sigma_i \geq \sigma_1 \Rightarrow T \in Tr_{i.}$$
Otherwise,
$$\forall\ i,\ 1 \leq i \leq 2,\ \sigma_i < \sigma_1 \Rightarrow T \in Wo_{i.}$$

The behaviour of Malicious Profiling section is displayed in figure 3. The purpose is to use the set of system functions passed from the separator section to identify possible Trojan and worm system functions of an executable program. By the time Malicious Profiling section receives the sets of system functions stored in *MST* and *MSW*, it attempts to identify Trojan and worm by using Chi square technique. Computation of a Chi square terms for Trojan is $CT \leftarrow MST - CTi$ and the one for worm is $CW \leftarrow MSW - CWi$ are used. *MST* and *MSW* are the observed total number of system functions for Trojan and worm, extracted by the separator section. *CTi and CWi* are the expected total number of system functions used by Trojan and the ones not used by worms. *CTi and CWi* are stored as definitions in the Malicious Profiling storage. The malicious profiling section is expected to interact with these definitions during its computation.

The final Chi square computation is $CM \leftarrow (CT*CT)/CWi + (CW)*(CW)/CTi$, which determines the degree of membership. Next, the degree of freedom is computed as *Degree of Freedom←number of attributes (2) – 1*. Since we are concerned with two attributes namely, Trojan and worm, then the computation for degree of freedom is 1. The next stage is to compute the threshold value *TV* where the null hypothesis judgment would be based upon. The threshold value *(TV)* is got from the Chi square table by reading degree of membership against the degree of freedom. To identify Trojan and worm, the following comparisons are made. When an executable program contains malicious system functions and CM < TV, then it has Trojan codes. Again, when an executable program contains malicious system functions and CM ≥ TV, then it has Worm codes. Then, when an executable program contains malicious system functions and does not have the conditions CM < TV and CM ≥ TV, then it is an unknown malicious codes. When $mal = \emptyset$ then the executable program being examine is benign. The final detection results are sent to the detection report section. The

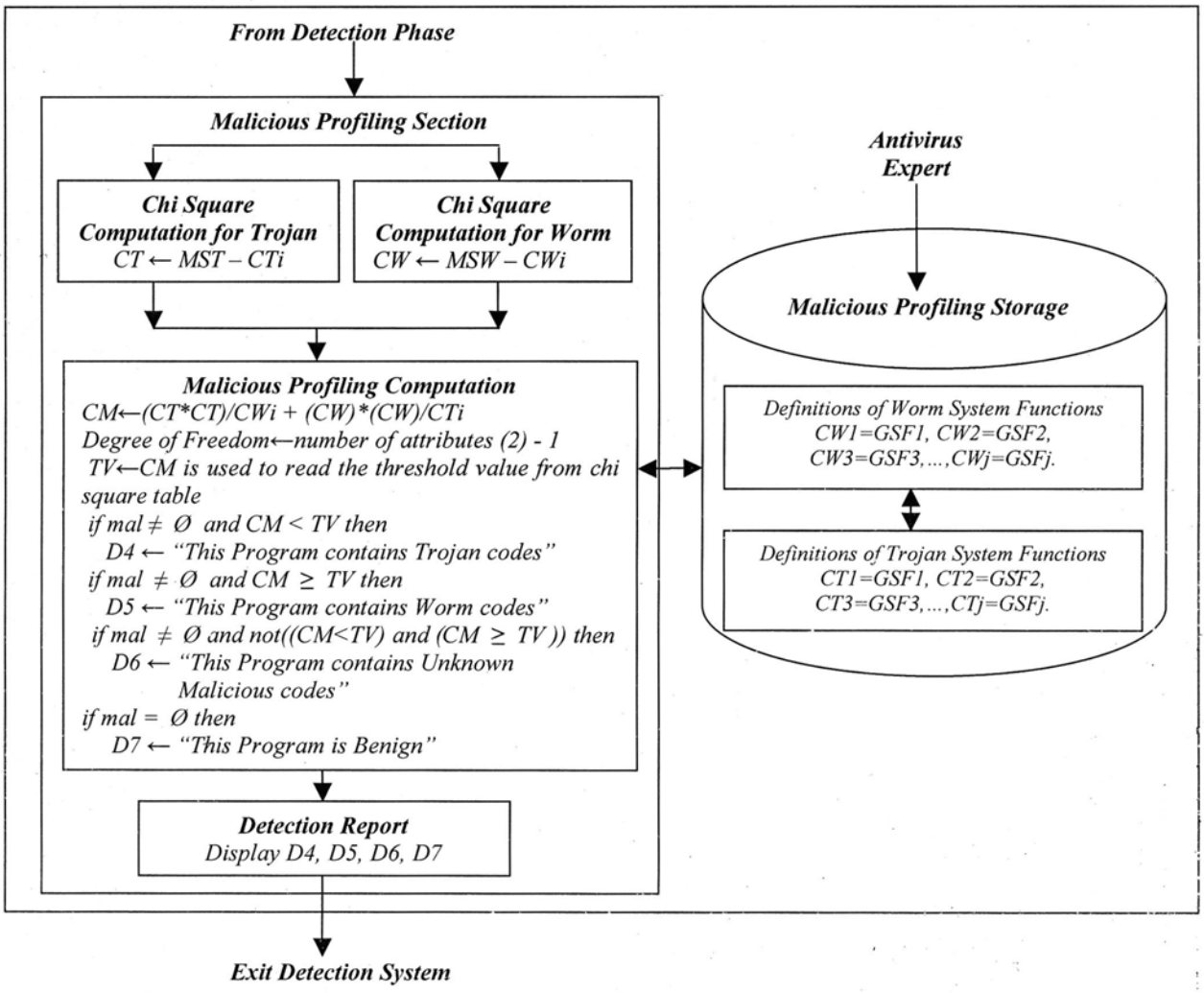


Fig. 3. Malicious Profiling Section.

Malicious Profiling storage keeps the set of definitions for the expected worm and Trojan system functions. These definitions are determined by the antivirus expert who knows the exact number of system functions that make up the expected number of sets of worm and Trojan functions. The definition for worm system functions are *CW1=GSF1, CW2=GSF2, CW3=GSF3,...,CWj=GSFj. CWj* is the total number of Trojan system functions extracted from the Group of system functions present in the operating system where the program is running. Another Definition for system functions not used by worm are *CT1=GSF1, CT2=GSF2, CT3=GSF3,...,CTj=GSFj. CTj* is the total number of system functions not used by Trojan, and they are extracted from the Group of system functions in the operating system the program is running on. The detection results got from the Malicious profiling section is sent to detection report section.

The detection report section displays the Trojan, worm, unknown malicious codes and benign detection results got from the executable program. After the detection results have been reported by the detection report section, the virus detector exits.

## CONCLUSION

In this paper, we designed a generic antivirus system that makes use of operating system functions rather than updating its malicious signature database. For an executable program to operate in the computer system, it must make use of the operating system functions also known as the system functions. As surprising as it seems, the operating system cannot differentiate between a set of system functions made by a benign program from the ones made by the malicious program. This paper has shown the design of a generic antivirus system which

makes use of deterministic finite state automata, Naïve Bayes and Chi square to accurately detect malicious codes from executable programs. The detection of malicious codes is done in the absence of malicious signature database component. The design of a generic antivirus system proposed in this paper will be highly appreciated by antivirus developers. The appreciation will be in terms of *reduction of human involvement*, *more scalable antivirus design* and *elimination of malicious signatures database from antivirus design*. There is reduction of running cost because fewer antivirus experts are required and there is no need to perform malicious signatures extractions from each malicious program. The antivirus system design will be more scalable because a generic signature is defined than having a numerous unique malicious signature definitions. The operating system functions are used to detect malicious code in executable programs rather than using malicious signature database. Our future research direction on design of generic antivirus system is to attempt to deploy its design to the Windows operating system functions. We are also going to develop algorithms for the generic and proposed Windows operating system designs. We shall also attempt to implement the proposed Windows operating antivirus design in C programming language and then test live malicious programs antivirus system to determine its efficiency.

**REFERENCES**

Babak, BR., Maslin, M. and Suhaimi, I. 2011. Evolution of Computer Virus Concealment and Anti-Virus Techniques: A Short Survey. International Journal of Computer Science. 8(1):113-121.

Devara, V. and Murali, K. 2012. Network Based Anti-virus Technology for Real-time Scanning. International Journal of Computer Science Issues. 9(4):304-310.

Feng, X. 2008. Attacking Antivirus. Nevis Labs, Nevis Networks, Inc.

Greensmith, J. and Aickelin, U. 2005. Firewalls, Intrusion Detection Systems and Anti-Virus Scanners. School of Computer Science and Information Technology, University of Nottingham, Jubilee Campus, Nottingham, UK.

Guo. F., Ferrie, P. and Chiueh, T. 2012. A Study of the Packer Problem and Its Solutions. (Retrieved from www.ecsl.cs.sunysb.edu/tr/ TR237.pdf).

Harley, D. and Lee, A. 2009. Heuristic Analysis: Detecting Unknown Viruses. ESET Corporation, Bratislava, Slovak Republic.

Kumar, S. and Spafford E. H. 1992. A Generic Virus Scanner in C++. The COAST Project, Department of Computer of Computer Sciences, Purdue University, West Lafayette.

Microsoft. 2004. The Antivirus: Defense-in-Depth Guide. Microsoft Corporation.

Morton, C. 2010. Bypassing Malware Defenses. The SANS Institute.

NetApp. 2006. Antivirus Scanning Best Practices Guide. Network Appliance Inc., (Retrieved from www.netapp.com on 15/10/2012).

Pedro, B., Inaki, U., Luis, C. and Josu, F. 2012. From Traditional Antivirus to Collective Intelligence: Panda's Technology Evolution. Panda Research, (Retrieved from research.pandasecurity.com on 15/10/2012).

Roberto, B., Emanuele, G. and Luigi, VM. 2004. A Host Intrusion Prevention System for Windows Operating Systems. Springer-Verlag, Berlin Heidelberg.

Speice, C. 2003. Designing a Managed Antivirus Solution for a Large Corporate Environment. SANS Institute.

Tikkanen, A. 2010. Antivirus Engines Basics. F-Secure Corporation.

Received: Sept 19, 2013; Accepted: Oct 30, 2013

SENRA Academic Publishers, British Columbia
Vol. 8, No. 1, pp. 2783-2787, February 2014
Online ISSN: 1920-3853; Print ISSN: 1715-9997

Canadian Journal of pure & applied sciences

**Short Communication**

# SOME PROBLEMS OF FINDING OF EIGENVALUES AND EIGENVECTORS FOR SH-WAVE PROPAGATION IN TRANSVERSELY ISOTROPIC PIEZOELECTROMAGNETICS

AA Zakharenko
International Institute of Zakharenko Waves (IIZWs)
660037, Krasnoyarsk-37, 17701, Krasnoyarsk, Russia

## ABSTRACT

This short theoretical work discusses some problems of finding of the suitable eigenvalues and eigenvectors. The eigenvalues and eigenvectors represent the solutions of the coupled equations of motion written in the well-known tensor form. These coupled equations of motion describe shear-horizontal (SH) wave propagation in the transversely isotropic piezoelectromagnetic materials of class 6*mm* when the SH-wave propagation is coupled with both the electrical and magnetic potentials. It is stated that as many as six eigenvalues can be soundly found for the problem. The problem is that some eigenvalues result in the corresponding certain eigenvectors and some eigenvalues allow existence of uncertain eigenvectors that can be chosen by a researcher. This uncertainty allows researchers to choose several certain forms for the uncertain eigenvectors. It is discussed that the author of this report has used the certain forms for the uncertain eigenvectors that are naturally coupled with the certain eigenvectors. However, some researchers suggest to use the following forms for the uncertain eigenvectors: (0,1,0) and (0,0,1). It is stated that the simplest and perhaps convenient eigenvectors in the forms of (0,1,0) and (0,0,1) are actually unsuitable because they are independent from the certain eigenvectors and the CMEMC coupling mechanisms. It is very important to use suitable eigenvectors because different forms of them can result in different final expressions for the velocities of the SH-waves. The SH-wave velocity is a very important wave characteristic and evaluation of its value can help for creation and optimization of novel technical devices based on surface, interfacial, and plate SH-waves.

**PACS:** 51.40.+p, 62.65.+k, 68.35.Gy, 68.35.Iv, 68.60.Bs, 74.25.Ld, 74.25.Ha, 75.20.En, 75.80.+q, 81.70.Cv
**Keywords**: Transversely isotropic piezoelectromagnetics, magnetoelectroelastic plates, magnetoelectric effect, new SH-waves.

## INTRODUCTION

This theoretical work discusses the problems of finding of suitable forms of the eigenvalues and eigenvectors. The found forms of the eigenvalues and the corresponding eigenvectors represent the solutions of the coupled equations of motion written in the well-known tensor form and can result in final expressions for the suitable propagation velocities of the shear-horizontal (SH) acoustic waves coupled with both the electrical and magnetic potentials. This difficulty touches the propagation problems of the surface (Zakharenko, 2010), interfacial (Zakharenko, 2012a), and plate (Zakharenko, 2012b) SH-waves in the transversely isotropic piezoelectromagnetics of class 6 *mm*.

The piezoelectromagnetic (composite) materials, also known as the magnetoelectroelastic media, are eminent as smart materials due to the fact that the electrical subsystem of the materials can interact with the magnetic subsystem via the mechanical subsystem, and vice versa. Therefore, it is vital to be familiar with the wave characteristics of such (composite) materials due to possible constitution of new technical devices with a high level of integration. It is understandable that this knowledge can help for further miniaturization of various technical devices and be used for the nondestructive testing and evaluation of piezoelectromagnetic (composite) materials. There is currently much review work on the magnetoelectric effect and the piezoelectromagnetics possessing this effect together with the other effects such as the piezoelectric and piezomagnetic effects. It is thought that the most complete list of review works on the subject is given in a first review paper by Zakharenko (2013a) concerning the SH-wave propagation problems in such smart materials.

The discussions highlighted in this short report are based on the results obtained in theoretical works (Zakharenko, 2010; Zakharenko, 2012a; Zakharenko, 2012b) that use certainly found eigenvalues and eigenvectors. However, some researchers believe that the natural eigenvalues and

*Corresponding author email: aazaaz@inbox.ru

the corresponding eigenvectors exploited in books (Zakharenko, 2010; Zakharenko, 2012a; Zakharenko, 2012b) for the transversely isotropic case cannot be the single possibility. They offer the other eigenvectors that actually represent an artificial case. This is also discussed below. Also, it is necessary to mention recent theoretical works (Wang *et al*., 2007; Liu *et al*., 2007; Wei *et al*., 2009; Melkumyan, 2007) that do not provide any eigenvalues and eigenvectors. The main expressions and discussions are given below in the following section.

**Problems of finding of eigenvalues and eigenvectors**

It is central to know the propagation directions of the shear-horizontal (SH) elastic waves when they can be coupled with both the electrical and magnetic potentials. For the transversely isotropic piezoelectromagnetic material of class 6 *mm*, the suitable propagation direction is given in the review paper written by Gulyaev (1998) and the coordinate system is shown in review paper by Zakharenko (2013a). This propagation direction for the 6 *mm* materials is different from the suitable propagation direction for the cubic piezoelectromagnetics (Zakharenko, 2013a; Zakharenko, 2011). Following this review paper, it is possible to state that the SH-wave propagation direction must be managed along the free surface of the piezoelectromagnetics when both the surface normal and the propagation direction are perpendicular to the sixfold symmetry axis of the 6*mm* material. In this configuration, the SH-waves are polarized along the sixfold symmetry axis. This is the case of pure waves where the pure SH-waves can be separately studied (Lardat *et al*., 1971; Dieulesaint and Royer, 1980). To study the SH-wave propagation, the quasi-static approximation (Dieulesaint and Royer, 1980; Auld, 1990) must be used when the SH-waves are coupled with both the electrical and magnetic potentials.

In the case of the pure SH-wave propagation, the corresponding tensor form of the equations of motion for the piezoelectromagnetic (6 *mm*) medium can be written (Zakharenko, 2010; Zakharenko, 2012a; Zakharenko, 2012b; Zakharenko, 2013a). Also, it is essential to mention the following nonzero material parameters (Zakharenko, 2010; Zakharenko, 2012a; Zakharenko, 2012b; Zakharenko, 2013a; Nye, 1989; Newnham, 2005): the elastic stiffness constant $C$, piezoelectric constant $e$, piezomagnetic coefficient $h$, dielectric permittivity coefficient $\varepsilon$, magnetic permeability coefficient $\mu$, and electromagnetic constant $\alpha$. These material constants are defined as follows: $C = C_{44} = C_{66}$, $e = e_{16} = e_{34}$, $h = h_{16} = h_{34}$, $\varepsilon = \varepsilon_{11} = \varepsilon_{33}$, $\mu = \mu_{11} = \mu_{33}$, and $\alpha = \alpha_{11} = \alpha_{33}$ (Zakharenko, 2010; Zakharenko, 2012[a]; Zakharenko, 2012[b]; Zakharenko, 2013[a]). Solving the corresponding equations of motion written in the tensor form (Zakharenko, 2010; Zakharenko, 2012a; Zakharenko, 2012b), it is possible to obtain all the eigenvalues and the corresponding eigenvectors. To discuss the problem of finding of suitable eigenvalues and eigenvectors is the main purpose for this short report.

When the SH-wave propagation is coupled with both the electrical ($\varphi$) and magnetic ($\psi$) potentials, the corresponding tensor form of the coupled equations of motion can be expressed by three homogeneous equations written in the following matrix form (Zakharenko, 2010; Zakharenko, 2012a; Zakharenko, 2012b):

$$\begin{pmatrix} C\left[m-\left(V_{ph}/V_{t4}\right)^2\right] & em & hm \\ em & -\varepsilon m & -\alpha m \\ hm & -\alpha m & -\mu m \end{pmatrix}\begin{pmatrix} U^0 \\ \varphi^0 \\ \psi^0 \end{pmatrix}=\begin{pmatrix} 0 \\ 0 \\ 0 \end{pmatrix} \quad (1)$$

where $m = 1 + n_3^2$ and $\left(U^0,\varphi^0,\psi^0\right)=\left(U_2^0,U_4^0,U_5^0\right)$ are unknown and must be found. $n_3$ represents the eigenvalues and $U^0$, $\varphi^0$, and $\psi^0$ are the eigenvector components. In equations (1), $\rho$ and $V_{ph}$ are the mass density of the piezoelectromagnetic material and the phase velocity, respectively. The phase velocity $V_{ph}$ is defined by the following relation: $V_{ph} = \omega/k$, where $\omega$ is the angular frequency and $k$ is the wavenumber in the propagation direction of the SH-waves. Also, $V_{t4}$ stands for the speed of the shear-horizontal bulk acoustic wave (SH-BAW) uncoupled with both the electrical and magnetic potentials, $V_{t4}=\sqrt{C/\rho}$.

All the suitable eigenvalues $n_3$ can be determined when the determinant of the coefficient matrix in equations (1) vanishes. Expanding this matrix determinant, the following secular equation representing a polynomial must be obtained:

$$m\times m\times\left[\left(1+K_{em}^2\right)m-\left(V_{ph}/V_{t4}\right)^2\right]=0.$$

This polynomial is already written in a convenient form of three factors because to find the polynomial roots means to write a polynomial as the suitable factors. So, the first, second, and third factors of the polynomial written above reveal the following eigenvalues:

$$n_3^{(1)}=-n_3^{(2)}=-\mathrm{j} \quad (2)$$

$$n_3^{(3)}=-n_3^{(4)}=-\mathrm{j} \quad (3)$$

$$n_3^{(5)}=-n_3^{(6)}=-\mathrm{j}\sqrt{1-\left(V_{ph}/V_{tem}\right)^2} \quad (4)$$

In definition (4), the velocity denoted by $V_{tem}$ represents the speed of the SH-BAW coupled with both the electrical and magnetic potentials. It is defined by the following expression:

$$V_{tem} = V_{t4}\left(1 + K_{em}^2\right)^{1/2} \quad (5)$$

In expression (5), $K_{em}^2$ stands for the coefficient of the magnetoelectromechanical coupling (CMEMC). It can be calculated with the following formula:

$$K_{em}^2 = \frac{\mu e^2 + \varepsilon h^2 - 2\alpha eh}{C\left(\varepsilon\mu - \alpha^2\right)} = \frac{e\left(e\mu - h\alpha\right) - h\left(e\alpha - h\varepsilon\right)}{C\left(\varepsilon\mu - \alpha^2\right)} \quad (6)$$

It is understandable in equality (6) that the CMEMC can be represented as the material parameter depending on the following three different coupling mechanisms (Zakharenko, 2013b; Zakharenko, 2013c):

$$e\mu - h\alpha\,,\; e\alpha - h\varepsilon\,,\; \varepsilon\mu - \alpha^2 \quad (7)$$

With the found eigenvalues defined by expressions (2), (3) and (4), it is necessary to determine the corresponding eigenvectors. Using coupled equations (1), it is also possible to determine the eigenvector explicit forms such as $\left(U^0, \varphi^0, \psi^0\right)$ for all the suitable eigenvalues $n_3$. It is natural to use the first equation in equations' set (1) to demonstrate the dependence of the eigenvector component $U^0$ on both the components $\varphi^0$ and $\psi^0$. Thus, this dependence reads

$$U^0 = -\frac{em}{A}\varphi^0 - \frac{hm}{A}\psi^0 \quad (8)$$

Exploiting equation (8) for the second and third equations in equations' set (1), one can exclude the eigenvector component $U^0$ to deal with only two equations in two unknowns such as $\varphi^0$ and $\psi^0$. Consequently, these two equations are composed as follows:

$$\left(\frac{me^2}{A} + \varepsilon\right)\varphi^0 + \left(\frac{meh}{A} + \alpha\right)\psi^0 = 0 \quad (9)$$

$$\left(\frac{meh}{A} + \alpha\right)\varphi^0 + \left(\frac{mh^2}{A} + \mu\right)\psi^0 = 0 \quad (10)$$

where

$$A = C\left[m - \left(V_{ph}/V_{t4}\right)^2\right] \quad (11)$$

It is now necessary to state that all the suitable eigenvector components can be obtained by means of the use of each of the found eigenvalues defined by equations from (2) to (4). As soon as each of the eigenvalues is used for equations from (8) to (10), the corresponding eigenvector components are determined. Indeed, each eigenvalue possesses its own certain set of the eigenvector components and it is natural to use the obtained equations from (8) to (10) to define the components because these equations follow from the coupled equations of motion written in matrix form (1). However, equations (9) and (10) allow each eigenvalue to naturally have two different sets of the eigenvector components. They are discussed below as cases (i) and (ii).

***Case (i)***

In this case, equations (8) and (9) are used. Accounting the fact that $m = 1 + n_3^2 = 0$ for eigenvalues (2) and (3), it is possible to have the following eigenvector components such as $U^0$, $\varphi^0$, and $\psi^0$:

$$\left(U^{0(1)}, \varphi^{0(1)}, \psi^{0(1)}\right) = \left(U^{0(3)}, \varphi^{0(3)}, \psi^{0(3)}\right) = \left(0, \alpha, -\varepsilon\right) \quad (12)$$

One can find that the found eigenvector components defined by expression (12) satisfy three homogeneous equations (1). This is true because $m = 0$ leads to all zero components for the second and third columns of the coefficient matrix in equations (1). Therefore, a wavevector of the following form is valid for this case: (0, $x$, $y$) where $x \neq 0$ and $y \neq 0$. This uncertainty is naturally resolved by the use of eigenvector (12) coupled with the certain eigenvector corresponding to eigenvalue (4). Employing expressions (8) and (9) for eigenvalue (4) with $m \neq 0$, the corresponding eigenvector components ($U^0$, $\varphi^0$, and $\psi^0$) can be written as follows:

$$\left(U^{0(5)}, \varphi^{0(5)}, \psi^{0(5)}\right) = \left(\frac{e\alpha - h\varepsilon}{CK_{em}^2}, -\frac{eh}{CK_{em}^2} + \alpha, \frac{e^2}{CK_{em}^2} - \varepsilon\right) \quad (13)$$
$$= \frac{1}{K_{em}^2}\left(\left(e\alpha - h\varepsilon\right)/C, \alpha\left(K_{em}^2 - K_\alpha^2\right), -\varepsilon\left(K_{em}^2 - K_e^2\right)\right)$$

It is very important to state that the found eigenvector components $\varphi^{0(5)}$ and $\psi^{0(5)}$ from expression (13) satisfy both equations (9) and (10).

The eigenvector components such as $\varphi^0$ and $\psi^0$ of eigenvectors (12) and (13) are naturally coupled as follows:

$$e\varphi^{0(1)} + h\psi^{0(1)} = e\varphi^{0(3)} + h\psi^{0(3)} =$$
$$e\varphi^{0(5)} + h\psi^{0(5)} = e\alpha - h\varepsilon \quad (14)$$

It is clearly seen in equalities (14) that the second coupling mechanism of three CMEMC mechanisms (7) couples the eigenvector components. This reveals the physical sense for the found eigenvectors (12) and (13).

In expression (13), the coefficient of the electromechanical coupling (CEMC) is denoted by $K_e^2$

and the other parameter denoted by $K_\alpha^2$ couples only the terms with the electromagnetic constant $\alpha$ in CMEMC (6). They are respectively defined as follows:

$$K_e^2 = \frac{e^2}{C\varepsilon},\ K_\alpha^2 = \frac{eh}{C\alpha} = \frac{\alpha eh}{C\alpha^2} \tag{15}$$

***Case (ii)***

In this second natural case, it is natural to utilize equations (8) and (10) to obtain the eigenvector components such as $U^0$, $\varphi^0$, and $\psi^0$. Using $m = 1 + n_3^2 = 0$, it is possible to have the following eigenvector components for eigenvalues (2) and (3):

$$\left(U^{0(1)}, \varphi^{0(1)}, \psi^{0(1)}\right) = \left(U^{0(3)}, \varphi^{0(3)}, \psi^{0(3)}\right) = (0, \mu, -\alpha) \tag{16}$$

For eigenvalue (4) with $m \neq 0$, the corresponding eigenvector components are found as follows:

$$\left(U^{0(5)}, \varphi^{0(5)}, \psi^{0(5)}\right) = \left(\frac{e\mu - h\alpha}{CK_{em}^2}, -\frac{h^2}{CK_{em}^2} + \mu, \frac{eh}{CK_{em}^2} - \alpha\right)$$
$$= \frac{1}{K_{em}^2}\left((e\mu - h\alpha)/C, \mu\left(K_{em}^2 - K_m^2\right), -\alpha\left(K_{em}^2 - K_\alpha^2\right)\right) \tag{17}$$

where

$$\varphi^{0(1)} + \psi^{0(1)} = \varphi^{0(3)} + \psi^{0(3)} = \varphi^{0(2)} + \psi^{0(2)} = \varphi^{0(5)} + \psi^{0(5)} \tag{18}$$

Equalities (18) also disclose the physical sense because eigenvector components $\varphi^0$ and $\psi^0$ in eigenvectors (16) and (17) are coupled via the first mechanism of three coupling mechanisms (7) of CMEMC (6).

It is vital to state here that the found eigenvector components $\varphi^{0(5)}$ and $\psi^{0(5)}$ from expression (17) also satisfy both equations (9) and (10). In expression (17), the non-dimensional parameter $K_m^2$ called the coefficient of the magnetomechanical coupling (CMMC) is defined by

$$K_m^2 = \frac{h^2}{C\mu} \tag{19}$$

***Case (iii)***

This case relates to the other mathematically possible forms for the eigenvectors that can be even mathematically more convenient but have no any physical sense. These eigenvectors are possible because of the uncertainty for the case of $m = 0$ for eigenvalues (2) and (3). Therefore, $m = 0$ leads to all the zero components in the second and third columns of the coefficient matrix in equations (1). As a result, some researchers suggest the use of the following form of the eigenvectors for eigenvalues (2) and (3): $(0, x, y)$ where either $x = 1$ or $y = 1$, or $x = y = 1$ occurs. The latter representing more complicated case will be not discussed in this report below. In addition to certain eigenvectors (13) and (17) for eigenvalue (4), some researchers believe that possible convenient eigenvector forms can be chosen for the eigenvalues defined by expressions (2) and (3) as follows:

(0,1,0), (0,1,0) (20)
(0,0,1), (0,0,1) (21)
(0,1,0), (0,0,1) (22)
(0,0,1), (0,1,0) (23)

It is clearly seen that none of the artificial eigenvectors defined by expressions from (20) to (24) has any connection to certain eigenvectors (13) and (17). It is thought that eigenvectors (20) and (21) of all the artificial eigenvectors are more referable compared with the other two eigenvectors defined by expressions (22) and (23) because it is natural to deal with the same eigenvectors in the case of identical eigenvalues (2) and (3). Indeed, eigenvectors (22) and (23) were composed by mixing eigenvectors (20) and (21). However, some researchers would like to exploit mixed eigenvectors (22) and (23) because they do not lead to uncertainty for the phase velocity in comparison with eigenvectors (20) and (21). It is necessary to state that eigenvectors (12) and (16) also leads to the uncertainty for the phase velocity that is readily resolved because the corresponding mechanism of three coupling mechanisms (6) of CMEMC (7) works. The artificial eigenvectors defined by expressions from (20) to (23) have no any connection with CMEMC coupling mechanisms (6) and certain eigenvectors (13) and (17). As a result, they can actually lead to fake results for the phase velocity.

## CONCLUSION

This report has briefly discussed the problem of finding of the eigenvalues and the corresponding suitable eigenvectors. Due to the discussed uncertainty for eigenvalues (2) and (3), the corresponding eigenvectors can be chosen in several different ways. Three cases were discussed, of which the first and second are natural because they are based on equations from (8) to (10) which were received from coupled equations of motion written in matrix form (1). On the other hand, it was also discussed the other eigenvectors given by expressions from (20) to (23) that have mathematically convenient forms but have no physical sense because they have no any connection with the certain eigenvectors defined by

expressions (13) and (17) and cannot demonstrate any connection with one of CMEMC coupling mechanisms (7).

## REFERENCES


Auld, BA. 1990. Acoustic fields and waves in solids. Krieger Publishing Company (vol. I & II) (2nd edi.). pp878.

Dieulesaint, E. and Royer, D. 1980. Elastic waves in solids: Applications to signal processing. J. Wiley, New York, USA. (translated by Bastin A. and Motz, M). Chichester. pp511.

Gulyaev, YV. 1998. Review of shear surface acoustic waves in solids. IEEE Transactions on Ultrasonics, Ferroelectrics, and Frequency Control. 45(4):935-938.

Lardat, C., Maerfeld, C. and Tournois, P. 1971. Theory and performance of acoustical dispersive surface wave delay lines. Proceedings of the IEEE. 59(3):355-364.

Liu, JX., Fang, DN. and Liu, XL. 2007. A shear horizontal surface wave in magnetoelectric materials. IEEE Transactions on Ultrasonics, Ferroelectrics, and Frequency Control. 54(7):1287-1289.

Melkumyan, A. 2007. Twelve shear surface waves guided by clamped/free boundaries in magneto-electro-elastic materials. International Journal of Solids and Structures. 44(10):3594-3599.

Newnham, RE. 2005. Properties of Materials: Anisotropy, Symmetry, Structure (Kindle edition). Oxford University Press Inc., Oxford-New York. (Reprinted 2008). pp391.

Nye, JF. 1989. Physical Properties of Crystals. Their Representation by Tensors and Matrices. Clarendon Press, Oxford. pp385.

Wang, BL., Mai, YW. and Niraula, OP. 2007. A horizontal shear surface wave in magnetoelectroelastic materials. Philosophical Magazine Letters. 87(1):53-58.

Wei, WY., Liu, JX. and Fang, DN. 2009. Existence of shear horizontal surface waves in a magneto-electro-elastic material. Chinese Physics Letters. 26(10):104301. pp3.

Zakharenko, AA. 2010. Propagation of seven new SH-SAWs in piezoelectromagnetics of class 6 *mm*. LAP LAMBERT Academic Publishing GmbH & Co. KG, Saarbruecken–Krasnoyarsk. pp84.

Zakharenko, AA. 2011. Seven new SH-SAWs in cubic piezoelectromagnetics. LAP LAMBERT Academic Publishing GmbH & Co. KG, Saarbruecken–Krasnoyarsk. pp172.

Zakharenko, AA. 2012[a]. Twenty two new interfacial SH-waves in dissimilar PEMs. LAP LAMBERT Academic Publishing GmbH & Co. KG, Saarbruecken–Krasnoyarsk. pp148.

Zakharenko, AA. 2012[b]. Thirty two new SH-waves propagating in PEM plates of class 6 *mm*. LAP LAMBERT Academic Publishing GmbH & Co. KG, Saarbruecken–Krasnoyarsk. pp162.

Zakharenko, AA. 2013[a]. Piezoelectromagnetic SH-SAWs: A review. Canadian Journal of Pure and Applied Sciences. 7(1):2227-2240.

Zakharenko, AA. 2013[b]. Peculiarities study of acoustic waves' propagation in piezoelectromagnetic (composite) materials. Canadian Journal of Pure and Applied Sciences. 7(2):2459-2461.

Zakharenko, AA. 2013[c]. New nondispersive SH-SAWs guided by the surface of piezoelectromagnetics. Canadian Journal of Pure and Applied Sciences. 7(3):2557-2570.


Received: Sept 4, 2013; Accepted: Dec 3, 2013

SENRA Academic Publishers, British Columbia
Vol. 8, No. 1, pp. 2789-2794, February 2014
Online ISSN: 1920-3853; Print ISSN: 1715-9997

Canadian Journal of pure&applied sciences

**Short Communication**

# RISKS ASSOCIATED WITH GEOPHAGIA IN GHANA

*Woode, A and Hackman-Duncan, SF
Department Of Civil Engineering, Accra Polytechnic, PO BOX 561 Accra

## ABSTRACT

An investigation was conducted to determine the risks associated with the ingestion of some geophagy clays mined in Ghana, Nigeria and Cote d'voire. These clays are widely distributed through major marketing centres in Ghana and within the West African sub-region. Samples of the geophagy clays were purchased from selected markets in the Greater Accra region and then subjected to X-ray fluorescence analysis to determine the levels of heavy metals present in them and their potential effects on consumers. The results indicate that the levels of arsenic, cadmium, mercury, lead and cobalt contained in 70g of the geopagy clay were far higher than the WHO/FAO and USDA approved maximum daily tolerable intake. This was interpreted to mean that consumers were at risk of heavy metal contamination which could lead to various diseases. The extent of bioavailability of these toxic elements to consumers of the clay was however not established. It was concluded that geophagy clay sold on Ghanaian markets could have potentially negative health impact on consumers if consumed at 70g per day or more and on regular basis.

**Keywords**: Harmful, heavy metals, geophagy, clay.

## INTRODUCTION

The mining and selling of geophagy clay is an important livelihood in the West African sub-region. Clay from Ghana, particularly obtained from Anfoega in the Volta Region, is sold for direct consumption in all parts of Ghana and in some West Africa countries, for either medicinal or cultural purposes and for pleasure (Vermeer, 1971). Other sub-Saharan states including Nigeria also produce and distribute geophagy clay for sale in markets in the West Africa sub-region (Hunter, 1973).

The consumption of clay is a common practice especially among women and is often associated with pregnancy, poverty and famine (Woywodt and Kiss, 2002; Al-Rmalli *et al*., 2010). In Ghana 28% of women of reproductive age who practice geophagy consume a daily average of 70g of clay (Tayie *et al*., 2013). Eating of clay and or soil as a habit was observed to be less frequent in boys than in girls. Geophagy in boys decreases with age (Bisi-Johnson *et al*., 2010). Geophagia has been shown to be prevalent among females in the teenage bracket and that by educating these females geophagia and its consequences can be reduced (Woode, 2013).

Some research works have confirmed a strong correlation between some harmful heavy metals such as arsenic, lead, mercury and cadmium and human health (WHO, 2013; Al-Rmalli *et al*., 2010). High levels of arsenic, lead and cadmium were detected in geophagy clay eaten by Bangladeshi pregnant women. There have also been other reports of the presences of these harmful elements in geophagy clays from other places such as Ghana and Kenya (Woywodt and Kiss, 2002; Gborbani, 2008; Tayie *et al*., 2013).

Excessive exposure to the harmful heavy metals could lead to one disease or another. For instance Selinus *et al*. (2010) have found that acute exposure to lead can affect the human central nervous system and may cause anemia and dysfunction of the kidney, liver and heart. It has also been reported by WHO (December 2012, 2013) that exposure to arsenic over a long time from drinking-water and food can cause cancer. Arsenic is also associated with cardiovascular disease and diabetes. WHO (2013, April 2012) has also reported that mercury can affect the nervous, digestive and immune systems, as well as the lungs, kidneys, skin and eyes. Another study Kippler *et al*. (2009) have also found that cadmium can inhibit the secretion of calcium in breast milk and may have toxic effects on the kidney, the skeletal and the respiratory systems.

Geophagy clay may contain some relatively non toxic mineral elements such as copper, iron, magnesium and zinc which are important and therefore could have useful health benefits to the consumer. On the contrary Kawai *et al*. (2009) observed that geophagy in pregnant women in sub-Saharan Africa resulted in iron deficiency associated anemia. Njiru (2011) confirmed this finding and indicated that clay soils may obstruct the bioavailability of micronutrients resulting in micronutrient deficiency.

Geophagy clay may also be a source of microbial infection (Tano-Debrah and Bruce-Baiden, 2010). Microbiological health effects associated with geophagia

*Corresponding author emails: pstwoode@yahoo.com

in humans include the beneficial use of kaolin (a form of clay) to treat diarrhoea and enhancement of bioactivities (Bisi-Johnson *et al.*, 2010) as confirmed by Ngole *et al.* (2010) in their study of the physicochemical properties of geophagic clayey soils from South Africa and Swaziland. The presence of iron oxide in clay and the water retention capacity of clay was founded to alleviate anemia and diarrhea respectively.

Even though geophagy clay consumption in Ghana has gone on for a very long time there are relatively few known publications on the risks that it poses to consumers and therefore its health implication. The aim of this study therefore is to determine the levels of the harmful heavy metals found in geophagy clays sold in some major markets in Ghana and to communicate the potential health risk associated with the consumption of the clay.

## MATERIALS AND METHODS

Materials

Samples of dry unprocessed geophagy clay were obtained from three major markets in the Greater Accra region of Ghana for analysis. The markets-Makola, Madina and Ashiaman markets were chosen because of the high level of trading in geophagy clay sourced from Nigeria, Abidjan in Cote d'ivoire and Ghana. A major source of supply of geophagy clay to most market places in Ghana is Anfoega in the Volta region and along the coastline of the Greater Accra region of Ghana. The geophagy clays samples obtained from the markets and sourced from same locations – Accra, Anfoega, Abidjan and Nigeria were bulked together for laboratory analysis.

Method

The clays obtained from the markets were crushed in turns in a crucible. The crushed samples were then sieved through the 180µm sieve. The crucible and sieve were cleaned after each sample prepared to avoid contamination. Four gram (4g) of each sieved sample and 0.9g wax added as a binder were then put into mix for 3minutes at 15Hz in a homogenizer (Model Retsch mm301). The mix was pressed into pellet discs for the test.

Three replicates of the pellet discs of each sample were placed in an X-ray Fluorescence Spectrometry (XRF) machine (Model Spectro X-Lab 2000) for the determination of the heavy metals. The results obtained are presented in table 1.

Table 1. Levels of heavy metals in twelve geophagy clay samples from Ghana (Anf, Acc), Cote d'ivoire (Abj) and Nigeria (Nig) in ppm.

| Heavy metals | Anf 1 | Anf 2 | Anf 3 | Acc 1 | Acc 2 | Acc 3 | Abj 1 | Abj 2 | Abj 3 | Nig 1 | Nig 2 | Nig 3 |
|---|---|---|---|---|---|---|---|---|---|---|---|---|
| V | 185.2 | 156.3 | 156.7 | 91 | 99 | 77 | 83 | 105 | 95 | 123 | 147 | 14 |
| Cr | 83.8 | 109 | 84 | 695 | 90 | 833 | 1213 | 1349 | 13 | 112 | 99 | 1031 |
| Co | 32.4 | 18.7 | 20.8 | 17 | 17 | 17 | 15 | 15 | 15 | 20 | 20 | 20 |
| Ni | 11.4 | 8.7 | 7.2 | 15.5 | 13.6 | 14.7 | 18.2 | 16.1 | 18.8 | 25.4 | 26.2 | 26.2 |
| Cu | 23.1 | 23.6 | 22.6 | 11.9 | 12.1 | 12.3 | 2.2 | 3.7 | 0.9 | 15.1 | 13.2 | 15.6 |
| Sn | 6.4 | 5.1 | 5.2 | 1.2 | 1.2 | 2.6 | 2 | 2.4 | 1.7 | 1.6 | 1.6 | 3.1 |
| Zn | 32.1 | 26.4 | 31.7 | 14.6 | 14.9 | 15.8 | 18 | 17.1 | 18.7 | 68 | 72.7 | 79.5 |
| Ga | 16.9 | 15.6 | 17.4 | 18 | 18.4 | 18.6 | 27.8 | 27.7 | 27.8 | 24 | 25.1 | 26.2 |
| As | 1.8 | 0.6 | 0.6 | 5.8 | 4.7 | 5.3 | 9.0 | 9.9 | 10.6 | 2.9 | 3.5 | 3.9 |
| Cd | 0.9 | 0.7 | 0.7 | 1.5 | 1.6 | 1.4 | 1.5 | 1.4 | 1.4 | 1.3 | 1.4 | 1.4 |
| Hg | 4.2 | 1.6 | 0.3 | 2.4 | 1.6 | 1.6 | 1.4 | 1.3 | 3.1 | 1.5 | 1.5 | 0.8 |
| Pb | 18.3 | 14.9 | 10.7 | 14.5 | 15.6 | 15.8 | 12.6 | 11.4 | 10.8 | 15.7 | 16 | 14.7 |

Anf = Anfoega; Acc = Accra; Abj = Abidjan; Nig = Nigeria

Table 2. PMTDI values for some heavy metals (after WHO/FAO, 2010) and the amount of the heavy metals in 70g of clay from Anf, Acc, Abj, and Nig. consumed.

| Heavy Metals | WHO/FAO PMTDI (µg/kg BW/day) | PMTDI for 60kg BW(µg/day) | Average amount of heavy metals in 70g of geophagy clays consumed(µg /day) | | | |
|---|---|---|---|---|---|---|
| | | | Anf | Acc | Abj | Nig |
| As | 3.0 | 180 | 126 | 371 | 688 | 240 |
| Pb | 3.0 | 180 | 1281 | 1071 | 812 | 1085 |
| Hg | 0.6 | 36 | 301 | 131 | 135 | 91 |
| Cd | 0.8 | 48 | 63 | 105 | 98 | 98 |

PMTDI- Permitted Maximum Tolerable Daily Intake

## RESULTS DISCUSSION

The amount of heavy metals in 70g of the clay consumed have been computed and presented in table 2. The 70g was adopted from Tayie *et al.* (2013) who indicated that to be the amount of clay ingested daily by the women who practice geophagia in Ghana. The amounts of heavy metals consumed were calculated using the average of three of the samples from the same source in table 1. The values obtained are then compared to the Permitted Maximum Tolerable Daily Intake (PMTDI) recommended by the World Health Organization (WHO) and the Food and Agriculture Organization (FAO) and are presented in table 2 and figures 1-4.

The Joint FAO/WHO Expert Committee on Food Additives (JECFA, 2010) estimated the total dietary exposure to arsenic to range between 2.0 and 7.0µg /kg BW/day. The committee fixed the mean exposure level at 3.0µg /kg BW/day. The Arsenic in the Anfoega clay sample ranges between 0.6 to1.8ppm (Table 1). This works out to a maximum of 126µg of As in 70g of the Anfoega clay consumed in a day (Table 2). The 126µg is lower than the 180µg permitted maximum tolerable daily intake for a 60kg adult and so adult consumers may not be at risk of arsenic (As) contamination unless they consume higher quantity. Children with body mass of less than 60kg who consume 70g of the clay may experience the effects of arsenic toxicity which includes skin and lung

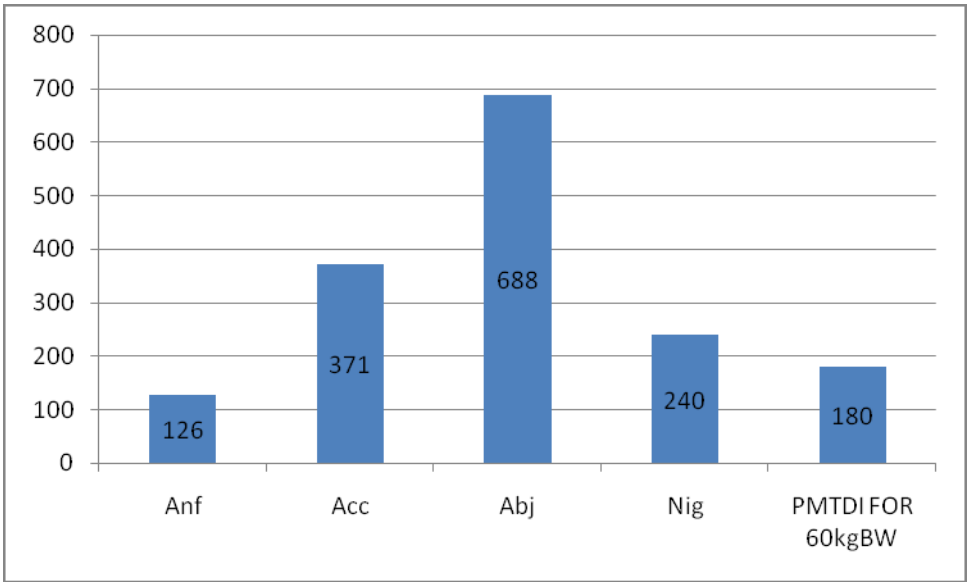


Fig. 1. The levels of Arsenic in clays compared to PMTDI.

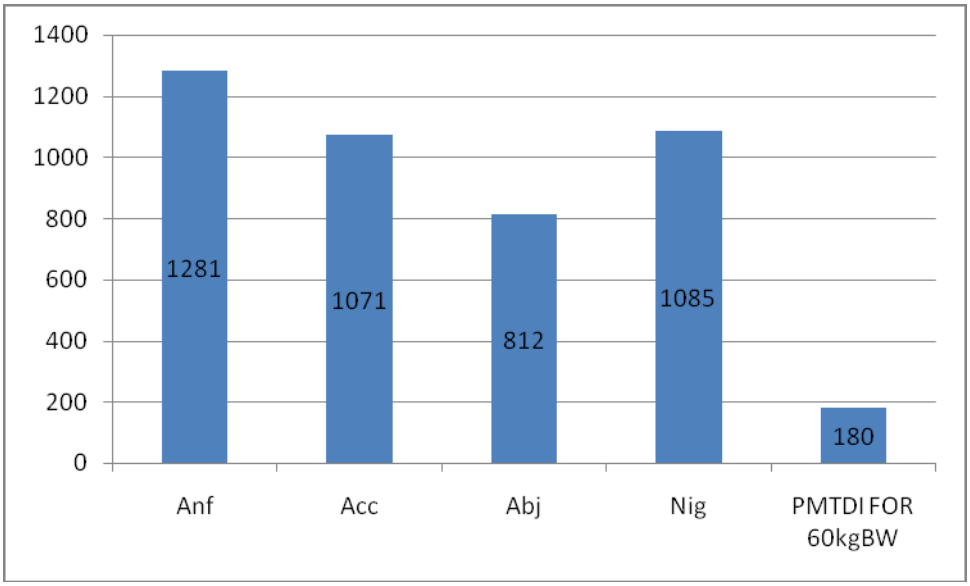


Fig. 2. The levels of lead in clays compared to PMTDI.

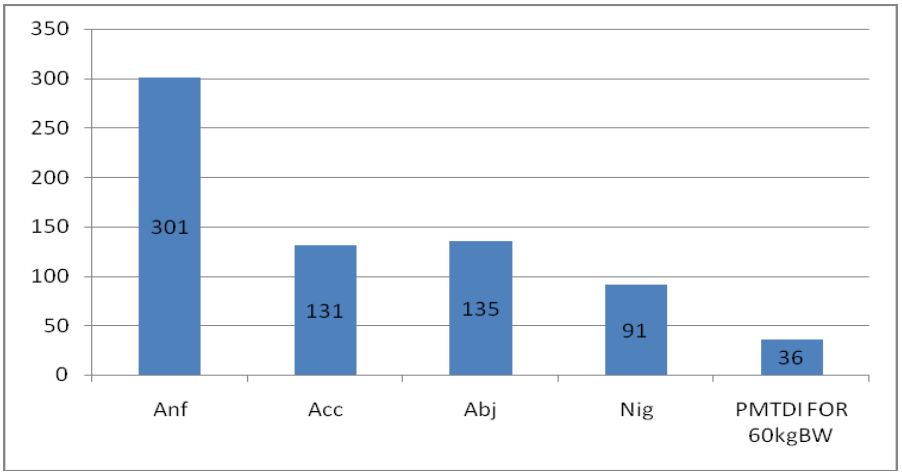


Fig. 3. The levels of mercury in clays compared to PMTDI.

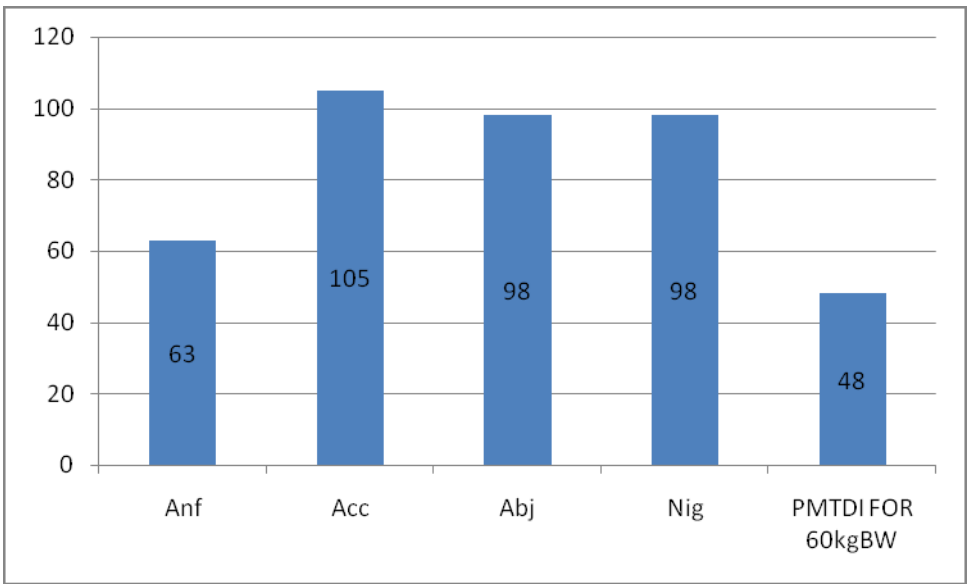


Fig. 4. The levels of cadmium in clays compared to PMTDI.

cancer. The level of arsenic in 70g of each of the other clays is higher than the PMTDI. The arsenic in the clay from Abidjan (Abj) is nearly four times that of PMTDI, and clay from Accra (Acc) contains about twice the PMTDI (Fig. 1).

Other harmful heavy metals in the Anfoega clay range between 10.7 and 18.3ppm for lead (Pb), 0.7 and 0.9ppm for cadmium (Cd) and 0.3 and 4.2ppm for mercury (Hg). The quantity of lead in 70g of Anfoega clay (1281µg) computed in table 2 is over seven times the required daily intake for an adult of 60kg weight. When consumed over a long time therefore, Anfoega clay could have very serious health effects such as the dysfunctioning of the kidney, liver and heart of the consumers (Selinus *et al*., 2010). Children who consume about 70g of the clay/day will in addition suffer damages including learning and behavior disorder. The lead values obtained for all the other clays are far higher than the PMDTI (Fig. 2).

From table 1 the maximum quantity of cadmium in the sample obtained from the XRF test is 0.9µg/g. Therefore, the cadmium in 70g of Anfoega clay consumed daily is 63.0µg. This value is about twice the level fixed by JECFA in 2010 for a 60kg adult (Table 2). This means that consuming clay from Anfoega over a period of time could result in kidney damage (Jarup *et al*., 1998). The Accra clay has the highest level of 105µg of cadmium in 70g compared to all the other clays. All the clays however, have higher cadmium than the PMTDI (Fig. 4). JECFA (Feb, 2010) fixed the weekly intake of mercury to be 4.0µg /kg BW/week. The daily intake therefore should be at most 0.6µg/kg BW/day. The mercury in 70g of Anfoega clay is estimated to be 301µg (Table 2). This

Table 3. Recommended Dietary Allowance (RDA) values of some heavy metals and the amount in sampled geophagy clays.

| Heavy Metals | Highest RDA for an adult (µg/day) | Tolerable Upper Intake Level by USDA (µg) | Average amount of heavy metals in 70g of geophagy clays consumed (µg /day) | | | |
|---|---|---|---|---|---|---|
| | | | Anf | Acc | Abj | Nig |
| Cr | 35 | N/A | 6,419 | 37,590 | 60,060 | 28,980 |
| Ni | 700 | >1,000 | 623 | 1022 | 1239 | 1799 |
| Mo | 45 | > 2,000 | 63 | 273 | 252 | 301 |
| Cu | 900 | > 10,000 | 1575 | 847 | 161 | 1022 |
| Co | 20 | > 250 | 1678 | 1190 | 1050 | 1400 |

Recommended Dietary Allowance values (after United States Department of Agriculture (USDA) Dietary Reference Intake, 2013).

means that the mercury in 70g of Anfoega clay is over eight times the required daily intake and therefore consumers are likely to suffer diseases associated with mercury toxicity. All the other clays have higher mercury than the PMTDI (Fig. 3).

Recommended Dietary Allowance values (after the United States Department of Agriculture (USDA) Dietary Reference Intake, 2013).

The amount of copper in 70g of geophagy clay ingested in a day is far less than the tolerable upper intake level by USDA (Table 3). None of the clays from the markets therefore contribute significant amounts of copper to the consumer. Cr values on the other hand are in some cases more than a thousand times over the recommended dietary allowance values in table 3. The clays therefore are a good source of chromium for the consumer. However, nickel is marginally more than the recommended dietary allowance. Clays from Accra, Nigeria and Abidjan have Ni values higher than the tolerable upper intake level in table 3. The levels of molybdenum in the clays are less than the tolerable upper intake levels by USDA. Cobalt values in 70g of the clays are all far higher than the tolerable upper intake levels. Consumers of the clays therefore are at risk of cobalt contamination and its consequence.

Even though very high amounts of As, Pb, Hg, Cd and Co have been recorded for the clays, indicating a possible risk to the consumer, the harmful metals may not be bioavailable to the consumer.

In order to determine whether the harmful elements will be bioavailable Tayie *et al*. (2013) simulated the acidic conditions in the human stomach by performing an extraction process on white clay from Anfoega and other areas using HCl and observed that arsenic and lead were not detected in the acid extract. They therefore concluded that the toxic minerals were not bioavailable and therefore the clay was safe for human consumption.

Some previous studies, on the contrary, have indicated that bioavailability of heavy metals in soil such as geophagy clay is dependent on many other factors other than the presence of acid in the stomach. The factors include the concentration of the metals, physical and chemical forms of the metals, pH, Eh, temperature, particulate and dissolved organic content (Luoma, 1989; Ernst, 1996; Violante, 2010).

An acid extraction therefore, may not adequately explain whether some heavy metals may be bioavailable or not. Further research may be necessary to establish the role of other factors in ensuring the availability of these harmful metals to consumers.

## CONCLUSION

The levels of arsenic, lead, mercury, cadmium and cobalt in all the geophagy clays sold in three major markets in Ghana are higher than WHO/FAO requirement and the levels established by the United States Department of Agriculture. The consumption of these clays by both adults and children therefore could lead to various life-threatening diseases. The clays are therefore risky for human consumption.

## ACKNOWLEDGEMENT

The XRF test was carried out in the laboratory of the Geological Survey Department of Ghana.

## REFERENCES

Al-Rmalli, SW., Jenkins, RO., Watts, MJ. and Haris, P. 2010. Risk of human exposure to arsenic and other elements from geophagy: Trace element analysis of baked clay using inductively coupled plasma mass spectrometry. Environmental Health. 9:79-88.

Bisi-Johnson, MA., Obi, CL. and Ekosse, GE. 2010. Microbiological and health related perspectives of

geophagia: An overview. African Journal of Biotechnology. 9(19):5784-5791.

Ernst, WHO. 1996. Bioavailability of heavy metals and decontamination of soils by plants. Environmental geochemistry. 11(1-2):163-167.

Gborbani, H. 2008. Geophagia, a soil-environment related disease. International meeting on soil fertility, land management and agroclimatology, Turkey. 957-967.

Hunter, JM. 1973. Geophagy in Africa and the United States: a culture-nutrition hypothesis. J. Geog. Rev. 63:170-195.

JECFA. 73rd Meeting Geneva 8-17, June 2010- Food additive and contaminants (Flavours; Cadmium and Lead).

JECFA, 72nd Meeting Rome 16-25, Feb. 2010- Contaminants (Acrylamide, Arsenic, Deoxynivalenol, Furan, Mercury, Perchlorate).

Jarup, L., Bellander, T., Hogstedt, C. and Spang, G. 1998. Mortality and cancer incidence in Swedish battery workers exposed to cadmium and nickel. Occup. Environ. Med. 55:755-759.

Kippler, M., Lönnerdal, B., Goessler, W., Ekström, EC., Arifeen, SE. and Vahter, M. 2009. Cadmium interacts with the transport of essential micronutrients in the mammary gland — a study in rural Bangladeshi women. Toxicology. 257:64-69.

Kawai, K., Saathoff, E., Antelman, G., Msamanga, G. and Fawzi, WW. 2009. Geophagy (Soil-eating) in relation to Anemia and Helminth infection among HIV-infected pregnant women in Tanzania. Am J Trop Med Hyg. 80:36-43.

Luoma, SN. 1989. Can we determine the biological availability of sediment-bound trace elements?: Hydrobiologia, v. 176/177:379-396.

Ngole, VM., Ekosse, GE., de Jager, L. and Songca, S. 2010. Physicochemical characteristics of geophagic clayey soils from South Africa and Swaziland. African Journal of Biotechnology. 9 (36):5929-5937.

Njiru, H. 2011. Geophagy During Pregnancy in Africa: A Literature Review**.** Obstetrical & Gynecological Survey. 66(7):452-459.

Selinus, O., Finkelman, RB. and Centeno, JA. 2010. Medical Geology. A regional synthesis. Pub. Springer. pp88.

Tano-Debrah, K. and Bruce-Baiden, G. 2010. Microbiological characterization of dry white clay, a pica element in Ghana, http://www.sciencepub.net/report.

Tayie, FA., Koduah, G. and Mork, SAP. 2013. Geophagia clay soil as a source of mineral nutrients and toxicants. African Journal of Food Agriculture, Nutrition and Development. 13(1):7157-7170.

USDA. 2013. Dietary Reference Intake.

Vermeer, DE. 1971. Geophagy among the ewe of Ghana. Ethnology. 10:56-72.

Violante, A., Cozzolino, V., Perelomov, L., Caporale, AG. and Pigna, M. 2010. Mobility and bioavailabilityof heavy metals and metalloids in soil environments. J. Soil Sci. Plant Nutr. 10(3):268-292.

Woywodt, A. and Kiss, A. 2002. Geophagia: The history of earth-eating. Journal of the Royal Society of Medicine. 95:143-146.

Woode, A. 2013. Factors influencing the ingestion of clay in the greater Accra region of Ghana. A paper presented at the CAPA International conference in Gambia, June 2013.

WHO. 2013. Fact sheet No361 on Mercury and Health, April 2012.

WHO. 2013. Ten chemicals of major public health.

WHO. 2013. Fact sheet No. 372 on Arsenic, December 2012.

Received: Aug 6, 2013; Accepted: Sept 25, 2013

SENRA Academic Publishers, British Columbia
Vol. 8, No. 1, pp. 2795-2799, February 2014
Online ISSN: 1920-3853; Print ISSN: 1715-9997

Canadian Journal of pure&applied sciences

**Short Communication**

# APPLICATIONS OF INFORMATION MEASURES FOR THE STUDY OF GAUSSIAN DISTRIBUTIONS

*Om Parkash[1] and Mukesh[2]
Department of Mathematics, Guru Nanak Dev University, Amritsar 143005, India

**ABSTRACT**

Finding the relationships between information measures and statistical constants leads to the applicability of information theory to the field of statistics. In the existing literature of information theory, there are many well known information theoretic measures, each with its own merits, limitations and areas of applications. In the present communication, we have developed new generalized parametric divergence measure and provided its applications along with the other parametric information theoretic measure to the field of Statistics by establishing the relationships of information contents with some statistical constants of Gaussian distribution.

**Keywords:** Gaussian distribution, entropy, divergence, chi-square statistics, covariance matrix.

## INTRODUCTION

In the literature, there exist certain analytical expressions for the entropy of univariate continuous distributions studied by Lazo and Rathie (1978) and Cover and Thomas (1991) whereas for multivariate distributions very few results have been provided by Ahmed and Gokhale (1989). Of course, Darbellay and Vajda (2000) developed a series of analytical expressions for the entropy and the mutual information of continuous multivariate distributions.

Another study Ginebra (2007) provided the applications of information measures to the field of statistics by stating a minimal set of requirements that must be satisfied by all such measures. By doing so, the author provided the links of information and uncertainty in a probability distribution. Kitsos and Toulias (2010) introduced a three-parameter generalized normal distribution to study the generalized measures of entropy and for this generalized normal measure, the Kullback-Leibler's (1951) information measure was evaluated to extend the well known result for the normal distribution. Parkash and Thukral (2010) emphasized that statistics is extensively used for the measurement of statistical constants whereas measures of information are used to study diversity and equitability. These two fields have been used independent of each other for data analysis. The authors developed the interrelations between the two and proved that statistical measures can be used as information measures.

Many researchers have provided axiomatic derivations of Shannon's (1948) measure of entropy, given by

$$H(P) = -\sum_{i=1}^{n} p_i \ln p_i \,, \tag{1.1}$$

of a discrete-variate probability distribution $P = (p_1, p_2, \ldots, p_n)$ from different sets of plausible axioms where a great deal of mathematical sophistication and rigour has been exercised in the process. However, when it comes to the derivation of the corresponding measure

$$H[f(x)] = -\int_a^b f(x) \ln f(x) dx \,, \tag{1.2}$$

which is called differential entropy, for the entropy of continuous-variate probability distribution with density function $f(x)$, all pretensions of rigour are given up and heuristic arguments are freely employed. The major argument in favour of (1.2) is not its rigorous derivation from clearly stated axioms, but the fact that it gives useful results. Similar arguments are used to deduce various measures of entropy for the continuous variate distributions. It is well known that the Gaussian distribution density has the greatest Shannon's (1948) entropy of all distribution densities. All the other distribution densities, having the same second order moments as the Gaussian distribution density, have smaller Shannon entropy than the Gaussian density.

In statistics, the entropy corresponds to the maximum likelihood method, in which Kullback-Leibler (1951) divergence measure given by

$$D(P;Q) = \sum_{i=1}^{n} p_i \ln \frac{p_i}{q_i} \,, \tag{1.3}$$

*Corresponding author email: omparkash777@yahoo.co.in

connects Boltzmann-Shannon entropy and the expected log-likelihood function.

Recently, Parkash and Mukesh (2013) have developed the relations between parametric information measures and chi-square statistic by using the optimization principles. Further, Parkash and Mukesh (2012) have provided the applications of divergence measure by developing an optimizational principle for minimizing risk in portfolio analysis. Parkash and Mukesh (personal communication) have also investigated and introduced a new generalized measure of entropy and provided its applications to the field of queueing theory. This new entropy measure with real parameters $\alpha$ and $\beta$ is given by

$$H_{\alpha,\beta}(P)=\frac{1}{\beta-\alpha}\left(\sum_{i=1}^{n} p_i^{\alpha-\beta+1}-1\right), \tag{1.4}$$

$\alpha\neq\beta, \beta<\alpha+1, -\infty<\alpha<\infty$.

Some other characterizations and generalization of the measures of entropy and directed divergence along with their detailed properties have been provided by Havrada and Charvat (1967) and Parkash and Mukesh (2012, 2011).

In the present communication, we have developed new generalized information measure and established the relationships between information measures and the statistical constants for Gaussian distribution densities.

## 2 A New generalized parametric measure of divergence

In this section, we propose a new generalized parametric measure of divergence for the probability distributions

$P=\left\{(p_1,p_2,\ldots,p_n), p_i\geq 0, \sum_{i=1}^{n} p_i=1\right\}$ and

$Q=\left\{(q_1,q_2,\ldots,q_n), q_i\geq 0, \sum_{i=1}^{n} q_i=1\right\}$ and study its properties. This new entropy measure with real parameters $\alpha$ and $\beta$ is given by

$$D_{\alpha,\beta}(P;Q)=\frac{1}{\alpha-\beta}\left(\sum_{i=1}^{n} p_i^{\alpha-\beta+1}q_i^{\beta-\alpha}-1\right), \tag{2.1}$$

$\alpha\neq\beta, \beta<\alpha+1, -\infty<\alpha<\infty$.

We have $\lim_{\alpha\to\beta} D_{\alpha,\beta}(P;Q)=\sum_{i=1}^{n} p_i\ln\frac{p_i}{q_i}$, which shows that $D_{\alpha,\beta}(P;Q)$ is a generalization of Kullback-Leibler's (1951) measure of divergence.

For $\beta=1$, we get $D_{\alpha,1}(P;Q)=\frac{1}{\alpha-1}\left(\sum_{i=1}^{n} p_i^{\alpha}q_i^{1-\alpha}-1\right)$.

Again $D_{\alpha,\beta}(P;Q)$ is the generalization of Havrada-Charvat's (1967) divergence measure.

Next, to prove that the measure (2.1) is a valid measure of directed divergence, we study its essential properties as follows:

1) $D_{\alpha,\beta}(P;Q)$ is a continuous function of $p_1,p_2,\ldots,p_n$ and $q_1,q_2,\ldots,q_n$.
2) $D_{\alpha,\beta}(P;Q)\geq 0$ and vanishes if and only if $P=Q$.
3) We can deduce from condition (2) that the minimum value of $D_{\alpha,\beta}(P;Q)$ is zero.
4) We shall now prove that $D_{\alpha,\beta}(P;Q)$ is a convex function of both $P$ and $Q$. This result is important in establishing the property of global minimum.

Let

$$D_{\alpha,\beta}(P;Q)=f(p_1,p_2,\ldots,p_n;q_1,q_2,\ldots,q_n)=\frac{1}{\alpha-\beta}\left(\sum_{i=1}^{n} p_i^{\alpha-\beta+1}q_i^{\beta-\alpha}-1\right).$$

Thus

$$\frac{\partial f}{\partial p_i}=\frac{1}{\alpha-\beta}\left[(\alpha-\beta+1)p_i^{\alpha-\beta}q_i^{\beta-\alpha}\right],$$

$$\frac{\partial^2 f}{\partial p_i^2}=(\alpha-\beta+1)p_i^{\alpha-\beta-1}q_i^{\beta-\alpha},\ \forall i=1,2,\ldots,n,$$

and $\frac{\partial^2 f}{\partial p_i\partial p_j}=0,\ \forall i,j=1,2,\ldots,n; i\neq j$.

Similarly

$$\frac{\partial f}{\partial q_i}=-p_i^{\alpha-\beta+1}q_i^{\beta-\alpha-1},$$

$$\frac{\partial^2 f}{\partial q_i^2}=(\alpha-\beta+1)p_i^{\alpha-\beta+1}q_i^{\beta-\alpha-2},\ \forall i=1,2,\ldots,n,$$

and $\frac{\partial^2 f}{\partial q_i\partial q_j}=0,\ \forall i,j=1,2,\ldots,n; i\neq j$.

Hence, the Hessian matrix of the second order partial derivatives of $f$ with respect to $p_1,p_2,\ldots,p_n$ is given by

$H=a_{ij}$,

where

$$a_{ij}=\begin{cases}(\alpha-\beta+1)p_i^{\alpha-\beta-1}q_i^{\beta-\alpha}, & i=j\\ 0, & i\neq j\end{cases}.$$

This Hessian matrix is positive definite. Similarly one can prove that the Hessian matrix of second order partial derivatives of $f$ with respect to $q_1,q_2,\ldots,q_n$ is positive

definite. Thus, we conclude that $D_{\alpha,\beta}(P;Q)$ is a convex function of both $p_1, p_2, \ldots, p_n$ and $q_1, q_2, \ldots, q_n$. Moreover, with the help of numerical data shown in the table 1, we have presented $D_{\alpha,\beta}(P;Q)$ as shown in the figure 1.

Table 1. $D_{\alpha,\beta}(P;Q)$ against $p$ for $n=2, \alpha=3$ and $\beta=1.1$.

Table. 1.

| $P$ | $Q$ | $D_{\alpha,\beta}(P;Q)$ |
|---|---|---|
| 0.0 | 0.5 | 1.4380 |
| 0.1 | 0.5 | 0.9233 |
| 0.2 | 0.5 | 0.5205 |
| 0.3 | 0.5 | 0.2317 |
| 0.4 | 0.5 | 0.0580 |
| 0.5 | 0.5 | 0.0000 |
| 0.6 | 0.5 | 0.0580 |
| 0.7 | 0.5 | 0.2317 |
| 0.8 | 0.5 | 0.5205 |
| 0.9 | 0.5 | 0.9233 |
| 1.0 | 0.5 | 1.4380 |

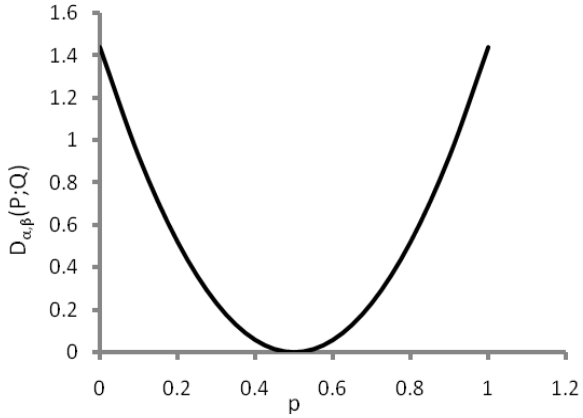


Fig. 1. Convexity of $D_{\alpha,\beta}(P;Q)$ with respect to $P$.

Under the above conditions, the function $D_{\alpha,\beta}(P;Q)$ is a valid parametric measure of directed divergence.

### 3 Relationships between information measures and Gaussian distribution

In this section, we make use of generalized information measures of entropy and divergence, discussed in the above sections, to establish their relationships with certain statistical constants for Gaussian distributed random variables.

#### 3.1 Generalized measure of entropy of Gaussian distributed random variable

We now consider the continuous version of the generalized two parametric measure of entropy (1.4) with density function $f_x(\xi)$ given by

$$H_{\alpha,\beta} = \frac{1}{\beta-\alpha}\left[\int_{-\infty}^{\infty} f_x^{\alpha-\beta+1}(\xi)d\xi - 1\right], \tag{3.1}$$

$\alpha \neq \beta, \beta < \alpha+1, -\infty < \alpha < \infty$.

The Gaussian distribution density $N(\mu, \sigma^2)$ with the expectation value $\mu$ and variance $\sigma^2$ is given by

$$f_x(\xi) = \frac{1}{\sqrt{2\pi}\sigma}\exp\left[-\frac{1}{2}\frac{(\xi-\mu)^2}{\sigma^2}\right]. \tag{3.2}$$

An extension to a multi-dimensional Gaussian random variable of dimension $n$ provides the distribution density

$$f_{\underline{x}}(\underline{\xi}) = \frac{1}{(2\pi)^{\frac{n}{2}}|\Sigma|^{\frac{1}{2}}}\exp\left[-\frac{1}{2}(\underline{\xi}-\underline{\mu})^T.\Sigma^{-1}.(\underline{\xi}-\underline{\mu})\right], \tag{3.3}$$

with the expectation vector

$\underline{\mu} = E\{\underline{x}\}$,

and the covariance matrix

$\Sigma = E\{(\underline{x}-\underline{\mu})(\underline{x}-\underline{\mu})^T\}$.

If we look at $H_{\alpha,\beta}$, we realize that this information is equal to the expected value of a distribution density

$$H_{\alpha,\beta} = \frac{1}{\beta-\alpha}\left[E\{f_x^{\alpha-\beta+1}(\xi)\}-1\right], \tag{3.4}$$

which is a typical form of an information function. Such functions often contain an expected value of a quantity, defined as information, which consist of a distribution density. Shannon's (1948) information has, for instance, such a form as $H = -E\{\ln[p(x)]\}$.

Now we insert the multi-dimensional Gaussian distribution density into the expectation function (3.4) and we get

$$H_{\alpha,\beta} = \frac{1}{\beta-\alpha}\left\{\left[\frac{1}{(2\pi)^{\frac{n}{2}}|P|^{\frac{1}{2}}}\right]^{\alpha-\beta}\int_{\Xi}\frac{1}{(2\pi)^{\frac{n}{2}}|\Sigma|^{\frac{1}{2}}}\exp\left[\begin{matrix}-\frac{1}{2}(\alpha-\beta+1)\\ .(\underline{\xi}-\underline{\mu})^T.\Sigma^{-1}.(\underline{\xi}-\underline{\mu})\end{matrix}\right]d\underline{\xi}-1\right\}, \tag{3.5}$$

and we use a new covariance matrix $\Sigma_{new} = \left[(\alpha-\beta+1)\Sigma^{-1}\right]^{-1}$ in the exponent, so that

$$\int_{\Xi}\frac{1}{(2\pi)^{\frac{n}{2}}|\Sigma_{new}|^{\frac{1}{2}}}\exp\left[-\frac{1}{2}(\underline{\xi}-\underline{\mu})^T.\Sigma_{new}^{-1}.(\underline{\xi}-\underline{\mu})\right]d\underline{\xi} = 1. \tag{3.6}$$

To obtain the determinant $|\Sigma_{new}|$, we have to calculate the matrix $\Sigma_{new}$ as given below

$$\Sigma_{new} = \left[(\alpha-\beta+1)\Sigma^{-1}\right]^{-1} = \frac{1}{(\alpha-\beta+1)}\Sigma,$$

and thus we are able to determine the determinant of the $[n\times n]$-dimensional matrix

$$|\Sigma_{new}| = \left|\frac{1}{(\alpha-\beta+1)}\Sigma\right| = \frac{1}{(\alpha-\beta+1)^n}|\Sigma|.$$

The integral of the new distribution density upon multiplying both sides by $(\alpha-\beta+1)^{-\frac{n}{2}}$ gives

$$\int_{\Xi}\frac{1}{(2\pi)^{\frac{n}{2}}|\Sigma|^{\frac{1}{2}}}\exp\left[\begin{array}{l}-\frac{1}{2}(\underline{\xi}-\underline{\mu})^{T}\\ .(\alpha-\beta+1)\Sigma^{-1}.(\underline{\xi}-\underline{\mu})\end{array}\right]d\underline{\xi}=(\alpha-\beta+1)^{-\frac{n}{2}}, \quad (3.7)$$

and thus the integral in equation (3.5) is solved. We therefore write

$$H_{\alpha,\beta}=\frac{1}{\beta-\alpha}\left\{\left[\frac{1}{(2\pi)^{\frac{n}{2}}|\Sigma|^{\frac{1}{2}}}\right]^{\alpha-\beta}(\alpha-\beta+1)^{-\frac{n}{2}}-1\right\}, \alpha\neq\beta. \quad (3.8)$$

Thus, the given information measure depends upon the determinant of the covariance matrix which describes the uncertainty of the expectation value of the Gaussian distribution density.

### 3.2 Generalized measure of divergence of Gaussian distributed random variable

We now consider the continuous version of the generalized measure of divergence (2.1) for the continuous-variate probability distributions with density functions $f_p(\xi)$ and $f_q(\xi)$. This measure is given by

$$D_{\alpha,\beta}=\frac{1}{\alpha-\beta}\left[\int_{-\infty}^{\infty}f_p^{\alpha-\beta+1}(\xi)f_q^{\beta-\alpha}(\xi)d\xi-1\right], \quad (3.9)$$

$\alpha\neq\beta, \beta<\alpha+1, -\infty<\alpha<\infty$.

In the computation of the divergence, we have to assume two Gaussian distribution densities, both with scalar random variables, to reduce the computational effort, given by the equations (3.2) and

$$f_{x_s}(\xi)=\frac{1}{\sqrt{2\pi}\sigma_s}\exp\left[-\frac{1}{2}\frac{(\xi-\mu_s)^2}{\sigma_s^2}\right]. \quad (3.10)$$

The dummy variable $\xi$ is the same for both densities. Otherwise one of the two distribution densities would be independent of the integration variable and could be extracted out of the integral.

Thus, corresponding to distribution densities (3.2) and (3.10), the equation (3.9) attains the following form:

$$D_{\alpha,\beta}=\frac{1}{\alpha-\beta}\left\{\int_{\Xi}\frac{(\sigma_s)^{\alpha-\beta}}{\sqrt{2\pi}(\sigma)^{\alpha-\beta+1}}\exp\left[\begin{array}{l}-\frac{1}{2}(\alpha-\beta+1)\frac{(\xi-\mu)^2}{\sigma^2}\\ +\frac{1}{2}(\alpha-\beta)\frac{(\xi-\mu_s)^2}{\sigma_s^2}\end{array}\right]d\xi-1\right\} \quad (3.11)$$

The exponent in the equation (3.11) is given by

$$E=-\frac{1}{2}(\alpha-\beta+1)\frac{(\xi-\mu)^2}{\sigma^2}+\frac{1}{2}(\alpha-\beta)\frac{(\xi-\mu_s)^2}{\sigma_s^2}$$

$$=-\frac{1}{2}\left[\begin{array}{l}\xi^2\left(\frac{\alpha-\beta+1}{\sigma^2}+\frac{\beta-\alpha}{\sigma_s^2}\right)-2\xi\left(\mu\frac{\alpha-\beta+1}{\sigma^2}+\mu_s\frac{\beta-\alpha}{\sigma_s^2}\right)\\ +\left(\mu^2\frac{\alpha-\beta+1}{\sigma^2}+\mu_s^2\frac{\beta-\alpha}{\sigma_s^2}\right)\end{array}\right]$$

$$=-\frac{1}{2}\left[a\xi^2-2b\xi+c\right]$$

$$=-\frac{a}{2}\left[\left(\xi-\frac{b}{a}\right)^2+\frac{c}{a}-\left(\frac{b}{a}\right)^2\right], \quad (3.12)$$

where

$$a=\frac{\alpha-\beta+1}{\sigma^2}+\frac{\beta-\alpha}{\sigma_s^2}, \quad (3.13)$$

$$b=\mu\frac{\alpha-\beta+1}{\sigma^2}+\mu_s\frac{\beta-\alpha}{\sigma_s^2}, \quad (3.14)$$

and

$$c=\mu^2\frac{\alpha-\beta+1}{\sigma^2}+\mu_s^2\frac{\beta-\alpha}{\sigma_s^2}. \quad (3.15)$$

Now using equation (3.12) into equation (3.11), we get

$$D_{\alpha,\beta}=\frac{1}{(\alpha-\beta)}\left(\begin{array}{l}\frac{(\sigma_s)^{\alpha-\beta}}{(\sigma)^{\alpha-\beta+1}}\exp\left\{-\frac{a}{2}\left[\frac{c}{a}-\left(\frac{b}{a}\right)^2\right]\right\}\\ \int_{\Xi}\frac{1}{\sqrt{2\pi}}\exp\left\{-\frac{a}{2}\left(\xi-\frac{b}{a}\right)^2\right\}d\xi-1\end{array}\right). \quad (3.16)$$

Using the identity

$$\int_{\Xi}\frac{1}{\sqrt{2\pi}\frac{1}{\sqrt{a}}}\exp\left\{-\frac{a}{2}\left(\xi-\frac{b}{a}\right)^2\right\}d\xi=1, \quad (3.17)$$

in the equation (3.16), we get

$$D_{\alpha,\beta}=\frac{1}{(\alpha-\beta)}\left(\frac{(\sigma_s)^{\alpha-\beta}}{(\sigma)^{\alpha-\beta+1}}\exp\left\{-\frac{a}{2}\left[\frac{c}{a}-\left(\frac{b}{a}\right)^2\right]\right\}\frac{1}{\sqrt{a}}-1\right). \quad (3.18)$$

Inserting the terms for $a$, $b$ and $c$ from equations (3.13), (3.14) and (3.15) in equation (3.18), we get

$$D_{\alpha,\beta}=\frac{1}{(\alpha-\beta)}\left(\begin{array}{l}\frac{(\sigma_s)^{\alpha-\beta}}{(\sigma)^{\alpha-\beta+1}\sqrt{\frac{\alpha-\beta+1}{\sigma^2}+\frac{\beta-\alpha}{\sigma_s^2}}}\\ \exp\left\{-\frac{\sqrt{\frac{\alpha-\beta+1}{\sigma^2}+\frac{\beta-\alpha}{\sigma_s^2}}}{2}\left[\frac{\mu^2\frac{\alpha-\beta+1}{\sigma^2}+\mu_s^2\frac{\beta-\alpha}{\sigma_s^2}}{\sqrt{\frac{\alpha-\beta+1}{\sigma^2}+\frac{\beta-\alpha}{\sigma_s^2}}}-\left(\frac{\mu\frac{\alpha-\beta+1}{\sigma^2}+\mu_s\frac{\beta-\alpha}{\sigma_s^2}}{\sqrt{\frac{\alpha-\beta+1}{\sigma^2}+\frac{\beta-\alpha}{\sigma_s^2}}}\right)^2\right]\right\}-1\end{array}\right) \quad (3.19)$$

Thus given parametric measure of cross entropy is expressible in terms of standard deviations of the Gaussian distribution densities.

If the expected values for both the random variables are equal, we get

$$D_{\alpha,\beta}=\frac{1}{(\alpha-\beta)}\left[\frac{(\sigma_s)^{\alpha-\beta}}{(\sigma)^{\alpha-\beta+1}\sqrt{\frac{\alpha-\beta+1}{\sigma^2}+\frac{\beta-\alpha}{\sigma_s^2}}}-1\right]. \quad (3.20)$$

## CONCLUDING REMARKS

We have derived the relationships between the information measures and the statistical constants of Gaussian distributions to develop the link between information theory and statistics. With similar arguments,

the relations between information measures and other standard distributions can be studied.

**ACKNOWLEDGEMENTS**

The authors are thankful to the University Grants Commission, New Delhi, for providing financial assistance for the preparation of the manuscript.

**REFERENCES**

Ahmed, NA. and Gokhale, DV. 1989. Entropy expressions and their estimators for multivariate distributions. IEEE Transactions on Information Theory. 35:688-692.

Cover, TM. and Thomas, JA. 1991. Elements of information theory. Wiley, New York, USA.

Darbellay, GA. and Vajda, I. 2000. Entropy expressions for multivariate continuous distributions. IEEE Transactions on Information Theory. 46:709-712.

Ginebra, J. 2007. On the measure of the information in a statistical experiment. Bayesian Analysis. 2:167-212.

Havrada, JH. and Charvat, F. 1967. Quantification methods of classification process: Concept of structural $\alpha$ -entropy. Kybernetika. 3:30-35.

Kitsos, CP. and Toulias, TL. 2010. New information measures for the generalized normal distribution. Information. 1:13-27.

Kullback, S. and Leibler, RA. 1951. On information and sufficiency. Annals of Mathematical Statistics. 22:79-86.

Lazo, ACGV. and Rathie, PN. 1978. On the entropy of continuous probability distributions. IEEE Transactions on Information Theory. IT-24:102-122.

Parkash, O. and Mukesh. 2013. A study of maximum entropy principle for queueing theory. Canadian Journal of Mathematics. (Communicated).

Parkash, O. and Mukesh. 2012. Development of optimizational principle for minimizing risk in portfolio analysis. Global and Stochastic Analysis: An International Journal. 2:21-26.

Parkash, O. and Mukesh. 2012. New generalized parametric measures of entropy and cross entropy. American Journal of Mathematics and Sciences. 1:91-96.

Parkash, O. and Mukesh. 2013. Relation between information measures and chi-square distribution. International Journal of Pure and Applied Mathematics. 84:517-524.

Parkash, O. and Mukesh. 2011. Two new symmetric divergence measures and information inequalities. International Journal of Mathematics and Applications. 4:165-179.

Parkash, O. and Thukral, AK. 2010. Statistical measures as measures of diversity. International Journal of Biomathematics. 3:173-185.

Shannon, CE. 1948. A mathematical theory of communication. Bell System Technical Journal. 27:379-423.

Received: Sept 27, 2013; Accepted: Nov 5, 2013

SENRA Academic Publishers, British Columbia
Vol. 8, No. 1, pp. 2801-2805, February 2014
Online ISSN: 1920-3853; Print ISSN: 1715-9997

Canadian Journal of pure&applied sciences

**Short Communication**

# QUALITY ASSESSMENT OF SELECTED GROUNDWATER SAMPLES IN AMIKE – ABA, ABAKALIKI EBONYI STATE, NIGERIA

*SO Ngele[1], E J Itumoh[1], NC Onwa[2] and F Alobu[1]
[1]Department of Industrial Chemistry, Ebonyi State University Abakaliki, Ebonyi State
[2]Department of Applied Microbiology, Ebonyi State University Abakaliki, Ebonyi State, Nigeria

## ABSTRACT

The quality of selected groundwater (borehole) samples in Amike – Aba, were assessed for physicochemical parameters, trace metals and bacteriological tests for a period of seven weeks following standard water sampling and analysis procedures. The results of the physicochemical parameters showed the range 6.38 – 6.44 for pH, 26.20 – 26.35 for temperature, 0.20 – 0.25 mg/L $O_2$ for $BOD_5$, 10.87 – 12.98 µS/cm for conductivity, 32.16 – 34.87 mg/L for total hardness and 4.00 – 6.00 TCU for colour. The result of the bacteriological analysis showed that the total heterotrophic bacteria count (THBC) of the samples ranged from $2.4 \times 10^2 – 4.2 \times 10^3$ CFU/mL. The total coliform count also ranged from 280 – 540 MPN/100 mL. The study revealed the presence of *Escherichia coli*, *Proteus sp.*, *Psedomonas aeuginosa*, *Enterobacter aerogenes*, *Streptococcus faecalis* and *Bacillus sp.* in the water samples. The results of the trace metals showed the range (in mg/L) 0.223 – 0.273 for Fe, 0.048 – 0.059 for Cr, 0.0081 – 0.099 for Pb, 0.032 – 0.040 for Cu, 0.021 – 0.024 for Mn and 0.097 – 0.143 for Mg. Compared with World Health Organization limits and Nigerian Standard for Drinking Water Quality, the results revealed the groundwater samples are facing various hydrological stress and possible contamination which could change the quality of the groundwater in the near future.

**Keywords**: Groundwater, quality assessment, trace metals, coliforms, physicochemical parameters.

## INTRODUCTION

Groundwater exists below the surface of the ground in the spaces between particles of rock or soil, or in the crevices and cracks in rocks, usually within 100 meters of the surface of the Earth (SGS, 2012). It plays an important role in both private and public water supplies all over the world (Pradhan and Pirasteh, 2011; Ibeh and Okplenye, 2005). This is because groundwater forms a major part of freshwater use globally (SGS, 2012). Also in most developing countries today, groundwater remains the only source of potable water supply, giving rise to high numbers of boreholes and wells. Again, it is likely that many people in developing countries have preferences for boreholes to other sources of water supply. This is also in line with view of World Health Organisation (WHO) that boreholes are resistant to many forms of natural and manmade disasters (except in cases of high magnitude earthquake), and the narrow opening at the top of the borehole often prevents contamination of the water source or damage to the pump components below ground (WHO, 2011).

However, in spite of the seemingly availability of water, the challenge of ensuring usable water in sufficient quantities remains a primary issue in most developing countries (Amangabara and Ejenma, 2012). The reasons for this are enormous. First, groundwater contains a variety of constituents such as microorganisms, gases, inorganic and organic materials, etc at different concentrations (Sundaram *et al*., 2009; SGS, 2012) which may constitute undesirable pollutant when they are not within WHO guidelines for drinking water (Nkamare *et al*., 2012). Anthropogenic contamination of the water even at the source is the second issue. For example, water contamination with trace metals can be related to polluted water infiltrating through soil, rock and eventually reaching the groundwater (Oladipo *et al*., 2011). Also, exposure of water to hostile environmental factors over a long period of time such as extreme sunlight, high temperature, segmentation, biological action, etc. tend to introduce either bacteria or viruses into the water (Okonkwo *et al*., 2012). Finally, water is an excellent solvent which tends to dissolve the minerals in the geological system. The greater part of the soluble constituents in groundwater comes from soluble minerals in soils and sedimentary rocks (Sundaram *et al*., 2009). According to Pradhan and Pirasteh (2011), the chemical nature of the ground water is influenced by several factors such as chemical weathering of the country rocks and interaction with the country rocks.

Abakaliki is a rapidly developing urban city where public water supply is nearly absent or in short supply especially

*Corresponding author email: sonngele@yahoo.com

in the suburb areas such as Amike – Aba. This has made groundwater (borehole) as a major source of water supply in the area for domestic use and for drinking. It is also pertinent to note that Abakaliki and Ebonyi State in general was before now one of the Guinea worm endemic areas of the country (Ekpo, 1990) and incidences of waterborne diseases such as cholera, dysentry, typhoid fever etc. are common. The recent upsurge in population in the area due to its current status as a State capital has given rise to unprofessional engaging in building/ construction of houses and sinking of boreholes without recourse to standard sanitary specifications (e.g. The WHO recommends that boreholes should be located at least 30 km away from latrines and 17m from septic tanks (Ibeh and Okplenye, 2005). Cases of some boreholes located close or adjacent to septic tanks/soak aways abound leading to contamination through underground seepages.

The quality assessment of groundwater samples in Amike – Aba has not been reported. There is also the need for regular monitoring and assessment of drinking water sources. This is because monitoring provides data on groundwater quantity and quality and it is an integral aspect of groundwater management (Sundaram *et al*., 2009).

The aim of this work is to estimate the presence of some of the parameters that are implicated in water pollution and ascertain their levels if present and compare their levels with that of WHO standard and Nigeria Industrial standards (NIS 554, 2007) for drinking water where applicable.

## MATERIALS AND METHODS

### The Study Area

Ebonyi State, South-East Nigeria, is an agrarian State with high mineral deposits. Abakaliki is on lat. 6.21N and long. 8.07E (Collins-Longman, 1981) and area falls within the climatic region of Southern Eastern Nigeria where the rainy season spans from April to October and the dry season from October to April (Ezeh and Ugwu, 2007). The average annual rainfall of the study area is about 1500mm with actual surface temperature (seasonal temperature) of between 24-36$^0$C during dry season and about 18 $^0$C during the rainy season (Ezeh and Ugwu, 2007; Collins-Longman, 1981).

### Sampling Protocols and Analysis

In order to avoid contamination, all glassware, high-density polyethylene (HDPE) storage bottles for reagent solutions and plastic items were acid cleaned following a standard procedure. All items for collecting and storing samples and reagents were first washed with distilled water, soaked in a 10% HCl solution for at least 24h (Prior and Johnes, 2002) and rinsed three times with distilled water. The washed items were dried and stored in zip locked polyethylene bags. However, the glass containers for microbial analysis were further sterilized using a hot air oven at 37$^0$C for 1h. All metallic wares were autoclaved at 121$^0$C for 15minutes.

The water samples were collected thrice-a-week for a period of seven weeks. Water samples were randomly collected in sterile, wide mouthed containers (*ca.* 1 litre) with cap. The water was allowed to run from the tap for about three minutes. The containers were completely filled with water and capped to prevent spillage. The samples for metal analysis were spiked with 1 mL of concentrated nitric acid. All the samples were protected from direct sunlight and transported to the laboratory in an ice-pack. The samples were kept in the refrigerator at 4$^0$C and analyses within one hour of collection and maximum of 24h. However, pH, temperature, dissolved oxygen; conductivity and turbidity were carried out *in-situ* at the sampling sites using probes (see Table 1).

The metallic contents of the samples were determined using atomic absorption spectroscopy (AAS) (Perkin-Elmer Buck Scientific VGP 210) according to standard procedures (Mendham *et al*., 2004). The Total Heterotrophic Bacteria Count (THBC) was carried out by the standard plate count procedures as described by (Benson, 2011) using plate count agar. Plates were incubated at 35$^0$C for 24h. The Total Coliform Count (TCC) was determined using the Most Probable Number (MPN) method (Benson, 2011) while morphological, physicological and biochemical characteristic method was used for identification of the bacterial species according to the scheme of (Holt *et al*., 1994).

## RESULTS AND DISCUSSION

The results of the physicochemical parameters are presented in table 2 which was compared with standards for drinking water. The parameters were within the acceptable limits and present the water samples as potable. The pH of the samples was not too acidic and was slightly stable over the range (6.38 – 6.44). Hence, the pH was not influenced by treatment breakdowns or other accidental spills which affect groundwater (Sundaram *et al*., 2009). The temperature range also had little impact on the levels of inorganic constituents and chemical contaminants (see Tables 4 and 5) and the range of the water temperature which was not high did not increase problems related to taste, odour and color. The fairly stable temperature observed (26.20 – 26.35$^0$C) is not surprising since ground water is stored underground it has a relatively constant temperature throughout the year (Sundaram *et al*., 2009). Although the temperature and ionic compositions of water significantly affects the electrical conductivity of water, the values recorded were far below the acceptable standard (1000µS/cm) which

Table 1. Physicochemical parameters and method of determination.

| Physicochemical parameters | Instrument/Method |
|---|---|
| pH | pH – 201 Lutron (Taiwan) |
| Conductivity | Lutron WA 300 Conductivity meter (Taiwan) |
| Dissolved Oxygen | Lutron 5509 DO meter (Taiwan) |
| Colour | Laser Beam Spectrometer DR 3000 HACH (USA) |
| Temperature | Portable digital multi-stem thermometer (Model – ST -9269) |
| Turbidity | Turbidimeter |
| BOD | Titration |
| Total Hardness | Titration |

Table 2. Mean variation of the physicochemical properties (± standard error, SE) of the samples compared with the WHO standards (n = 7).

| Parameter/unit | Range | Mean ± SE | Standard |
|---|---|---|---|
| pH | 6.38 – 6.44 | 6.39 ± 0.015 | 6.5 – 8.5[a,b] |
| Temperature ($^0$C) | 26.20 – 26.35 | 26.30 ± 0.028 | Ambient[a] |
| $BOD_5$ (mg/L $O_2$) | 0.20 – 0.25 | 0.23 ± 0.013 | < 3.0[a] |
| Conductivity (μS/cm) | 10.87 – 12.98 | 11.89 ± 0.346 | 1000[a] |
| Total hardness (mg/L) | 32.16 – 34.87 | 33.34 ± 0.542 | 150[a] |
| Turbidity (NTU)* | 0.00 – 0.00 | 0.00 ± 0.00 | 5[a,b] |
| Colour (TCU)* | 4.00 – 6.00 | 4.80 ± 0.374 | 15.0[a] |

[a]Nigerian Standard for Drinking Water Quality (Nigerian Industrial Standard NIS 554:2007) (Standard Organisation of Nigeria (SON), 2007), [b]Guidelines for Drinking-water Quality (WHO, 2011).
*NTU = nephelometric turbidity unit, TCU = true colour units

Table 3. Total heterotrophic bacterial count (THBC) (CFU/mL) and total coliform count (TCC) (MPN/100 mL) (n = 7).

| S. NO. | Sample code | Range of THB count (CFU/mL) | Mean THB count (CFU/mL) | Range of total coliform (MPN/100 mL) | Mean total coliform (MPN/100 mL) |
|---|---|---|---|---|---|
| 1 | S – A | $2.4 \times 10^3 – 3.1 \times 10^3$ | $2.8 \times 10^3$ | 350 – 390 | 380 |
| 2 | S – B | $3.9 \times 10^3 – 4.5 \times 10^3$ | $4.2 \times 10^3$ | 520 – 560 | 540 |
| 3 | S – C | $1.1 \times 10^3 – 1.8 \times 10^3$ | $1.4 \times 10^3$ | 250 – 300 | 280 |
| 4 | S – D | $2.2 \times 10^2 – 2.6 \times 10^2$ | $2.4 \times 10^2$ | 330 – 350 | 340 |
| 5 | S – E | $3.6 \times 10^3 – 4.3 \times 10^3$ | $4.2 \times 10^3$ | 440 – 460 | 440 |

*MPN = Most probable number

implied little or no contributions of the parameters to its elevation. The water samples were not hard (32.16 – 34.87mg/L) or turbid and significantly had no visible coloration (4.00 – 6.00 TCU).

The result of the bacteriological test is presented in table 3. Samples S – B and S – E had the highest THBC of $4.2 \times 10^3$ CFU/mL respectively while sample S – D had the lowest count of $2.4 \times 10^2$ CFU/mL. The result of the TCC showed that sample S – B had the highest count of 540 while S – C had the least count of 280. The presence of coliforms in the water samples indicates inadequate treatment and contamination (WHO, 2008). Bacterial species isolated included *Escherichia coli*, *Proteus sp.*, *Psedomonas aeuginosa*, *Enterobacter aerogenes*, *Streptococcus faecalis* and *Bacillus sp*. The presence of *E. coli* indicates that the groundwater samples are contaminated with faecal matter (WHO, 2008; Madigan *et al*., 2000). As observed by Uzoigwe and Agwa (2012), who also observed high total coliform in the water samples analyzed, the presence of these indicator organisms in drinking water sources provides an indication of water-borne problems and direct threat to human health and should be viewed as a matter of serious concern.

The results of the chemical constituents (metals) of the groundwater samples are presented in tables 4 and 5. Table 4 shows the mean concentration (mg/L) of the metals per sample while table 5 shows the range of the metals in the samples compared to standards. The concentrations of these metals (Fe, Cr, Pb, Cu, Mn and

Table 4. Mean concentration (mg/L) of trace metals (± standard error, SE) of the samples compared with the WHO standards (n = 7).

| Parameter/sample | S – A | S – B | S – C | S – D | S – E |
|---|---|---|---|---|---|
| Fe | 0.254 ± 0.001 | 0.022 ± 0.001 | 0.223 ± 0.000 | 0.273 ± 0.001 | 0.226 ± 0.000 |
| Cr | 0.048 ± 0.001 | 0.051 ± 0.002 | 0.052 ± 0.001 | 0.049 ± 0.003 | 0.059 ± 0.001 |
| Pb | 0.091 ± 0.001 | 0.096 ± 0.000 | 0.099 ± 0.001 | 0.081 ± 0.001 | 0.082 ± 0.002 |
| Cu | 0.040 ± 0.002 | 0.032 ± 0.001 | 0.033 ± 0.001 | 0.029 ± 0.001 | 0.036 ± 0.001 |
| Mn | 0.024 ± 0.002 | 0.025 ± 0.001 | 0.021 ± 0.001 | 0.024 ± 0.001 | 0.023 ± 0.000 |
| Mg | 0.014 ± 0.001 | 0.097 ± 0.001 | 0.099 ± 0.001 | 0.114 ± 0.002 | 0.126 ± 0.003 |

Table 5. Mean concentration (mg/L) of trace metals of the samples compared with the WHO standards (n = 7).

| Parameter | Range | Mean | Standard |
|---|---|---|---|
| Fe | 0.223 – 0.273 | 0.240 | 0.03[a] |
| Cr | 0.048 – 0.059 | 0.052 | 0.05[a,b] |
| Pb | 0.0081 – 0.099 | 0.089 | 0.01[a,b] |
| Cu | 0.032 – 0.040 | 0.034 | 2[b] |
| Mn | 0.021 – 0.024 | 0.023 | 0.2[a] |
| Mg | 0.097 – 0.143 | 0.119 | 0.2[a] |

[a]Nigerian Standard for Drinking Water Quality (Nigerian Industrial Standard NIS 554:2007) (Standard Organisation of Nigeria (SON), 2007)
[b]Guidelines for Drinking-water Quality (WHO, 2011)

Mg) are relatively within the limits of the standards. The high concentrations of Pb, almost close to the NIS and WHO standards, could be attributed to geology of the area since Abakaliki is one of the well known lead-zinc mineralized districts in Africa (Hutchison and Meema, 1987). The relatively high concentration of Fe is probable from the soil geochemistry and abundance of the metal in the soil. The concentrations of Cr may have contributions from waste water discharges, seepages and from soil geochemistry. The concentrations of Mn from the study probably from rocks and aquifers since Mn occur in rocks and soils and are widespread in the environment (Krauskopf and Bird, 1995). The relative low concentrations of Mg compared to standard are also reflected in the hardness of water.

## CONCLUSION

This work assessed the quality of selected groundwater (borehole) samples in Amike – Aba, for physicochemical parameters, trace metals and bacteriological tests for a period of seven weeks following standard water sampling and analysis procedures. Compared with World Health Organization limits and Nigerian Standard for Drinking Water Quality, the results revealed the groundwater samples are facing various hydrological stress and possible contamination which could change the quality of the groundwater in the near future.

Generally, the results of this study, except for the bacteriological tests, are not indicative of high pollution of the potable water sources and require caution in the interpretation of the results. Based on the result of the bacteriological analysis, it is recommended that the groundwater (borehole) in Amike – Aba be treated to disinfect contaminating microorganisms and to reduce the bioload. However, to meet the millennium development goal of potable water supply, efforts are required to improve water supply, sanitation coverage and it is important to regularly assess the pollution risks to groundwater posed by improper on-site sanitation systems.

## REFERENCES

Amangabara, GT. and Ejenma, E. 2012. Groundwater Quality Assessment of Yenagoa and Environs Bayelsa State, Nigeria between 2010 and 2011. Resources and Environment. 2(2):20-29.

Benson, HJ. 2011. Microbiological Applications Laboratory Manual in General Microbiology (8th edi.). McGraw-Hill Companies, New York, USA.

Collins-Longman. 1981. New Secondary Atlas (Rev. edi.). Sheck-Wah Tong Printing Press Ltd., Hong Kong.

Ekpo, I. 1990. Nigeria Water Management Strategy: The Journey so far. Proceedings of the 1st Biennial National Symposium on Hydrology, Maidugri. 294-301.

Ezeh, H. and Ugwu, S. 2007. Geo-electric Investigation of Sulphide Mineralization at Egu-Echaraunuhu, Abakaliki, S.E. Nigeria. J. Applied Natural Sciences. 1(1):59-63.

Holt, JG., Krieg, NR., Sneath, PH. and William, ST. 1994. Bergeys Manual of Determinative Bacteriology (8th edi.). The Williams and Wilkins Company, New York, USA.

Hutchison, TC. and Meema, KM. 1987. Lead, Mercury, Cadmium and Arsenic in the Environment. John Wiley Ltd, New York, USA.

Ibeh, SN. and Okplenye, JI. 2005. Bacteriological Analysis of Borehole in Uli, Nigeria. African Journal of Applied Zoology & Environmental Biology. 7:116-119.

Johnston, D. 2007. EPA Guidelines: Regulatory Monitoring and Testing Groundwater Sampling. Environment Protection Authority, Adelaide, Australia.

Krauskopf, K. and Bird, D. 1995. Introduction to Geochemistry (3rd edi.). McGraw-Hill, London.

Madigan, MT., Martinko, JM. and Parker, J. 2000. Brock Biology of Microorganisms (9th edi.). Prentice Hall, New Jersey.

Mendham, J., Denney, RC., Barnes, JD. and Thomas, M. 2004. Vogel's Textbook of Quantitative Chemical Analysis (6th edi.). Pearson Education Ltd, Delhi, India.

Nkamare, MB., Ofili, AN. and Adeleke, AJ. 2012. Physico-chemical and Microbiological Assessment of Borehole Water in Okutukutu, Bayelsa State, Nigeria. Advances in Applied Science Research. 3(5):2549-2552.

Okonkwo, SI., Eme, L. and Swift, O. 2012. Optimization Modeling of Borehole Water Quality in Rumuogwunama in Eneka of Obio-Akpor L.G.A in Rivers State, Nigeria. 2012 International Conference on Environmental, Biomedical and Biotechnology. IACSIT Press, Singapore. 41:255-258.

Oladipo, M., Njinga, RL., Baba, A. and Mohammed, I. 2011. Contaminant Evaluation of Major Drinking Water Sources (Boreholes Water) in Lapai Metropolis. Advances in Applied Science Research. 2(6):123-130.

Pradhan, B. and Pirasteh, S. 2011. Hydro-Chemical Analysis of the Ground Water of the Basaltic Catchments: Upper Bhatsai Region, Maharastra. The Open Hydrology Journal. 5:51-57.

SGS. 2012. Groundwater Analysis. SGS Environmental Services-ENV 068: www.environment.sgs.ca or www.environment.sgs.ca/fr-FR/ Retrieved April 5, 2013.

Standard Organisation of Nigeria (SON). 2007. Nigerian Standard for Drinking Water Quality (Nigerian Industrial Standard NIS 554:2007). Standard Organisation of Nigeria (SON), Abuja.

Sundaram, B., Feitz, A., Caritat, PD., Plazinska, A., Brodie, R., Coram, J. and Ransley, T. 2009. Groundwater Sampling and Analysis - A Field Guide. Geoscience Australia, Record 2009/27, Canberra, Australia.

Uzoigwe, CI. and Agwa, OK. 2012. Microbiological Quality of Water Collected from Boreholes sited near Refuse Dumpsites in Port Harcourt, Nigeria. African Journal of Biotechnology. 11(13):3135-3139.

World Health Organisation-WHO. 2008. Guidelines for Drinking-water Quality (3rd edi., vol. 1). World Health Organisation, Geneva.

World Health Organisation-WHO. 2011. Guidelines for Drinking-water Quality. World Health Organisation (WHO), Geneva.

World Health Organisation-WHO. 2011. Technical Notes on Drinking Water, Sanitation and Hygiene in Emergencies 2. Water Sanitation, Hygiene and Health. World Health Organisation, Geneva.

Received: Aug 18, 2013; Received: Oct 3, 2013